



University  
of Glasgow

Rawcliffe, Heather Joanne (2016) *Lava-water-sediment interaction: processes, products and petroleum systems*. PhD thesis.

<http://theses.gla.ac.uk/7204/>

Copyright and moral rights for this thesis are retained by the author

A copy can be downloaded for personal non-commercial research or study

This thesis cannot be reproduced or quoted extensively from without first obtaining permission in writing from the Author

The content must not be changed in any way or sold commercially in any format or medium without the formal permission of the Author

When referring to this work, full bibliographic details including the author, title, awarding institution and date of the thesis must be given

# **Lava-Water-Sediment Interaction: Processes, Products and Petroleum Systems**

**Heather Joanne Rawcliffe**

M.E.Sci (Hons) University of Liverpool

Submitted in fulfilment of the requirements for the  
Degree of Doctor of Philosophy

School of Geographical and Earth Sciences  
College of Science and Engineering  
University of Glasgow

December 2015

© Heather J. Rawcliffe, 2015

## Dedication

For my loving Grandparents.

*“To believe in yourself and what you can do is to take the first step on the road to success.” Anonymous*

*“The best geologist is one who has seen the most rocks.” H.H. Read, 1940.*

---

## Abstract

Lava-water-sediment interaction encompasses the processes and products created as lava is emplaced over, or into sediment (and/or water). The lithologies preserved at the lava-sediment interface include pillow lavas, hyaloclastite and peperite, which are well documented within the literature. However, little work captures the full scope of the interaction between sub-aerially emplaced, invasive lava and (clastic) sediment (+/- water). Furthermore, the scales and geometries of interaction at the lava-water-sediment interface are yet to be fully understood. This research uses four field localities from a variety of environmental and tectonic settings to assess the remarkably variable, complex and intricate fragmental textures and geometries preserved at the lava-sediment interface, many of which are documented for the first time. The processes and lava/sediment properties that influence interaction are then interpreted.

This research identifies a continuum of lava-water-sediment interaction, from minimal and passive interactions, to dynamic and complex interactions, predominantly between basalt lavas and siliciclastic and volcanoclastic sediments. The continuum recognises that the variability of sedimentary properties (e.g. saturation, grain size, cohesion, compaction), rather than lava properties (e.g. effusion rates/flux, composition, temperature, viscosity, shear strength etc.), is the dominant influence on interaction products. The variability of sedimentary properties can occur on the micro- to macro-scale, producing a range of scale-invariant lava-sediment products. When sediment is partially consolidated and compacted, with relatively little to no water content, loading and passive interaction, including the formation of passive peperite, occurs. Sediment that is very fine grained, compacted, semi-saturated and only slightly consolidated, is typically more cohesive and produces coherent sedimentary inclusions. Sediment inclusions within lava and peperite domains are abundant, and interpreted as the product of lava invading and entraining fragments of more cohesive, consolidated sediment. When sediment is saturated (with pore water), unconsolidated, and uncompacted, dynamic peperite forms and sediment fluidisation occurs. Sediment fluidisation is also the main product at the interface between pillow lavas and sediment. Measurement analysis of pillow-sediment contacts establishes that pillow invasion is scale invariant.

An understanding of the lateral variability of the processes and products of lava-water-sediment interaction is developed, along with the concept of individual sedimentary 'barrier' layers that may impede lava-invasion, and influence the geometries of the system. The geometries of lava-water-sediment domains, particularly where dynamic

interaction occurs, may be further influenced by palaeoenvironment (e.g. fluvial drainage systems may focus aggressive interaction and peperite formation in channels). The products and processes of lava-water-sediment interaction, and the geometries of the lava-sedimentary systems, are presented in a series of models, all of which highlight the variable sediment properties at the time of lava invasion.

The results of this research are directly applicable to the petroleum industry in aiding exploration within volcanic-rifted margins. Application of these findings is of particular importance during the development of regional and basin-scale depositional environment models. The field data is applied to wireline and borehole image log interpretations, which provides greater understanding of how potential reservoir units may be disrupted by lavas, both physically and by “compartmentalization” of the reservoir. Together, these results demonstrate how lavas have the potential to considerably fragment on interaction with sediment and/or water, informing our understanding of the interplay of volcanic and sedimentary systems.

---

## Table of Contents

Dedication .....	ii
Abstract .....	iii
List of Figures .....	x
List of Tables .....	xiv
Acknowledgments .....	xv
Author's Declaration .....	xviii
Abbreviations.....	xix
<b>Chapter 1: Introduction .....</b>	<b>21</b>
1.1 Research Rationale.....	21
1.2 Research Aims and Objectives .....	24
1.3 Methods.....	25
1.3.1 Fieldwork: .....	26
1.3.2 Samples and Petrography: .....	26
1.3.3 Industry: .....	27
1.4 Thesis Outline.....	27
<b>Chapter 2: Geological Background .....</b>	<b>29</b>
2.1 Introduction.....	29
2.2 Terminology and basic concepts .....	29
2.2.1 Lava types and emplacement .....	29
2.2.2 Volcaniclastic Rocks.....	32
2.2.2.1 Classification .....	32
2.2.2.2 Volcaniclastic sub-categories .....	35
2.3 Lava-water interaction .....	38
2.4 Lava-sediment interaction.....	39
2.5 Offshore data collection in petroleum systems.....	43
2.5.1 Wireline logs .....	43
2.5.2 Borehole imaging.....	45
<b>Chapter 3: Kinghorn, Fife, Scotland, UK.....</b>	<b>48</b>
3.1 Introduction.....	48
3.2 Geological Setting.....	49
3.3 Field Relationships .....	51
3.3.1 Volcanic Units.....	53
3.3.1.1 Lava.....	53
3.3.1.2 Hyaloclastite unit .....	56
3.3.1.3 Lapilli tuff.....	57

3.3.2	Sedimentary Units.....	59
3.3.2.1	Epiclastic units .....	59
3.3.2.2	Volcaniclastic unit (V1), Locality 2.....	60
3.3.2.3	Carbonate units .....	67
3.3.3	Lava-Sedimentary Contacts.....	70
3.4	Interpretation.....	73
3.4.1	Volcanic Units.....	73
3.4.1.1	Lava .....	73
3.4.1.2	Hyaloclastite.....	74
3.4.1.3	Lapilli Tuff .....	74
3.4.2	Sedimentary Units.....	75
3.4.2.1	Clastic Units .....	75
3.4.2.2	Volcaniclastic Unit (V1) .....	76
3.4.2.3	Carbonate Units .....	76
3.5	Discussion.....	78
3.5.1	Loading and soft-sediment deformation .....	78
3.5.2	Peperite - ‘passive’ interaction .....	79
3.5.3	Peperite - ‘dynamic’ interaction.....	80
3.6	Conclusions.....	84
<b>Chapter 4: Mountain Home, Idaho, USA.....</b>		<b>86</b>
4.1	Introduction.....	86
4.2	Geological History.....	86
1.1	Field Relationships .....	88
1.1.1	Brief overview of the area .....	88
1.1.2	LSP1 .....	91
1.1.2.1	Lava: .....	91
1.1.2.2	Sedimentary: .....	92
1.1.2.3	L1 and S1 contact: .....	97
4.2.1	LSP2 .....	97
4.2.1.1	Lava: .....	97
1.1.2.4	Sedimentary .....	98
4.2.1.2	L2 and S2 contact: .....	101
4.2.2	LSP3 .....	102
4.2.2.1	Lava: .....	103
4.2.2.2	Hyaloclastite and Pillow breccia (HPb): .....	104
4.2.2.3	Sedimentary: .....	107
4.2.2.4	HPb and S3 contact (sedimentary inclusions):.....	116
4.2.2.5	Interaction and penetration of the HPb with the VSst .....	119

4.2.3	LSP4 .....	124
4.2.3.1	Lava: .....	124
4.2.3.2	Sedimentary/Volcaniclastic: .....	124
4.3	Interpretation.....	125
4.3.1	LSP1 .....	125
4.3.1.1	Lava: .....	125
4.3.1.2	Sedimentary units:.....	125
4.3.1.3	Interaction .....	126
4.3.2	LSP2 .....	126
4.3.2.1	Lava: .....	126
4.3.2.2	Sedimentary: .....	127
4.3.2.3	Interaction .....	127
4.3.3	LSP3 .....	128
4.3.3.1	Lava: .....	128
4.3.3.2	Sedimentary .....	129
4.3.3.3	Interaction .....	130
4.3.4	LSP4 .....	131
4.4	Discussion.....	132
4.4.1	Pillow Analysis .....	132
4.4.2	Coherent sediment inclusions .....	134
4.4.3	Sedimentary Marker Bed and Barrier .....	136
4.4.4	Emplacement Model .....	138
4.5	Conclusions.....	141
<b>Chapter 5: Gran Canaria, Canary Islands, Spain .....</b>		<b>142</b>
5.1	Introduction.....	142
5.2	Geological Background .....	143
5.3	Observations .....	146
5.3.1	Sedimentary Units.....	148
5.3.2	Volcanic Units.....	160
5.3.2.1	Hyaloclastite Pillow breccia.....	160
5.3.2.2	Pillow lava .....	163
5.3.3	Lava-Sediment Interface .....	170
5.4	Interpretation.....	176
5.4.1	Sedimentary Units.....	177
5.4.2	Volcanic Component .....	178
5.4.2.1	HPb.....	178
5.4.2.2	Sheet lava .....	178
5.4.3	Lava-sediment interaction .....	179

5.5 Discussion.....	181
5.5.1 Pillow measurements .....	181
5.5.2 Fluidisation.....	185
5.6 Conclusions.....	187
<b>Chapter 6: St. Cyrus, Scotland, UK.....</b>	<b>188</b>
6.1 Introduction.....	188
6.2 Geological Setting.....	189
6.3 Field Relationships .....	191
6.3.1 Lavas .....	196
6.3.2 Sedimentary Units.....	197
6.3.2.1 Conglomerate.....	199
6.3.2.2 Sandstone and siltstone .....	201
6.3.3 Mixed lava-sedimentary domains .....	204
6.3.3.1 Sedimentary inclusions within lava.....	204
6.3.3.2 Isolated lava lobes .....	206
6.3.3.3 Isolated sedimentary units with localised peperite.....	207
6.3.3.4 Stacked lava lobes with sediment .....	208
6.3.3.5 Peperite .....	212
6.4 Interpretation.....	218
6.4.1 Lava .....	218
6.4.2 Sedimentary Units.....	218
6.4.2.1 Conglomerate.....	218
6.4.2.2 Sandstone and Siltstone.....	218
6.4.3 Mixed lava-sediment domains .....	219
6.4.3.1 Sedimentary inclusions within lava:.....	219
6.4.3.2 Isolated lava lobes: .....	220
6.4.3.3 Isolated sedimentary units with localised peperite.....	220
6.4.3.4 Stacked lava lobes with sediment .....	221
6.4.3.5 Peperite .....	222
6.5 Discussion.....	225
6.5.1 Sediment Properties .....	225
6.5.2 Depositional Environment.....	226
6.6 Conclusions.....	229
<b>Chapter 7: Discussion and Application to Petroleum Systems .....</b>	<b>230</b>
7.1 Introduction.....	230
7.2 Field Synthesis: Fundamental Concepts .....	231
7.2.1 Lava-water-sediment Continuum .....	232
7.3 Industry Application of Field Analogues .....	240

---

7.3.1 Borehole Imaging .....	240
7.3.2 Combining borehole images with field analogues .....	241
7.3.3 Basin-scale implications of lava-water-sediment interaction.....	249
7.4 Further work .....	252
<b>Chapter 8: Conclusions .....</b>	<b>253</b>
<b>References .....</b>	<b>254</b>
<b>Appendix 1 .....</b>	<b>267</b>

# List of Figures

Figure 1-1: Map indicating the areas of current hydrocarbon exploration around the globe.....	22
Figure 1-2: Map of the Faroe Shetland Basin, indicating the structure, extent of the flood basalts (red dot-dash), and volcanic centres. ....	24
Figure 2-1: Basalt lava flow type morphologies. ....	30
Figure 2-2: Schematic model illustrating the development and growth of a pāhoehoe basalt lava sheet flow through inflation, both through lateral ( $V_x$ ) and vertical ( $V_y$ ) expansion.....	31
Figure 2-3: The main classification schemes for volcanoclastic rocks as proposed by Fisher (1961), 1966); Cas and Wright (1987); McPhie et al. (1993); White and Houghton 2006. ....	34
Figure 2-4: Examples of the typical volcanoclastic deposits. ....	37
Figure 2-5: Typical characteristics and morphology of pillow lava. ....	39
Figure 2-6: Summary of the characteristics of peperite from Skilling et al. (2002). ....	42
Figure 2-7: Field photograph, sketch and wireline data of the typical internal structure of a pahoehoe lava flow. ....	44
Figure 2-8: Schematic diagram representing the typical wireline log responses of lithofacies found within lava-dominated sequences. ....	44
Figure 2-9: A typical FMI image of basalt lava. ....	46
Figure 2-10: Classification of lava facies with FMI interpretation. ....	47
Figure 3-1: A) Locality map of Kinghorn, Scotland, which lies within the Midland Valley of Scotland (MVS). B) A geological map of the MVS, showing the three main basins present during the Dinantian Epoch, Carboniferous (dashed transparent circles). ....	50
Figure 3-2: Location map of Kinghorn with the main field localities, and corresponding stratigraphic log through the ~485 m thick succession. ....	52
Figure 3-3: Typical columnar jointed lava (L8) exposed above Locality 4 at Kinghorn, Fife. The lava is ~ 10 m thick and columns range in width from 0.5 -1.5 m. ....	53
Figure 3-4: Inter-lava red-weathered units are observed at several locations at Kinghorn. ....	54
Figure 3-5: Photomicrographs of the red-weathered unit, R2, (paleosol) between two lavas (L14 and L15) at Locality 8.....	55
Figure 3-6: Photomicrographs of basaltic lava from the hyaloclastite (H1) sub-aerial lava (L11) boundary, Locality 6.....	55
Figure 3-7: Hyaloclastite at Kinghorn.....	56
Figure 3-8: Lapilli tuff at the top of the Kinghorn succession, Locality 9. ....	57
Figure 3-9: Photomicrographs of lapilli tuff from Locality 9, Kinghorn.....	58
Figure 3-10: Green-weathered fine volcanoclastic sandstone (S3) at, Kinghorn. ....	59
Figure 3-11: Fine-grained volcanoclastic sandstone (S7) underlying the lapilli tuff at Locality 9. ....	60
Figure 3-12: Upper contact of the volcanoclastic unit (V1) at Locality 2.....	61
Figure 3-13: (Next page) Graphic log of the volcanoclastic unit, V1, at Locality 2. ....	61
Figure 3-14: Detailed graphical sketch logs through the volcanoclastic unit (V1) at Locality 2. ....	63
Figure 3-15: Features of the volcanoclastic unit, V1, at Locality 2, Kinghorn.....	65
Figure 3-16: (Previous page) Photomicrographs of the volcanoclastic unit, V1, at Locality 2. ....	67
Figure 3-17: The lower limestone unit in the Kinghorn succession. ....	68
Figure 3-18: Characteristics of the two main carbonate units within the Kinghorn succession. ....	69
Figure 3-19: The lava-sedimentary contact at Locality 1, Kinghorn.....	70
Figure 3-20: Features of the lava (L2) and interaction with underlying siltstone and claystone, at Locality 1.....	71
Figure 3-21: Peperite at the base of lava (L8) at Locality 4.....	72
Figure 3-22: Typical outcrop view of Locality 7 at Kinghorn.....	72
Figure 3-23: Loading features observed at Locality 7, Kinghorn.....	73
Figure 3-24: Schematic illustration of soft-sediment deformation and loading of sedimentary units by lava. ....	79
Figure 3-25: “Passive” interaction and the formation of peperitic margins ( $\pm$ pillows/hyaloclastite), typically at the base and frontal margins of the lava.....	80
Figure 3-26: “Dynamic” interaction and the formation of invasive disaggregated peperite. ....	81
Figure 3-27: A simplistic, schematic model highlighting the three main lava-sediment interaction types at Kinghorn, and the likely sediment saturation levels that facilitate interaction. ....	83
Figure 4-1: A) Location map and B) simplified geological map of the field area close to the C.J. Strike Dam of the Snake River, near Mountain Home, Idaho, USA. ....	88

Figure 4-2: A shaded relief map of the field area along the Snake River, indicating the log locations. ....	89
Figure 4-3: Schematic overview and sketch log through the lava-sedimentary stratigraphy at C. J. Strike Dam, Idaho. ....	90
Figure 4-4: Basalt (tholeiitic) lava in Mountain Home, ID. ....	91
Figure 4-5: An overview of the area where LSP1 and L1 are visible. ....	92
Figure 4-6: Logs of LSP1. ....	93
Figure 4-7: The lower units of S1 at Log localities 5 and 3. ....	94
Figure 4-8: The upper part of S1 comprises a significant volcanoclastic component, including beds of massive lapilli tuff with accretionary lapilli (acclap). ....	95
Figure 4-9: Upper' sedimentary units of LSP1, including logs 1 and 2 of S1 sedimentary package. ....	96
Figure 4-10: A) a panorama of the outcrop in the south of the field area, close to the reservoir and road cut of the Strike Dam (looking East). ....	98
Figure 4-11: Correlation panel of sedimentary logs through S2 in LSP2. ....	99
Figure 4-12: Log 14 at the reservoir displays the upper units of S2 directly underlying L2. ....	101
Figure 4-13: Petrography of LSP2. ....	102
Figure 4-14: An overview of the stratigraphy exposed within the north of the field area. ....	103
Figure 4-15: An overview of LSP3. ....	105
Figure 4-16: Pillow-dominated and hyaloclastite-dominated foresets within the HPb of LSP3. ....	106
Figure 4-17: Typical small scale features of the HPb. ....	107
Figure 4-18: A correlation panel of the sedimentary logs of S3. ....	108
Figure 4-19: Petrography of S3. All images PPL. ....	110
Figure 4-20: Field view of the VSst unit of LSP3. ....	111
Figure 4-21: Petrography of the VSst of LSP3. ....	112
Figure 4-22: Field view of S3 and log 25, where the VSst is not recorded. ....	113
Figure 4-23: Field view of S3, showing the VSst marker bed and Log 23. Person for scale. ....	113
Figure 4-24: Discontinuous, oragned-stained beds within the sedimentary units overlying the VSst and underlying the HPb. ....	114
Figure 4-25: Logs depicting the sedimentary units observed at the road cut along CJ Strike Dam Reservoir, Mountain Home. ....	115
Figure 4-26: Annotated field photographs of the LSP3 lava-sediment interface. ....	116
Figure 4-27: The relationship between S3, the VSst and the HPb at Locality 24. ....	117
Figure 4-28: Petrography of the HPb-sediment contact at LSP3. ....	118
Figure 4-29: A flame structure of S3 sediment, including the VSst (dashed line). ....	120
Figure 4-30: Interaction at the HPb and S3 interface at locality 19-21. ....	120
Figure 4-31: The complex contact relationship between S3 and the HPb. ....	122
Figure 4-32: Field view (A) and interpretative field sketch (B) depicting a large, isolated, coherent sediment block within the HPb. ....	123
Figure 4-33: Field photographs of L4 and LSP4. ....	124
Figure 4-34: Comparison of pillow lava size and penetration depth into the underlying sediment. ....	133
Figure 4-35: Sketch showing bulldozing lava and sediment mingling within the HPb. ....	135
Figure 4-36: A series of schematic sketches depicting how invasive lava deforms and mingles with sediment. ....	137
Figure 4-37: Schematic model showing the emplacement of the Mountain Home lavas of LSP3 into a large lake, and the relationships between lava, water and sediment. ....	140
Figure 5-1: Map of the Island of Gran Canaria, Canary Islands, Spain. ....	143
Figure 5-2: View of field locality across the Barranco de Tamaraciete, Gran Canaria, illustrating the stratigraphy of the Las Palmas Detritic Formation (LPDF). ....	145
Figure 5-3: Overview of the ~600 m long roadside exposure in Barranco de Tamaraciete, Las Palmas, Gran Canaria. ....	147
Figure 5-4: Correlation panel of the sedimentary logs across the field section. ....	149
Figure 5-5: Annotated field photographs and corresponding logs for the lava-sedimentary interface at a number of localities along the section. ....	151
Figure 5-6: Log 1 through the lava-sedimentary succession, where the cobble/boulder conglomerate is relatively thick. ....	152
Figure 5-7: The contact between the basal conglomerate unit, the volcanoclastic sandstone package, and the overlying HPb. ....	153
Figure 5-8: Petrography of the volcanoclastic sandstone directly overlying the basal conglomerate (Sample GC.001), Log 2 (Figure 5-4). ....	154

Figure 5-9: Characteristic features and structures within the volcanoclastic units of the main sedimentary section. ....	155
Figure 5-10: Volcanoclastic siltstone (Sample GC.002) Log 2, (Figure 5-4), and fine grained claystone (Sample GC.011), underlying the lava in Log 4 (Figure 5-4).....	156
Figure 5-11: Distinctive orange beds (O <sub>1-3</sub> ) are observed close to the top of the sedimentary unit at the top of Log 5 (Figure 5-4). ....	158
Figure 5-12: Characteristic features at the lava-sedimentary contact.....	158
Figure 5-13: Petrography of orange-stained beds (Sample GC.006) collected from the top of Log 7 (Figure 5-3 and Figure 5-4). ....	159
Figure 5-14: Interbedded claystone and siltstone with pumice-rich layers (Sample GC.007), top of Log 7 (Figure 5-4). ....	159
Figure 5-15: The HPb at the northern part of the section (Locality F). ....	161
Figure 5-16: Sketch log through the HPb, depicting the facies changes, and diffuse stratification within the hyaloclastite-dominated and pillow-dominated foresets.....	162
Figure 5-17: Schematic illustration (A) and field view (B) of the different pillow measurements obtained along the section.....	163
Figure 5-18: Field view of locality A (Figure 5-3). ....	167
Figure 5-19: Field view of lava tubes at Locality C. ....	168
Figure 5-20: Photomicrographs of the shark's tooth lava at Locality C (Figure 5-3). ....	168
Figure 5-21: Field view at Locality E, where a coherent lava sheet is present between the sedimentary unit (pink solid line) and the overlying HPb (yellow dashed line). ....	169
Figure 5-22: Annotated field view depicting the flame structure produced as sediment (sed.) is fluidised and squeezed between two overlying pillow lavas. ....	171
Figure 5-23: The largest pillow in the section, possibly a feeder pillow, at locality D.....	172
Figure 5-24: Lava-sediment mingling at Log locality 9 (Figure 5-3) occurs between the pillows, HPb and the sediment.....	173
Figure 5-25: Photomicrographs of basalt juvenile lava clasts within a volcanoclastic matrix at the lava-sediment boundary (XPL).....	173
Figure 5-26: Field view (A) and sketch (B, slightly oblique to photograph) showing the features of a heavily fluidised zone, at Locality D. ....	175
Figure 5-27: The lava-sedimentary contact between localities E and F, near log 6, (Figure 5-3).....	176
Figure 5-28 (previous page): Scatter plots illustrating the relationship between pillow size and the depth to which the pillows penetrate into the sediment. ....	183
Figure 5-29: A comparison of pillow measurement data between Mountain Home and Gran Canaria field sites. ....	184
Figure 5-30: Schematic diagram of an invasive pillow lava (P) and the variety of sedimentary products that may form as a consequence of lava-water-sediment interaction. ....	186
Figure 6-1: A) Location map of St. Cyrus, and the Midland Valley of Scotland (MVS) (adapted from Macdonald and Fettes 2007). B) Regional geological map of the Strathmore Basin, north east MVS (adapted from Haughton 1989; Browne et al. 2002; Hole et al. 2013).....	190
Figure 6-2: Lithostratigraphy of the Midland Valley of Scotland (MVS) during Old Red Sandstone deposition of the Silurian and Devonian (Browne et al. 2002; Hole et al. 2013). ....	190
Figure 6-3: Map of the St. Cyrus succession, detailing the locations of the panorama photographs (P1-6). ....	192
Figure 6-4: Panoramas, P1, P2, and P3 (see Figure 6-3), of the western part of the field area at St. Cyrus Beach. ....	193
Figure 6-5: Panoramas of the northern part of the field area at St. Cyrus (P4-7). ....	195
Figure 6-6: Features of the lava at St. Cyrus. ....	196
Figure 6-7: Representative sedimentary logs at St. Cyrus (locations on Figure 6-3). ....	198
Figure 6-8: Conglomerates at St. Cyrus.....	199
Figure 6-9: Cliff section, Locality 2 (P1, Figure 6-4) and location of Log 3 (Figure 6-7). ....	200
Figure 6-10: Sketch of the lava-sedimentary contact at the top of Log 3, Locality2 (Figure 6-3). ....	201
Figure 6-11: The lava-sedimentary relationship at Locality 1 (Figure 6-4). ....	202
Figure 6-12: Photomicrographs of typical sandstone and siltstone units observed at St. Cyrus. ....	203
Figure 6-13: The base of the sedimentary section at Locality 13.....	203
Figure 6-14: Sediment inclusions (S) within the lava (L) at St. Cyrus. ....	205
Figure 6-15: Field view and sketch log at Locality 10. ....	206
Figure 6-16: Lava-sediment interaction at Locality 1 (P1 Figure 6-4).....	207
Figure 6-17: Isolated sedimentary units (see Panorama 4) near Locality 9. ....	208

Figure 6-18: Annotated field view and sketch of the lava-sedimentary contact at Locality 3.....	208
Figure 6-19: Lava-sedimentary relationships at Locality 7 (Figure 6-3). .....	209
Figure 6-20: Stacked lava lobes at Localities 10 and 11.....	210
Figure 6-21: Photomicrographs of the lava-sediment interface between stacked lava lobes and intercalated sediment layers.....	211
Figure 6-22: Variations in peperite textures at St. Cyrus.....	213
Figure 6-23: Sediment inclusions within peperite domains are a common feature at St. Cyrus. ....	214
Figure 6-24: Close-packed peperite at locality 6 (P1 and P2, Figure 6-4). .....	215
Figure 6-25: Pillow-like peperite at Locality 4, (P1 and P2, Figure 6-4).....	216
Figure 6-26: Rootless peperite observed at Locality 5. ....	217
Figure 6-27: Schematic diagram showing various features and morphologies of lava-water-sediment interaction, as observed at St. Cyrus. ....	221
Figure 6-28: A simplified, schematic diagram of the characteristic features of lava-water-sediment interaction within a small sedimentary column. ....	223
Figure 6-29: A schematic model of the interpretation of pillow-like peperite and sediment inclusions...	224
Figure 6-30: (next page) A schematic model illustrating the development of a lava-flow field within a braided river drainage system, and the associated lava-water-sediment interactions that occur. .	227
Figure 7-1: Diagrammatical representation of the main types of lava-water-sediment interaction documented within this research.....	234
Figure 7-2: Conceptual flow diagram illustrating the processes and products of lava-water-sediment interaction. ....	235
Figure 7-3: Large scale FMI and wireline logs of lava and interlava lithofacies. ....	242
Figure 7-4: Flattened FMI images, wireline data and interpretation of a pahoehoe lava with irregular lava- sediment contacts.....	243
Figure 7-5: FMI images, wireline data, and interpretation of peperite at the base of a lava. ....	244
Figure 7-6: FMI images wireline data and, interpretation of sediment inclusion within the base of a lava. .....	245
Figure 7-7: FMI images, wireline logs and interpretation of graded hyaloclastite packages observed within the Cambo Field data. ....	246
Figure 7-8: (next page): A 3D model through an interbedded lava-sedimentary succession, with a sketch log, FMI responses and field examples through a hypothetical well site. ....	247
Figure 7-9: (next page) Hypothetical well log interpretation and correlation of a lava-dominated sequence (~175 m thick) at basin scale (km). ....	250

---

## List of Tables

<b>Table 1: A summary of the existing grain size classification schemes for sedimentary and volcanoclastic particles. ....</b>	<b>33</b>
<b>Table 2: Lithostratigraphy of the Midland Valley of Scotland during the Carboniferous (adapted from Underhill et al. 2008). ....</b>	<b>51</b>
<b>Table 3: Summary of the key features of passive and dynamic peperite. ....</b>	<b>81</b>
<b>Table 4: Characteristics and depositional environments of the members of the LPDF as presented by Perez-Torrado et al. (2014). ....</b>	<b>145</b>
<b>Table 5: Pillow measurements, including width, height, penetration depth of the pillow into the underlying sediment and sediment thickness. ....</b>	<b>166</b>
<b>Table 6: A summary table of the mixed lava-sediment domains identified at St. Cyrus and the interpreted sediment properties that facilitate the interaction. ....</b>	<b>225</b>
<b>Table 7: A summary of the main features of lava-water-sediment interaction observed at each field locality (chapters 3-6). ....</b>	<b>232</b>

---

## Acknowledgments

This research has been sponsored by ENI, through the Volcanic Margins Research Consortium (VMRC) based at the Universities of Durham, Glasgow, and Aberdeen.

I must first thank my supervisors Dr. David Brown and Dr. Brian Bell, for giving me such a wonderful opportunity filled with experiences of a lifetime. You chucked me in at the deep end with a fieldtrip to Mull - a truly wet Scottish welcome, and that was just the beginning. Thank you for your help and guidance throughout this research, from the many fieldtrips to the writing, edits and advice. Brian, your knowledge, experience and realism have been invaluable. Davie, I think it is now fair to say that my character is built. Thanks for enduring my last-minute-itous, for reassurance that my “fantasmagrams” are worth the time and effort, and for all the amazing travelling and volcano hunting!! Your enthusiasm for volcanology and fieldwork has been inspiring, and your support, and banter, excellent; thank you.

VMRC members, both past and present, including academics and sponsors alike, have eagerly listened, questioned and helped me through this complex research. I would like to thank all those that have helped me grow through this process including: Dave Ellis, Giles Pickering, Nick Crabtree, Simon Passey, Nick Schofield, and Rich Brown. Thanks to all the fellow students, colleagues and now friends who provided help, great advice and were in this together: Sam (“PhD and thin-section guru”), Kirstie Wright (PhD big sister- from fellow students to close friends that lunch with large glasses of wine), Pete, Bansri, Joanne, Clayton, and Tim, thank you.

Through the members of VMRC I have been lucky enough to complete 2 internships at 2 companies. To Nick Crabtree at Premier Oil, thank you so much for the brief but invaluable work placement, introducing me to 3D seismic, and for your boundless energy and encouragement. Huge thanks to Giles Pickering at OMV and the exploration and production teams, for organising my 3 month internship; I truly felt part of the team. The projects have inspired my thesis further and provided me with some true ‘light-bulb’ moments.

To my fellow postgrad colleagues and friends at Glasgow, we’ve certainly had a rollercoaster journey, but being in it together has made it so much more fun. Thanks to all of you for endless advice, hugs, tears, laughter, joy, coffee, cake, and wine, along the way: Jill, Penne, Rebecca, Eric, Heidi, Mark, Callum, Crystal, Caroline, Hazel and

---

Daisy (plus Dylan and Milo). Jill, we started together and ended together - what a pair we are. Thank goodness I had you for moral support throughout this journey!

Charlotte, the best field assistant anyone could ask for, without you the last 2 years would have been so much harder. Here's to Iceland, Mountain Home, Gran Canaria and Indonesia!! Thanks a million for making the fun times more exceptional, and the not so fun times bearable. Your work ethic and intelligence have spurred me on further and for this I am truly grateful.

Thanks also to Jonny and Sapphire (the newbies of Vo@G), and to my surrogate-pseudo-supervisor Rhian Meara, for all those cake emergencies and practical PhD advice. I'd also like to thank: John Gilleece and Robert Macdonald for being the friendly and helpful faces around the department, and Nick Kamenos for plenty of laughter and life advice (and that you're kinda from Blackburn too!).

This has been a long journey on which many people, friends of old and new, have helped. Thanks to Lydia and Jonny, Emma, Michael, Vicky, Shona, Ash and Mike. Though your support may have been given unknowingly it is much appreciated. I owe Lydia and Jonny an extra huge thank you for putting up with me and putting me up for 3 months! Thanks for your help, wind-ups, and continuing friendship - you really are true friends. I'd also like to thank Kirstie and Di at Wanamoka for all your support and understanding, which has been incredible! Thanks for giving me the opportunity to bake cakes, fuel my coffee addiction, and briefly escape this thesis.

Special thanks go to the members of Glasgow Lions Touch Rugby Club, of whom there are too many of you to name individually! The Lions provided me with a much needed Glasgow family, which got me through the rubbish points, gave me some escapism, a fitness plan, many close friends, and Ryan. Your friendship, wisdom, and silliness, made me truly feel at home and settled in Glasgow, and will never be forgotten.

Ryan, to whom I will be eternally thankful, you somehow found the most incredible amount of patience to stick with me and support me through the last year(s) of my PhD, especially the last bit, and I know I couldn't have done this without you. You, and your family, have been the endless encouragement, and distraction, that was needed so many times. If I thanked you a million times over it wouldn't be enough, but here's a small list of gratitude for your awesomeness: thank you for all the fun times (may they long continue), all the cups of tea and coffee, being the motivator, believing in me, tolerating my 'mess', accepting all the travelling, taking me on hillwalking and camping

adventures, looking after me, being my rock, providing wine/gin/chocolate, and being there with a cuddle and reassurance at the end of every day. You're the Best.

Finally, the unwavering support, love, and pride from my family, deserves enormous thanks; Mum, Dad, Granny, Grandad, Grandma, and Philip, thank you. Your continual encouragement, emotionally, financially, and unconditionally, throughout my studies has instrumental to my success. Thank you for enabling me to do "what makes me happy". I hope I've made you proud.

---

## Author's Declaration

I declare that this thesis, except where acknowledged to others, represents my own work carried out in the School of Geographical and Earth Sciences, University of Glasgow. The research presented here has not been submitted for any other degree at the University of Glasgow, nor at any other institution. Any published or unpublished work by authors has been given full acknowledgement in the text.

A handwritten signature in black ink, appearing to read 'H Rawcliffe', with a stylized flourish at the end.

Heather J. Rawcliffe

---

# Abbreviations

CPIP - Carboniferous-Permian Igneous Province

FMI - Formation Micro Imager

FSB - Faroe Shetland Basin

HBF - Highland Boundary Fault

HL - Hurler Limestone

KVF - Kinghorn Volcanic Formation

LPDF - Las Palmas Detritic Formation

LSP - Lava-Sediment Package

MVF - Montrose Volcanic Formation

MVS - Midland Valley of Scotland

NAIP - North Atlantic Igneous Province

ORS - Old Red Sandstone

SCF - Sandy Craig Formation

SMWL - St. Monans White Limestone

SRP - Snake River Plain

SUF - Southern Upland Fault

VMRC - Volcanic Margins Research Consortium

---

**Lithofacies:**

acc - accretionary lapilli

dsLT - diffusely stratified lapilli tuff

dsT - diffusely stratified tuff

//dstT - planar laminated diffusely stratified tuff

//sT - planar laminated stratified tuff

dsxLTp - pumice rich diffusely cross-stratified lapilli tuff

dxsLT - diffusely cross-stratified lapilli tuff

HPb- Hyaloclastite Pillow breccia

LT - Lapilli Tuff

mLT - massive lapilli tuff

mT - massive tuff

VSst - Volcaniclastic Sandstone

xsLT - cross stratified lapilli tuff

# Chapter 1: Introduction

The way in which lava interacts with water and sediment is complex. Several lithologies, including pillow lavas, hyaloclastite and peperite, are produced as a result of such interaction (e.g. Silvestri 1963; Kokelaar 1982; White et al. 2000; Skilling et al. 2002); however, the processes and products of these interactions are not yet fully understood. This investigation has used detailed field and petrographical analysis from several case studies, from a variety of environmental and tectonic settings, to characterise the highly variable fragmental geometries and textures of the lithologies that are created at the lava-water-sediment interface, and to understand the processes that occur.

This research is part of a wider group of projects, the Volcanic Margins Research Consortium (VMRC), an industry-funded initiative designed to answer broad questions concerning volcanic margin geology and the influence of volcanic rocks within hydrocarbon systems. Together, the projects aim to improve our understanding of the influence of volcanic rocks on hydrocarbon exploration and development, enabling and advancing the exploitation of frontier basins. This research focuses on the lava-clastic sediment interface, the processes and products that occur, and what affects these might have on the petroleum system, or may need to be considered during exploration and development.

## 1.1 Research Rationale

Lava-water-sediment interactions are well documented within literature, including the formation and occurrence of peperite, with identification at the margins of intrusions and sub-aerial lava. There is however, an emphasis on juvenile clast morphology description and interpretation, and the controls of magma/lava on peperite formation. The geometries of peperite domains are rarely discussed, and whilst host sediment grain size is considered, depth of discussion and argument for the influencing factors of sediment on interaction processes is minimal. This research has identified a variety of peperite domains and associated features, and recognised a continuum of lava-water-sediment interactions based on variable host sediment properties rather than the controlling properties of the lava. The geometries of mixed-lava-sedimentary domains are also discussed, with reference to basin-scale systems.

With rapidly diminishing hydrocarbon reserves, the petroleum industry is turning towards more 'unconventional' reservoir systems and basins to find further resources and meet the energy demands of the 21st century. This project focuses on systems that

have a significant volcanic component, which poses both interesting and complex problems and questions for the petroleum industry. Volcanic rocks have the potential to act as reservoirs, seals, traps, barriers or baffles, and cause compartmentalisation of the petroleum system. There are several basins worldwide that hold abundant hydrocarbon resources, and which include volcanic and volcanoclastic rocks, many of which are linked with LIP's (Figure 1-1). Examples of these basins include: Western Australia (Hawlder 1990), Brazil (dos Anjos et al. 2000), China (Wu et al. 2006; ZOU et al. 2008; Zou 2013), Indonesia (Willumsen and Schiller 1994), Japan (Shimazu 1985; Sakata et al. 1989; Levin 1995; Mitsuata et al. 1999), Pakistan (Berger et al. 2009) and the North Atlantic Margin (Knott et al. 1993; Doré et al. 1999; Lamers and Carmichael 1999; Larsen et al. 2010).

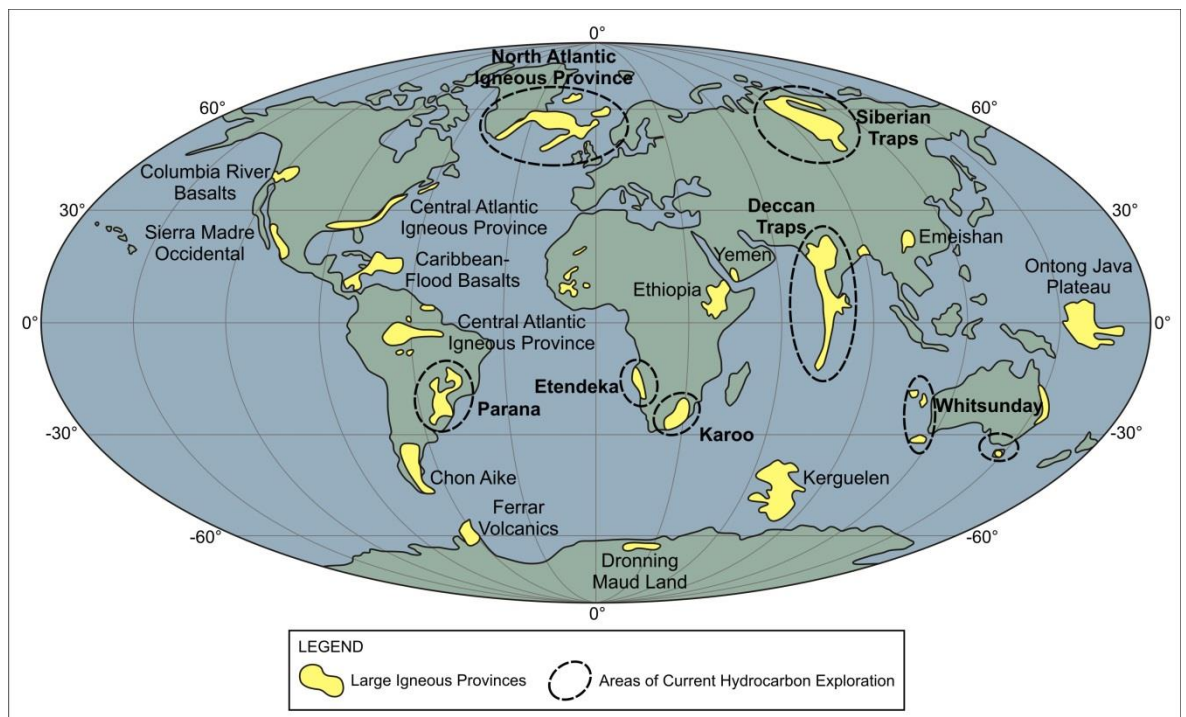


**Figure 1-1: Map indicating the areas of current hydrocarbon exploration around the globe. Many of the areas are linked with large igneous provinces such as the North Atlantic Igneous Province, the Siberian Traps, Deccan Traps and the Parana Basin. Figure adapted from Wright (2013).**

The Faroe-Shetland Basin (FSB), west of the Shetlands Isles, North Atlantic (Figure 1-2), is a good example of a frontier basin that is both volcanic-dominated and hydrocarbon-rich. This area has become a focus for exploration as companies move away from the North Sea area towards the West and North Atlantic Margins. The FSB contains a number of prospects that are undergoing extensive research and exploration by multinational petroleum companies. The Rosebank Field (Figure 1-2), North Atlantic, discovered in 2004 by Chevron, OMV, Statoil, and DONG (Duncan et al. 2009; Helland-Hansen 2009; Schofield and Jolley 2013), is a good example, and has been the focus of

much of this research thus far. The Rosebank Field, and much of the FSB, holds large amounts of oil and gas, found within a thick sequence of Palaeogene strata dominated by basaltic lavas. The lavas are interbedded with siliciclastic and volcanoclastic units, with both the latter and the lavas, acting as cap rocks to siliciclastic reservoirs. Whilst this discovery is perceived as a successful example of a volcanic dominated petroleum system, the field is yet to commence production. Other adjacent prospects, such as Cambo (Figure 1-2), however, are still facing difficulties with development and in particular understanding the complexity of the volcanic and volcanoclastic system. The Brugdan Well (6104/21-1) is an example of a failed well, which did not reach the target reservoir sandstone of the Vaila Formation. Instead larger thicknesses of Paleocene basalt lavas, more than was previously estimated, were identified, with no significant hydrocarbons found. Despite these difficulties interest and exploration in the area continues.

Whereas traditional siliciclastic petroleum systems are relatively well understood, it is apparent that there is a lack of knowledge, and many unanswered questions, concerning volcanic-sedimentary systems and their hydrocarbon potential. This is true both in academia, where volcano-sedimentary facies models are relatively poorly developed, and particularly within the petroleum industry where the study of such interactions has not been a priority. The architecture, geometries and scale of the competing volcano-sedimentary systems are poorly understood, primarily due to the complexities created by the volcanic input. Two significant complications of a volcanic input into a sedimentary basin are the interaction of volcanic material with siliciclastic sediment and its potential for reservoir heterogeneity (e.g. Mathisen and McPherson 1991; Schutter 2003; Rohrman 2007; Holford et al. 2012) and, the potential destruction and/or compartmentalisation of the reservoir (Schutter 2003; Rohrman 2007; Cukur et al. 2010; Schofield et al. 2012). Understanding these problems in potential hydrocarbon systems is problematic, especially in volcanic-dominated sequences, as offshore data (e.g. seismic, wireline data, core) are limited and difficult to obtain. Furthermore, seismic data in volcanic-dominated basins are difficult to interpret, and complexities created by volcanic input into the system may be beyond seismic resolution (Maresh et al. 2006; Nelson et al. 2009; Schofield et al. 2010). Therefore, the study of suitable onshore examples is essential to our understanding of such systems and the future development of offshore prospects.

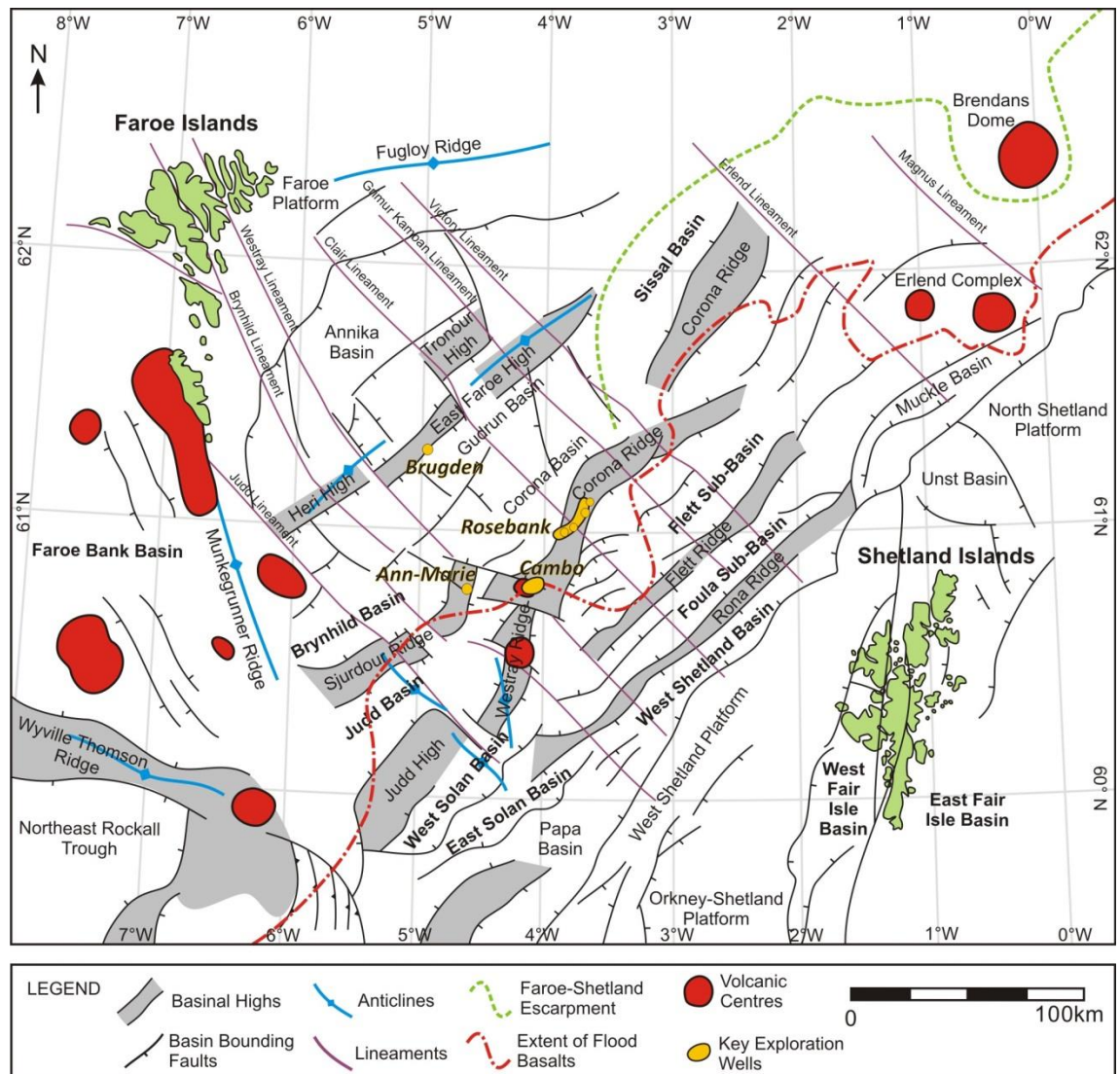


**Figure 1-2: Map of the Faroe Shetland Basin, indicating the structure, extent of the flood basalts (red dot-dash), and volcanic centres. From Wright (2013), modified from Stoker et al. (1993), Ritchie and Hitchen (1996); Ritchie et al. (1999), Sørensen (2003); Ellis et al. (2009); Moy and Imber (2009)**

## 1.2 Research Aims and Objectives

In order to gain a comprehensive understanding of the nature and scale of lava-water-sediment interaction the following research objectives have been set:

- To understand the architecture, geometries and scale of volcanic-sedimentary systems and their interaction through detailed mapping and logging of suitable onshore field analogues;

b) To document and characterise the range of geometries and textures that are created at the lava-sediment interface during lava-water-sediment interaction, both on a macro- and micro-scale;

c) To create detailed facies models and interpretative models from combined field observations and petrographic analysis, and develop conceptual models of lava-water-sediment products and processes;

d) To compare these datasets (e.g. lithological logs, facies models, conceptual models) with limited offshore datasets, especially wireline logs. Together, these can be used by the hydrocarbon industry to better inform its understanding and decision making during the exploration and production stages. These results will provide further information to allow the industry to recognise and interpret volcanic-sedimentary lithofacies and processes in their data sets, and better target viable hydrocarbon resources in such systems.

It is important to note that ‘seismic-scale’ comparisons are beyond the scope of this thesis, which typically focuses on macro and micro-scale observations of the lava-sediment interface. For examples of basin-wide studies with a seismic focus, see Wright et al. (2012); Grove (2013); Schofield and Jolley (2013); Watton et al. 2013.

### **1.3 Methods**

This research is primarily field-based which involved detailed mapping and logging of siliciclastic, volcanoclastic and volcanic units within four individual field areas. The study has concentrated on basaltic lavas and how they interact with bodies of clastic sediment and water. More evolved lavas may undergo different interactions with sediment; however, studies of these rocks are beyond the scope of this thesis, and less relevant to the basins currently targeted by industry in the North Atlantic. The main focus of the field studies has been the geometries and scale of the units, as well as the interaction between the various lithologies, in particular, at the interface between volcanic and sedimentary components. Macroscopic study of lava-sediment interfaces using detailed logging and quantitative analysis has been undertaken, in order to record how the materials physically interact and the products formed. Petrography is used in conjunction with the field data, to provide a link between the macroscopic and microscopic scales. Offshore borehole data is used as a comparison to the onshore analogues, which provides context to a wider industry audience.

### 1.3.1 Fieldwork:

The four field areas were chosen for the following reasons:

- ubiquitous subaerial lavas and volcanoclastic deposits;
- the volcanic rocks are interbedded with sedimentary, predominantly clastic and volcanoclastic units, broadly similar to those sequences within hydrocarbon plays, such as the Faroe-Shetland Basin, North Atlantic Igneous Province (NAIP);
- a wide range of lava-water-sediment interactions are observed;
- the areas include several depositional (e.g. fluvial, lacustrine, shallow marine) and tectonic (typically rift-related, but including continental rifts and back-arc spreading) settings;

The fieldwork involved detailed data collection, which involved: detailed field observations, and the preparation of small-scale maps and graphic logs with correlation panels. Rock samples were also collected for petrographical analysis and represent a comprehensive range of lava-water-sediment types and interfaces (and interactions), adjacent and distant from the lava-sediment contacts. These are key to determining the lithofacies and the micro-scale interaction relationships. The individual investigations/chapters detail any data collection specific to that area.

### 1.3.2 Samples and Petrography:

Thin sections were produced for petrographical use (John Gilleece, University of Glasgow). Standard size and large format, 30  $\mu\text{m}$  thick, polished and unpolished thin sections were produced from each field site. They represent the main lithofacies and lava-sediment contacts present within each site. Off-cuts from the hand specimens and thin sections were preserved, allowing comparison between hand specimen and thin section. All thin sections were analysed using a polarising microscope, and photomicrographs were collected using an Olympus DP25 camera.

### 1.3.3 Industry:

Work was carried out during a three-month industry internship at OMV UK, London, facilitated by Giles Pickering, Subsurface Team. This involved the organisation and interpretation of borehole well data from the Cambo Field, FSB, including both wireline logs and FMI image data, processed using Techlog software. Some of the data has been reproduced and included within the Discussion chapter (Chapter 7), with the permission of OMV UK. The advantage of this work is that it provides an offshore example of the type of data, and resolution, that the field study analogues can be applied to.

## 1.4 Thesis Outline

Chapters 2-7 are briefly summarised below. The individual field case studies (chapters 3-6), are produced to stand-alone; therefore, each chapter contains an introduction, a geological history of the area, descriptions and interpretations, discussion, and conclusions. Each case study (chapter) involves progressively complex systems of lava-water-sediment interaction.

*Chapter 2:* an introduction to volcanoclastic rocks and the principle processes and products of lava, water, and sediment interactions. In addition, the methodologies of interpreting wireline logging tools and borehole images are described, with respect to volcanoclastic rocks and lava-sediment interfaces/interactions, and their relevance to petroleum systems.

*Chapter 3:* a field study of the coastal geology between Burntisland and Kinghorn, Fife, Scotland, UK. The succession displays numerous interbedded Carboniferous volcanic and clastic lithologies, which are described and interpreted. A basic continuum of the types and styles of lava-water-sediment interaction is established.

*Chapter 4:* a field study of an area south of Mountain Home, Idaho, USA, situated within the Snake River Plain. A succession of Miocene to Pleistocene interbedded volcanic and sedimentary/volcanoclastic rocks are exposed within a canyon along the Snake River and records the emplacement of lava into a large lake. This chapter focuses on sediment properties and the concepts of “barriers” to interaction.

---

*Chapter 5:* a small, focused field study of a single locality on the island of Gran Canaria, Canary Islands, Spain. The locality records the emplacement of Miocene sub-aerial lava into the shallow marine environment during the island-building phase. Detailed descriptions and interpretations of the lava-sediment interface are provided, as well as quantitative measurement data for the penetrations depths of pillow lavas into the (underlying) sediment. This chapter focuses on sediment properties and the scale of lava interaction/penetration.

*Chapter 6:* a comprehensive field study of the Devonian volcanic and sedimentary rocks exposed along the coastal section at St. Cyrus, Angus, Scotland, UK. The stratigraphic sequence comprises fluvial conglomerates and sandstones, lacustrine siltstones and volcanoclastic sandstones, and is dominated by basaltic lava that has thoroughly interacted with the sedimentary units. The lava-sediment contacts are described and interpreted in detail, with focus on sediment properties and the thorough disruption of sedimentary bodies.

*Chapter 7:* a comprehensive discussion of the main findings from the field studies, highlighting the observed similarities and differences of the various examples of lava-water-sediment interaction. A conceptual flow diagram of the processes and products of lava-water-sediment interaction, and the role of sediment properties, is presented. The application to the hydrocarbon industry is addressed and discussed using borehole image log data interpretation, which is combined with facies models from the onshore field analogues.

*Chapter 8:* the key conclusions of the thesis and their significance for the hydrocarbon industry.

## Chapter 2: Geological Background

### 2.1 Introduction

Lithologies and facies linked with lava-water, and lava-sediment interactions are well documented; however, as outlined in the introductory chapter the detailed processes and products of lava-water-sediment interaction are relatively poorly understood. Furthermore, little of this work has been assessed in the context of application to the petroleum industry. This chapter introduces the terminology and basic concepts that are the foundation to this thesis. It is important to note that comprehensive process discussion, in conjunction with new observations and interpretations, is associated with each of the case study chapters, and therefore, this chapter is not exhaustive and serves as a more basic introduction to existing accepted terminology/concepts. Furthermore, discussions of the regional geology are contained in the appropriate chapters.

This chapter introduces the basic lava types and terminology, in particular, lava morphologies, and the process of lava inflation. It highlights the wide range of terminology associated with volcanoclastic rocks/sediments, and the different processes involved, with particular focus on our existing knowledge of the processes and products of lava-water-sediment interaction. Also described, are wireline log and borehole image data collection and interpretation, which are useful methods for determining lava-water-sediment interactions in the sub-surface; an important application to the petroleum industry.

### 2.2 Terminology and basic concepts

#### 2.2.1 Lava types and emplacement

Basalt lavas are typically classified based on their surface and internal morphology into 'a'a or pahoehoe flow types (Macdonald 1953) (Figure 2-1). 'A'a lava has a basal breccia, a massive core, and a characteristic rough, clinker flow-top breccia (Macdonald 1953) formed through auto-brecciation. In comparison, pāhoehoe flows have individual lava tubes with smooth or ropey surfaces (Macdonald 1953; Walker 1971; Rowland and Walker 1990). Morphological differences are related to surface processes and flow dynamics that occur during lava emplacement. Effusion rates determine the lava-flow type that develops. 'A'a flows typically develop from high effusion rates and pāhoehoe forms with lower flow rates (below  $5\text{-}10\text{ m}^3\text{s}^{-1}$ ) and below a certain viscosity threshold (Rowland and Walker 1990).

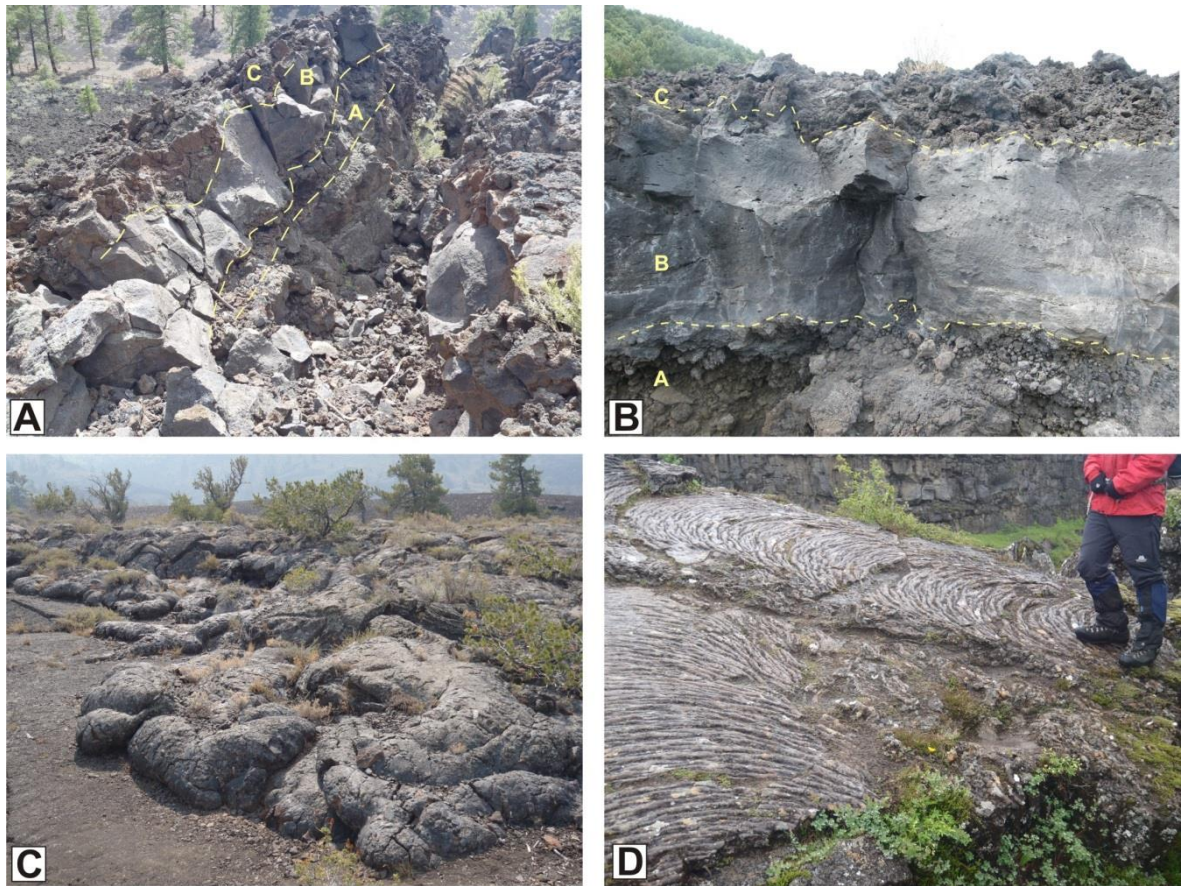


**Figure 2-1: Basalt lava flow type morphologies.**

Classification is based on their morphology, as either 'a'a (A, B), or pahoehoe (C, D). A) 'A'a lava, Flagstaff, Arizona. 'A'a flow typically comprise a basal breccia (A), a coherent massive core (B) and a clinker, autobrecciated top (C). Core is ~ 1m thick. B) Cross-section through a typical 'a'a lava Etna, Sicily, Italy. A, B, C as before. The core (~ 1.5 m thick) has a massive basal portion, and vesiculated upper portion. C) Pahoehoe lava lobes have smooth surfaces, and advance through budding/breakouts and inflation of individual lobes. Lava lobe front is ~30 cm thick; Craters of the Moon, Idaho. D) Ropey textures are indicative of pahoehoe lava, (Thingvellir, Iceland, person for scale). Pahoehoe surfaces often display ropey surfaces, which from due to ductile movement and deformation of the cooled lobe crust.

'A'a lavas flow rapidly in narrow, open-channels, typically 0.1-2.5 km wide. The margins of the flow stagnate and form levees through accretion, which cause the central channelized portion to become more concentrated (Rowland and Walker 1990). The channelized part of the flow has a high flow velocity, up to 60 km/h (Macdonald 1953), but also a significant radiative heat loss, which leads to continual turnover of the flow and development of a rapidly cooling crust (Crisp and Baloga 1994). 'A'a clinker (ragged, slightly cooled clumps of lava) is produced when the cooler flow crust is continuously disrupted by the fast moving flow, with shear stresses exceeding the tensile stress of the cooled crust (Brown et al. 2011). The clinker can be incorporated back into the flow as it is forced to the flow front and then falls to the base of the flow, resembling a caterpillar track motion (Macdonald 1953).

Pāhoehoe lavas advance slowly with multiple small flow lobes, typically  $<1 \text{ m}^2$ , active at any one time (Macdonald 1953; Self et al. 1998; Thordarson and Self 1998). The surface chills quickly forming a crust that allows continual flow within the core and endogenous growth or inflation of the lobe (Figure 2-2). This thermally efficient transport structure enables the lava to flow for great lengths, up to 100s to 1000 km, (Hon et al. 1994; Self et al. 1998; Brown et al. 2011), as heat is retained from source to flow margins. As the lobe inflates, a viscous crust is formed, with a brittle fractured outer crust (Figure 2-2). Solidified sheet lobes typically display a thin ( $<10 \text{ cm}$ ) basal crust, a massive core, and an upper fractured, vesiculated flow top (Figure 2-2). Coalescence of pāhoehoe lobes form typical compound sheet flows, which are characteristic of this lava style and flood basalt provinces (Hon et al. 1994; Self et al. 1998). Hummocky flows may also form, with tumuli, or uplifted ridges, which occur during discontinuous lava emplacement (Self et al. 1998), where effusions rates are stalled during inflation, or because the underlying flow surface is irregular (Self et al. 1998).

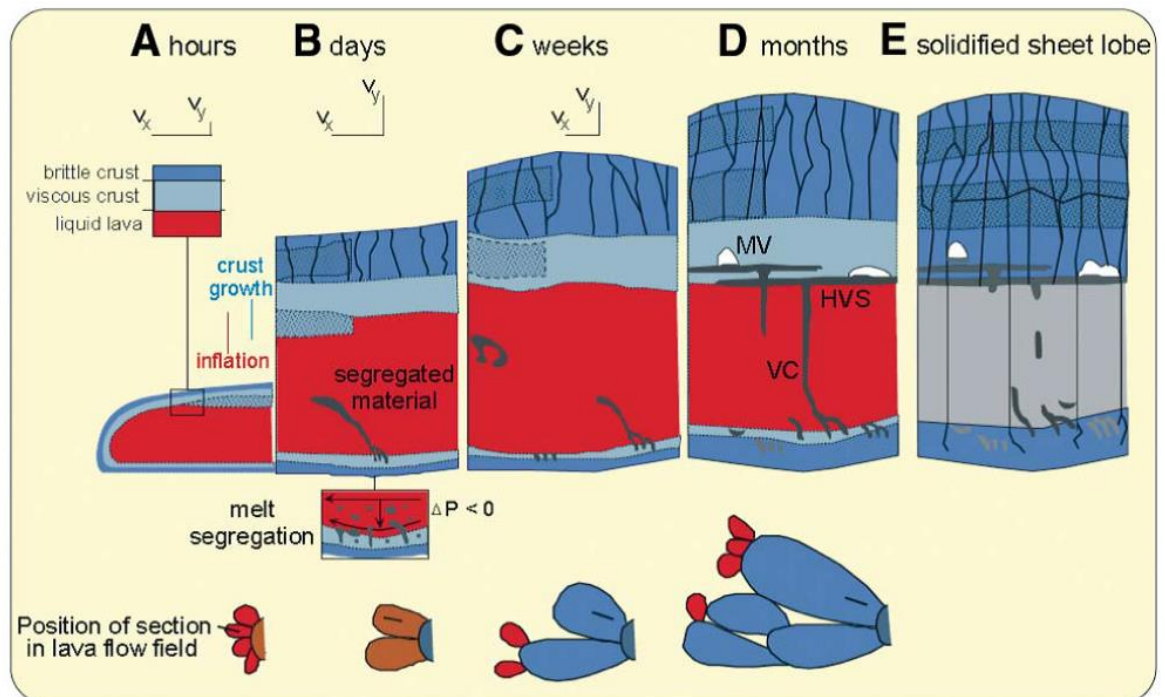


**Figure 2-2: Schematic model illustrating the development and growth of a pāhoehoe basalt lava sheet flow through inflation, both through lateral ( $V_x$ ) and vertical ( $V_y$ ) expansion. The basalt flow field develops as lobes coalesce and thicken. Schematic plan view of growing lava flow field is given beneath each stage. MV—megavesicles; HVS—horizontal vesicular sheets; VC—vesicle cylinders (from Self et al. 2014, after Thordarson and Self 1998).**

## 2.2.2 Volcaniclastic Rocks

### 2.2.2.1 Classification

Volcaniclastic rocks can be very simply defined as clastic rocks that contain a significant amount of volcanic fragments. The classification of volcaniclastic rocks and deposits, however, is complex, with a number of schemes used to characterise them (see: Fisher 1961; Cas and Wright 1987; McPhie et al. 1993; White and Houghton 2006; Manville et al. 2009). Volcaniclastic rocks are differentiated by those that form directly from volcanic eruptions (primary volcaniclastic), and those that form due to the reworking of material from earlier eruptions (i.e. epiclastic/"ordinary" sedimentary rocks) (White and Houghton 2006). Those volcaniclastic rocks that form directly from volcanic eruptions typically use classic pyroclastic terminology (e.g. tuff, lapilli tuff), whereas those that are formed by reworking typically utilised classic sedimentary terminology (Table 1). A summary flow diagram each scheme is provided below (Figure 2-3). Fisher (1961), was the first to describe volcaniclastic rocks according to the primary origin of the grains/fragments and grain size (Figure 2-3). The classification scheme allows the distinction between pyroclastic, autoclastic and rocks, and includes a non-genetic category for rocks that do not fit or are difficult to distinguish. This scheme has now widely been superseded.

Cas and Wright (1987), centred their classification on depositional mode and fragmentation rather than origin as in Fisher (1961). All deposits formed by normal sedimentary processes (both syn- and post -eruptive) are defined as non-primary, or epiclastic. This causes difficulties as the distinction between syn-eruptive and post-eruptive processes is unclear, and deposits such as those formed during subaqueous volcanic activity should not be classified as epiclastic. However, the scheme does provide a useful generic descriptive terminology, which is particularly useful where identification/interpretation of genesis is difficult (e.g. in core, cuttings). This scheme is still widely used, particularly in industry.

McPhie et al. (1993), combined aspects of the two previous schemes of Fisher (1961) and Cas and Wright (1987), to use grain origin, transport and depositional mechanisms for classification. Four types of deposit are described: pyroclastic, autoclastic, re-sedimented syn-eruptive volcaniclastic, and volcanogenic sedimentary (Figure 2-3). Volcanogenic sedimentary deposits are those that involve reworking of pre-existing volcanic deposits before final deposition. Re-sedimented syn-eruptive deposits comprise primary material that is deposited during the eruption, but under the

influence of an external control (e.g. water or gravity). This scheme is very complex and rarely used.

Unlike the other schemes that use descriptive volcanoclastic terminology (i.e. volcanoclastic breccia etc.), White and Houghton (2006) determine transportation and depositional processes initially, followed by grain size, and thus lose the descriptive volcanoclastic term as used by Cas and Wright (1987) (Figure 2-3). Their scheme uses both primary pyroclastic terminology, and clastic grain size terminology. Primary volcanoclastic deposits include those directly related to eruptions and those that are syn-eruptively reworked, and they are divided into pyroclastic, autoclastic, hyaloclastite and peperite. Reworked and post-eruptive deposits are considered ordinary sedimentary deposits and given clastic grain sizes. Epiclastic is not used. This scheme is extensively used by volcanologists, but has not been adopted widely in industry.

In this thesis, determining whether certain volcanoclastic materials had been reworked was extremely difficult, especially given their fine grain size. Furthermore, detailed genetic determination of these materials was not the focus of this study. Therefore, for simplicity, the general descriptive terminology of Cas and Wright (1987), has been used to describe these materials, unless however, clear evidence for primary fragmentation exists, in which case the primary volcanoclastic terminology of White and Houghton 2006 is used.

Sedimentary: Udden-Wentworth (1914, 1922) Blair and McPherson (1999)			Grain size Upper limit:		Volcanoclastic: Cas & Wright (1987)	Primary volcanoclastic: after Fisher (1961), White and Houghton (2006)	
L	U	Class	(mm)	$\Phi$	L	L	U
Conglomerate (Breccia)	Gravel	Boulder	4096	-12	Volcanoclastic breccia or conglomerate	Breccia	Blocks/ bombs
		Cobble	256	-8		Lapilli-tuff	Lapilli
		Pebble	64	-6			
		Granule	4	-2			
Sandstone	Sand	Sand	2	-1	V. sandstone	Tuff	Ash
Mudstone or Shale	Mud	Silt	0.063	4	V. siltstone		
		Clay	0.004	8	V. claystone		

**Table 1: A summary of the existing grain size classification schemes for sedimentary and volcanoclastic particles.**  
(After: Wentworth 1922; Fisher 1961; Cas and Wright 1987; Blair and McPherson 1999; White and Houghton 2006). L = Lithified; U = Unconsolidated.

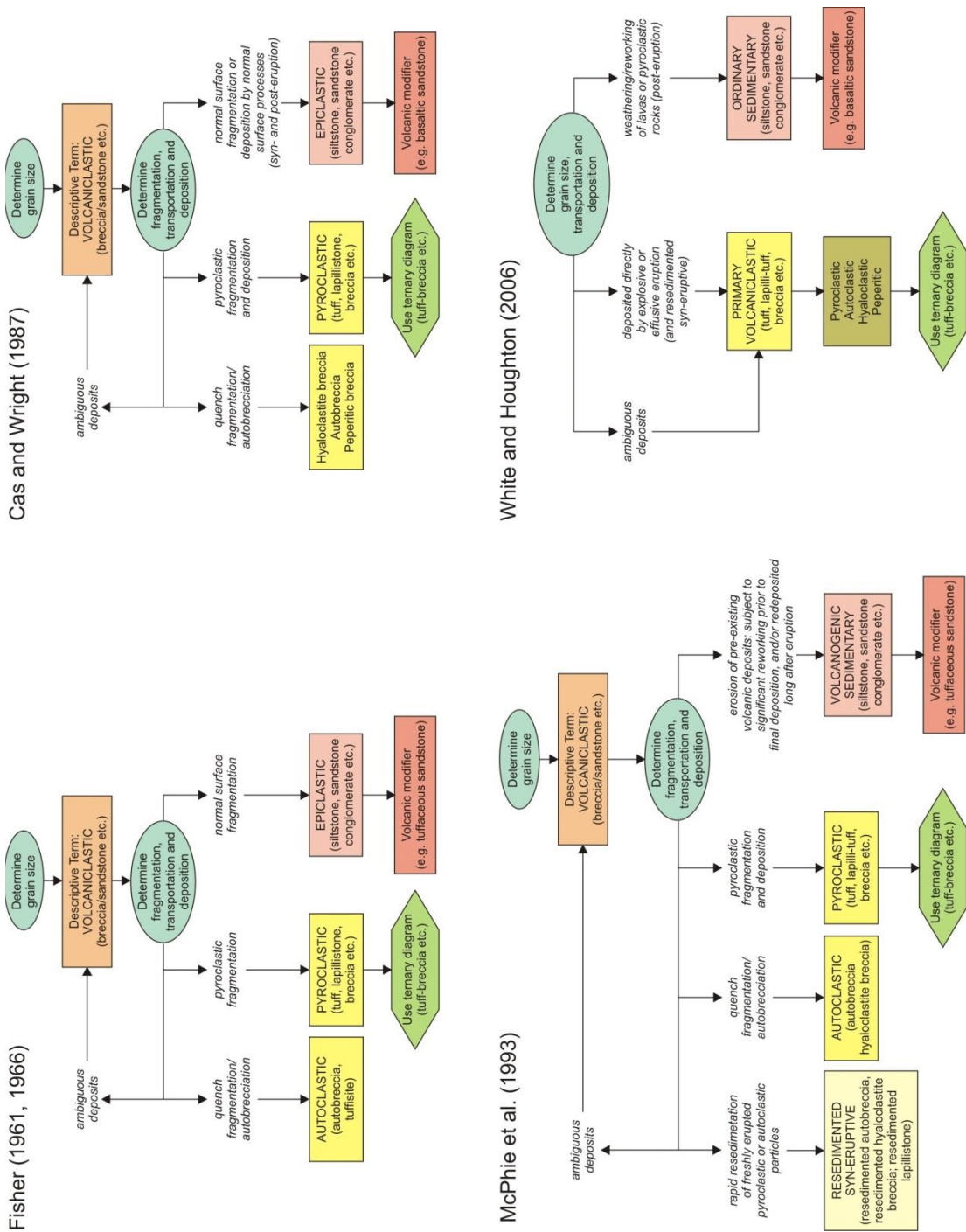


Figure 2-3: The main classification schemes for volcaniclastic rocks as proposed by Fisher (1961, 1966); Cas and Wright (1987); McPhie et al. (1993); White and Houghton 2006.

### 2.2.2.2 Volcaniclastic sub-categories

Several groups or sub-categories of volcaniclastic rocks are typically recognised: pyroclastic, autoclastic, hyaloclastite, peperite and epiclastic/reworked. Brief descriptions of these are given below.

- Pyroclastic deposits are produced by explosive fragmentation and are directly linked to volcanic eruptions. They form from volcanic plumes, and/or pyroclastic density currents (White and Houghton 2006). Deposits include ignimbrites, spatter, and scoria (Figure 2-4), (Schmid 1981; Branney and Kokelaar 2002).
- Autoclastic rocks are produced by mechanical self-fragmentation of a lava flow (or dome), during effusive volcanism (Manville et al. 2009, White and Houghton 2006). The exterior of the lava flow cools and fragments on contact with air, and the fragments are deposited as the flow continues (e.g. clinker) (Figure 2-4) (White and Houghton 2006).
- Hyaloclastite is produced by quench fragmentation of magma and/or lava that comes into contact with water or ice. The fragments produced during rapid cooling, quenching and fragmentation are deposited during continued magma/lava emplacement (White and Houghton 2006b). Deposits are characteristically glassy, angular, (basaltic) shards of quenched magma, supported by a fine-grained, typically, glassy matrix (Figure 2-4).
- Peperite is a heterogeneous rock that forms essentially *in situ* as magma fragments and mingles with unconsolidated, typically wet, sediment (White et al. 2000; Skilling et al. 2002; White and Houghton 2006). Peperite forms in a variety of palaeo-environments where sedimentation and magmatism are contemporaneous. It is also commonly associated with syn-volcanic intrusions in submarine sedimentary sequences (Kokelaar 1982; Lorenz 1984; Kokelaar et al. 1985; Busby-Spera and White 1987; Kano 1989; Kano 1991; Hanson and Wilson 1993; McPhie et al. 1993; Doyle 2000; Squire and McPhie 2002) as well as at the bases of lavas in lacustrine and sub-aerial successions (Cas et al. 2001; Skilling et al. 2002; Zimanowski and Büttner 2002). Peperite domains comprise juvenile lava clasts supported by host sediment (Figure 2-4). Peperite is discussed in detail below.

- 
- Epiclastic deposits (i.e. reworked volcanic materials), are a result of re-sedimentation of pre-existing rocks/unconsolidated tephra. The deposits contain fragments derived from previous volcanic eruptions, through the processes of weathering and erosion (Fisher 1961; Cas and Wright 1987) (Figure 2-4). They can form in any type of depositional environment, involving a wide variety of depositional processes.

A range of volcanoclastic deposits are described within this thesis, however, peperite, which directly involves the processes of magma/lava-sediment mingling, is the main focus.

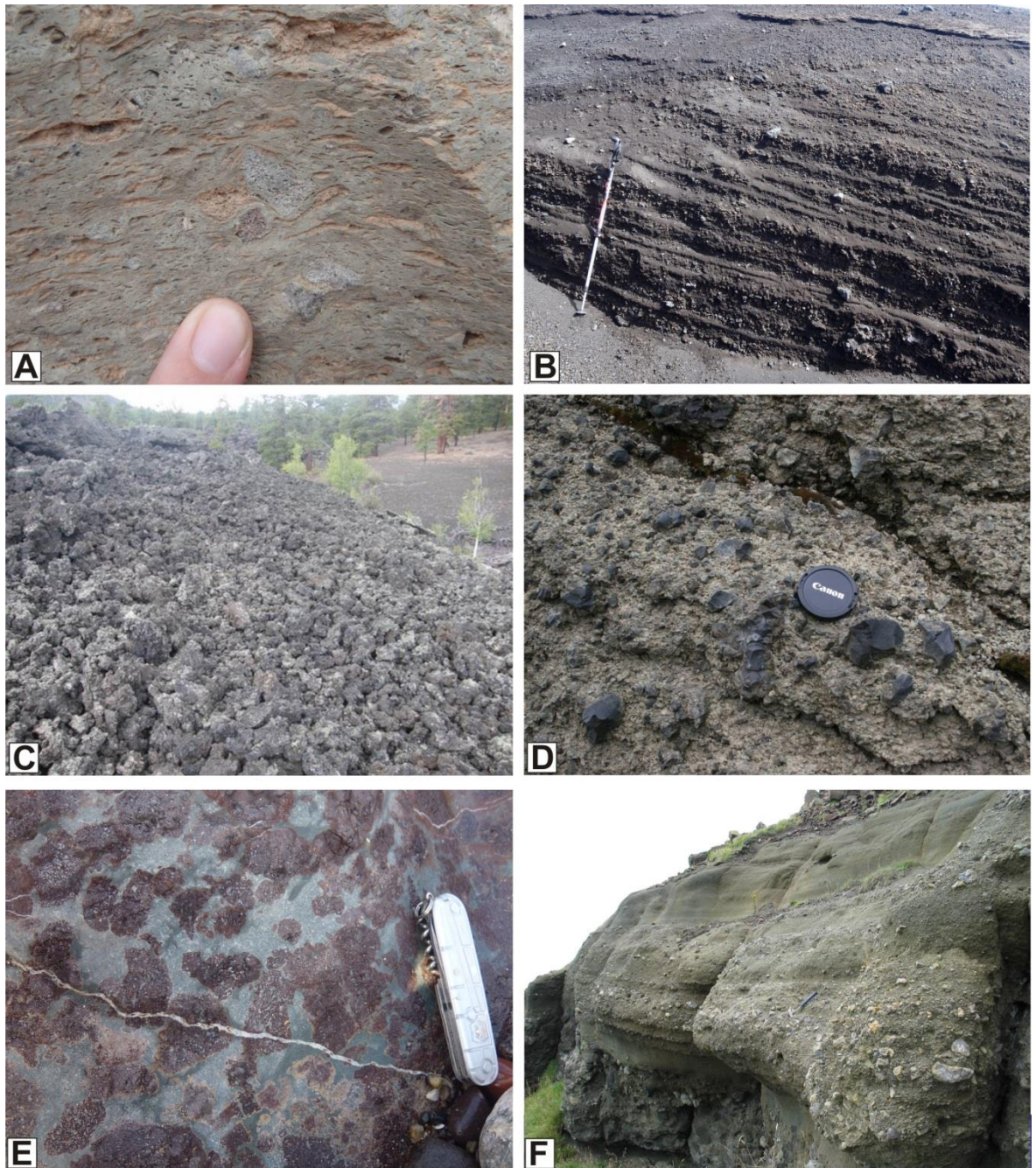


**Figure 2-4: Examples of the typical volcaniclastic deposits.**

A) Welded ignimbrite, with lithic lapilli and fiamme, Gran Canaria, Spain. Fingernail is 1 cm wide. B) Scoriaceous pyroclastic fall deposits, Laki, Iceland. Walking pole is ~1 m. C) Autoclastic flow top breccia, Flagstaff, Arizona. D) Hyaloclastite, Solheimajokull, Iceland. Glassy basalt fragments (black) are supported by a fine grained glassy matrix. Camera lens is ~8 cm diameter. (Photo credit: B. Bell). E) Peperite, St.Cyrus, Scotland. Juvenile lava clasts (red/purple) within a fine grained siltstone host sediment matrix (green). Pen knife is ~8 cm. F) Reworked volcaniclastic sandstone, Malcolm's Point, Mull. Rock hammer is ~ 30 cm. (Photo credit: D. Brown).

## 2.3 Lava-water interaction

Pillow lavas form as lava is erupted into, or is emplaced into, a water body (Moore 1975). They dominate the ocean floor through eruption at ocean ridges, and are also found in association with emplacement of sub-aerial lava along the shoreline of ocean islands and lakes, or under ice. Pillow lavas are typically viewed in cross-section as the characteristic elliptical (pillow) shape, and are most closely related to pahoehoe morphologies (Self et al. 1998; Bear and Cas 2007) (Figure 2-5). They have thin cooled outer crusts that insulate the inner core, and allow growth and propagation of the ductile lava. Multiple chilled crusts, or rinds, are formed through continuous lava emplacement and cracking of the crust (Goto and McPhie 2004) (Figure 2-5). Adjacent pillows deform around each other during the growth process; concentric vesicles and radial joints at the outer rims are common (Skilling 2002; Goto and McPhie 2004) (Figure 2-5). Fracturing of the glassy outer rinds can lead to the generation of spalled glassy material, hyaloclastite, which forms a matrix between pillows.

Sub-aerial basalt lavas that enter water typically form delta-like sequences comprising prograding clinofolds of pillow lava and hyaloclastite breccia (Furnes and Fridleifsson 1974; Porębski and Gradziński 1990; Schmincke et al. 1997; Batiza and White 2000; Skilling 2002; Watton et al. 2013). The deltas associated with hyaloclastite are comparable to Gilbert-style, coarse grained, gravity driven flows (Porębski and Gradziński 1990; Skilling 2002; Watton et al. 2013). Within the delta, hyaloclastite can also be reworked by gravity and wave action.

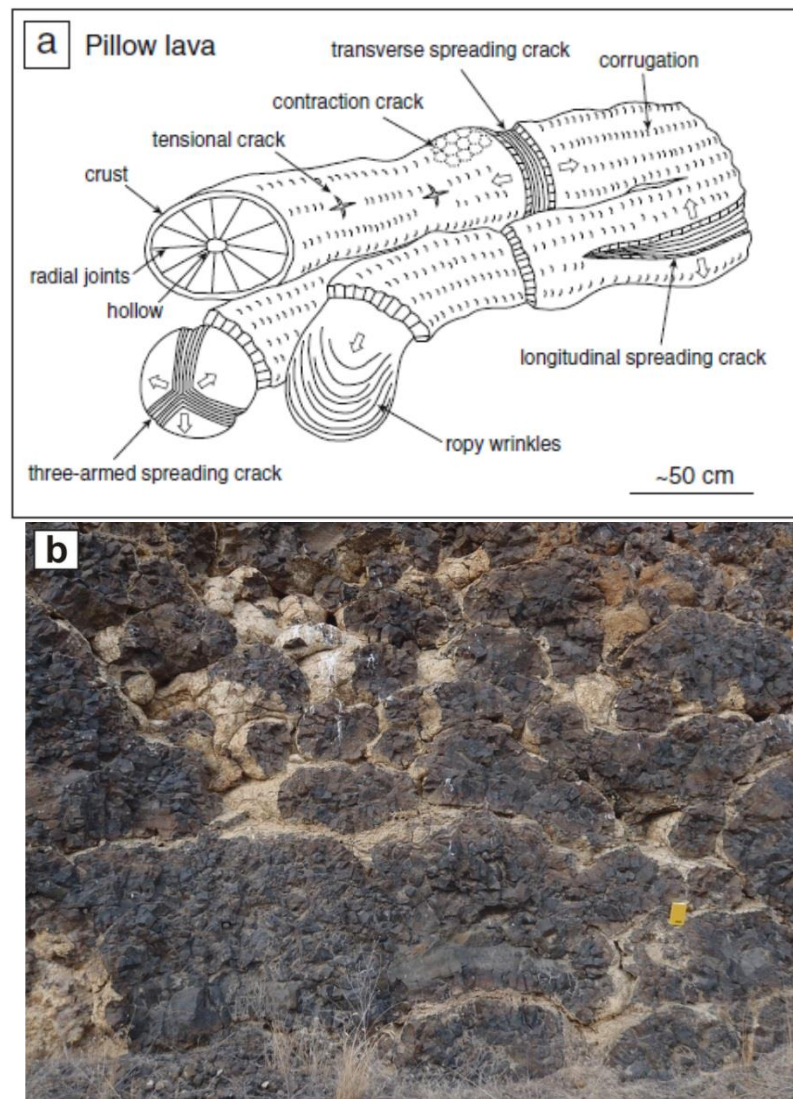


**Figure 2-5: Typical characteristics and morphology of pillow lava.**

a) Schematic sketch of morphology and surface features of pillow lavas (from Goto and McPhie 2004). b) Pillow lavas in cross-section, Columbia River, USA. Pillows are elliptical, and deform around each other to fill the open space. Yellow notebook is ~ 15 cm.

## 2.4 Lava-sediment interaction

Peperites are widely reported to form at the margins of intrusions, with domains of several km<sup>3</sup>, and at the base of lava flows, where domains are significantly smaller, ~1 m<sup>3</sup> (Skilling et al. 2002). Geometries of these domains are wide ranging, from lobes, to sheets, and interconnected pods (Doyle 2000; Skilling et al. 2002) (Figure 2-6). Formation of peperite is influenced by a number of factors that include (but are not restricted to): nature of the ‘parent’ igneous body (intrusive vs sub-aerial), lava type and environment of emplacement (Jerram and Stollhofen 2002; Petry et al. 2007), host sediment grain size (coarse vs. fine) (Busby-Spera and White 1987; Skilling et al. 2002),

host sediment consolidation and saturation (Skilling et al. 2002, Waichel et al. 2007; Hole et al. 2013) and magma-sediment density contrasts (Zimanowski and Büttner 2002).

On contact with unconsolidated sediment, magma/lava disintegrates and fragments, forming juvenile clasts, which mix and mingle to varying degrees with the sediment. Juvenile clasts display a range of morphologies from blocky to fluidal (Busby-Spera and White 1987), which reflect the differing brittle and ductile fragmentation processes that take place during peperite formation (Skilling et al. 2002) (Figure 2-6b). Blocky clasts are sub-equant, polyhedral to tabular, and have curvilinear to planar surfaces (Skilling et al. 2002), whereas fluidal clasts have globular morphologies, characterised by their intricate, irregular outlines, and range in shape from amoeboid to globules, to tendrils and wisp-like structures (Lorenz 1984; Busby-Spera and White 1987; Skilling et al. 2002). Groups of blocky clasts commonly display jigsaw-fit texture, characteristic of *in situ* fragmentation (Skilling et al. 2002). However, mixtures of juvenile clast morphologies are observed within the same peperite domain, inferring a mixture of both thermal and mechanical fragmentation processes (Skilling et al. 2002). Individual clasts that display both fluidal and sub-planar margins are interpreted as a product of multistage fragmentation (Skilling et al. 2002). The internal structure of a peperite is determined by the dispersal, orientation and grading of the juvenile clasts (Figure 2-6a). The dispersal of juvenile clasts within the host sediment has been used to define “close-packed” (high concentration of juvenile clasts) and “dispersed” (low proportion of juvenile clasts) peperite (Hanson and Wilson 1993; Skilling et al. 2002). Juvenile clasts may also display preferred orientation within the host sediment (Busby-Spera and White 1987; Brooks 1995; Doyle 2000; Skilling et al. 2002; Brown and Bell 2007). Peperite domains are typically non-stratified, ungraded and highly discordant to bedding; however, grading of the juvenile clasts can locally be preserved (e.g. Hanson and Wilson 1993; Doyle 2000; Brown and Bell 2007). Original stratification within the host sediment is typically lost (Doyle 2000; White et al. 2000; Skilling et al. 2002).

Host sediment variables affecting peperite formation include grain size, composition, sorting, cohesiveness, porosity and permeability (Lorenz 1984; Busby-Spera and White 1987; Squire and McPhie 2002; Skilling et al. 2002). A number of features observed within host sediments are used to infer the sediment was unconsolidated and likely wet; these include: polycrystalline host-sediment grains, textural homogenisation; vesiculated sediment; sediment in vesicles and hairline cracks of juvenile clasts and the parent igneous body, and elutriation pipes (Kokelaar 1982; Busby-Spera and White 1987; Hanson 1999; Dadd and Van Wagoner 2002; Skilling et al. 2002; Squire and McPhie 2002) (Figure 2-6c). However, blocky peperite has been identified in association with

unconsolidated, dry sediment (e.g. aeolian) (Jerram and Stollhofen 2002). Sediment fluidisation (Figure 2-6e) is the main process inferred to occur during magma-sediment interaction and peperite formation (Skilling et al. 2002), and requires sufficient particle support and transport of the host sediment grains by fluid movement (Skilling et al. 2002). Other processes that occur include soft-sediment deformation (sediment liquefaction), forceful magma intrusion, magma-sediment density contrasts, pore-water steam explosions (fuel-coolant interactions), magmatic gas explosions, and hydrodynamic mingling (Kokelaar 1982; McPhie et al. 1993; Lorenz et al. 2002; Skilling et al. 2002; Zimanowski and Büttner 2002; Schipper et al. 2011) (Figure 2-6d, e). These processes are thought to occur simultaneously and as a result of magma intrusion into the host sediment.

Current understanding surrounding peperite is that it occurs at both intrusive and extrusive igneous contacts. Most studies concentrate on intrusive contacts, between intrusions and host sediment/rock, or interpret peperite at the basal contact of sub-aerial lava. Some studies report shallow invasion of sedimentary bodies by sub-aerial lavas (Reidel 1998; Thordarson and Self 1998; Ebinghaus et al. 2014). However, the effects that invasive lava can have on unconfined sedimentary bodies of variable consolidation and saturation levels are poorly understood. This research considers lava-sediment (clastic) interactions during the emplacement of sub-aerial lava as it flows over and invades the underlying sediment, which is typically unconsolidated and saturated. It captures the full scope of lava-sediment interaction products, which include, but are not exclusive to, peperite.

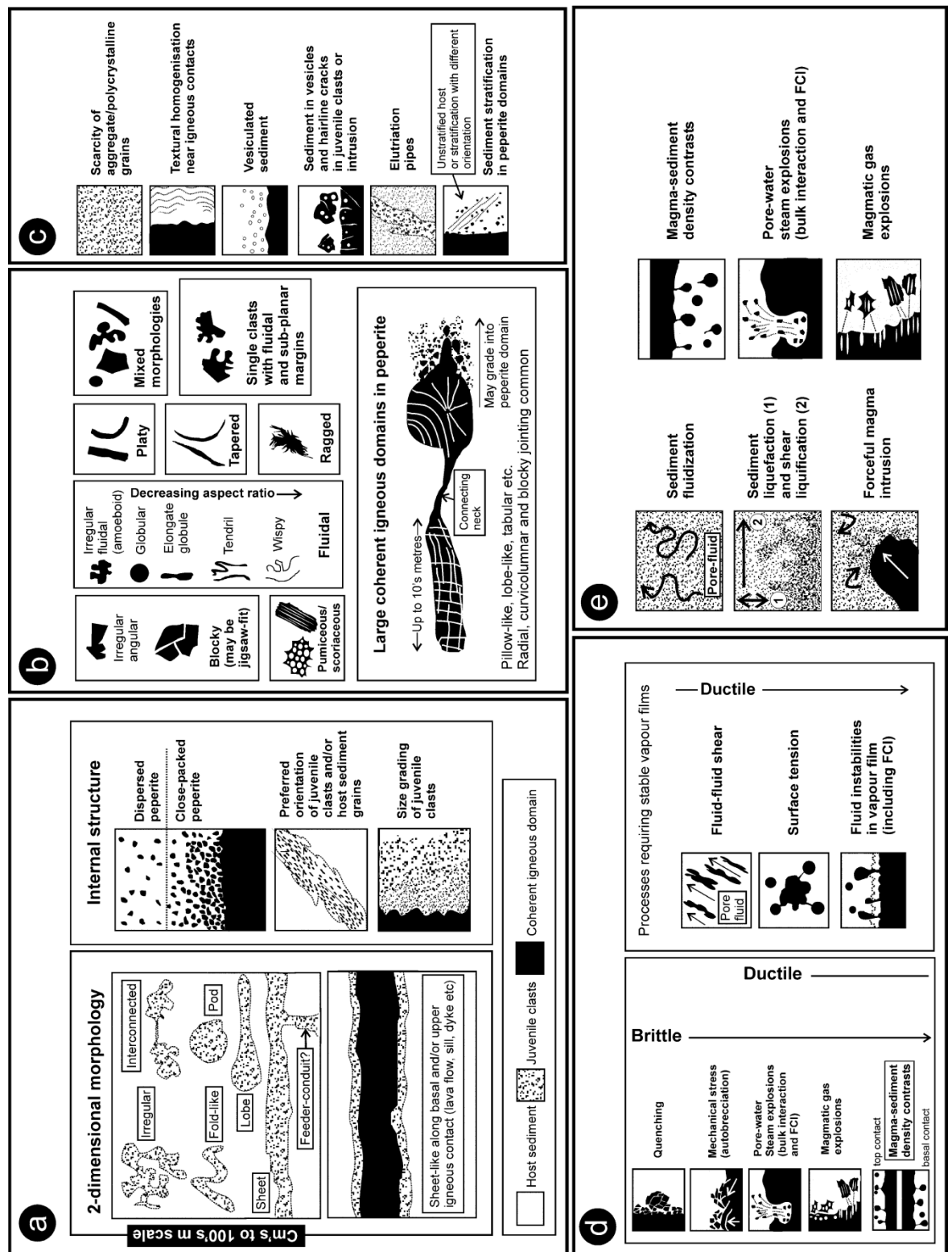


Figure 2-6: Summary of the characteristics of peperite from Skilling et al. (2002). a) peperite domain morphologies and internal structure, b) juvenile clast morphology, c) host sediment characteristics, d) process of juvenile clast generation, e) mingling processes of juvenile lava clasts and host sediment.

## 2.5 Offshore data collection in petroleum systems

### 2.5.1 Wireline logs

Wireline logging tools provide a continuous record of the subsurface in attributes that can be linked and interpreted as specific features including lithology porosity, permeability and saturation (Serra et al. 1984; Asquith et al. 2004; Wright 2013). These data provide a high resolution control to seismic data and are used for basin analysis and reservoir modelling.

Wireline logging tools comprise several individual log responses that are interpreted together to provide an accurate representation of the subsurface and rock lithofacies (Serra et al. 1984; Asquith et al. 2004; Wright 2013). The standard suite of log responses usually collected and evaluated includes: bulk density ( $\text{g/cm}^3$ ), natural gamma-ray, neutron porosity, resistivity, and velocity logs (Asquith et al. 2004). Different lithologies have different characteristic responses such that both a gross interpretation of rock formation, followed by detailed lithofacies interpretation can be assessed (Asquith et al. 2004; Wright 2013). For example, resistivity logs can be used to identify changes in siliciclastic rocks as sandstones typically have higher log responses than shales, which have low resistivity responses (Asquith et al. 2004). Development of log response interpretation and calibration to rock lithology was initially for interpretation of sedimentary rocks, but has since been successfully applied to the interpretation of igneous rock facies (Figure 2-7) (e.g. Helm-Clark et al. 2004; Nelson et al. 2009; Wright 2013; Watton et al. 2014). For volcanic rocks resistivity, velocity and neutron porosity logs are the most useful for lithofacies identification and smaller-scale changes, such as internal lava flow structures (Figure 2-7, Figure 2-7, Figure 2-8) (Schutter 2003; Helm-Clark et al. 2004; Nelson et al. 2009; WRIGHT 2013; Watton et al. 2014). Wireline logs give a theoretical numerical 'picture' of the subsurface lithologies; however, borehole imaging provides a high-resolution resistivity-based image for more detailed lithofacies analysis, which is particularly useful when core is not recovered.

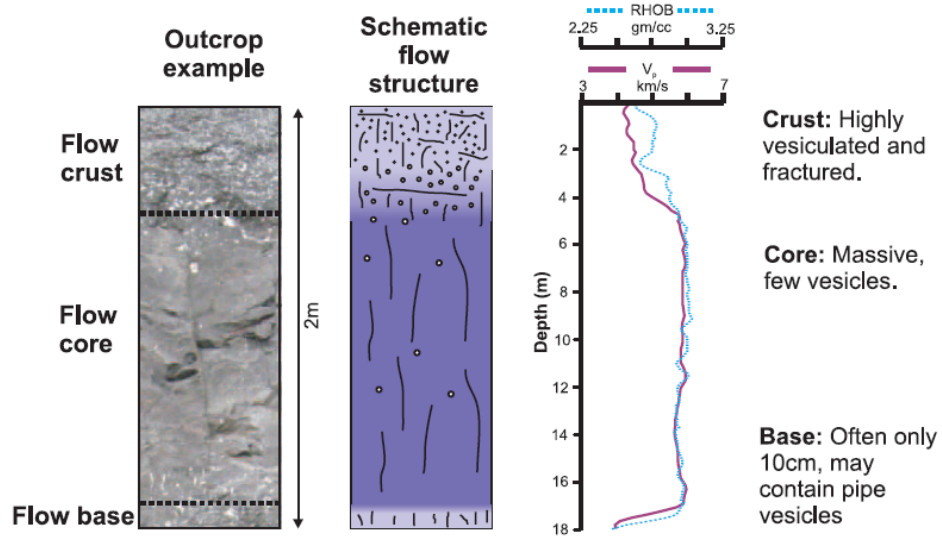


**Figure 2-7: Field photograph, sketch and wireline data of the typical internal structure of a pahoehoe lava flow.**  
 The graph shows wireline log velocity ( $V_s$ ) and density (RHOB) responses to the changes in lava structure. Log data is at a different scale to the outcrop but the lava structure is scale invariant. Image from Nelson et al. (2009).

Formation Lithology	Gamma Ray		Bulk Density			Neutron Porosity		Resistivity		Velocity				
	-50	API 200	1.0	g/cm <sup>3</sup>	5.0	-3.9713	m <sup>3</sup> /m <sup>3</sup>	1.5011	0.2	ohmm	2000	1000	s/m	6000
Siliciclastic Interbed	[Log trace]													
Volcaniclastic Material	[Log trace]													
Siliciclastic Interbed	[Log trace]													
Lava Flow Crust	[Log trace]													
Lava Flow Core	[Log trace]													
Lava Flow Base	[Log trace]													
Siliciclastic Interbed	[Log trace]													
Sill Aureole	[Log trace]													
Sill	[Log trace]													
Sill Aureole	[Log trace]													
Siliciclastic Interbed	[Log trace]													

**Figure 2-8: Schematic diagram representing the typical wireline log responses of lithofacies found within lava-dominated sequences.**  
 Image from Wright (2013) (after Planke 1994; Planke et al. 2000; Bell and Butcher 2002; Smallwood and Maresh 2002; Helm-Clark et al. 2004; Boldreel 2006; Nelson et al. 2009).

## 2.5.2 Borehole imaging

Borehole wireline image data is acquired using either microresistivity or acoustic velocity measurements, and provides visualisation of lithofacies structures and geometries, particularly in sedimentary facies (Shahinpour 2013). A variety of different tools exists for the collection of these data, and have been developed for industry use, such as the Schlumberger designed Fullbore Formation Microimager (FMI), which is used within this research. This down-well tool uses a set of pads that are pressed against the borehole wall, and record formation microresistivity during the wireline and drilling process (Prensky 1999; Gaillot et al. 2007; Shahinpour 2013; Watton et al. 2014). Typically, a resolution of 5 mm or less is collected for 80-100% of the borehole, providing excellent data recovery and 360° borehole coverage (Gaillot et al. 2007; Watton et al. 2014). Processing of the high-resolution dataset provides a normalised, vertical “unwrapped”, calibrated borehole electrical image that is northerly orientated so that South is the centre point of the image (Figure 2-9). Normalisation produces two colour-coordinated images, ‘static’ and ‘dynamic’, which are produced during averaging of the down-hole resistivity values. Static images have the same colour scaling over the entire log, which highlights larger scale resistivity variations related to lithology. Whereas dynamic images are averaged every ~2 m, which provides maximum detail, upto ~50 µm, allowing identification of small scale features such as bedding and fractures (Figure 2-9). Both static and dynamic images are used in conjunction with each other, and correlated with wireline logs during interpretation. The advantage of using this technology within volcanic-dominated sequences has recently been highlighted, and the identification and interpretation of internal lava structures and features, and volcanoclastic facies is possible (Watton et al. 2014) (Figure 2-10).

The data used within this study (Chapter 7) has focused on the identification of lava-sedimentary contacts within borehole images and how this can advance well-log correlations and inform depositional environment interpretations. FMI and wireline log data was provided by OMV from wells within the Cambo field in the Faroe-Shetland Basin.

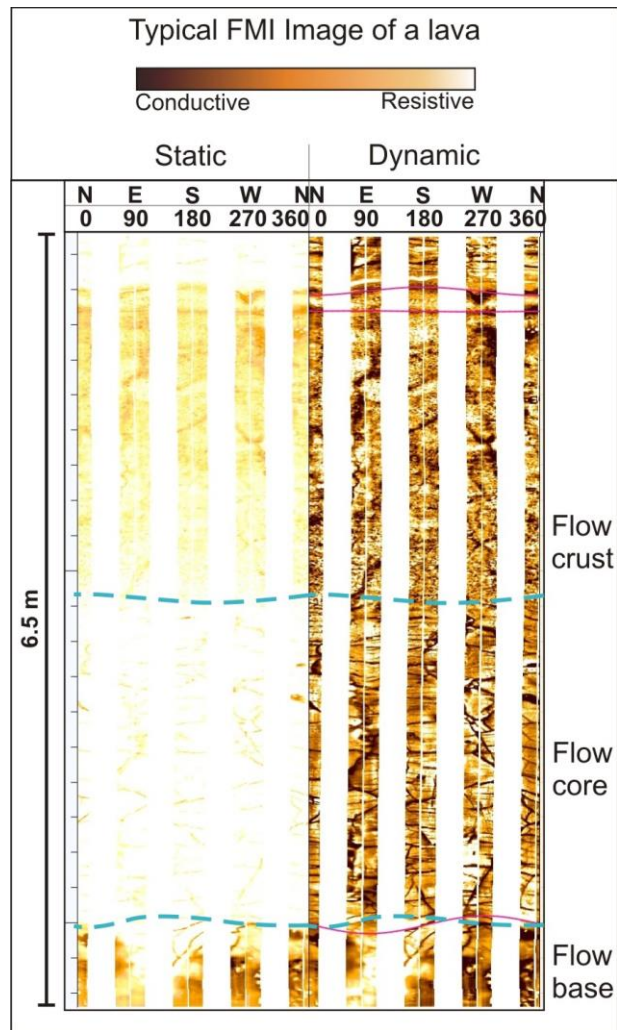


**Figure 2-9: A typical FMI image of basalt lava.**

The two images provided, static and dynamic, are a measure of the resistivity of the down-well lithofacies. The images provide an unwrapped 360° view of the borehole, orientated to the south. The static image provides lithological identification; in this example, basalt lava is highly resistive (pale yellow/white), with the flow core having the strongest resistive signature. The dynamic image provides detailed facies information such as bedding, and small-scale internal structures, for example clear fracturing within the flow core, and vesiculation within the flow crust.

FMI facies	FMI Identification	Composite log Attributes	Interpretation Volcanic lithofacies	FMI Image		Resistive Interpretation		Field analogue
				Static	Dynamic	Conductive	Interpretation	
<b>Mottled Upper</b>	High conductivity in comparison to flow core. Resistive 'spots' pepper the interval. Often overall grading to higher resistivity values in both static and dynamic logs at the top of the unit. Higher fracture abundance can differentiate interval from the core where gradational changes are lost. Flow top, Core and Base have been identified by $V_p$ distribution see Fig. 2.	<ul style="list-style-type: none"> <li>• Low GRAP1 &lt;30</li> <li>• Lower Resistivity (deeper) than flow core (10-80 Ohms)</li> <li>• <math>V_p</math> decrease (4-6 km s<sup>-1</sup>)</li> <li>• Density decrease (2.5-3gm/cc)</li> <li>• PEF remains constant (5-6.5)</li> </ul>	<p><b>Flow Crust.</b> Higher conductivity 'spots' represent vesicles which can be banded. Once buried these vesicles can be filled with calcite and zeolite to form amygdalae. These features have been confirmed when the FMI logs have been compared to core data.</p> <p>Sharp relationships mark the transitions between flows.</p>	Static	Dynamic	Conductive	Interpretation	 <p>Highly vesicular flow tops grade into glassy chilled contacts indicated by a change in resistivity values.</p>
<b>Uniform Conductive</b>	High conductivity overall, some vertical fractures which are drilling induced. Near constant resistivity values on static FMI. Noticeable lack of features separates the unit from the flow top. Flow top, Core and Base have been identified by $V_p$ distribution see Fig. 2.	<ul style="list-style-type: none"> <li>• Low GRAP1 &lt;15</li> <li>• Higher Resistivity (deeper) &gt;100 Ohms</li> <li>• <math>V_p</math> increase (5-6.5 km s<sup>-1</sup>)</li> <li>• Density decrease (2.7-3.3gm/cc)</li> <li>• PEF remains constant (5-6.5)</li> </ul>	<p><b>Flow Core</b> Finely crystalline vesicle poor central segment of a lava flow. Can be fractured or jointed but often absent of any features hence uniform appearance in the image log. Flow cores are formed as magma cools more slowly as insulated by the crust.</p>	Static	Dynamic	Conductive	Interpretation	 <p>Basalt flow core absent in vesicles. In this example the core is much thicker than the surrounding crust.</p>
<b>Mottled Lower</b>	Similar to flow tops with a resistive base and increasing in conductivity towards the core. Small resistive spot are again visible but can be elongate perpendicular to the flow base. The basal contact can be locally irregular. Flow top, Core and Base have been identified by $V_p$ distribution see Fig. 2.	<ul style="list-style-type: none"> <li>• Low GRAP1 &lt;30</li> <li>• Lower Resistivity (deeper) than flow core. (10-80 Ohms)</li> <li>• <math>V_p</math> decrease (4-6 km s<sup>-1</sup>)</li> <li>• Density decrease (2.5-3gm/cc)</li> <li>• PEF remains constant (5-6.5)</li> </ul>	<p><b>Flow Crust (Base).</b> At the flow base vesicles or occasionally infilled amygdalae occur. They originate from cooling and volatile release. Segregation of a more silica rich component can lead to the formation of elongate vesicles at the flow base. Vesiculation can be partially laminated upon ductile deformation of the flow during cooling.</p>	Static	Dynamic	Conductive	Interpretation	 <p>Flow bases can be highly vesicular and fractured (as above) especially in contact with a water saturated sediment or soil.</p>
<b>Resistive contact</b>	Resistive contact in FMI image between two flows. Mottled, diffuse appearance with patches of higher and lower resistivity. The contact changes are gradation with no sharp contacts. Usually only 0.2-0.7m thickness. Where present flow to facies can be difficult to determine.	<ul style="list-style-type: none"> <li>• High GRAP1 &gt;40</li> <li>• Higher Resistivity (deeper) than flow top (40-80 ohms)</li> <li>• <math>V_p</math> decrease (2.5-3 km s<sup>-1</sup>)</li> <li>• Density decrease (2.3-2.7gm/cc)</li> <li>• PEF decrease to lower values (2-4)</li> </ul>	<p><b>Palaeosol or laterite</b> derived from the weathering and leaching of basalt flow tops. In outcrop they often have a reddened appearance due to oxidising iron. Palaeosols are important as they marks breaks in activity in volcanism and can provide useful stratigraphic markers. Recognition of palaeosols in image logs can be difficult.</p>	Static	Dynamic	Conductive	Interpretation	 <p>Reddened laterite horizon, note the leaching (yellow) surrounding the reddened interval.</p>

**Figure 2-10: Classification of lava facies with FMI interpretation.** The variability of lava facies can be recognised and interpreted within FMI data. A classification scheme of the main types, including lava flow crust and core, is provided from Watton et al (2014). The data provided includes typical FMI signatures, typical identifiable features and field examples.

## Chapter 3: Kinghorn, Fife, Scotland, UK

### 3.1 Introduction

Kinghorn, Fife, is located on the east coast of Scotland (Figure 3-1). The succession under investigation comprises eastward-dipping basaltic lavas interbedded with a variety of siliciclastic, carbonate, and volcanoclastic rocks. The 485 m thick succession is part of the Kinghorn Volcanic Formation (KVF), of the Early Carboniferous Fife-Midlothian Basin, produced during the late Visean (Stage) (345.5-326.5 Ma) of the Dinantian (Epoch), Early Carboniferous. This is part of the Carboniferous-Permian Igneous Province of northern Britain (Macdonald and Fettes 2007). The sequence broadly records a marine transgression; however, various uplift and subsidence events and fluctuating accommodation space have controlled the intra-basinal drainage system. A range of depositional environments from sub-aerial through fluvio-deltaic to shallow marine are recorded.

The basaltic lavas at Kinghorn were typically emplaced sub-aerially, but the presence of hyaloclastite, locally with pillow fragments, and peperite, indicate eruption into standing bodies of water and/or interaction with unconsolidated wet sediment. The presence of phreatomagmatic lapilli-tuffs and ash aggregates also records interaction of magma with water. Sedimentation is dominated by siliciclastic input to fluvial and marginal marine environments at the base of the sequence, and carbonate deposition at the top of the succession. Locally, and periodically, pulses of reworked volcanic material inundated the basin.

Detailed analysis of the interfaces between the volcanic and sedimentary units at Kinghorn has enabled the characterisation of three types of lava-water-sediment interaction: i) loading and soft-sediment deformation; ii) “passive” interaction with the formation of peperitic margins; and iii) “invasive” interaction where the interaction is more “dynamic” and the host sediment is disaggregated. It is proposed that the sedimentary properties at the time of interaction strongly influenced the type of interaction that occurred.

## 3.2 Geological Setting

The early Carboniferous of northern Britain was dominated by back-arc N-S extension (Stephenson 2003; Macdonald and Fettes 2007; Underhill et al. 2008; Leeder 2009), as a consequence of the Variscan Orogeny (320-290 Ma) and its tectonic controls on southern Britain, Europe, and the Iberia-America-Massif Central region (Wilson et al. 2004; Woodcock and Strachan 2008). Alkali basaltic magmatism in Britain was driven by pressure-release melting of the upper mantle during extension (Smedley 1986; Stephenson 2003), related to subduction in the south. Extension controlled sedimentation and igneous activity throughout the Carboniferous, resulting in a series of interconnected subsiding basins, associated with extension-related magmatism (Macdonald and Fettes 2007; Underhill et al. 2008).

During the Late Visean, NNE-SSW trending basins formed in the Caledonian Terrane (Underhill et al. 2008), recording E-W extension (Stephenson 2003; Macdonald and Fettes 2007) with volcanism concentrated at the basin hinges and margins. The continental, rift-related style of basaltic magmatism formed the Carboniferous-Permian Igneous Province (CPIP) of northern Britain (Trewin and Thirlwall 2002; Upton et al. 2004). It is concentrated within the Midland Valley of Scotland (MVS), and ~90 % is thought to have erupted during the Visean, 345.5-326.5 Ma (Macdonald and Fettes 2007). The rapid onset of magmatism occurred simultaneously with subsidence, sedimentation and extension within the MVS. The MVS is a WSW-ESE trending basin, ~80 km wide, and >150 km long (Underhill et al. 2008) (Figure 3-1). It is bounded by the Highland Boundary Fault (HBF) to the North, and the Southern Upland Fault (SUF) to the South, and contains numerous N-S trending folds (Figure 3-1), one of which is the Burntisland Anticline (Underhill et al. 2008). The MVS comprises a number of smaller subsiding basins that developed along north-south axes, including the Fife-Midlothian Basin in the eastern MVS (Figure 3-1). The margins of these basins became the focus of CPIP volcanism, as in Kinghorn, Fife, and the Bathgate Hills (Stephenson 2003). Volcanic activity was characterised by composite volcanic fields comprising scoria cones, lava shields and fissure vents (Macdonald and Fettes 2007), along with explosive phreatomagmatic activity due to interactions with surface and ground waters, as well as water-saturated sediment (Macdonald and Fettes 2007). Table 1 illustrates the lithostratigraphy of the MVS during the Carboniferous.

A marine transgression is recorded within the MVS throughout the early Carboniferous, although numerous subsidence and uplift events controlled the accommodation space and intrabasinal drainage system (Macdonald and Fettes 2007; Underhill et al. 2008). Sedimentary input to the subsiding basins was typically restricted; however, lacustrine,

marginal marine and fluvio-deltaic conditions dominated deposition (Stephenson 2003; Macdonald and Fettes 2007), resulting in marine shales, deltaic siltstones, and fluvial sandstones, as well as thin carbonate units, such as the Lower Limestone Formation of the Late Dinantian (Woodcock and Strachan 2008). During periods of restricted deposition, stratified water columns formed, resulting in the preservation of organic matter and the accumulation of oil shales (Underhill et al. 2008; Woodcock and Strachan 2008).

The lava-dominated succession at Kinghorn, Fife, is part of the Fife-Midlothian Basin of the MVS, and belongs to the late Visean age KVF (Stephenson 2003; Upton et al. 2004). The KVF (Table 2), is localised to the area surrounding the Burntisland Anticline, is <20 km across (Underhill et al. 2008), and is typically grouped with the Sandy Craig Formation (SCF) (Table 2). The KVF comprises sub-aerial basaltic lavas intercalated with sedimentary rocks of the SCF (Underhill et al. 2008), which comprises both siliciclastic and carbonate units of fluvio-deltaic and lacustrine (non-marine) depositional environments (Stephenson 2003). These units are overlain by the Pathhead Formation (Table 1), which comprises cyclic units of marine siliciclastic mudstones, siltstones and carbonates, and has its upper boundary with the base of the Hurllet Limestone of the Lower Limestone Formation (Table 2) (Browne et al. 1999). The Hurllet Limestone marks the top of the succession within this study.

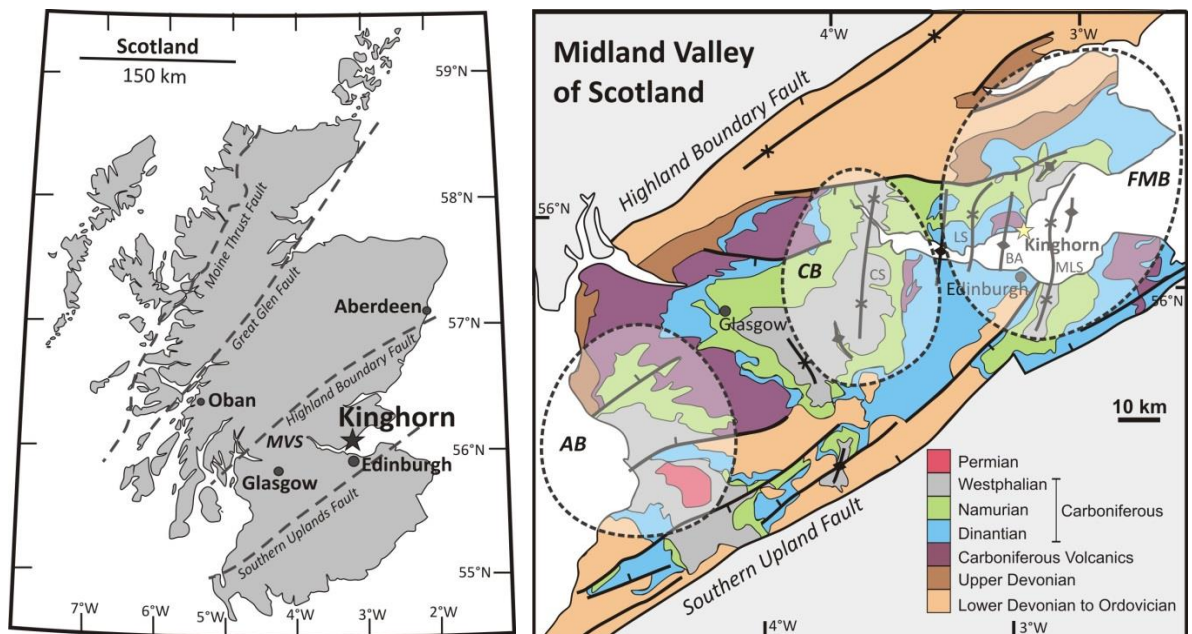


**Figure 3-1: A) Locality map of Kinghorn, Scotland, which lies within the Midland Valley of Scotland (MVS). B) A geological map of the MVS, showing the three main basins present during the Dinantian Epoch, Carboniferous (dashed transparent circles). Ayrshire Basin (AB), Central Basin (CB), Fife-Midlothian Basin (FMB). BA - Burntisland Anticline, CS - Clackmannan Syncline, LS - Lochore Syncline, MLS - Midlothian-Leven syncline. (A) adapted from, Macdonald and Fettes 2007, B) adapted from Underhill et al. 2008 and Woodcock and Strachan 2008).**

Period	Epoch	Stage	Lithostratigraphic Classification			
			Groups	Formations		
				West Lothian	East Lothian	<b>Fife</b>
CARBONIFEROUS	SILESIAN	Westphalian	Coal Measures	Upper Coal Measures		
				Middle Coal Measures		
				Lower Coal Measures		
		Namurian	Clackmannan Group	Passage Formation		
				Upper Limestone Formation		
				Limestone Coal Formation		
	<b>Lower Limestone Formation</b>					
	DINANTIAN	Visean	Strathclyde Group	West Lothian Oil-Shale Formation	Aberfeldy Formation	<b>Pathhead Fm</b>
						<b>Sandy Craig Fm</b>
				Gullane Formation		Pittenweem Fm
						Anstruther Fm
						Fife Ness Fm
	Tournaisian	Inverclyde Group	Clyde Sandstone Formation			
			Ballagan Formation			
			Kinnesswood Formation			

**Table 2: Lithostratigraphy of the Midland Valley of Scotland during the Carboniferous (adapted from Underhill et al. 2008).**

**The Sandy Craig, Pathhead, and Lower Limestone formations are seen in the succession at Kinghorn, and are highlighted in bold. The Kinghorn Volcanic Formation is grouped within the Sandy Craig Formation.**

### 3.3 Field Relationships

The field area is situated along the coastal path and shoreface between Burntisland and Kinghorn, Fife, covering ~3 km. The main field locations, referred to in the text, are shown in Figure 3-2. The succession youngs towards the NE, with the oldest rocks at Locality 1, and the youngest at Locality 9. Figure 3-2 shows a schematic stratigraphical log through the Kinghorn succession. It is dominated by sub-aerial basalt lavas, which are interbedded with thin, siliciclastic, volcanoclastic, and carbonate units. The main lithofacies are described further below.

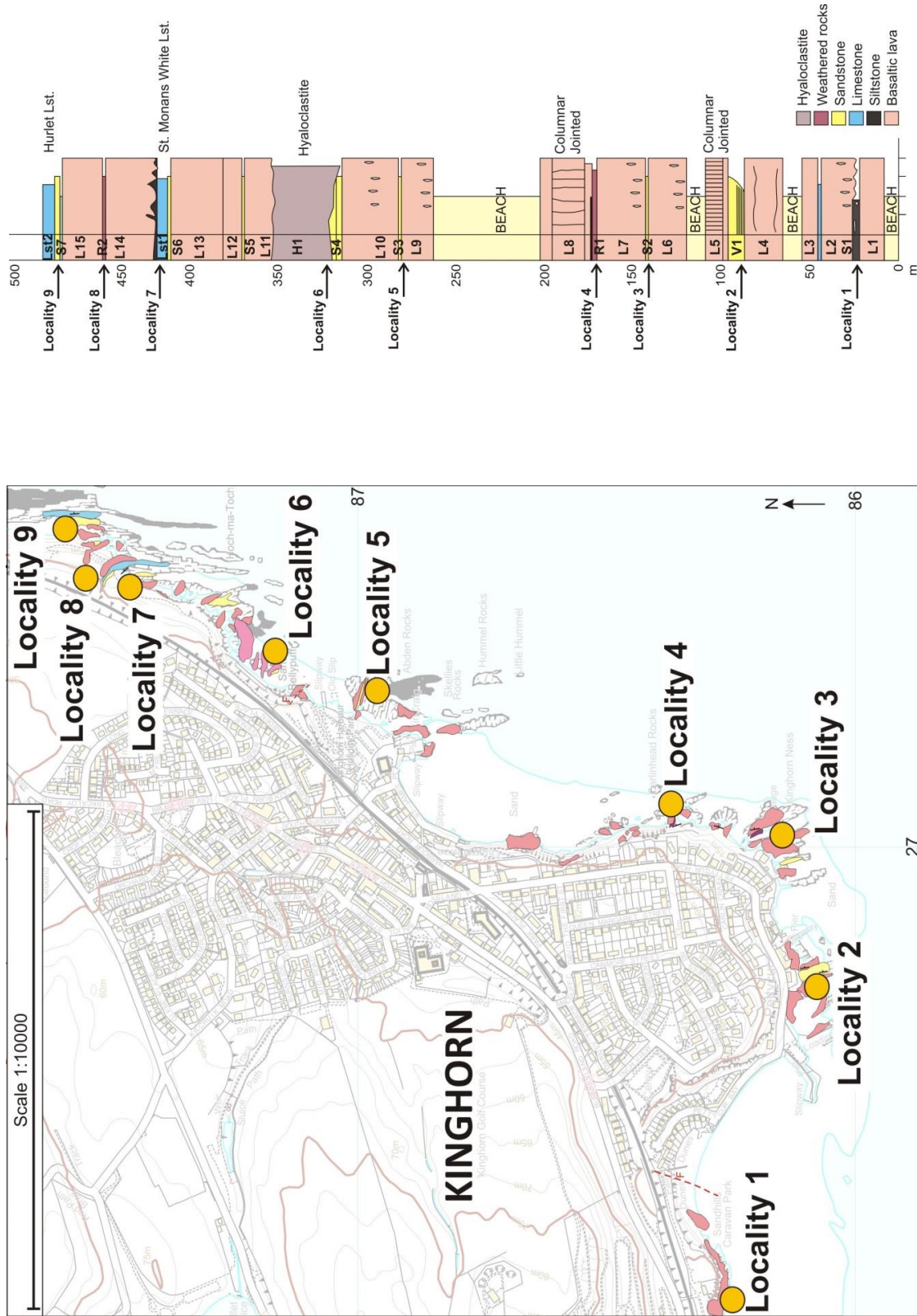


Figure 3-2: Location map of Kinghorn with the main field localities, and corresponding stratigraphic log through the ~485 m thick succession. Key: L=lava, S=sedimentary unit, V1 = Volcanic unit, Lst = Limestone unit, R=red-weathered bed, H=Hyaloclastite.

### 3.3.1 Volcanic Units

#### 3.3.1.1 Lava

The lavas exposed throughout the section at Kinghorn, are typically highly amygdaloidal basalt, with massive cores and vesicular, brecciated margins. The lavas dip  $\sim 32^\circ$ , towards ENE and locally display prismatic to pseudo-columnar and columnar joints (with 0.5-3 m wide columns) (Figure 3-3). Veins of quartz and calcite are widespread and disrupt the lavas. Amygdales are typically 1-3 cm across, and comprise quartz and calcite. The oldest lavas, L1, L2 and L3, at Locality 1 (Figure 3-2), have large quartz and calcite amygdales, 5-10 cm across, concentrated at the upper margins of the lavas. Some amygdales are zoned with a blue rim of chalcedony (crypto-crystalline silica). Pipe amygdales (2-7 cm long) are concentrated at the base of the lavas and are observed throughout the succession.



**Figure 3-3: Typical columnar jointed lava (L8) exposed above Locality 4 at Kinghorn, Fife. The lava is  $\sim 10$  m thick and columns range in width from 0.5 -1.5 m.**

Red-weathered surfaces and contacts between lavas are common throughout the field area. At Locality 4 (Figure 3-2), the basal lava (L7) has a red weathered top (R1),  $\sim 60$  cm thick, and displays spheroidally weathered corestones. The overlying lava (L8) has a brecciated flow base, which is clast-supported, with sub-angular to sub-rounded lava clasts, 4-6 cm across, in a silt to sand- grade volcanoclastic matrix. Coherent siltstone clasts, 2-3 cm across, are also present within the basal breccia. At Locality 8 (Figure 3-2) another red-weathered upper lava surface (R2),  $\sim 30$ -100 cm thick, is observed

(Figure 3-4). The upper brecciated surface comprises sub-angular to rounded clasts of basalt, 2-8 cm, with a fine sandstone and siltstone matrix. The upper part (top ~30 cm), in contact with the overlying lava is stained red.

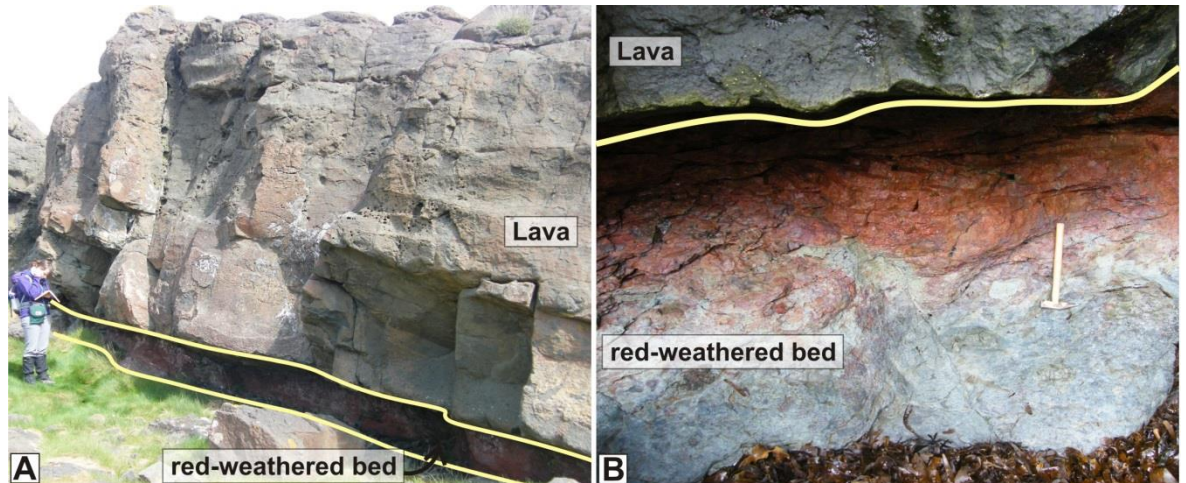


**Figure 3-4: Inter-lava red-weathered units are observed at several locations at Kinghorn. A) Lavas are separated by a red-weathered unit (paleosol), as seen at Locality 8. Person for scale. B) Close up of the red-weathered bed, which shows weathering/oxidation of the underlying lava top prior to the emplacement of the overlying lava. Hammer is ~35 cm long.**

The mineralogy and petrography of the Kinghorn lavas (and red-weathered surfaces) (Figure 3-5) indicate that they are of basaltic composition, and are dominated by plagioclase feldspar phenocrysts within a fine-grained glassy groundmass (Figure 3-6). Altered olivine phenocrysts are also present, replaced by clay minerals. Thin sections of the red-weathered surfaces at Locality 8 (Figure 3-5), show rounded spheroidal grains, <500  $\mu\text{m}$  across, of volcanoclastic material, potentially of altered scoria or clinker, within a fine-grained matrix. Figure 3-5 C and D highlight larger, irregular clasts of altered basaltic material and volcanoclastic sediment that are prominent within the surrounding granular sediment.

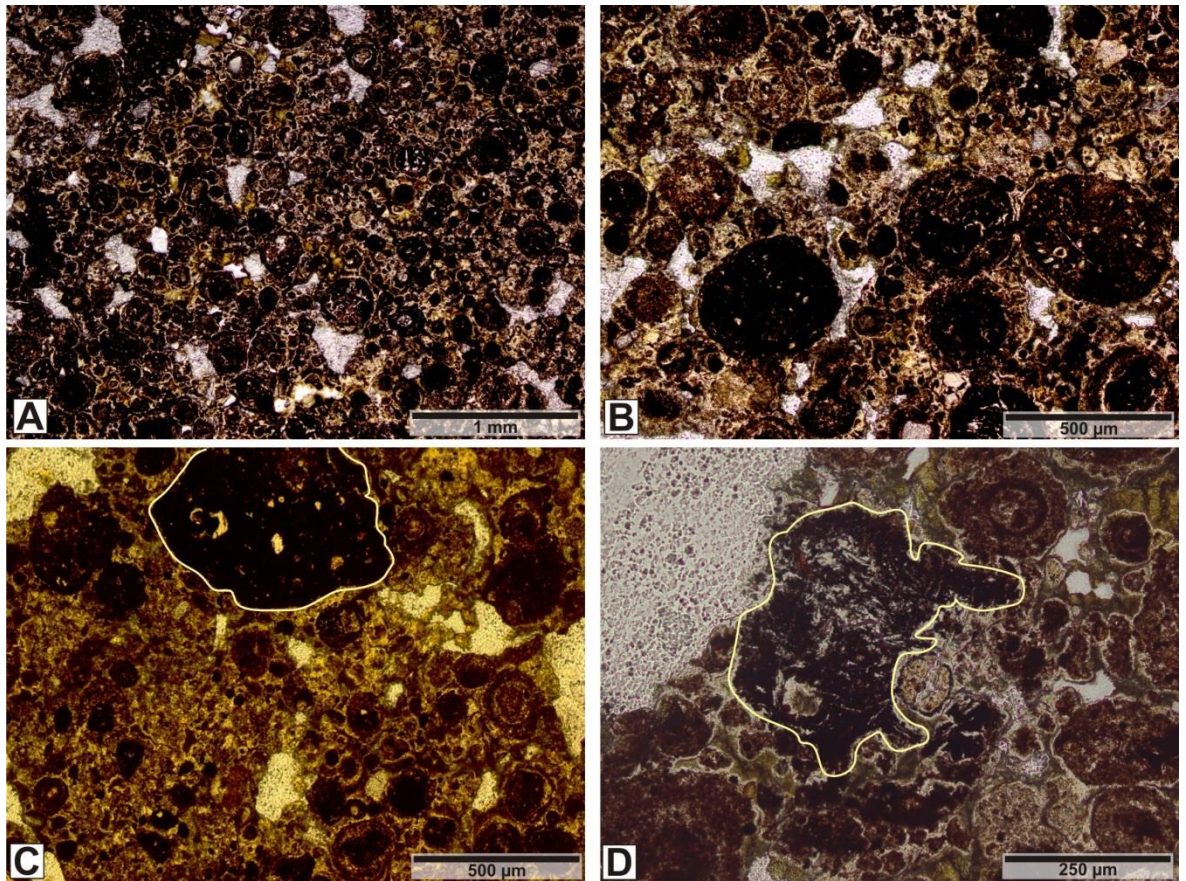


Figure 3-5: Photomicrographs of the red-weathered unit, R2, (paleosol) between two lavas (L14 and L15) at Locality 8.

All images are in plane-polarised light. A) The unit is dominated by rounded, spherical and ovoid clasts of reddened volcaniclastic material, within a fine grained matrix. B) A magnified image of the volcaniclastic sediment, including rounded clasts that have defined nuclei (e.g. quartz grains, volcanic lithics, or sediment). C) Larger clasts of siltstone (yellow outline) are also present, in contrast to the well rounded and well sorted grains that dominate. D) Yellow line outlines a clast of glassy basalt, which has an irregular, globular margin.

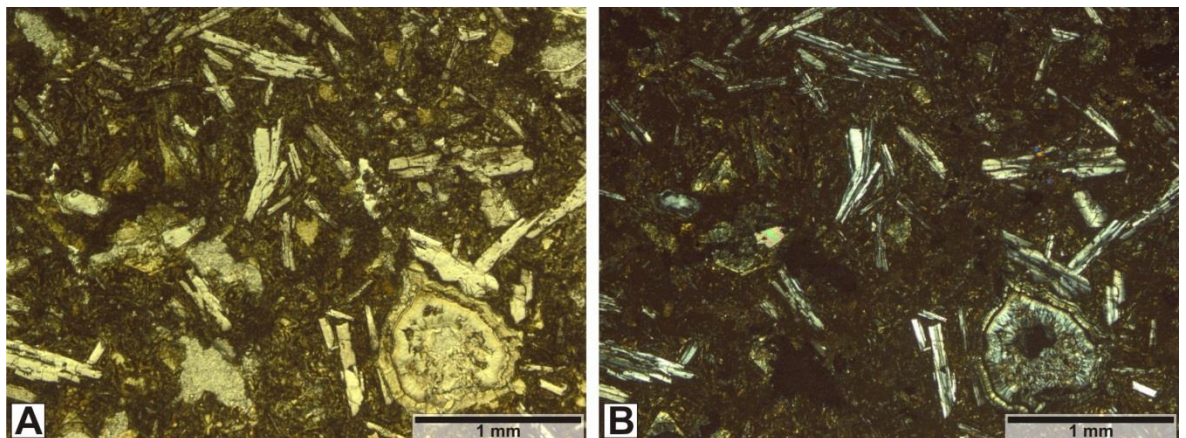


Figure 3-6: Photomicrographs of basaltic lava from the hyaloclastite (H1) sub-aerial lava (L11) boundary, Locality 6.

A) PPL B) XPL. The lava comprises plagioclase phenocrysts within a glassy groundmass. The amygdale in the lower right hand corner comprises calcite and zeolite.

### 3.3.1.2 Hyaloclastite unit

In the central portion of the succession, at Locality 6 (Figure 3-2), is an 30 m thick hyaloclastite unit (H1) (Figure 3-7). The hyaloclastite comprises a breccia of glassy basalt clasts supported by a fine sand-grade glassy matrix (basalt glass, weathered clays). The fragmented basalt clasts range in size from 5-50 cm, show little sorting, and have angular to sub-rounded morphologies. Larger pillow fragments are present (Figure 3-7B and 8C), and have chilled margins. The hyaloclastite unit grades upwards from a coarse breccia with pillow fragments, to finer hyaloclastite with blocky, vitric clasts. At the top of the hyaloclastite, there is a transitional or passage zone into sub-aerial lava, with interdigitating lava fingers and hyaloclastite.

Underlying the hyaloclastite is a sedimentary unit, which comprises laminated siltstone and fine sandstone sub-litharenite beds (~60 cm thick), capped by a 20-30 cm thick quartz cemented quartz arenite sandstone unit (Figure 3-7A). The latter is loaded and truncated by the hyaloclastite.

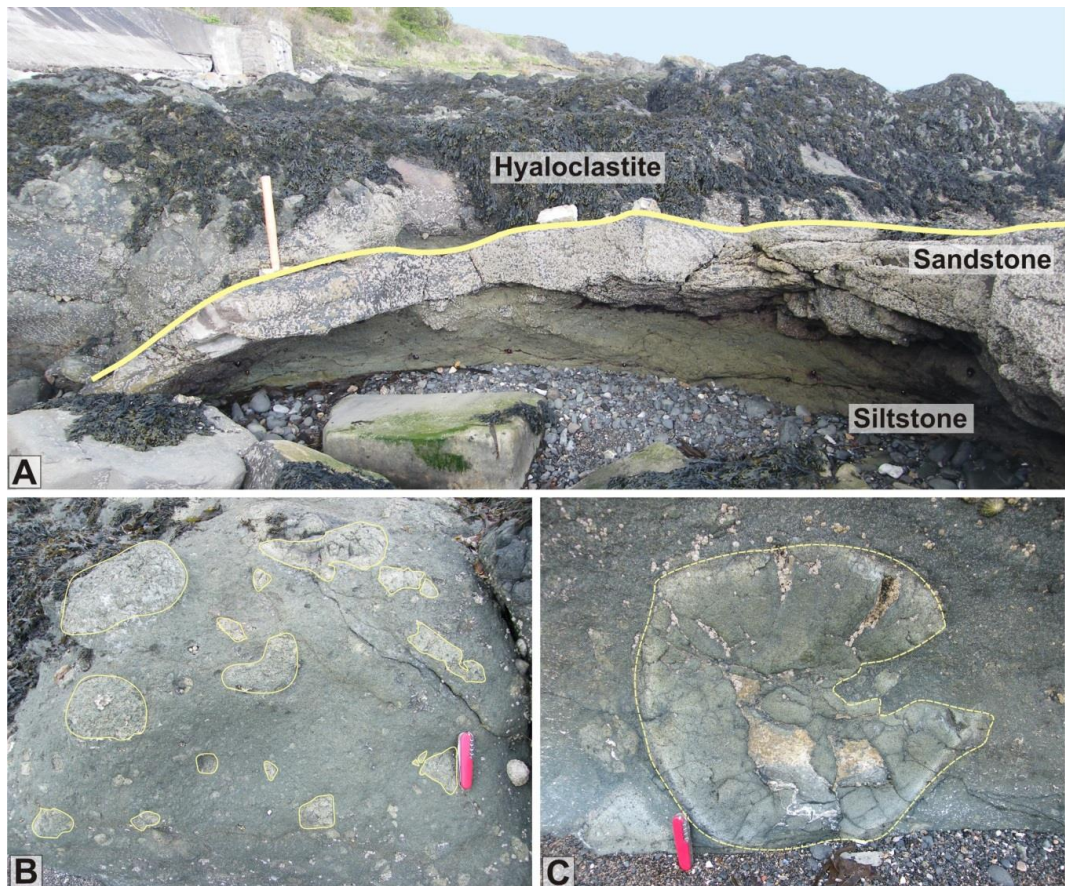


**Figure 3-7: Hyaloclastite at Kinghorn.**

**A)** The hyaloclastite overlies a relatively thin, isolated sedimentary unit, comprising thin sandstone beds, and a ~20 cm thick quartz cemented sandstone. Hammer is ~35 cm long. **B)** Typical hyaloclastite comprises quenched basalt lava fragments (yellow outlines, ~3-20 cm across) within a fine, glassy basaltic matrix. **C)** A relict pillow structure (yellow dashed outline, 35 cm across) is preserved within the hyaloclastite. Pen knife is ~8 cm long.

### 3.3.1.3 Lapilli tuff

Overlying the uppermost lava at Locality 9 (Figure 3-2), is a thin, <10 cm thick, finely laminated lapilli tuff, which fills palaeo-topography. It comprises thin layers that grade from fine tuff, to fine-medium tuff with disaggregated ash pellets (lapilli size), to a densely packed ash pellet (ash aggregate) supported layer, which in turn grades upwards to fine tuff (Figure 3-8). Pellets are typically 0.5-1 cm across, and each has a well-defined outer rim, or coating, with a structureless nucleus (Figure 3-8). Within the pellet supported layer some of the coated pellets are partially coalesced. Clastic and carbonate units overlie the tuff unit (Section 3.4.2).

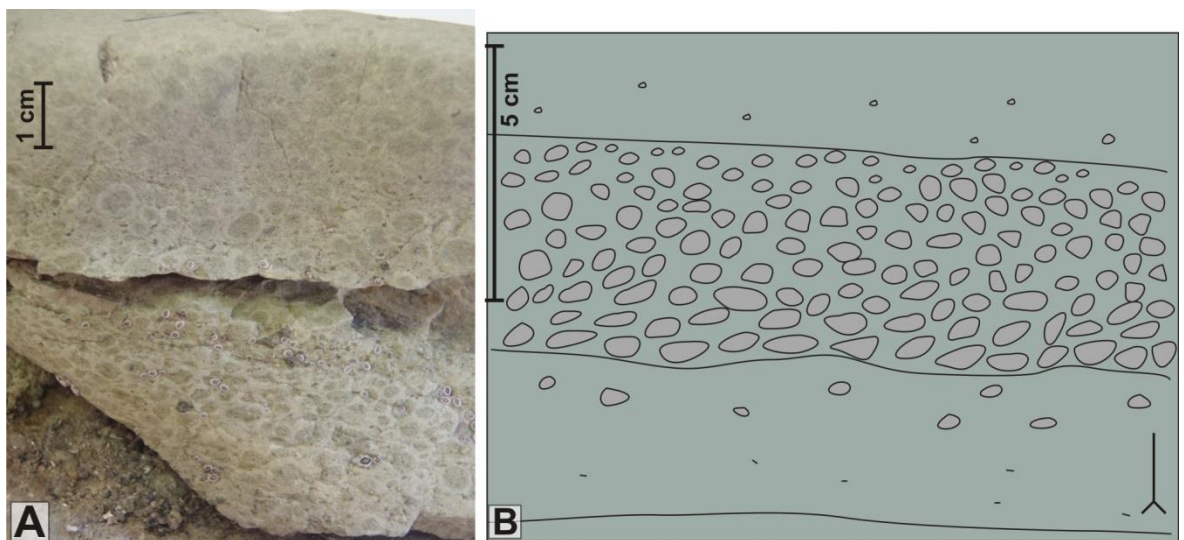


**Figure 3-8: Lapilli tuff at the top of the Kinghorn succession, Locality 9.**

**A) Hand specimen, with well defined coated ash pellets. B) A schematic sketch of the tuff that is composed of a densely packed ash aggregate layer with ash pellets, between layers of fine tuff.**

Petrographic analysis of the lapilli tuff reveals large coated pellets, with structureless nuclei, within a graded ash matrix (Figure 3-9). The pellets have a thin, fine-ash coating around the nucleus, which has a similar composition to the matrix. Basalt lithic grains, relict tube pumice and devitrified shards are also present within the tuff.

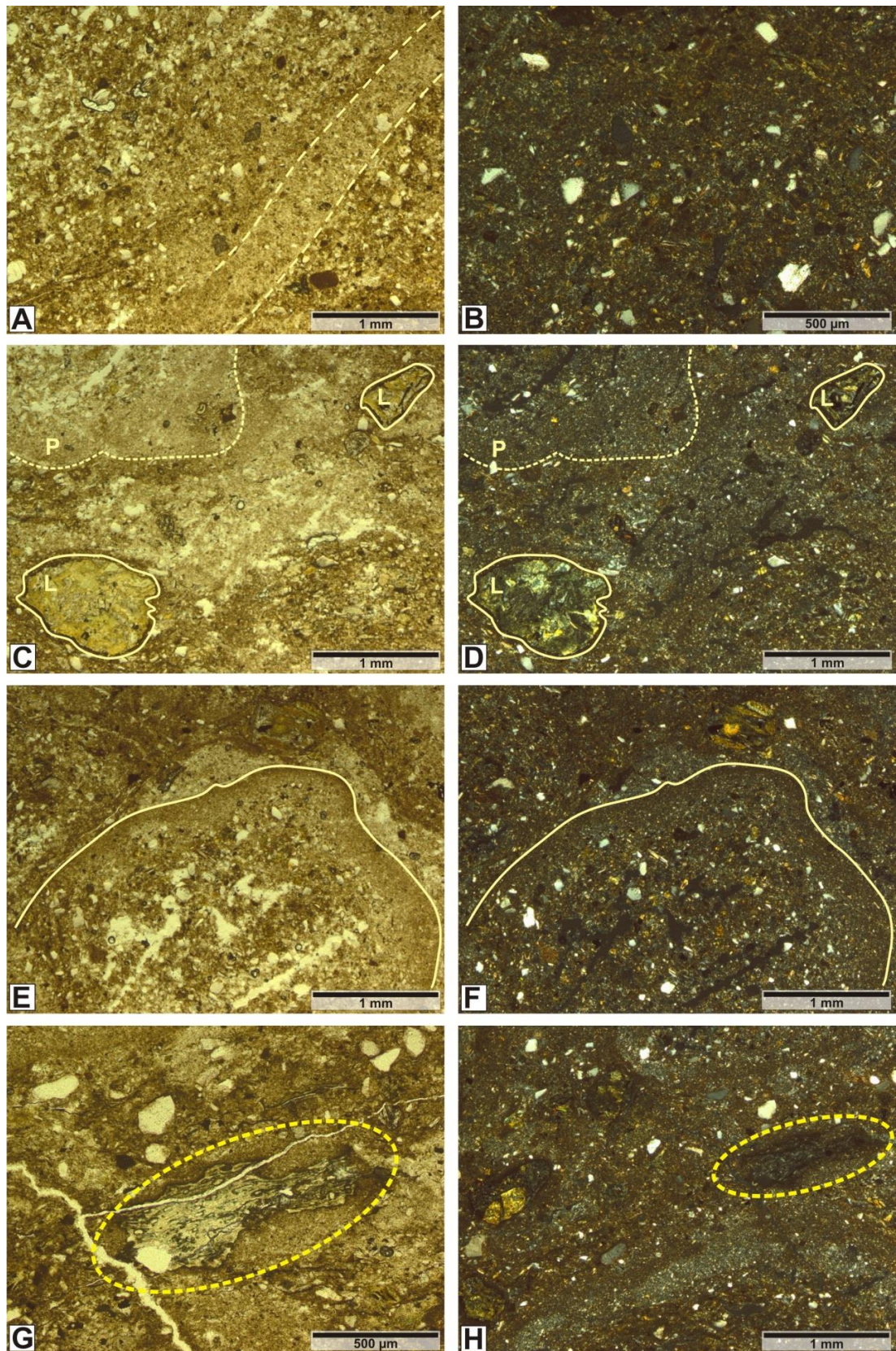


**Figure 3-9: Photomicrographs of lapilli tuff from Locality 9, Kinghorn.** A, C, E and G in PPL; B, D, F and H in XPL. A) Fine-grained tuff, with preserved laminae and grading (yellow dashed lines). B) Higher magnification of the tuff, which comprises sub-angular grains of quartz, lithics, and volcanic glass. C) and D) highlight grains of basalt lithic fragments (L, yellow outlines). The large grain in the upper left hand corner is a coated pellet (P, dashed yellow outline). E) and F) A coated pellet within the pellet supported layer. A clear fine ash coating to the pellet is preserved around the agglutinated nucleus. G) and H) highlight a relict vesicular pumice shard within the tuff (dashed outline). Relict shards are indicative of explosive volcanism.

### 3.3.2 Sedimentary Units

#### 3.3.2.1 Epiclastic units

Discrete sedimentary units occur throughout the succession, such as S2 at Locality 3 (Figure 3-2). Each is typically green-grey, 2-5 m thick, and comprises siliciclastic and volcanoclastic siltstone and sandstone lithologies. Where bedding is preserved, it is planar to wavy. Some sedimentary units are capped by a fine-grained, quartz cemented quartz arenite bed, ~3 m thick, that has planar contacts with the underlying sedimentary units, and the overlying basaltic lava. Petrographically, the units display volcanoclastic sandstone characteristics, as in Figure 3-10 and Figure 3-11. The fine-grained sandstone in Figure 3-10 comprises a green/grey clay-rich matrix with sub-angular to sub-rounded grains of quartz, feldspar, and basalt fragments.

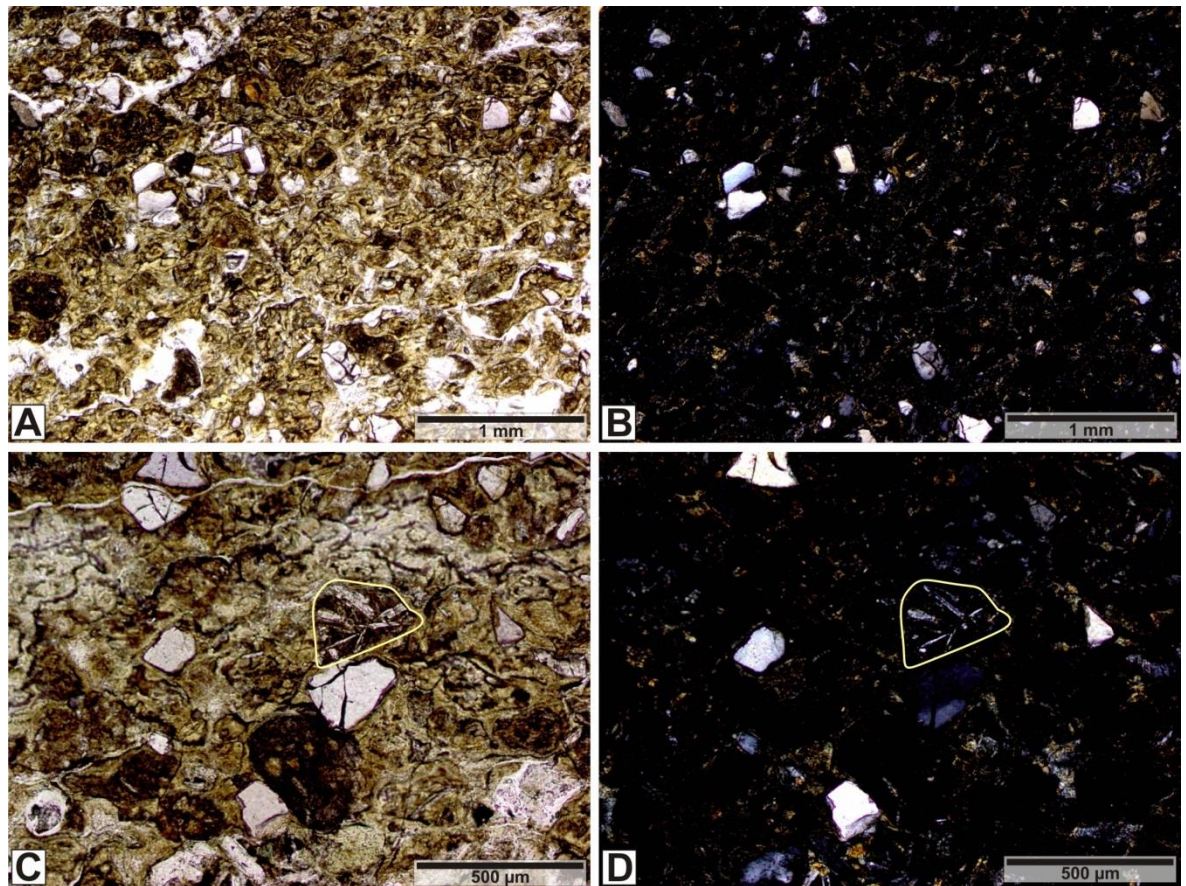


**Figure 3-10: Green-weathered fine volcanoclastic sandstone (S3) at Kinghorn.** A and C PPL, B and D XPL. A) and B) Typical fine-grained volcanoclastic litharenite, with basalt lithic clasts as well as quartz and feldspar. The glass-rich matrix has altered to clays and chlorite. C) and D) Higher magnification highlighting a basalt lithic grain with microphenocrysts of feldspar (yellow outline) within the clay-rich volcanoclastic matrix. The sandstone was likely transported from and over a volcanoclastic landscape (reworked) before deposition.

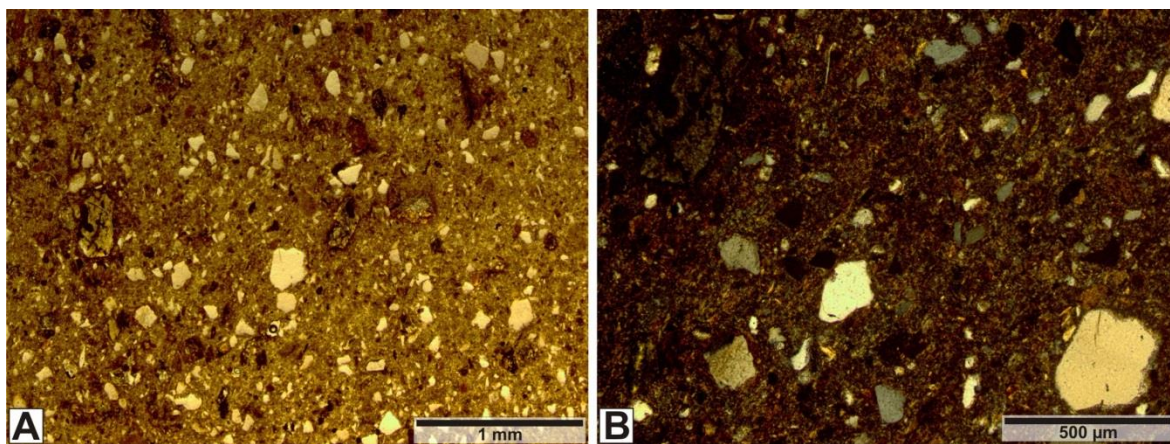


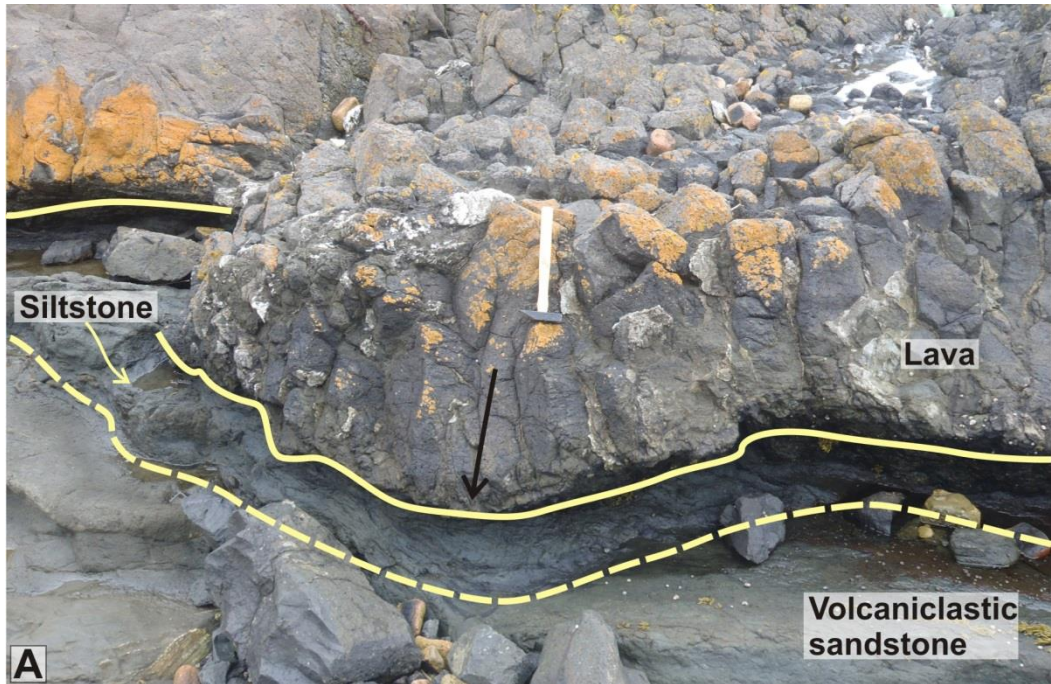
**Figure 3-11: Fine-grained volcaniclastic sandstone (S7) underlying the lapilli tuff at Locality 9.**

**A) Fine grained volcanic sub-litharenite comprised dominantly of sub-angular to sub-rounded grains of quartz and volcanic lithics within a fine grained, clay-rich matrix; (PPL). B) A higher magnification of the sub-litharenite (XPL). Although not in this field of view, a bubble-wall shard of palagonitised basalt glass is observed in this unit, together with other volcanic lithic grains.**

### 3.3.2.2 Volcaniclastic unit (V1), Locality 2

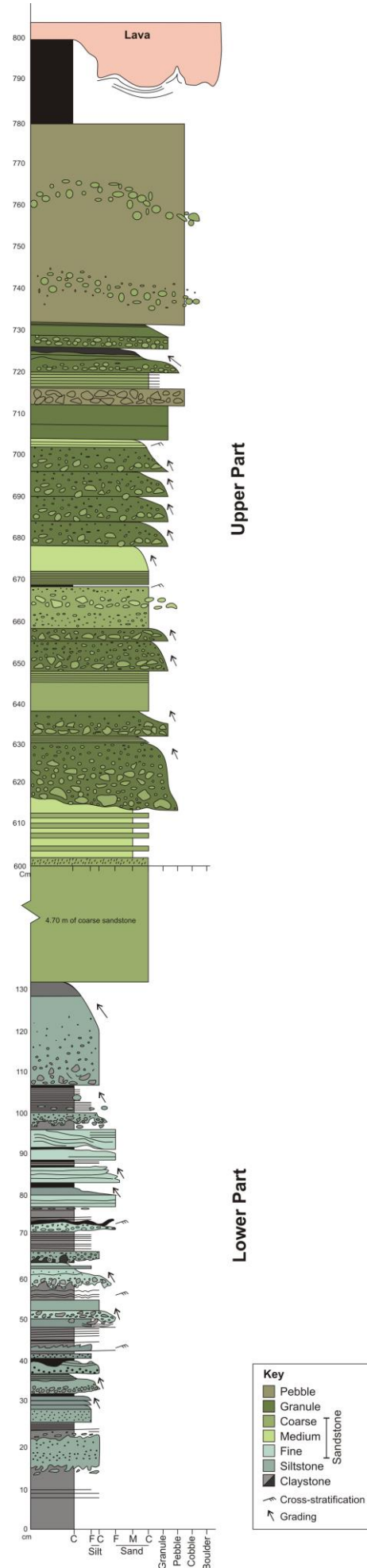
At Locality 2, an 8-10 m thick volcaniclastic unit (V1) is present between lavas L4 and L5 (Figure 3-2). The basal contact is not visible, whereas the upper contact reveals loading of the overlying columnar jointed lava onto a graded siltstone package, ~20 cm thick (Figure 3-12). The lavas, ~10 m thick, are basaltic, amygdaloidal, and have vesicular tops and bases, with massive coherent cores.

This volcaniclastic unit shows an overall graded sequence from finely laminated, siltstone and fine sandstone, ~1 m thick, into packages of medium to coarse sandstone. Some of the upper beds are granular, and have sub-rounded to rounded pebble-cobble sized clasts, which typically comprise vesicular basalt, ~5-10 cm across. Bedding (134/30° NE) is observed ~7 m from the base of the unit. The sequence can be divided into two parts, lower and upper, as shown in Figure 3-13 and Figure 3-14, and these are described below.



**Figure 3-12: Upper contact of the volcaniclastic unit (V1) at Locality 2.** The unit is capped by a thin siltstone and claystone unit, ~20 cm thick, that is overlain by basaltic, columnar jointed lava, ~10 m thick. The columnar joints display an irregular entablature style pattern. At the lava-sedimentary contact, the lava loads the underlying sediment (arrow), but peperite does not occur.

**Figure 3-13: (Next page) Graphic log of the volcaniclastic unit, V1, at Locality 2.** The unit can be split into 2 parts: lower and upper as shown. The lower part comprises fine-grained silt- and sandstone beds, whereas the upper part comprises sandstone and granular packages. The unit is capped by a siltstone bed, which is loaded by the overlying sub-aerial lava (L5).



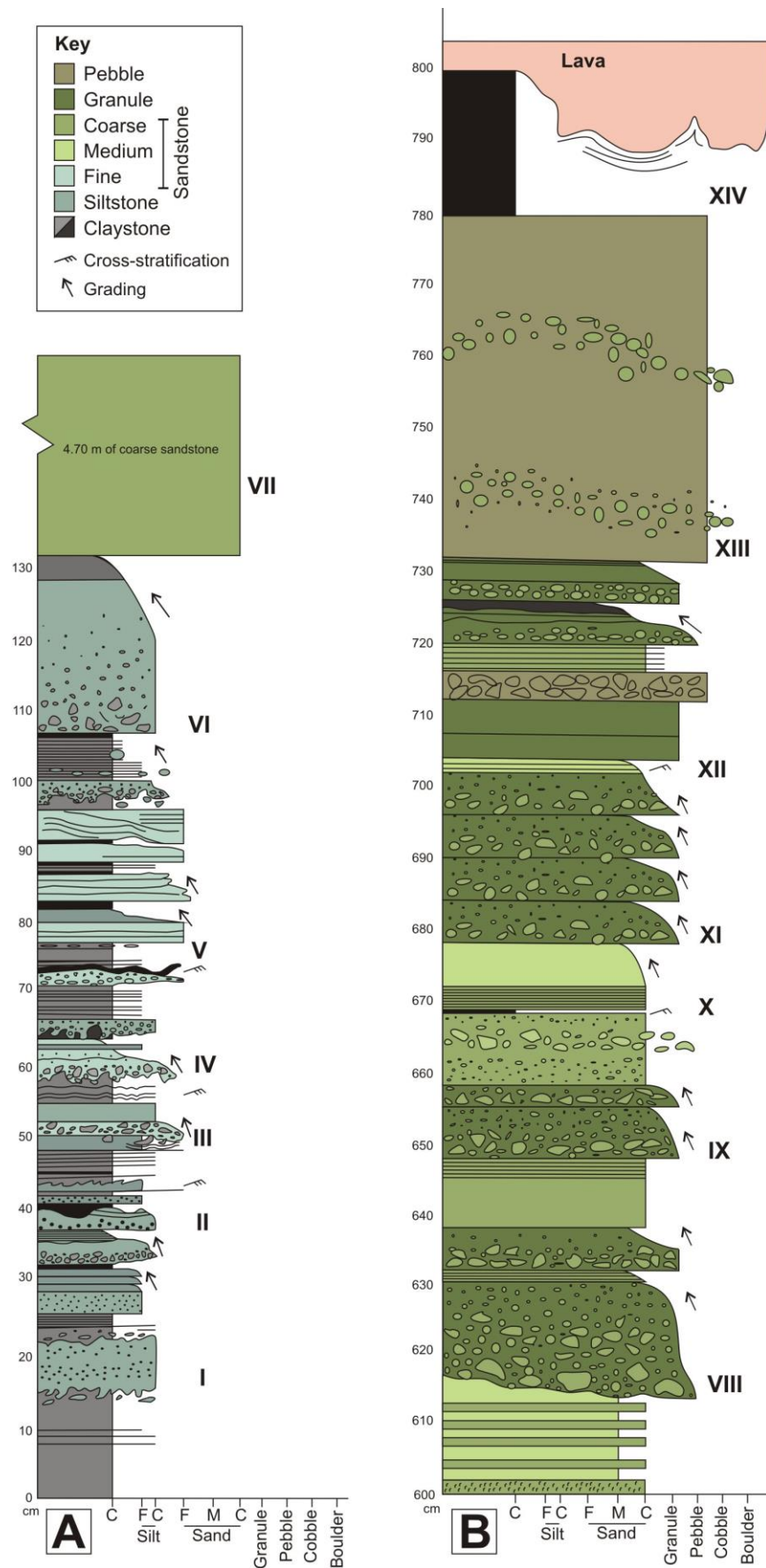


**Figure 3-14: Detailed graphical sketch logs through the volcaniclastic unit (V1) at Locality 2. A) the lower part is characterised by fine-grained claystone and siltstone packages, whereas B) the upper part is characterised by medium to coarse grained sandstone granular packages. Subdivisions I-XIV are key features referred to in text.**

The lower part of the volcanoclastic unit V1, (Figure 3-13 Figure 3-14 A) comprises interbedded dark grey claystone and siltstone, with light grey/green volcanoclastic siltstone (reworked tuff?) beds (Figure 3-15 A and B). There are ~40 beds in the lower 1.3 m, each ~1 cm thick, and they typically display normal grading. Within V1, wavy to ripple cross-laminations are observed, with common erosional and loaded bed surfaces (e.g. I, II, III Figure 3-14 A). Thicker beds are dominated by coarse siltstone to fine sandstone (pale green Figure 3-14 A), with some grains comprised of sub-angular to sub-rounded lithics and pumice fragments, <6 mm (e.g. I-IV, Figure 3-14, Figure 3-13 A, Figure 3-15 B). Small lenses of grey carbonate 'concretions' are present along a single interval at ~75 cm (V, Figure 3-14 A), near the top of a planar laminated siltstone bed that ranges in thickness from 6-15 cm. Within the upper coarse siltstone package at ~110 cm (VI, Figure 3-14 A), clasts of basalt lithics and pumice-like material occur ~1 cm above the base. Above 1.3 m (VII, Figure 3-14 A) V1 changes, comprising green/brown, fine to coarse sandstone fining-upwards packages. The basal packages are ~2-6 cm thick and interbedded with medium sandstone, which become coarser and thicker up sequence above 4 m. Fossil fragments, likely of brachiopod shells (VII Figure 3-14), are observed within the coarse sandstone.

The petrography of the lower part of V1 (Figure 3-14 A) is displayed in Figure 3-16. The lower units comprise fine scale bedding and laminae of graded volcanoclastic siltstone and fine sandstone (e.g. units III-V, Figure 3-14 A), with lithic clasts, relict bubble-wall shards and pumice fragments.

The upper part of V1, above 6 m (Figure 3-14 B), comprises fining upward packages of medium to coarse sandstone and granular packages, which range in thickness from 3-10 cm, although most are 8-10 cm (Figure 3-14 B, and Figure 3-15). Coarse granules, 1-3 cm, are dominant at the base of most packages before fining upwards to coarse, laminated sandstone (e.g. VIII, IX, XI and XII, Figure 3-14). Granules and pebbles predominantly comprise vesicular, sub-rounded, basaltic clasts and pumiceous fragments (Figure 3-15 E). Wavy to ripple cross-lamination is observed within the coarse sandstone bed at 6.7 m (X) and 7 m (XII, Figure 3-14 B). At ~ 6.2 m (VIII), 6.5 m (IX) and 6.8 m (XI, Figure 3-14), sandstone laminae are loaded by occasional and isolated, sub-angular, vesicular basalt clasts, ~5-6 cm (Figure 3-15 F). The top of the sequence is capped by 20 cm of finely laminated claystone and siltstone, and overlying basalt lava (Figure 3-12, Figure 3-14 B).



**Figure 3-15: Features of the volcanoclastic unit, V1, at Locality 2, Kinghorn.**

**A)** Finely bedded lower portion of V1. Pen knife is ~8 cm. **B)** Hand specimen of the lower part of V1 highlights the detail of ~8 beds within this unit. Fine, cm-scale bedding and laminae are observed, with normally graded beds (arrows) and loading (dashed lines/clast outlined in yellow). Coarser, granular beds with lithics and pumice-like grains are observed, such as the one above the dashed line. Letters (A-K) refer to petrography images in Figure 17. Scale on ruler is cm. **C)** Fossil fragments observed within the lower part of the V1, VII (Figure 15), ~2 m (yellow outline). Lens cap is ~5 cm diameter. **D)** Medium-coarse grained sandstone beds (a-d) within the upper part of V1 (yellow dashed lines). Displacements and drag indicate minor, possibly syn-sedimentary faulting. Ruler covers the interpreted fault. **E)** Pebbles and cobbles of sub-rounded vesicular basalt (yellow outlines) are typical of the upper part of V1. Ruler is 15 cm long. **F)** Isolated vesicular basalt cobble, ~7 cm across (yellow outline), within a medium sandstone bed, found at ~6.2 m, VIII (Figure 3-14).

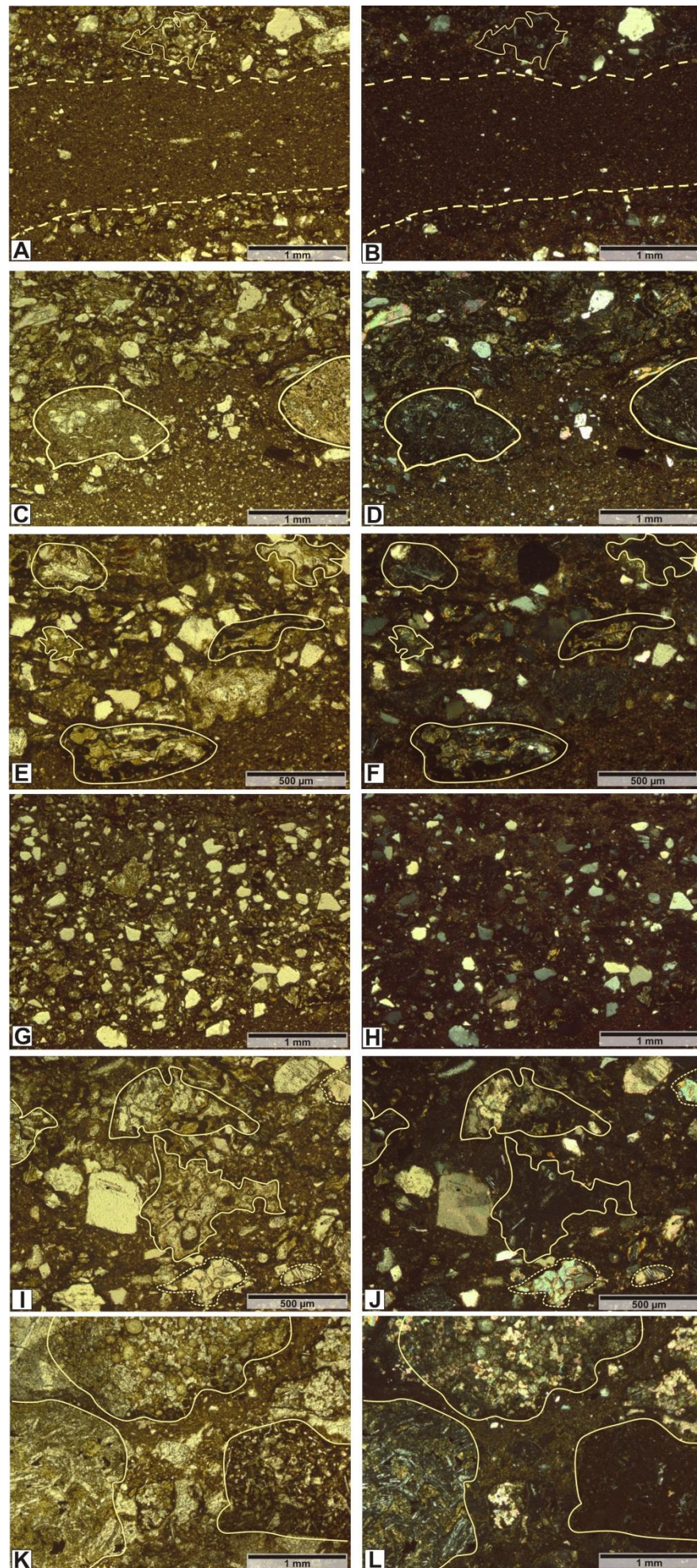


**Figure 3-16: (Previous page) Photomicrographs of the volcanoclastic unit, V1, at Locality 2.**

Images A, C, E, G, I, K are PPL, B, D, F, H, J, L are XPL. Locations of images are shown in Figure 16 B (A-K). A and B) A thin (~1 mm) very fine grained siltstone bed has sharp lower and upper contacts with coarser sandstone beds. The sharp contacts are typical of the sequence. In the upper coarse sandstone, angular grains of basalt are observed (yellow outline). C and D) The contact between two graded beds within the lower part of V1. Large basalt lithics lie at the base of a graded volcanoclastic siltstone and fine sandstone bed. E and F) A coarse granular volcanoclastic bed with relict bubble wall shards and basaltic lithic grains (yellow outline) at its base. G and H) Typical fine grained volcanoclastic sandstone, as seen throughout the lower V1. Grains include a high abundance of quartz, with volcanic lithics, plagioclase crystals and clay minerals. I and J) Scoriaceous fragments are preserved within the reworked volcanoclastic sediment. K and L) Coarse grained granular lithic-dominated bed, with basalt lithics (yellow outline).

### 3.3.2.3 Carbonate units

There are two distinctive carbonate units within the succession: the St. Monans White Limestone (SMWL) (Locality 7) and the Hurllet Limestone (HL) (Locality 9), both well-known units of the Carboniferous within the Fife and Midland Valley area.

The SMWL is the older of the two units and is observed at Locality 7 (Lst1 Figure 3-2), where it overlies siltstone and sandstone units belonging to the Pathhead Fm. The SMWL comprises massive, light grey carbonate beds (Figure 3-17 and Figure 3-18), typically 15-85 cm thick, locally interbedded with thin beds of claystone and fine siltstone (2-5 cm). Fossils are mostly absent, but *Zoophycus* traces occur at the top of some limestone beds (Figure 3-18). The unit is capped by laminated fine sandstone that grades into siltstone (~20-30 cm thick), which is overlain by basaltic lava (L14). Loading and flame structures are observed at the lava-sediment contact, and are described further in section 3.3.3.



**Figure 3-17: The lower limestone unit in the Kinghorn succession. This comprises the St. Monans White Limestone, which is overlain by a siltstone unit and sub-aerial basalt lava. The limestone unit comprises massive carbonate beds with *Zoophycus* trace fossils. Seated person for scale.**

The HL at Locality 9 (Lst2 Figure 3-2) forms the base of the Lower Limestone Formation and overlies pyroclastic and sedimentary units (S7) at the top of the succession (Figure 3-2). The HL is ~3.5 m thick and comprises multiple fossil-rich, bioclastic limestone beds, ~15-35 cm thick (Figure 3-18 C and D) that are interbedded with fissile, organic-rich mudstone and coal beds. The limestone beds contain numerous Carboniferous fossils, typically broken, including bivalves, brachiopods, crinoid ossicles and coral (Figure 3-18).

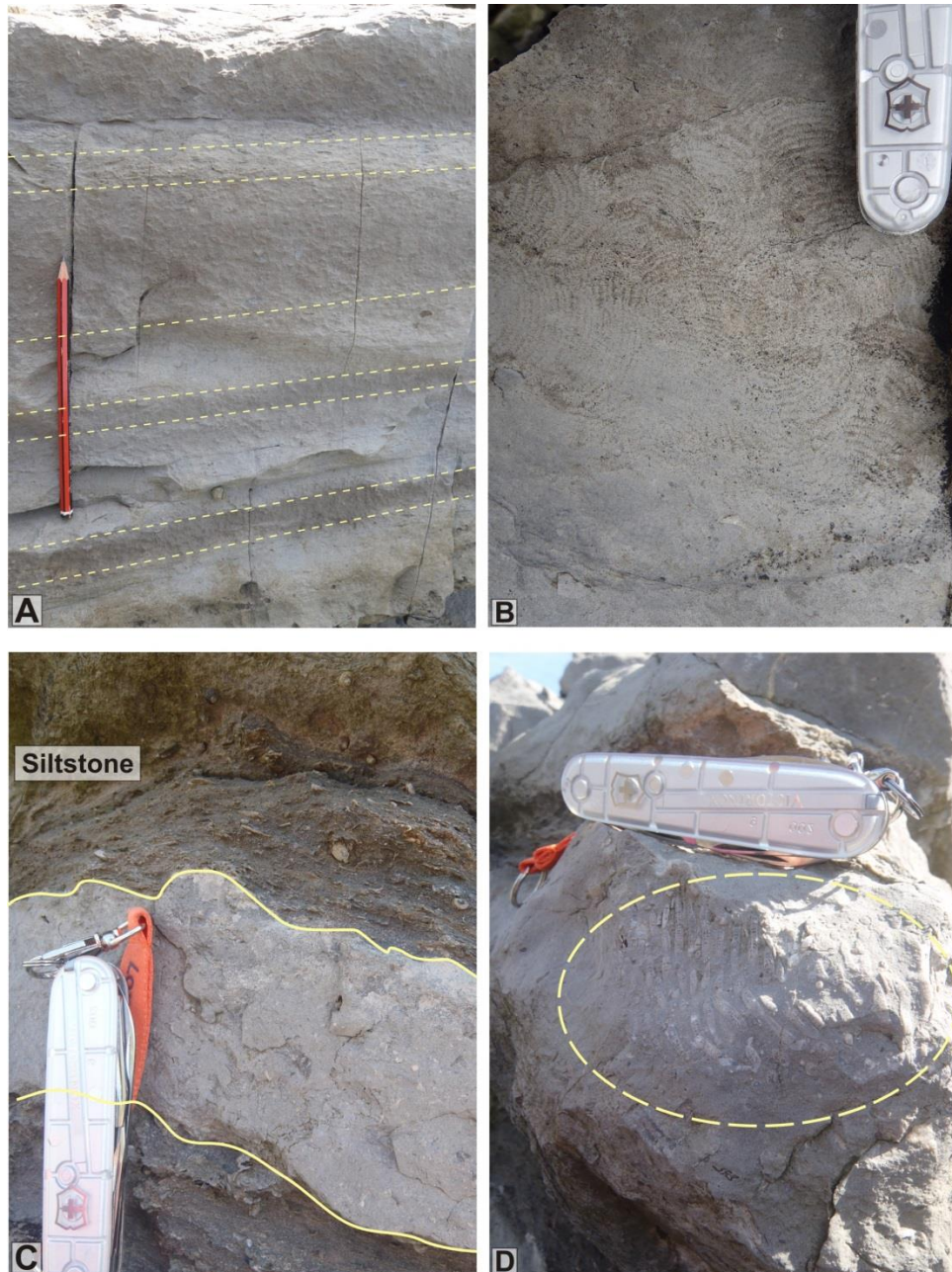


Figure 3-18: Characteristics of the two main carbonate units within the Kinghorn succession.

A) Typical view of the St Monans White Limestone (SMWL), Locality 7 (Lst1). Feint lamination (dashed lines) is observed within the otherwise massive carbonate beds. B) *Zoophycus* trace fossils are preserved within the tops of the carbonate beds of the SMWL indicating a shallow marine, possibly lagoonal environment. C and D) are from the upper carbonate unit, the Hurlet Limestone (HL) at Locality 9 (Lst2). C) Small individual carbonate beds, ~3-5 cm thick (pale grey with yellow outline), are interbedded with fissile, fine siltstone beds that contain fragmented fossil shells. D) Numerous coherent fossils, including coral (yellow dashed outline), are found within the carbonate beds of the HL. Scale: pencil is 15 cm long; pen knife is ~8 cm long.

### 3.3.3 Lava-Sedimentary Contacts

Throughout the succession the nature of the lava-sediment interface ranges from planar with no interaction, to peperitic. These contacts are described below, from oldest to youngest.

Figure 3-19 illustrates the relationships between lava and sediment at Locality 1. The finely laminated siltstone bed (S1) underlying the lava (L2) (Figure 3-19) is ~60-120 cm thick and contains lens-shaped nodules, ~15 cm thick. The lava-siltstone contact is irregular with small, cm size, load structures. There are a variety of relationships on a small (2 m) scale at the same contact, such as isolated lava blebs. An isolated, detached, lava bleb, (Figure 3-20 D), which is 20 cm wide and globular with irregular edges, is exposed close to the base of the siltstone unit. Small, 2-8 cm, irregular siltstone inclusions are also found within the lava (Figure 3-20 A). A “melange” (no tectonic implication) of basaltic lava (pale grey), siltstone (dark grey) and pale grey laminated claystone (possibly reworked volcaniclastic material) is also observed at Locality 1 (Figure 3-20 C). In places, small-scale peperite (~4-6 cm) is present, where the siltstone and juvenile lava clasts mingle (Figure 3-20 B). Juvenile clasts are 0.2-10 mm across and have irregular and blocky morphologies.

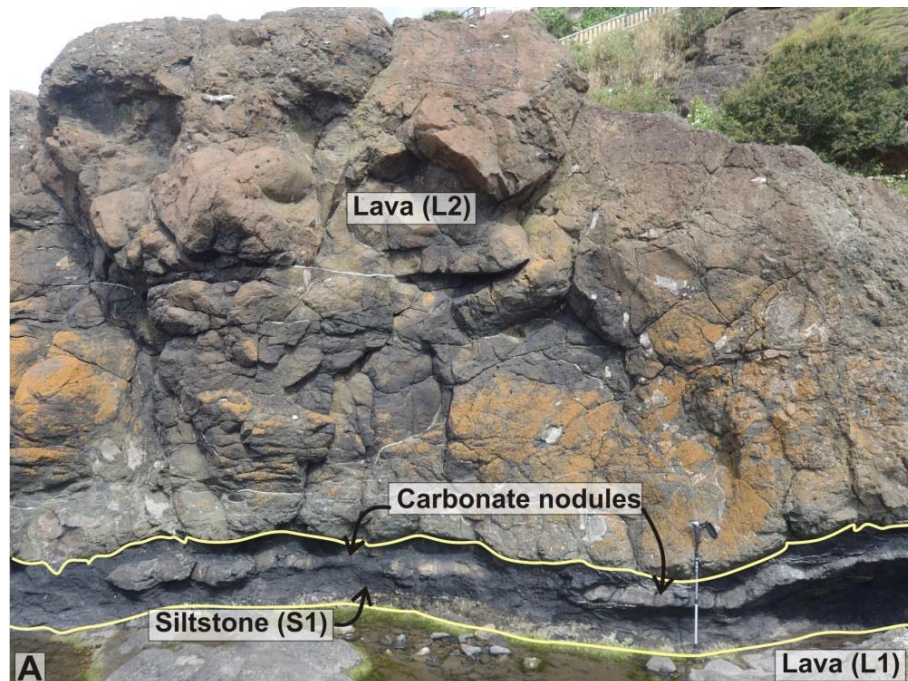


**Figure 3-19: The lava-sedimentary contact at Locality 1, Kinghorn. A thin bed of siltstone (S1), containing lenticular carbonate nodules is overlain by amygdaloidal basalt lava (L2). The lava-siltstone contact is typically sharp, but locally involves small scale (mm-cm) loading and deformation of the siltstone.**

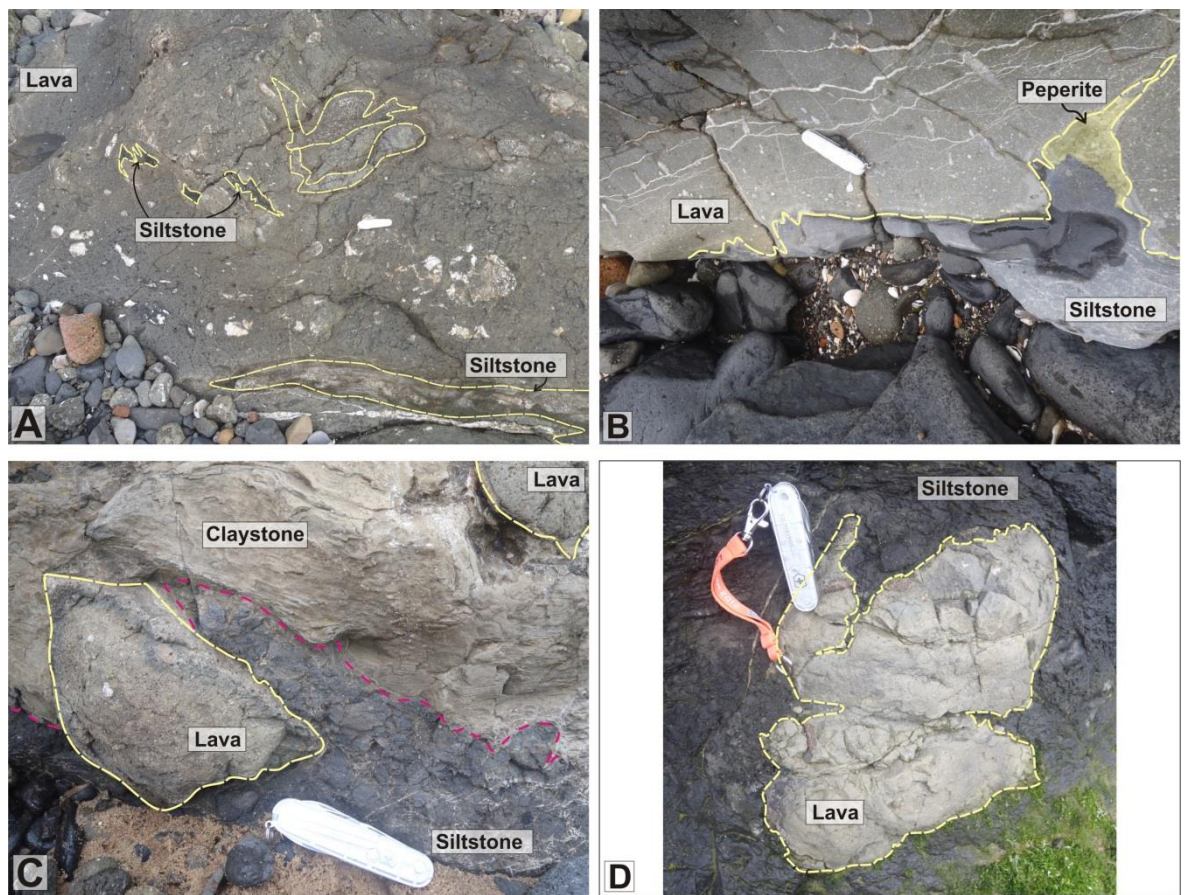


**Figure 3-20: Features of the lava (L2) and interaction with underlying siltstone and claystone, at Locality 1.**

**A)** Amygdaloidal basalt with small, ~5 cm, sediment inclusions (areas highlighted with yellow dashed outlines) at the lava base. Inclusions suggest sediment was fractured and incorporated into the lava during emplacement. **B)** Irregular lava-sediment contact with small-scale peperite, comprising mm-cm size juvenile lava clasts (yellow shading). **C)** A “melange” of lava (dashed yellow outline), siltstone (dark grey) and claystone (pale grey). The contact is irregular (red dashed line) and slightly invasive between lava blebs and sediment. **D)** A large (~12 cm across) detached and apparently isolated mass of basaltic lava with ‘fluidal’ margins, implying its juvenile (magmatic) character at the time of interaction and incorporation into the originally unlithified silt(stone). Penknife is 8 cm long.

At Locality 4, the lava (L8) is massive and prismatically jointed, forming pseudo-columns each ~0.5-1.5 m across and 10 m long (Figure 3-3), and overlies a red-weathered volcanoclastic sandstone (R1). At its base, the lava is locally peperitic (Figure 3-21), with the zone of magma-sediment interaction typically 60-70 cm thick. Juvenile lava clasts are 3 to 10 cm in diameter, and typically have crenulated fluidal margins and morphologies. Some clasts have small-scale blocky jigsaw-fit textures, but these are rare and difficult to distinguish as the peperite is, in most places, extremely weathered. The matrix comprises fine-grained sandstone (Figure 3-21). Rare clasts of siltstone are also found within the peperite and are distinguishable from the fine-grained matrix.

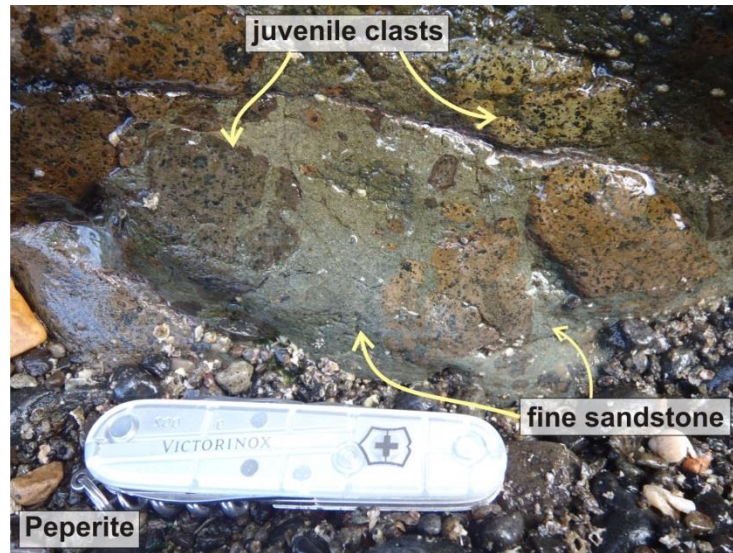


**Figure 3-21: Peperite at the base of lava (L8) at Locality 4.**

The juvenile clasts show a range of morphologies from globular to blocky with jigsaw-fit textures, and are held within a fine sandstone host. Pen knife is 8 cm long.

The lava -sediment contact, at Locality 7 (L14, Figure 3-2) overlying the SMWL (Figure 3-22), displays distinctive flame structures, ~50 cm long (Figure 3-23). The sandstone and siltstone interval, ~20-30 cm thick, is loaded by the overlying lava, which forms load casts with cusp and dome geometries (8-25 cm across) (Owen 2003), and ball and pillow structures (Hall and Els 2002) as well as flame structures (20-50 cm long). Lamination within the siltstone is mostly preserved, and is typically deformed around the load structures. Isolated detached lava blebs (from the main lava body) or pseudonodules are not observed and there is no evidence of peperite formation.



**Figure 3-22: Typical outcrop view of Locality 7 at Kinghorn.**

The St. Monans White Limestone (blue) is overlain by fine-grained sedimentary units of the Pathhead Fm (yellow), which the overlying lava (L14) loads. Person for scale (sat down).

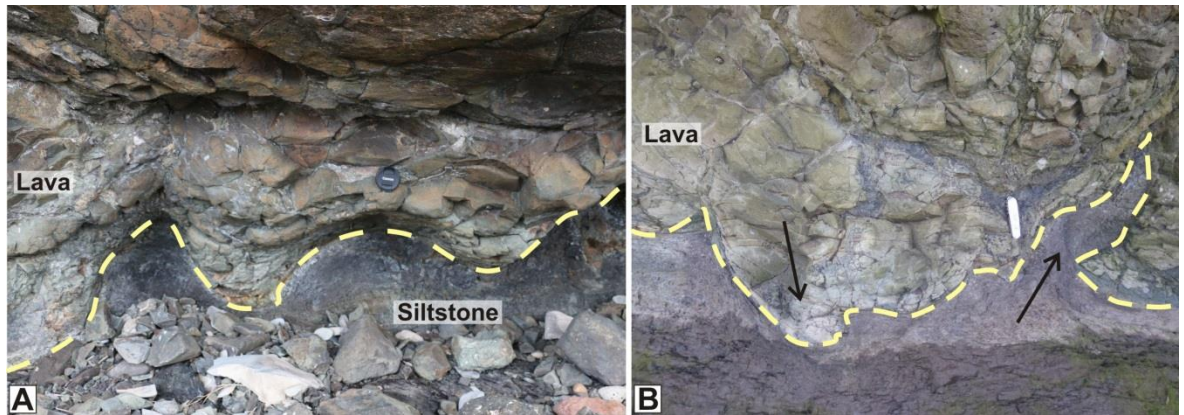


**Figure 3-23: Loading features observed at Locality 7, Kinghorn.**

Lava loads onto the underlying siltstone, forming load casts with cusp and dome geometries, or ball and pillow structures (A) and flame structures (B). Bedding is mostly retained within the siltstone at and near the contact. Scale: A) Camera lens cap, ~5 cm diameter. B) pen knife for scale ~8 cm.

## 3.4 Interpretation

### 3.4.1 Volcanic Units

#### 3.4.1.1 Lava

The basaltic lavas of the Kinghorn Volcanic Formation with their massive cores and vesicular tops and bottoms, and the absence of basal and upper autobreccias typical of 'a' a lavas, are interpreted as sub-aerial inflated pahoehoe-type flows (Self et al. 1998). Characteristic ropey textures are not preserved, possibly as a consequence of weathering and erosion. The development of columnar joints, suggests the flows ponded prior to the final crystallisation (Long and Wood 1986; Williamson and Bell 1994; Lyle 2000; Williamson and Bell 2012). Reddening of the tops of certain lavas, and of inter-lava beds, suggests hiatuses in the effusion history and prolonged exposure to weathering (oxidisation) and erosion, before resumption of volcanic activity and further lava emplacement. This period of volcanic quiescence enabled re-establishment of the drainage system and deposition of the various inter-lava siliciclastic/volcaniclastic units. The presence of pyroclastic material (see petrographic details in Figure 3-7 and 3.3.1.3) suggests volcanic activity did not cease, but changed from effusive to explosive. This is indicative of a landscape that developed volcanic cones, which were possibly phreatomagmatic (Rex and Scott 1987, Stephenson et al. 2003). Although the majority of the lavas were emplaced sub-aerially, some have encountered water and/or saturated sediment (Stephenson et al. 2003), leading to the formation of hyaloclastite and pillow breccia, and peperite at the lava-sedimentary interface.

### 3.4.1.2 Hyaloclastite

The H1 unit at Locality 6 (Figure 3-2, Section 3.3.1.2) is hyaloclastite, formed as lava quenched and fragmented during emplacement into a water body. The characteristics of the passage zone and the overlying sub-aerial lavas suggest that the lava was initially sub-aerial and emplaced into a water body, rather than wholly sub-aqueously erupted. Depth of the water body can be inferred from the thickness of the hyaloclastite unit, which is ~30 m thick (Schmincke et al. 1997). Grading of the hyaloclastite from coarser fragmental material (5-50 cm), to fine grained material (<2 mm) suggests that the hyaloclastite was possibly reworked within the water column and down slope, as continual emplacement built a lava delta and filled accommodation space (Jones and Nelson 1970; Furnes and Fridleifsson 1974; Furnes and Sturt 1976; Cas and Wright 1987; Skilling 2002; White and Houghton 2006; Watton et al. 2013). At this point in the succession, a significant basin (with accommodation space) was established, possibly related to subsidence and extension and sea level rise (Macdonald and Fettes, 2007), with volcanism extending beyond the basin margins.

### 3.4.1.3 Lapilli Tuff

The development of a lapilli tuff unit (Section 3.3.1.3, Figure 3-8), with a layer of coated pellets (ash aggregates), suggests that localised phreatomagmatic eruptions occurred, indicating the likely presence of groundwater, and/or surface water, and/or atmospheric moisture (Gilbert and Lane 1994; Ritchie et al. 2002; Branney et al. 2008; Durant et al. 2008; Durant and Rose 2009; Brown et al. 2010; Brown et al. 2012). Coated pellets (e.g. Figure 3-9), form as particle aggregation and agglomeration occurs during explosive volcanic eruptions (e.g. Brown et al. 2010). They are typically associated with pyroclastic density currents (PDCs) and the co-ignimbrite/phoenix-clouds that are lofted above the PDC (Self 1983; Branney and Kokelaar 2002; Brown et al. 2010; Brown et al. 2012). Brown et al. (2010) proposed a model for the temporal formation of ash pellets and accretionary lapilli. Finer-grained ash particles that are lofted within the phoenix clouds (above the ground-hugging density current) agglutinate within the moisture-rich cooler parts of the cloud, forming ash pellets. As the ash pellets become heavier they drop into main part of the density current where, subject to turbulence, they accrete concentric laminae around the original nucleus, forming accretionary lapilli (Brown et al. 2010). They are then deposited alongside ash and pumice. Ash pellets that remain in the buoyant plume fall out in the wake of the main current where they accrete just a single outer layer, and form coated ash pellets (Brown et al. 2010). Any pellets that remain after the passing of the plume fall out as ash pellets (Brown et al. 2010). Van Eaton et al. (2012) interpret ash pellets to have

formed during saturated conditions (phreatomagmatic), with nucleation and coalescing of the particles, followed by transportation and deposition in a saturated environment (e.g. a lake).

The ash aggregates observed at Kinghorn, are akin to the coated pellets described by Brown et al. (2010), or massive and coalesced ash pellets described by Eaton and Wilson (2012) (i.e. ash pellets with defined single outer rims of finer grained ash, typically of 2-6 mm). Their presence most likely indicates phreatomagmatic eruptions from monogenetic volcanoes, which generated PDCs and built maars/tuff rings/tuff cones. Such volcanism is widely reported in the Carboniferous of the Midland Valley (e.g. Macdonald and Fettes 2007; Gernon et al. 2013). The relatively thin layer of coated ash pellets, encased between layers of fine tuff may indicate a relatively short-lived eruption, bypassing of the depositing PDC (explaining the lack of accretionary lapilli in the tuff underlying the coated ash pellets, (Branney and Kokelaar 2002), or a distal source. Further evidence for explosive activity is provided by relict tube pumice shards observed in the petrographic analysis (Figure 3-9).

The change in eruptive style from lava effusion to explosive phreatomagmatism may also record a change in the local environment, with a dominantly sub-aerial lava field, giving way to a landscape with shallow lagoons or lakes (possibly swampy due to deposition of organic-rich shales) punctuated by small volcanic cones (Scott 1990; Van Eaton et al. 2012). This supports the previous interpretation of Rex and Scott (1987); Stephenson (2003).

## **3.4.2 Sedimentary Units**

### **3.4.2.1 Clastic Units**

The siliciclastic and volcanoclastic units between Localities 1-5 (Figure 3-2) belong to the Sandy Craig Fm (Table 2), whilst those above the hyaloclastite unit at Locality 6 (Figure 3-2), belong to the Pathhead Fm (Table 2). The thin units (2-5 m thick) of volcanoclastic siltstone and sandstone, which comprise sub-rounded grains of quartz, feldspar and reworked basalt lithics, and display planar to wavy bedding, are interpreted as fluvial to nearshore/lacustrine deposits, or were possibly deposited within small isolated water bodies (Rex and Scott 1987; Stephenson 2003). Deposition would have occurred within troughs and hollows in the underlying volcanic landscape. These intercalations represent a renewed sediment drainage system that reworks the

---

volcanic landscape during periods of volcanic quiescence (e.g Dohrenwend et al. 1987; Williamson and Bell 2012; Schofield and Jolley 2013; Ebinghaus et al. 2014).

### **3.4.2.2 Volcaniclastic Unit (V1)**

During a hiatus in lava emplacement, sedimentation re-established within the basin, depositing fine clay and silt, both siliciclastic and volcaniclastic in nature (Section 3.3.2.2). Individual units show cross-bedding and erosional features (e.g. rip-up clasts) suggesting a depositional environment with at least a moderate energy, but not strong enough to indicate a tidal or shallow marine environment. The most likely environment was a small lake, as sedimentation is both quick to recover and disappear. The lake was possibly hypersaline, within close proximity to the marine basin, allowing carbonate muds and broken shells to be deposited, most likely due to storm influences (Kreisa 1981; Allen 1982; Mount 1984; Leeder 2009). The coarsening-upward motif of the unit suggests further development of a fluvial-lacustrine setting with fine material eroded and deposited first, followed by more substantial erosion of the volcanic landscape and inundation of basaltic material into the sedimentary system. The presence of basaltic blocks, up sequence, suggests a potential explosive phase of volcanic activity, which produced primary ballistic blocks, or alternatively, basalt blocks were transported and reworked within the fluvial system (Kataoka 2005; Paredes et al. 2007; Umazano et al. 2008; Manville et al. 2009). Reworking of volcanic material into the lacustrine environment is most likely. The reworked fine ash and lapilli deposits observed at the base of the unit (Figure 3-13, Figure 3-16, V1) further support the reworking of explosive volcanic material within an otherwise volcanic hiatus. The top of the unit is marked by a siltstone bed, indicating a return to background sedimentation, and perhaps a halt in fluvial input. The overlying, sub-aerial columnar jointed lavas mark the resumption of effusive volcanism.

### **3.4.2.3 Carbonate Units**

Both of the carbonate units present in the sequence have previously been described and interpreted within the Fife-Midlothian Basin and are representative of the tropical climates that dominated during the Carboniferous. The lower of the two, the St. Monans White Limestone unit of the Pathhead Fm (Stephenson 2003; Upton et al. 2004; Underhill et al. 2008), provides evidence for a lagoonal/shallow marine environment with the onset of carbonate production, followed by a shallowing and choking of carbonate production by a siliciclastic input. A small transgression and regression is inferred with a movement from siliciclastic to carbonate and back to siliciclastic dominated sedimentation. This may also have been controlled on a regional level, by

---

tectonics, subsidence and associated volcanism (Macdonald and Fettes 2007; Underhill et al. 2008). The Hurlet Limestone Fm marks a change in carbonate production, with thin, fossil-rich beds interbedded with organic-rich shale and coal. This represents a lagoonal/swamp environment with possible marine storm influences and deposits; this setting is typical of the Carboniferous Period (Rex and Scott 1987; Browne et al. 1999; Stephenson et al. 2003; Upton et al. 2004; Macdonald and Fettes 2007).

## 3.5 Discussion

The succession of interbedded basaltic lavas and sedimentary rocks at Kinghorn provides evidence for three main types of lava-water-sediment interaction, (hyaloclastite ± pillow lava are also present): i) loading and soft-sediment deformation; ii) 'passive' peperite; and ii) 'dynamic' peperite. These products are indicative of a dynamically changing environment dominated by both sedimentation and volcanic activity. The interaction types are discussed further, using models to illustrate the processes of interaction.

### 3.5.1 Loading and soft-sediment deformation

Loading and soft-sediment deformation by lava may occur on a number of scales. At Locality 7 (Figure 3-2, Figure 3-22, Figure 3-23) the deformation is decimetre scale and well defined with minimal interaction between the lava and sediment. Flame structures and ball and pillow structures are observed (Figure 3-23), and bedding is typically preserved (Figure 3-23). These features have been related to Rayleigh-Taylor instabilities (Visher and Cunningham 1981; Owen 2003), shear stresses exerted by the lava flow, and reverse density gradient contrasts at the lava-sediment interface (Visher and Cunningham 1981; Hall and Els 2002). Hal and Els (2002) have interpreted loading and flame structures as the result of the sediment being water-saturated, enabling an increase in both hydrostatic and lithostatic pressures, and eventually leading to fluid escape into the overlying lava. However, the term 'saturation' has not been formally defined, and it is likely that a scale of saturation along with other sediment properties plays a role in the development of loading and deformation structures.

In this study, where loading and soft-sediment deformation is observed, and peperite is absent, the sediment state is interpreted as slightly compacted and consolidated, with minimal pore water at the time of lava emplacement (Figure 3-24). The sediment is (further) compacted by the overlying lava and, due to density contrasts and the presence of minimal pore water, flame structures and pseudonodules may develop (Figure 3-24). Consolidation of the sediment means that the bedding structures are preserved within the deformed sediment (Figure 3-24) and that fluidisation and liquefaction is inhibited (Busby-Spera and White 1987; Skilling et al. 2002\_ ). This sediment state (a combination of all properties) also impedes the quenching and fragmenting of the lava, and therefore mingling does not occur.

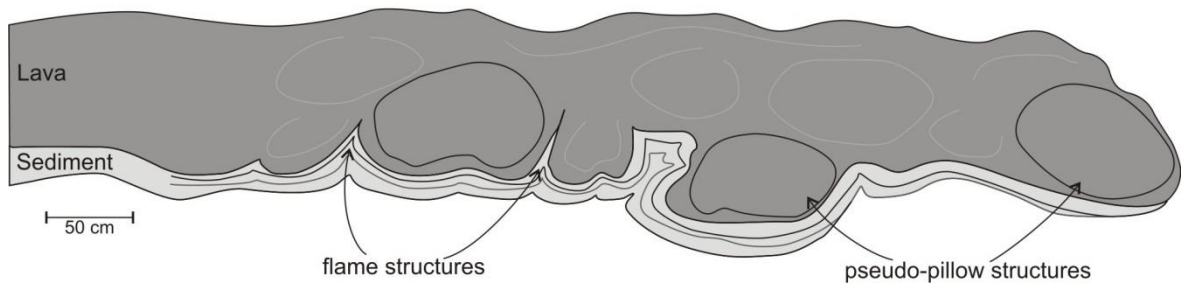


**Figure 3-24: Schematic illustration of soft-sediment deformation and loading of sedimentary units by lava.**

**Minimal lava-water-sediment interaction occurs, but flame structures form as the lava loads the underlying sediment, and bedding is preserved. The lava may form pseudo-pillow/ball-and-pillow structures that do not detach from the lava body. Sediment is likely to be partially consolidated and compacted with minimal to no pore water.**

### 3.5.2 Peperite – ‘passive’ interaction

At Kinghorn, localised peperite is observed at the base of lava, L8 (Locality 4). Typical peperite characteristics are recorded, such as mixed morphologies of globular and blocky juvenile clasts, and jigsaw-fit textures (Figure 3-21). Peperite has been documented as forming at the base of lava flows, and at the margins of intrusions (e.g. Kokelaar 1982; White et al. 2000; Skilling et al. 2002; Zimanowski and Büttner 2002). As sub-aerial lava is emplaced and flows over unconsolidated, wet sediment, it quenches and fragments, forming juvenile clasts, whilst simultaneously mingling with the host sediment (White et al. 2000; Skilling et al. 2002). Sedimentary structures away from the mingling zone are preserved, and truncated by the peperite (e.g. Figure 3-25 and Skilling et al. 2002).

This *in situ* interaction process is typically localised rather than occurring ubiquitously along the lava-sediment contact, most likely due to minor differences in the sediment state. For this style of limited ‘passive’ interaction, the sediment properties most likely control the degree of interaction and mingling of the lava and host sediment. The sediment is likely unconsolidated, uncompacted, and relatively saturated with saturation due to substantial pore water or infiltration from an overlying isolated water body. The well-developed fluvial-lacustrine depositional system interpreted for Kinghorn supports these conditions. Nonetheless, the sediment stat does not support the thorough mixing and extensive disaggregation of the lava.

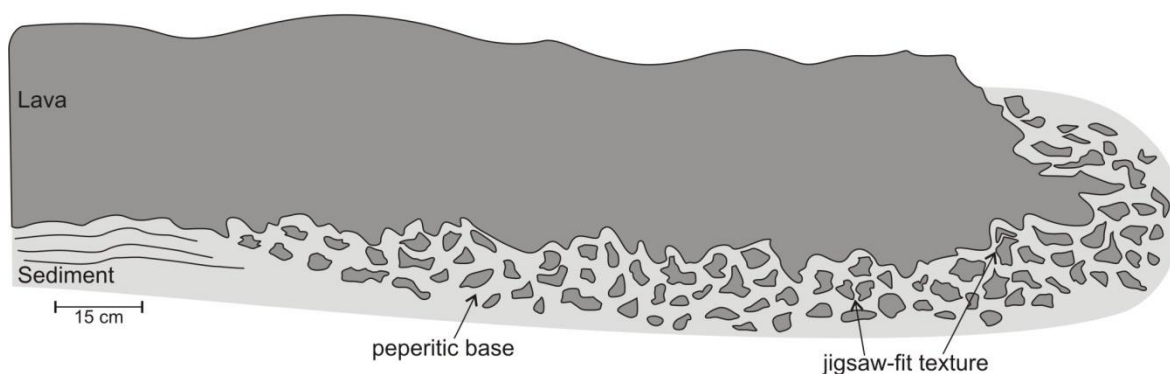


**Figure 3-25: “Passive” interaction and the formation of peperitic margins ( $\pm$  pillows/hyaloclastite), typically at the base and frontal margins of the lava.**

**The base of the lava interacts with the unconsolidated, saturated sediment, forming juvenile clasts that mingle with the sediment. Sedimentary bedding and structure is destroyed within the mingling zone but preserved elsewhere.**

### 3.5.3 Peperite - ‘dynamic’ interaction

Examples of dynamic magma-sediment interaction are not common within the Kinghorn section; however, some features are preserved at Locality 1 and 7.

Sub-aerial lava invades the host sediment by burrowing and bulldozing of lava fingers, which disaggregate and mingle with the disrupted host sediment (Jerram and Stollhofen 2002; Brown and Bell 2007; Palinkaš et al. 2008). Peperite occurs at both the upper and basal margins of the lava fingers (Figure 3-26), with larger, isolated lava blebs detached from the main lava body (Locality 1, Figure 3-20), and sediment inclusions found within the lava lobes (Locality 1, Figure 3-20 and Locality 7). For this interaction to occur, the sediment is interpreted as being unconsolidated, uncompacted, and supersaturated (excessive water content and availability), thus enabling the lava to disrupt the sediment whilst simultaneously fragmenting/disaggregating and mingling, forming a complex interface. Key characteristics of this ‘dynamic’ interaction include upper peperite margins to the lava fingers, and sedimentary inclusions within the lava, although these are not mutually exclusive features.

Table 3 summarises the main features of passive and dynamic peperite, highlighting the differences and similarities between them. Differences in the sedimentary properties, such as saturation, appear subtle; however, the degree of interaction, and resultant peperite domains that form, are remarkably diverse.

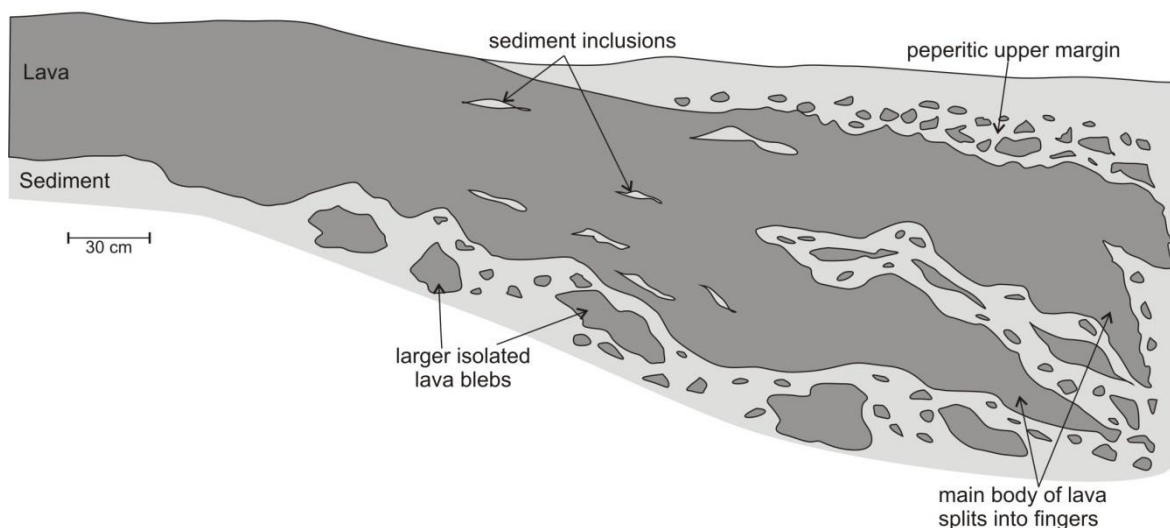


**Figure 3-26: “Dynamic” interaction and the formation of invasive disaggregated peperite. Lava invades and shallowly burrows into the unconsolidated, saturated sediment, producing peperite at both the basal and upper margins of the lava fingers. Sedimentary inclusions may also be incorporated into the main lava body.**

Key Features	Passive Peperite	Dynamic Peperite
Location	Forms at the base and frontal margins of sub-aerial lava as it flows over underlying sediment	Occurs at all margins, including the upper margins, of the lava lobes as the sub-aerial lava invades and bulldozes the sediment
Peperite domain	Limited to the base of the lava and the upper parts of the sedimentary domain	Interaction is unconfined as the lava shallowly burrows into the sediment, typically mingling with the entire sedimentary domain.
Mingling zone/ interface	Simple with typical peperite characteristics, including a range of juvenile clast morphologies	A complex interface between invasive lava and sediment forming a disaggregated peperite.
Peperite characteristics	Peperite typically comprises similar sized, or graded, juvenile lava clasts within a sedimentary host.	Peperite comprises juvenile lava clasts, with additional larger, isolated lava blebs and coherent sedimentary inclusions with a sedimentary host.
Host sediment features	Sedimentary structures close to the mingling zone are preserved but truncated by the peperite. Sediment inclusions are rare.	No preservation of sedimentary structures, but sediment inclusions found within the lava and peperite domain.
Host sediment properties	Sediment is interpreted as: unconsolidated, uncompacted-slightly uncompacted and (semi) saturated. Saturation is either by pore water or infiltration from overlying water body.	Sediment is interpreted as: unconsolidated, uncompacted and (super)saturated. Saturation is due to pore water or infiltration from overlying water body.

**Table 3: Summary of the key features of passive and dynamic peperite.**

A simplistic, overall model that integrates the three types of lava-sediment interaction with the representative sedimentary properties is presented (Figure 3-27). The model highlights the scale of lava-water-sediment interaction from minimal (loading and soft-sediment deformation), through passive to dynamic (peperite), within a single succession, as seen within this field study. The main influencing factor of interaction is interpreted as the properties of the host sediment (e.g. the degree of consolidation, saturation level, cohesion, and grain size of the sediment) (e.g. Busby-Spera and White 1987; Doyle 2000; Dadd and Van Wagoner 2002; Skilling et al. 2002), together with the key properties of the lava (e.g. effusion rate/flux, composition, viscosity) (e.g. Busby-Spera and White 1987; Doyle 2000; Dadd and Van Wagoner 2002; Skilling et al. 2002). This study has concentrated on the sediment properties, assuming that these control the overall evolution of interaction with lava, and that the driving mechanisms and properties of the lava (i.e. effusion rate, thickness, morphology and density) are essentially the same throughout (all the lavas in the Kinghorn section display similar compositions and field relationships). Consequently, water saturation and consolidation levels of the sediment are considered the most significant influencing factors of interaction between lava and sediment in this study, and their resultant products (Table 3).

The three 'end-member' styles are produced in this single, relatively thin succession (Figure 3-27), and this is significant when considering other field case studies. Peperite is widely reported from intrusion margins, but less so from sub-aerial lavas. This study demonstrates that lava-water-sediment interaction is more common than previously thought, and that a subtle, but complex, range of products may develop. Both temporal and spatial changes in sediment properties can produce diverse products at lava-sedimentary contacts, and provide important palaeo-environmental information.

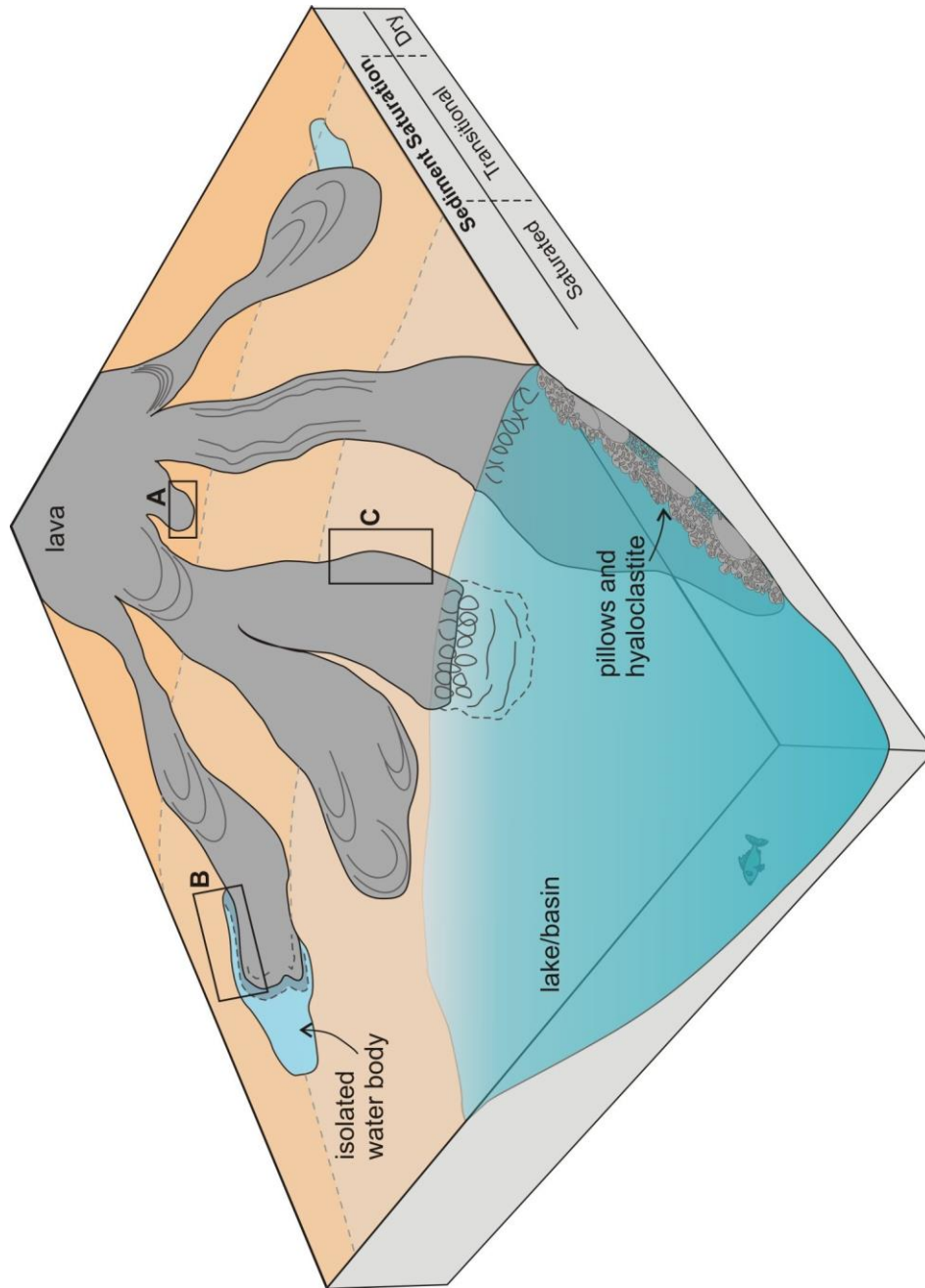


Figure 3-27: A simplistic, schematic model highlighting the three main lava-sediment interaction types at Kinghorn, and the likely sediment saturation levels that facilitate interaction. The sediment saturation scale ranges from dry, with minimal pore-water, to saturated, and then supersaturated (e.g. those within the lake). Boxes refer to the individual interaction models (Figures 26-28). A) Loading and soft-sediment deformation likely occurs where sediment has minimal pore water (dry) (Figure 3-24). B) Passive interaction and peperite formation at the lava base mostly likely occurs where sediment has sufficient pore water, and may or may not involve an isolated body of water (Figure 3-25). C) Dynamic interaction with the shallow bulldozing of sediment by lava likely occurs with sediment that is (super-)saturated (Figure 3-26). Other sedimentary properties (e.g. consolidation and compaction), as well as lava properties may also influence interaction.

## 3.6 Conclusions

The Kinghorn succession provides an Early Carboniferous example of interbedded basaltic lavas and sediments within a dynamic depositional environment. The sedimentary interbeds comprise a mixture of siliciclastic, carbonate and volcanoclastic units that record sub-aerial to fluvial-lacustrine and shallow-marine environments. The typically sub-aerial basalt lava dominated sequence also features hyaloclastite with pillow fragments, peperite, and phreatomagmatic lapilli tuffs and ash aggregates. This provides evidence for emplacement and interaction of both lava and magma with water in large standing bodies, ground water, or sediment pore waters, and both with and without the presence of sediment.

Three types of lava-water-sediment interaction are documented: loading and deformation; 'passive' interaction and peperite formation ( $\pm$  hyaloclastite and pillow formation); and 'dynamic' interaction and peperite formation. These three types are presented as end-members on a formal, variable scale. Interaction is influenced by sediment properties, such as saturation, consolidation, and compaction, at the time of lava emplacement and interaction. Loading and deformation of the sediment by overlying lava occurs when sediment is consolidated, slightly compacted and has minimal pore water, whereas peperite formation requires an unconsolidated, uncompacted sediment that is saturated. As the sediment saturation level differs between semi-saturated to super-saturated so does the interaction type, from passive to dynamic.

This study has demonstrated that lava-water-sediment interaction involving sub-aerial lava is more common than previously thought. Subtle changes in sediment properties, both spatially and temporally, can produce diverse and complex products at lava-sedimentary contacts. This also provides palaeo-environmental information that can be applied to larger-scale field studies or used as a field analogue.

Understanding the nature of the lava-sediment contact is also necessary for industry (i.e. hydrocarbon reservoir exploration). An appreciation for the range in possible contacts (e.g. loading, passive, dynamic), the varying degrees in scale, and the possible effects they may have, along with palaeo-environmental information is important. For example: when considering the degree of disruption to the sediment (e.g. peperite), alteration due to heat transfer and diagenesis, and/or compartmentalisation of the sedimentary unit by lava.

---

This case study provides a “base level” knowledge and understanding of the variety of lava-water-sediment interaction that occurs at Kinghorn, and how these may be applied more generally. This basic model is applied and further developed within the other, more complex, case studies presented in this thesis.

## Chapter 4: Mountain Home, Idaho, USA

### 4.1 Introduction

Four packages of strata, comprising various sedimentary/volcaniclastic units overlain by basalt lava, and hereafter referred to as lava-sediment packages (LSP), are identified at Mountain Home, Idaho, USA (Figure 4-1). The sedimentary units comprise a mixture of lacustrine and volcaniclastic units. The lavas are typically sub-aerial pahoehoe type, although in LSP3 it comprises pillow lava and hyaloclastite. In this study, the processes of lava-water-sediment interaction are characterised at both the basin and interface scale.

The interface at each lava-sediment contact displays varying degrees of interaction, from soft-sediment deformation, to passive interaction (peperite), and fragmentation (Hyaloclastite pillow breccia). In summary, LSP1 shows no evidence for emplacement of lava into water. LSP2 involved negligible interaction through the emplacement of magma onto unconsolidated, possibly wet sediment. LSP3 records entry of lava into a large lake and disruption of near-shore sediments with complex mingling of hyaloclastite and sediment. A marker bed of volcaniclastic sandstone displays variable interaction from no interaction to fragmentation and incorporation into the overlying hyaloclastite pillow breccia. Locally, the VSst is absent.

Quantitative data (pillow and sedimentary thickness measurements) were collected to gain an insight into the relationship between pillow size and observed penetration into the sediment. This revealed no apparent correlation, suggesting that lava-water-sediment interaction is scale invariant, which is further supported by petrographic observations. It is suggested that variable sediment properties, lava effusion rate/flux, and/or water depths control and influence the morphologies and scales of lava-water-sediment interaction.

### 4.2 Geological History

The western Snake River Plain (SRP), in SW Idaho, is a NW-trending, fault-bounded, intra-continental rift basin, ~70 km wide and 300 km long (Wood and Clemens 2002; Shervais et al. 2005; Beranek et al. 2006). The graben lies obliquely to the central and eastern Snake River plains (ENE), which are aligned with the motion vector of the North American Plate over the Yellowstone Hotspot (Beranek et al. 2006; Jean et al. 2014). Movement of the plate over the Yellowstone Hotspot caused the western SRP to form and begin subsidising around ~12-11 Ma, NW of the Bruneau-Jardbidge bimodal eruptive

centre (Beranek et al. 2006; Bonnicksen et al. 2008), which is coeval with the onset of volcanic activity. Volcanic activity in the western SRP began in the Miocene with silicic volcanism at ca. 11.8-9.2 Ma (Clemens and Wood 1993; Wood and Clemens 2002), followed immediately by basaltic volcanism (Late Miocene to Pleistocene) (Shervais et al. 2002; Wood and Clemens 2002; Shervais et al. 2005; Beranek et al. 2006; Bonnicksen et al. 2008; Jean et al. 2014).

Basaltic volcanism within the western SRP occurred during two dominant episodes: 9-7 Ma and ~2.2-0.4 Ma (Godchaux et al. 1992; Shervais et al. 2002; White et al. 2002; Bonnicksen et al. 2008). The first basaltic episode (9-7 Ma) comprises basalt lavas and phreatomagmatic vents intercalated with sediments of the Idaho Group (Malde and Powers 1962; Malde and Powers 1972; Shervais et al. 2002; White et al. 2002; Wood and Clemens 2002; Shervais et al. 2005). Between periods of volcanic activity, extensive lacustrine, fluvial-deltaic and phreatomagmatic sediments, belonging to the Idaho Group were deposited (Malde and Powers 1962; Godchaux et al. 1992; Jenks et al. 1998; Wood and Clemens 2002; Shervais et al. 2005). This occurred in Lake Idaho, which covered most of the western SRP during the Miocene to Pliocene (Middleton et al. 1985; Jenks and Bonnicksen 1989; Malde 1991; Godchaux et al. 1992; Sadler and Link 1996; Shervais et al. 2005). The freshwater lake is thought to have covered ~20,000 km<sup>2</sup> at its maximum highstand (Branney et al. 2008), but frequently waxed and waned during periods of decreased subsidence, increased accommodation fill, and cycles of evaporation (Jenks et al. 1998; Beranek et al. 2006; Bonnicksen et al. 2008; Branney et al. 2008). Incision by the ancestral Snake River into underlying sediments, provided canyons for small ephemeral lakes to form, and for lavas to exploit and infill (Godchaux and Bonnicksen 2002).

The resumption of basaltic volcanism at 2.2 Ma (Pleistocene) occurred after active volcanism in the adjacent eastern SRP had ceased (Shervais et al. 2005), and as Lake Idaho was draining. The volcanic activity is characterised by effusive plateau-forming eruptions of tholeiitic basalt (belonging to the Snake River Group of Malde and Powers, 1962 (Shervais et al. 2005), that were focused along a line of NW-trending vents and shield volcanoes (Wood and Clemens 2002). The plateau-forming lavas are capped by younger lavas erupted from vents, shield volcanoes, and Pleistocene cinder cones (Bonnicksen and Godchaux 2002; Shervais et al. 2005).

Late Pliocene to Pleistocene basalt lavas, intercalated with lacustrine and volcanoclastic sedimentary units of the Idaho Group (Shervais et al. 2005) are exposed along a canyon adjacent to the CJ Strike Dam of the Snake River, south of Mountain Home, Idaho (Figure 4-1). The strata at Strike Dam comprise the Glens Ferry Formation of the Idaho

Group (Shervais et al. 2005), deposited as the base level of Lake Idaho decreased again, and lacustrine units were deposited (Wood and Clemens 2002). The basalt lavas were likely sourced from vents situated to the north and north-west of the field area, the exact locations, of which are unknown as they are covered by overlying lavas (Bonnichsen and Godchaux 2002; Shervais et al. 2005). Although largely sub-aerial, the upper basalt lava unit records sub-aerial emplacement into the margins of a lake, with associated pillow and hyaloclastite deltas (Shervais et al. 2005). Further afield of Mountain Home, lavas are separated by fluvial gravel and sand deposits (Shervais et al. 2005), indicative of an active fluvial system (possibly the ancestral Snake River) draining into a diminishing lake.

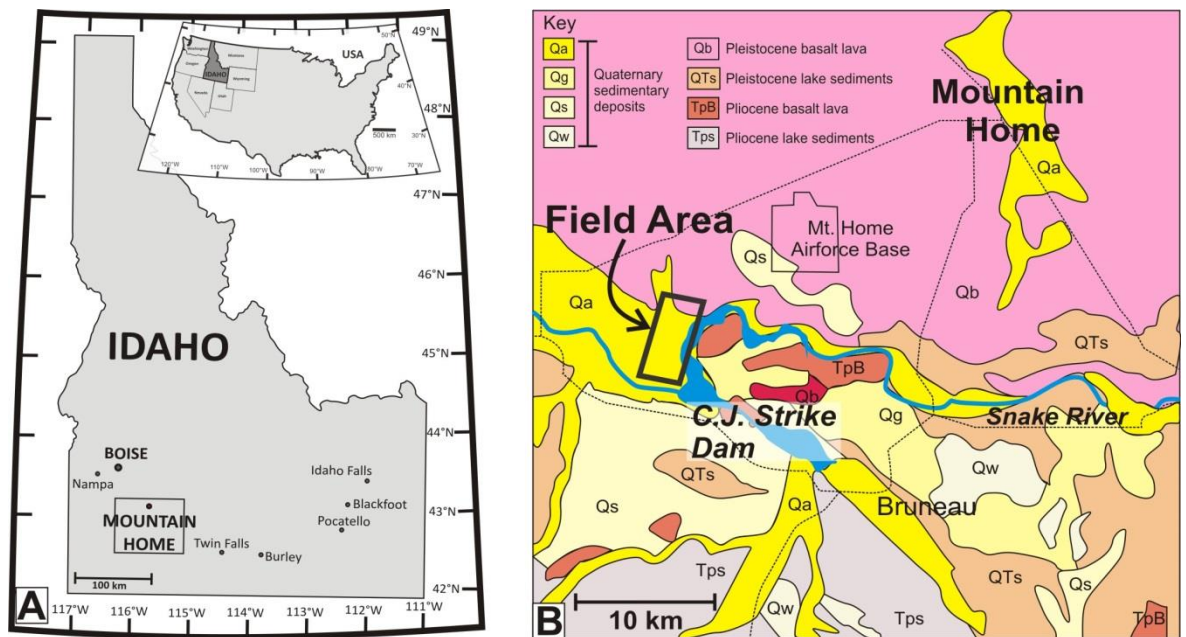


**Figure 4-1: A) Location map and B) simplified geological map of the field area close to the C.J. Strike Dam of the Snake River, near Mountain Home, Idaho, USA. Black boxes indicate field area. Geological map adapted from Jenks et al (1993).**

## 1.1 Field Relationships

### 1.1.1 Brief overview of the area

The field area near Strike Dam reservoir covers  $\sim 10 \text{ km}^2$  and is split into two main sections (Figure 4-2). The sequence is exposed along a road cut in the south of the field area, and also extensively within the canyon to the north (Figure 4-2). The lavas capping the sequence form a plateau that has been cut by the Snake River and its tributaries, exposing the Pliocene-Pleistocene sequence. Numerous graphic logs,

measurements, and samples were collected over a 15 day period, and thin sections were produced. The location of each log is shown in Figure 4-2 for reference.

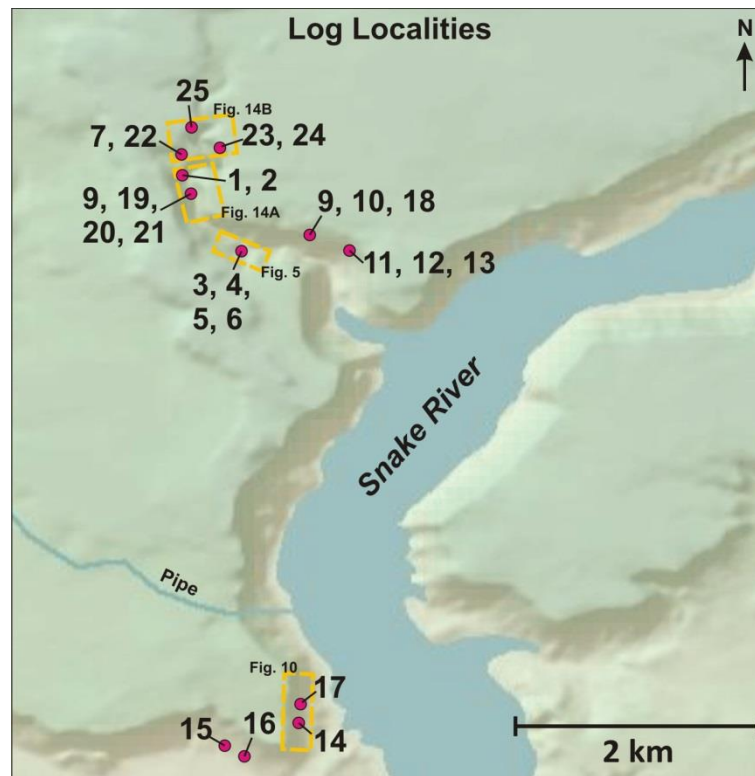


**Figure 4-2: A shaded relief map of the field area along the Snake River, indicating the log locations.**

**Where multiple numbers are given, multiple logs were taken within close proximity.**

The four LSPs identified in the sequence are shown within the generalised vertical section (Figure 4-3). Each LSP comprises a lacustrine-dominated basal sedimentary unit, and an overlying inflated pahoehoe basalt lava with a massive core and ropey to rubbly crust. LSP1 comprises a ~20 m thick sequence of lacustrine and volcanoclastic units and a sub-aerial lava. LSP1 is inclined at 20-40° towards S/SE and is unconformably overlain by LSP2, which comprises ~15-20 m of lacustrine and volcanoclastic units and a sub-aerial lava. LSP3 comprises ~8 m of volcanoclastic and lacustrine sedimentary units overlain by a ~10 m thick, laterally continuous zone of hyaloclastite and pillow breccia (HPb), which grades up into sub-aerial lava. This lava is locally overlain by a thin sub-aerial scoriaceous fall deposit and a sub-aerial lava-4 (LSP4). The lavas are all tholeiitic basalt (Figure 4-4) and the field relationships are described in detail below.

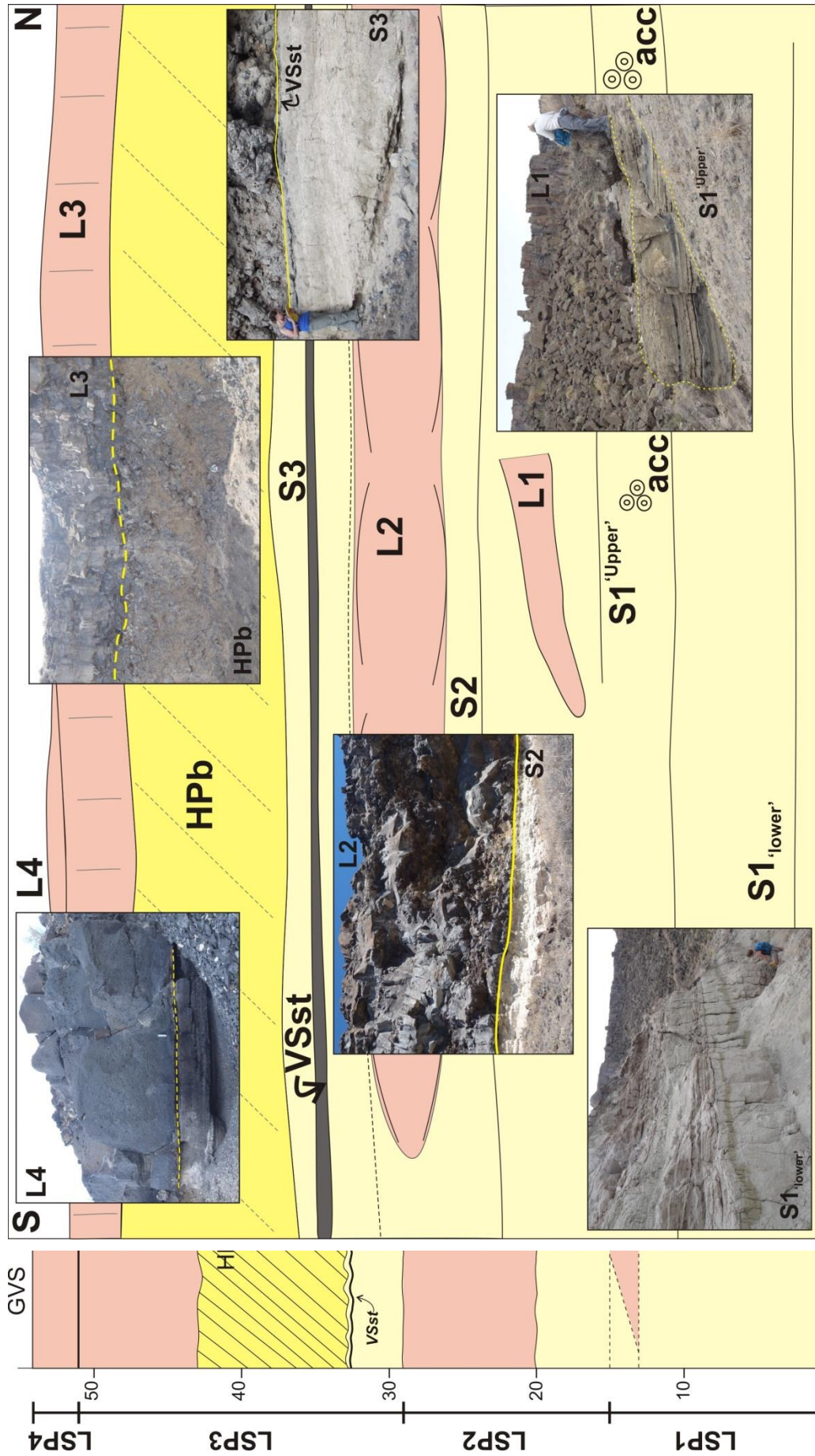


Figure 4-3: Schematic overview and sketch log through the lava-sedimentary stratigraphy at C. J. Strike Dam, Idaho. A) A generalised vertical section through the lava (L) and sedimentary (S) packages (LSP). B) A schematic sketch through the field area, for simplicity, illustrating the relationship of the LSP's and the key distinguishing features. HPb = Hyaloclastite and Pillow breccia, VSst = Volcaniclastic Sandstone, acc = accretionary lapilli.

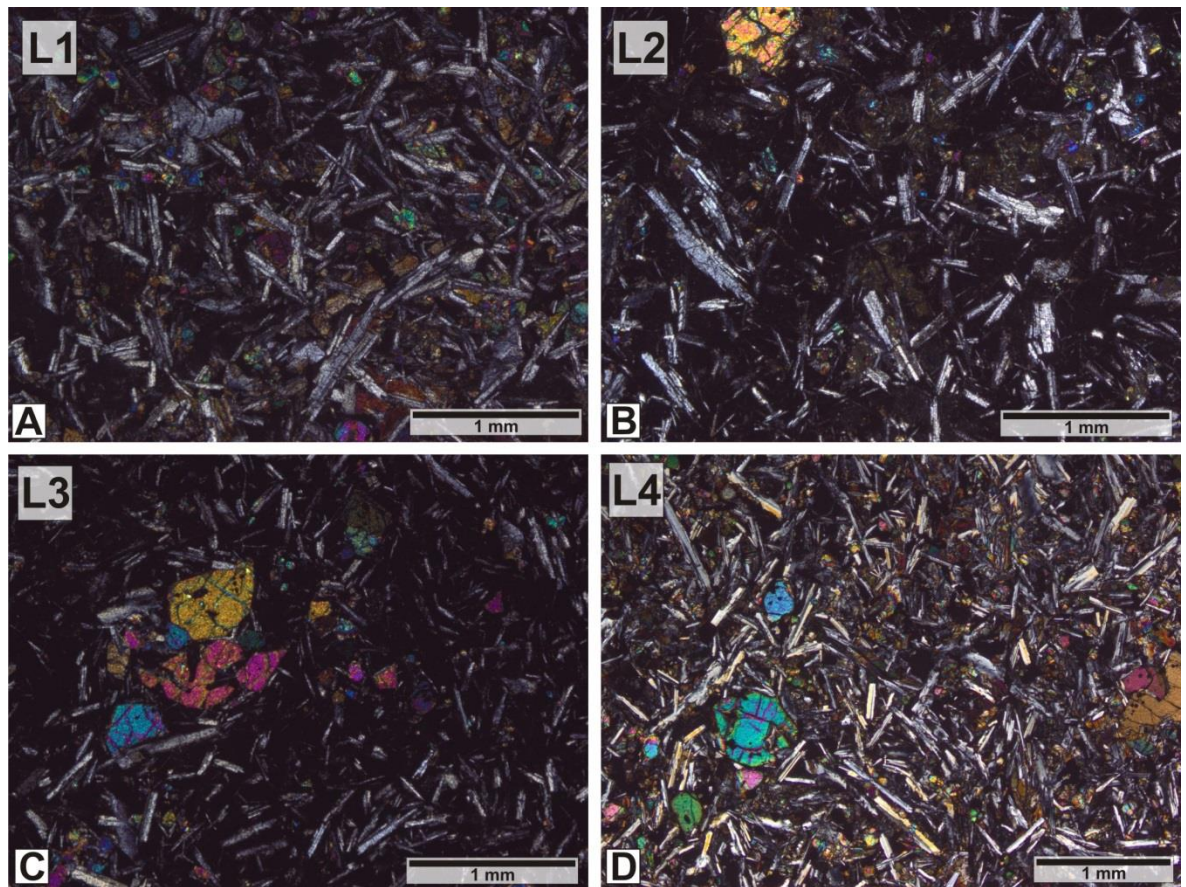


Figure 4-4: Basalt (tholeiitic) lava in Mountain Home, ID.

A-D represent lavas L1-L4, which are compositionally similar. All fields of view are in XPL. The lavas comprise microphenocrysts of plagioclase feldspar and olivine, with olivine glomerocrysts common in L3 (C) and L4 (D).

### 1.1.2 LSP1

LSP1 comprises sub-aerial lava and a thick sedimentary sequence (Figure 4-5). Exposure of the lava is limited to the west side of the canyon near localities 3-6 (Figure 4-2), whilst the sedimentary package is visible throughout the field area.

#### 1.1.2.1 Lava:

Lava 1 (L1) is 4-6 m thick, massive, and with large horizontal elongate vesicles, up to 20 cm. Pseudo-columnar joints (1.5 m spacing) are common throughout and the lava has a ropey top. A rubbly base is not observed. L1 is exposed over ~600 m, unlike the laterally continuous lavas of LSP2 and LSP3, and dips at 20-40° towards the S and SE (Figure 4-5). Petrographical analysis of L1 indicates it is of basalt to tholeiitic basalt composition (Figure 4-4), comprising abundant plagioclase feldspar with olivine and rare pyroxene, within a basaltic glass matrix.

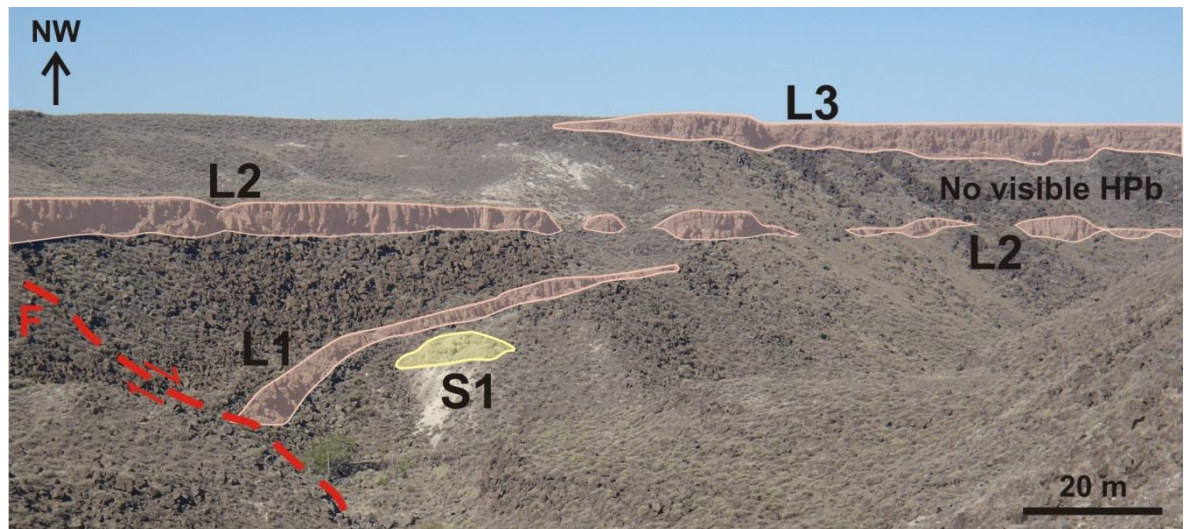


Figure 4-5: An overview of the area where LSP1 and L1 are visible.

L1 is not extensive, but the area is faulted. L = lava package, S = sedimentary package, F = fault.

### 1.1.2.2 Sedimentary:

Most sedimentary units at the bottom of the canyon stratigraphically underlie L1 and L2, although L1 is only locally observed. Overall, sedimentary unit S1 of LSP1 is at least ~20 m thick, not including the large areas of no exposure. S1 comprises units of highly weathered/altered white to green/grey, coarse to fine siltstone and claystone and reworked basalt. The lower units show little variation from massive fine siltstone and claystone, to infrequent packages of fine sandstone with planar to cross laminations. The upper sedimentary units, however, have more small-scale, internal structural variation, with large-scale cross bedding and erosional surfaces. There is an overall coarsening upwards of S1, and the presence of reworked basaltic material increases up sequence.

The correlation panel in Figure 4-6 shows the logs taken from all visible outcrops of S1 within the canyon (Figure 4-2 for locations). Logs 1 and 2 form the 'upper' units of S1 and logs 5 and 6 show the 'lower' units of S1. Logs 3 and 4 link the upper and lower units and are located on opposite sides of the canyon floor.

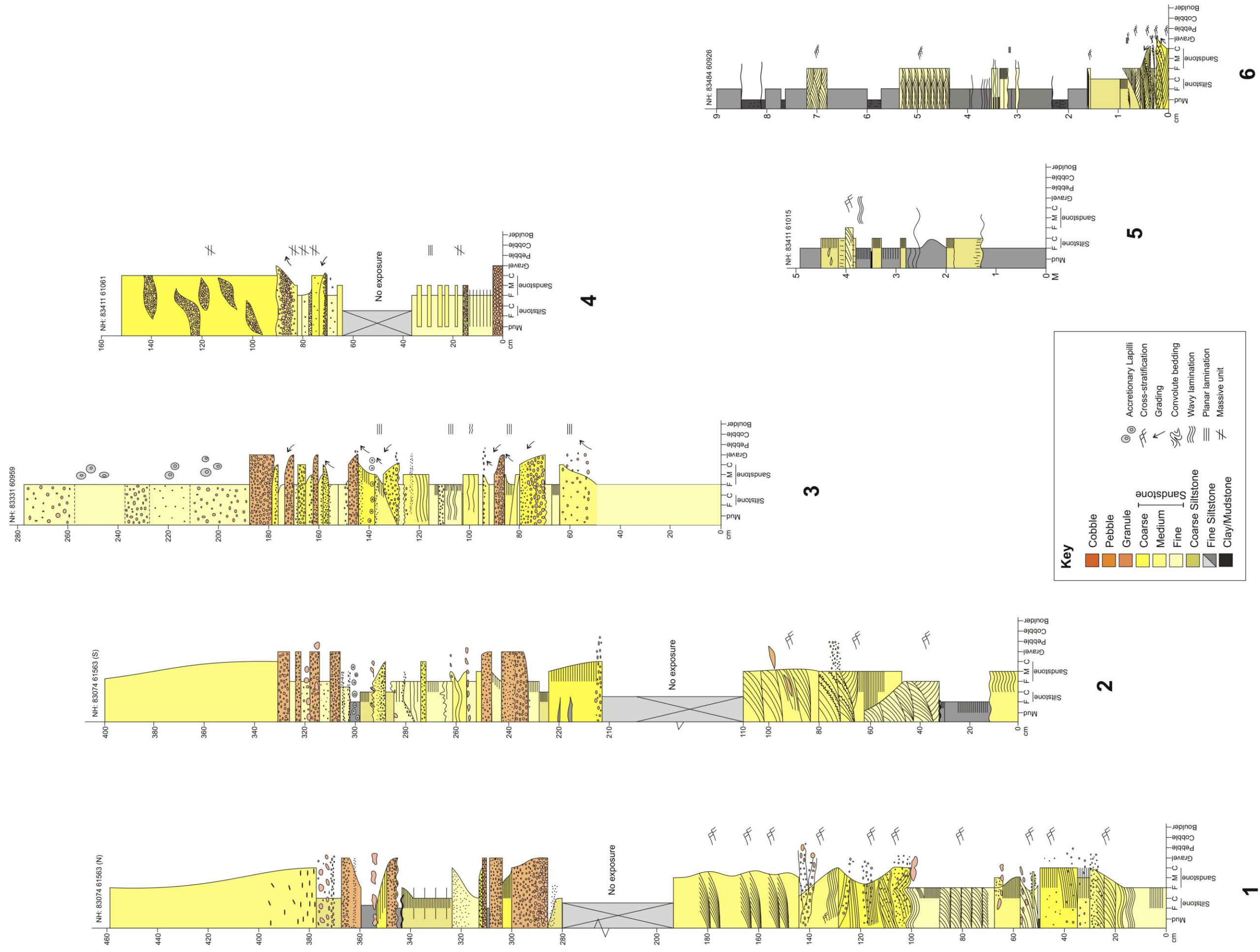
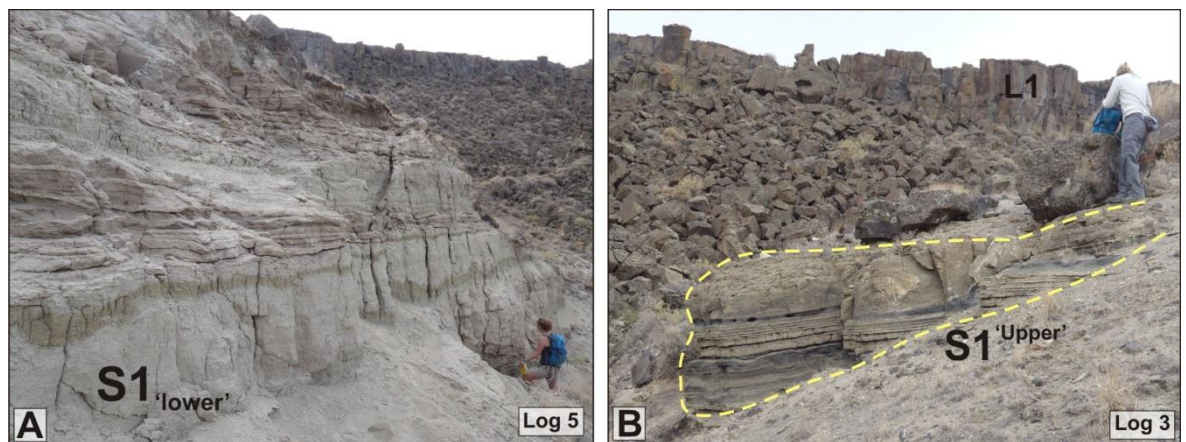


Figure 4-6: Logs of LSP1. Logs 1, 2, and 3 can be correlated but only Log 3 is observed below and near the Lava 1 contact. Log 4 correlates with Log 3 on the opposite side of the palaeo-canyon. Logs 5 and 6 show the lowermost sedimentary units of LSP1. Logs 1 and 2 are shown at outcrop scale in Figure 6.

The lower sedimentary units of S1 (logs 5 and 6, Figure 4-6) give measured thicknesses of 5 and 9 m, respectively, although neither the bases nor the tops of the sedimentary units are exposed, and are likely much thicker. The majority of the units are massive, pale white/yellow/green, fine and coarse siltstones interbedded with coarser packages of fine sandstone (Figure 4-7). Planar to wavy laminations are present within the sandstone packages. At the base of Log 6 (Figure 4-6) there is ~80 cm of coarse to medium sandstone that displays mm- and cm-scale, high angle, cross-bedding. Basalt lithoclasts accentuate the cross-beds, forming clast supported laminae with sub-angular grains and pebbles of basalt and quartz, ~1 cm across. This material also forms coarse, granular lenses as the packages fine upward. Contacts between packages are wavy and erosional, with flame structures interpreted as evidence of dewatering. Several packages of fine sandstone display trough cross bedding, with beds ~10-20 cm thick, and mm-cm scale laminations. Organic material, most likely plant fragments, occurs at the base of a fissile, grey/green, finely laminated (mm-scale), coarse siltstone unit that contained rare lithics (Log 5). Some bioturbation is also observed. Organic material, likely diatoms, is also observed within the petrography.



**Figure 4-7: The lower units of S1 at Log localities 5 and 3.**

**A) The lower units of S1 comprise massive units of fine to coarse siltstones interbedded with planar – wavy laminated fine sandstone beds. B) The upper parts of S1 comprise coarse siltstones, sandstones and granular packages, which are dominated by volcanoclastic material, such as tuff, basalt lithoclasts and accretionary lapilli beds. Person for scale ~ 175 cm.**

The ‘upper’ units of S1 (logs 1 and 2, Figure 4-2, Figure 4-6) comprise coarse siltstone, sandstone and granule-grade sandstone packages, all of which are lithic rich. Logs 1 and 2 show two distinctive packages of sandstone separated by ~1 m of no exposure ( ). The lower parts of the sequence are dominated by coarse siltstone to sandstone and granular siliciclastic packages. The uppermost 3 m has a substantial volcanoclastic

component comprising (possibly reworked) massive tuff, massive lapilli tuff, massive lapilli tuff with accretionary lapilli (mT, mLt, mLtacc (see abbreviations for definitions)), scoriaceous fall deposits (mm ~3 cm clasts, beds 1-15 cm), and siltstones with vesicular basalt lithoclasts (<5 cm). Beds with accretionary lapilli (broken) (Figure 4-8) help to correlate Logs 1 and 2 with Log 3 (further south in the canyon). They occur at a height of ~3 m in logs 1 and 2 (Figure 4-8) and multiple times between 140 and 250 cm in Log 3 (Figure 4-6 and Figure 4-9). Large-scale cross-bedding, channel structures and erosional surfaces are observed.

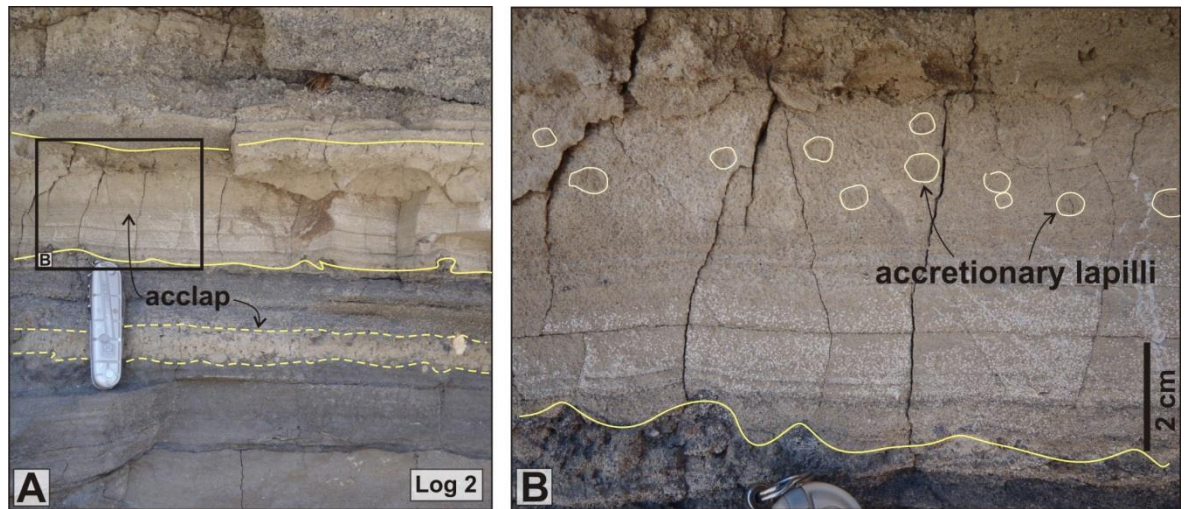


**Figure 4-8:** The upper part of S1 comprises a significant volcanoclastic component, including beds of massive lapilli tuff with accretionary lapilli (acclap).  
**A)** At Log locality 2, a thin unit of accretionary lapilli is bounded by grey coarse sandstone-granular units of basalt lithoclasts. The thicker unit of fine sandstone to siltstone contains broken pellets and accretionary lapilli. Pen knife is ~8 cm. **B)** A close-up of the accretionary lapilli in the upper part of S1.

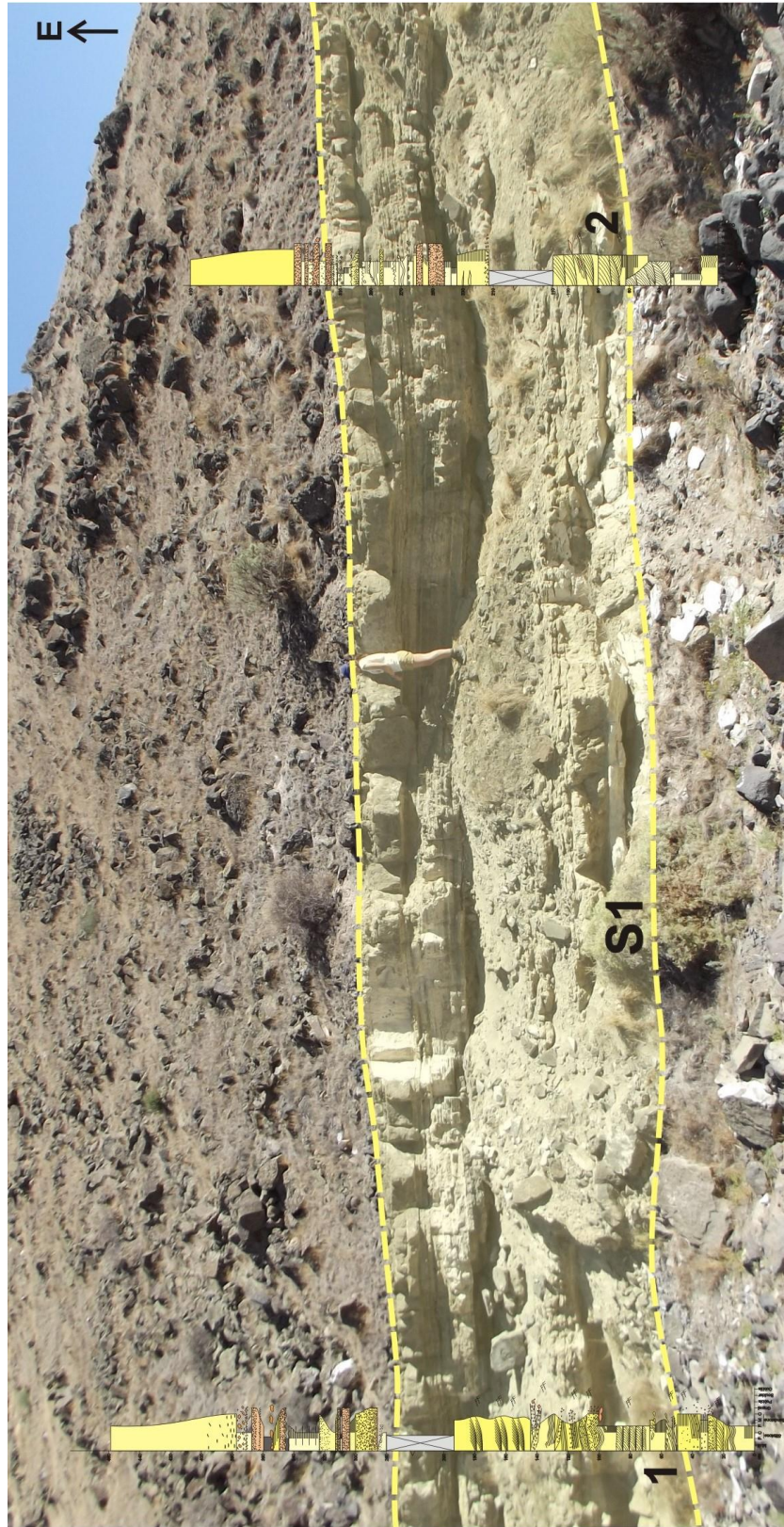


Figure 4-9: Upper' sedimentary units of LSP1, including logs 1 and 2 of S1 sedimentary package. The logs through this section show variable channel flows with a range of lacustrine and volcanoclastic sediment. Accretionary lapilli (reworked) are present in one bed. Person for scale.

### 1.1.2.3 L1 and S1 contact:

The contact between L1 and S1 is not observed. Faulting within the area may have caused the lava to dip strongly, or it may simply cross-cut the sedimentary sequence. However, given the nature of the overlying lavas, it is mostly likely that faulting and tilting have locally affected L1 and S1, resulting in a lack of exposure.

## 4.2.1 LSP2

LSP2 comprises ~15-20 m of fine-grained sedimentary and volcanoclastic units overlain by a sub-aerial lava. The lava-sedimentary interface can be observed in most exposures.

### 4.2.1.1 Lava:

Lava 2 (L2) is an ~8-9 m thick, grey, aphyric basalt (Figure 4-4), comprising multiple flow lobes. It has a massive core (~1-2.5 m thick) and a vesicular top and base, both with large, rounded - elongate vesicles (from 0.5-4 cm). Crust thickness typically ranges from 10-60 cm at the base, and 25-80 cm at the top. Both the basal and upper crusts are locally rubbly. Lobe-geometries (hummocky) are common, and the fractures and joints of the lava curve to reflect this feature. The basal lava typically has horizontally aligned elongate vesicles within the basal 60 cm that are 3.5 - 4 cm across with 3:1 aspect ratios, and trend E-W. Vertical elutriation pipes (clusters of vesicles) are also present (~10-30 cm long), above the aligned vesicles. Fine white siltstone and sandstone, and quartz spherulites are present within vesicles up to 20 cm from the basal contact. The base of the lava varies laterally over a typical distance of ~2 m, from a rubbly and erosional base with sediment filling the gaps, to a planar contact, with some minor sediment-lava interaction (as depicted in Log 8). The uppermost lobe is the thickest, and has a rubbly base, a massive core, and a fractured, rather than rubbly, top. Large circular/oval clusters of concentrated vesicles, typically 1-8 cm across, are relatively abundant where the top surface is exposed and weathered. The top surface of the lava has a hexagonal, pseudo-columnar joint pattern (<75 cm spacing) as shown on Log 25 (Figure 4-2). No palaeosols are observed.

In the southern part of the section (Figure 4-10), close to the reservoir, L2 has lobate geometries that can be followed the length of the exposure. It pinches out towards the south, with the last exposure seen at near to the locations of Logs 14 and 16). This exposure is small and rubbly, ~2 m high, and most likely represents the end toe of the

lava. Log 14 (Figure 4-10) shows L2, which has a ropey and vesicular base, with pseudo-columnar joints, above which is an entablature and a slabby crust with ropey textures. This is, however, atypical when compared to the other exposures of L2.

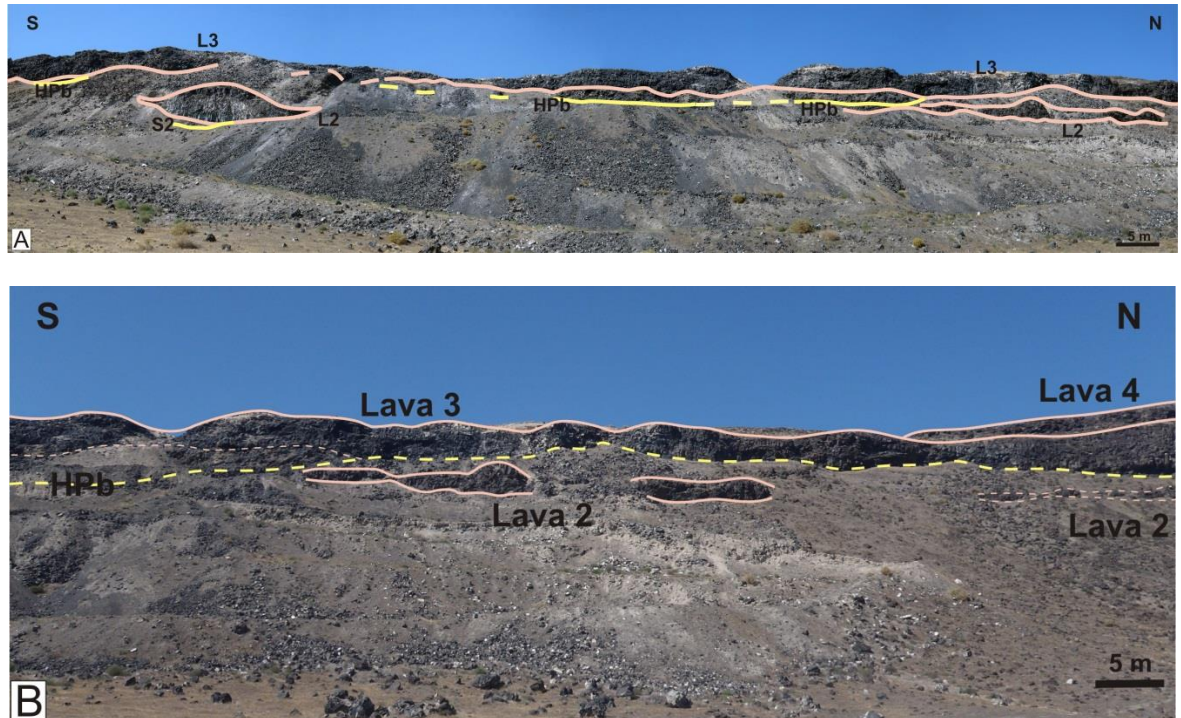


**Figure 4-10:** A) a panorama of the outcrop in the south of the field area, close to the reservoir and road cut of the Strike Dam (looking East).

B) An enlarged view highlighting the stratigraphy. The HPb of LSP3 pinches out (or starts) towards the north. At this end of the section Lava 4 is observed.

#### 1.1.2.4 Sedimentary

Much of the sedimentary package S2, underlying L2, is arguably the same as that underlying L1. S1 and S2 are typically undistinguishable due to a lack of contacts and exposure, and are therefore described as part of LSP1 (see above). However, here, the sedimentary units directly underlying and in contact with L2, are described and interpreted.

Where S2 directly underlies L2 it predominantly comprises fine, white siltstone. A 2-10 cm massive tuff (pyroclastic) with uncommon lapilli is present at the top of S2. This tuff has a gradational boundary with the underlying siltstone but is distinct due to its hardness and the presence of mm-scale aligned elongate vesicles at the top of the unit. The tuff thins through logs 10-13 (Figure 4-11). In logs 7-9, S2 is similar, with fine grained white siltstone underlying L2.

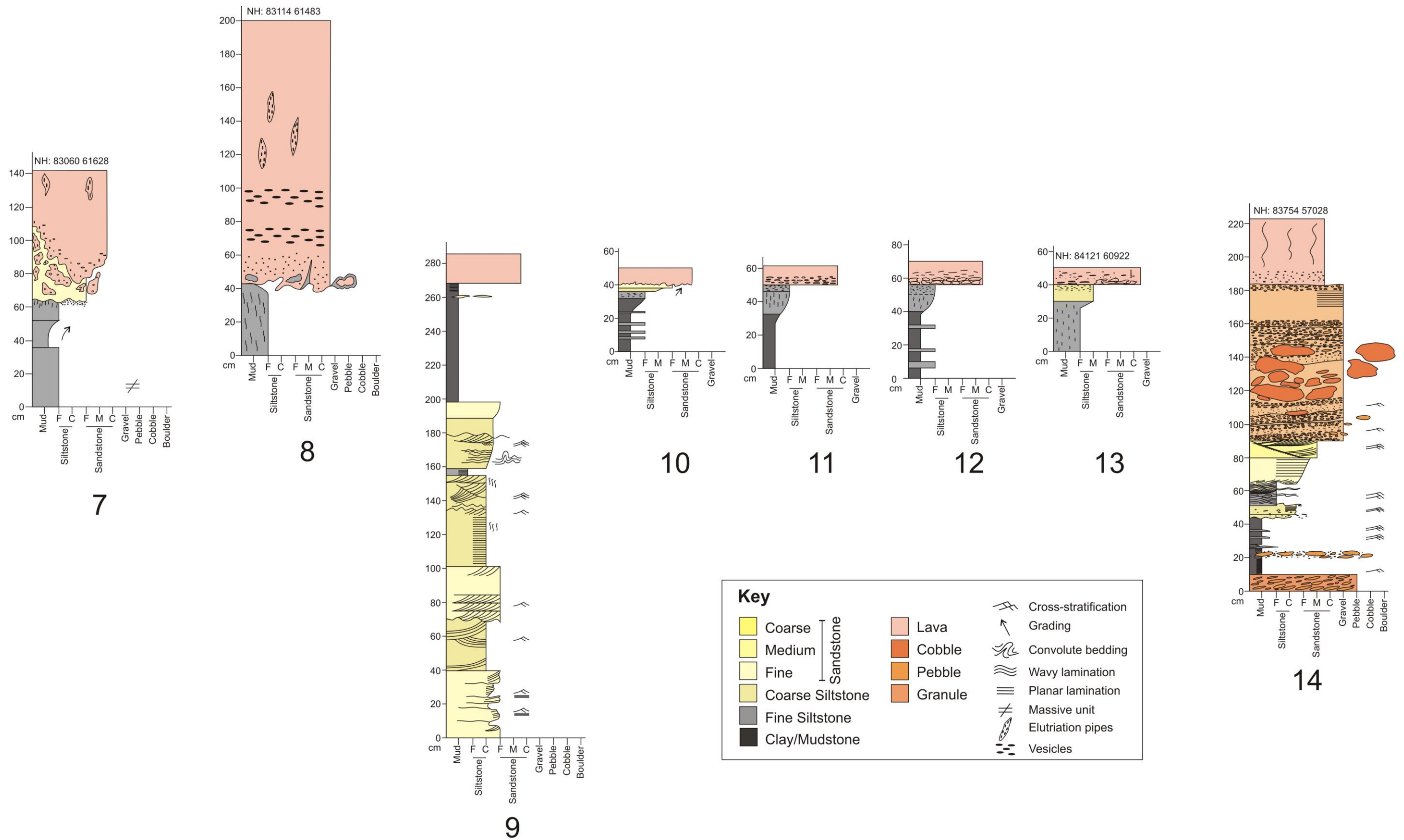
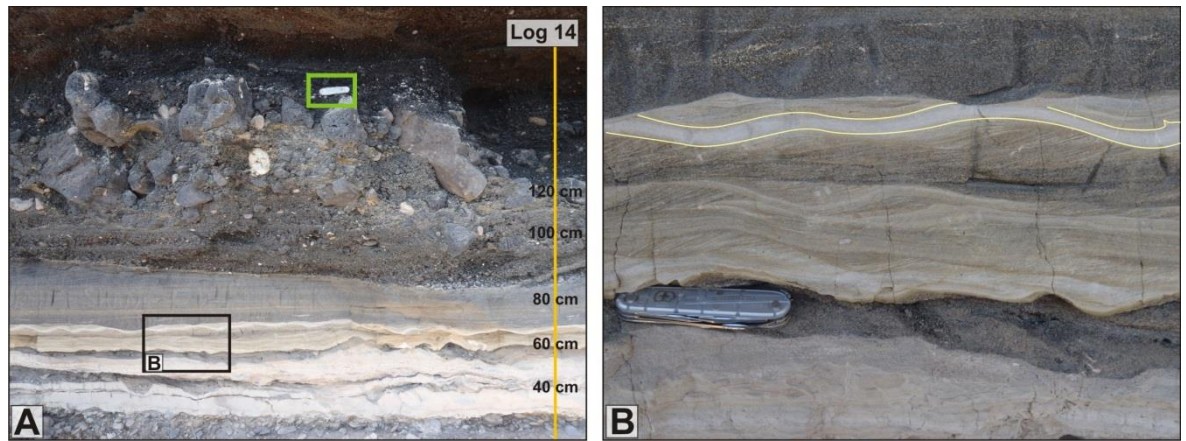


Figure 4-11: Correlation panel of sedimentary logs through S2 in LSP2. N-S (left-right). S2 is typically fine-grained at the contact with Lava 2.

Log 9 displays the greatest thickness of S2, with beds comprising interbedded grey/white, fine sandstone and coarse siltstone that display cross bedding and planar and ripple laminations. Bioturbation occurs in the units at 120 and 150 cm. Erosional surfaces are common throughout, with loading and convolute laminations above intervals with bioturbation. A 70 cm unit of fine white claystone, which contains hard, discontinuous nodules of carbonate-rich siltstone is in the uppermost 8 cm, directly below the capping L2 lava.

In the south of the field area (by the reservoir), S2 is coarser and more volcanic dominated (than further north within the canyon). The log for Locality 14 (Log 14, Figure 4-2, Figure 4-11) shows a measured thickness of ~1.8 m, although the base is not seen. The units include an imbricated pebble/cobble conglomerate (indicating a palaeo-flow direction towards the south) at the base, and comprising rounded to sub-rounded basalt clasts of 2 mm-10 cm in a siltstone matrix. This is overlain by a fine, chalky white claystone that is planar to ripple cross stratified, and contains rare discontinuous siltstone lenses and wavy pebble lenses. The sedimentary package typically grades from this fine claystone to volcanic-dominated granule grade units. Individual beds alternate from pale white to grey, have erosional bases that cross-cut the underlying beds, and commonly display trough and hummocky cross laminations (Figure 4-12). Many beds appear discontinuous over the 5 m exposure length, and small basalt clasts, < 5 mm, are randomly distributed throughout certain beds. At ~60 cm, there is a continuous uniform pale white tuff layer (reworked(?) fall deposit, 1-2 cm thick), which mantles the underlying bed (Figure 4-12). Above this, the sediment coarsens upwards from fine to medium sandstone with planar laminations and low angle cross beds (palaeoflow to the south) in the top 10 cm. The uppermost unit, 90 cm thick, comprises a cross-bedded, granule grade, clast-supported volcaniclastic conglomerate, dominated by scoriaceous basalt. Pebbles and cobbles, which are rounded, comprise rhyolite, quartzite, andesite and basalt, and range in size from 0.5 to 15 cm. In the middle of the sequence, which is predominantly scoriaceous, large clasts (pebbles, cobbles and boulders) are randomly distributed and occur in lags and lenses. The large basalt cobbles and boulders are up to 40 cm across. The top of this unit is dominated by laminated glassy volcanic clasts with minimal (< 5%) sediment. Small pebbles of country rock, < 5 cm, and scoriaceous clasts, <5 %, are present within the uppermost 10 cm. The top of the sedimentary unit, directly below the lava, is slightly reddened.



**Figure 4-12: Log 14 at the reservoir displays the upper units of S2 directly underlying L2. A) S2 comprises wavy to ripple cross-stratified claystone and siltstone beds, which grade to a clast-supported volcanoclastic conglomerate that is dominated by scoriaceous basalt. B) The lower claystone and siltstone packages display trough and hummocky cross-stratification and have erosional bases. A white reworked tuff layer, 1-2 cm thick, is present at ~60 cm (yellow outline). Pen knife (Green box A) is ~8 cm.**

#### 4.2.1.2 L2 and S2 contact:

The contact between S2 and L2 is variable across the field area, ranging from a planar contact with no evidence of interaction, to an erosive/invasive contact with mingling between the rubbly lava and sediment. This can be seen locally within a few metres, and also on a cm-mm scale.

Typically L2 has a rubbly base at the sediment contact. Small ‘fingers’ of basalt, 10-20 cm in length, protrude into the sediment. The sediment is squeezed, deformed and/or mingled with the rubbly lava base, with flame structures locally present. Sediment of S2 is incorporated into the base of the lava by the infilling of minor fractures and vesicles in the basal ~20 cm of the lava (Log 8, Figure 4-2, Figure 4-13). Coherent sediment inclusions, 8-12 cm long, of fine to medium sandstone, are also incorporated within the rubbly lava base.

Mixed domains of sediment and basaltic lava clasts are present at, or within, the rubbly base of the lava. They are localised and discontinuous, and typically 40-50 cm thick and 60-80 cm wide. Basaltic (juvenile) clasts are typically in the mm-cm range, highly vesicular, globular, and without a chilled margin. Fine siltstone is present throughout, filling vesicles in larger clasts. Micro ‘clasts’, <1 cm across, are grouped together within the sediment and are fluidal. These typically form a ‘minor’ peperite at the lava-sediment contact (Log 7, Figure 4-11).

At locality 7 (Figure 4-11) the sediment below L2 is white claystone and fine siltstone. The rubbly base of the lava forms peperite (with a 45 cm mingling zone) with the underlying sediment (Figure 4-13). Within the mingling zone, basalt clasts are ~1 cm, and up to 30 cm across. They have fluidal margins, although vesicles are not filled with sediment. The main lava body however, does have sediment-filled vesicles.

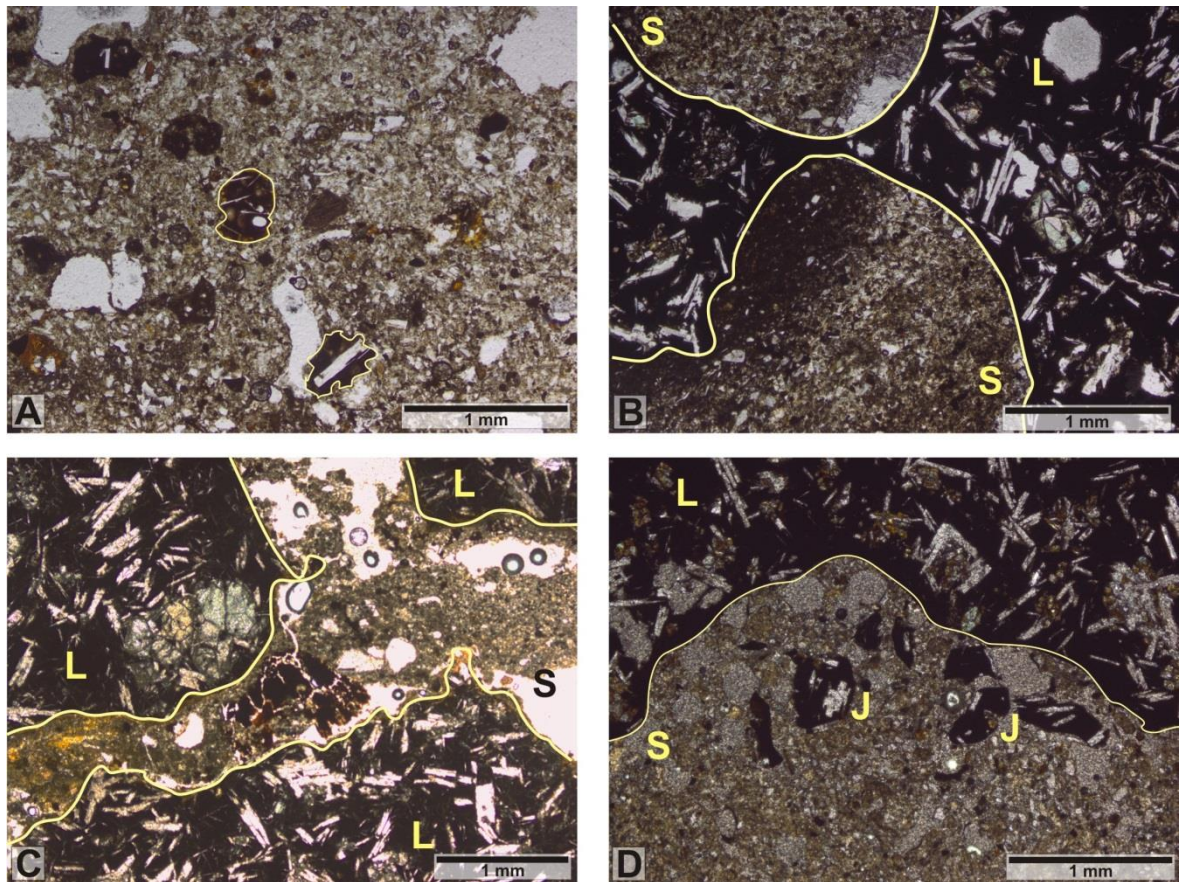


**Figure 4-13: Petrography of LSP2.**

**A)** S2, fine-grained sandstone, with basalt lithoclasts (e.g. yellow outline). **B)** Sediment-lava contact. Sediment (S) fills vesicles and is found as inclusions within the lava (L). **C)** Irregular and fluidal lava-sediment contact. The sediment (S) appears to 'invade' the lava (L). **D)** The lava-sediment contact is irregular to globular, and small, juvenile (J) clasts with blocky and irregular morphologies are present within the siltstone (S) at the contact.

### 4.2.2 LSP3

LSP3 is ~20 m thick, and comprises a basal sedimentary unit (S3) with a distinctive volcanoclastic marker bed, which is overlain by an interval of laterally continuous hyaloclastite and pillow breccia (HPb) that transitions upwards into sub-aerial lava L3.

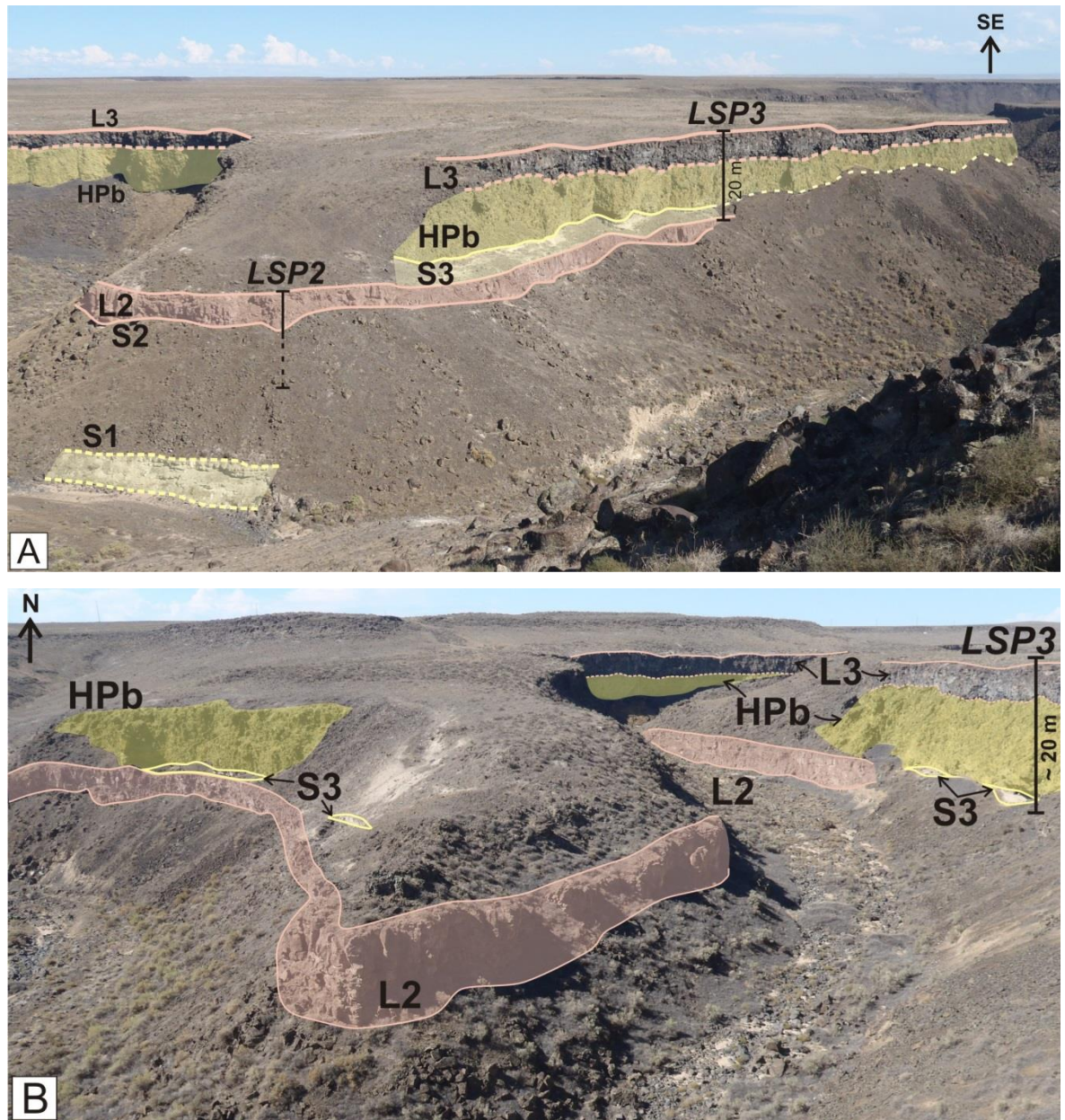


Figure 4-14: An overview of the stratigraphy exposed within the north of the field area. A) An overview of the field area looking west, showing LSP2 and LSP3. B) An overview of the northern section of the field area, by C.J. Strike Dam, where LSP3 and L2 are exposed. LSP = Lava Sedimentary Package; S = sedimentary; L = lava; HPb = Hyaloclastite Pillow breccia.

#### 4.2.2.1 Lava:

L3 is ~7.5-10 m thick and comprises multiple basaltic lobes, typically 0.9-1 m thick, although the upper lobes are typically thicker (~1.5-2 m). The lava (sub-aerial pahoehoe) has a ropey and rubbly brecciated base, with a passage zone, downwards, into lava tubes and pillows (indicating an initial subaqueous environment of eruption). The ropey base comprises a vesicular crust (~20 cm), overlain by a massive core (~60-150 cm) and a vesicular, rubbly and ropey top (~30-90 cm). Ropey textures are

observed at the base and top of the lava. Vesicles are predominantly spherical, but at the top of individual lobes are elongate and aligned horizontally. Pseudo-columnar joints occur in thicker lobe cores (60-80 cm across) towards the top of the lava.

The passage zone at the base of L3 into lava tubes and pillows occurs throughout the field area, but is best observed in the north, at locality 25. The passage zone typically transitions from sub-aerial lava, with a rubbly, vesicular base, to pillow tubes, which have ropey textures closest to the main lava body, giving way to brecciated surfaces and quenched rinds. The pillow lavas have multiple chilled margins and rinds that are fractured and broken. These are orange-stained in alternate layers (black and orange striped rinds). The pillow cores are vesicular. Hyaloclastite breccia occurs between pillows and contains abundant broken rind fragments, and is also heavily palagonitised (orange weathered).

#### **4.2.2.2 Hyaloclastite and Pillow breccia (HPb):**

The HPb is ~10 m thick and comprises dipping foreset packages of pillow lavas and hyaloclastite breccia (Figure 4-15). Apparent dip of the foresets is 034/30°SE assuming a strike of 034° into the cliff exposure. However, this is not quantitative, nor does it necessarily indicate a palaeoflow, as foresets range dramatically in apparent dip direction (i.e. they commonly dip in opposing directions throughout the exposures). The HPb is displayed within the cliff exposures throughout the field area, although it pinches out in the central portion.

The HPb is predominantly clast supported, with a matrix of silt- to sand grade palagonitised basaltic material. Locally, however, the matrix comprises white fine siltstone, particularly near the HPb/S3 contact (where there is a high sediment content). Throughout the field area, the HPb contains coherent sediment inclusions, typically ~3-25 cm that are present up to a height of ~5 m from the base of the HPb/sediment contact. These inclusions are also found within pillows.

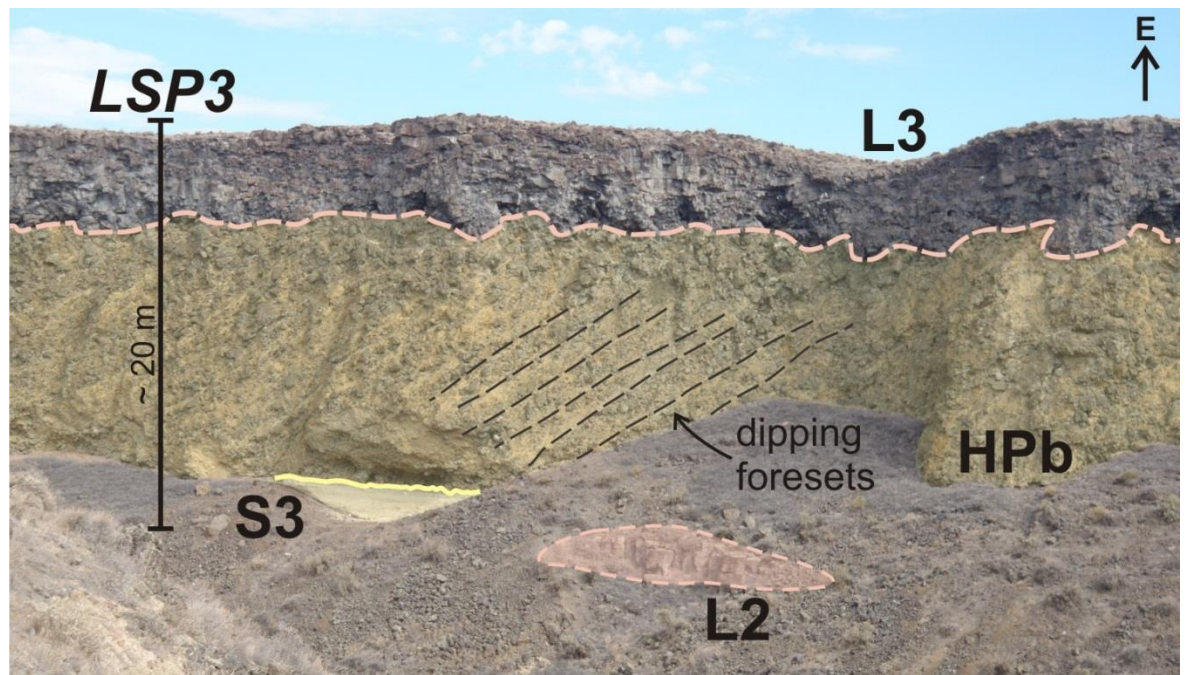


**Figure 4-15: An overview of LSP3.**

**LSP3 consists of sediment, S3, the HPb and Lava 3. The HPb has strongly defined dipping foresets.**

The pillow-dominated foresets are typically 3 m thick (maximum) (Figure 4-16) with pillows ranging from ~15 cm (minimum) to ~80-120 cm (average). Spalled, broken and brecciated pieces are smaller (5-15 cm) and have ropey textures. The larger pillows, with widths of up to 230 cm, have flattened bases, whereas the smaller pillows maintain their rounded structure and have more complex relationships with the surrounding sediment (for example, at log location 24, where the pillows protrude and deform the underlying sediment). Large sediment inclusions, <15-20 cm across, are present within pillows, commonly within the core, as well as coherent chunks within the breccia. Sediment also fills fractures within the pillows (Figure 4-17.C). The pillow breccia matrix contains basalt clasts, <1 mm.

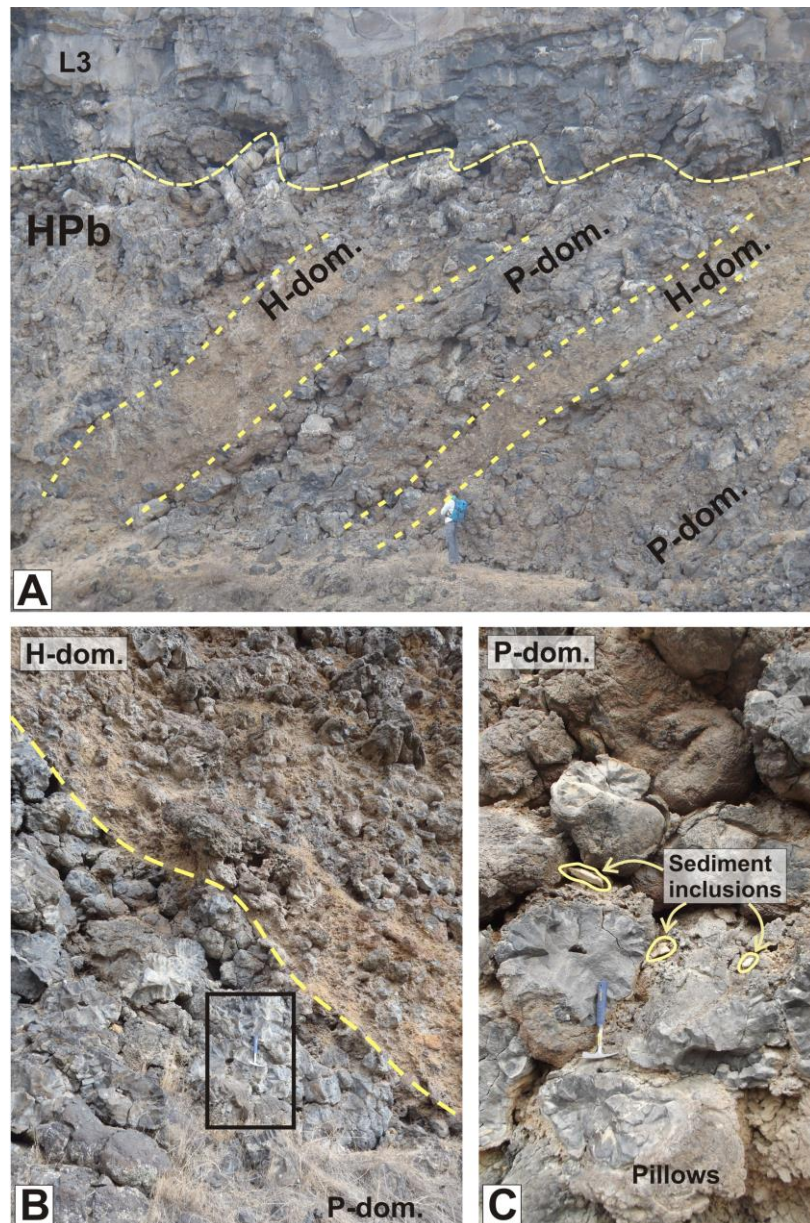


**Figure 4-16: Pillow-dominated and hyaloclastite-dominated foresets within the HPb of LSP3.**

A) Highlighted are pillow-dominated (P-dom) and hyaloclastite-dominated (H-dom.) foresets of the HPb, below L3. The pillow-dominated foresets are typically thicker than the hyaloclastite-dominated foresets. Person for scale. B) A close-up of the boundary between pillow-dominated and hyaloclastite-dominated foresets. Inset is image C. Hammer for scale. C) Pillows within a pillow-dominated foreset. Sediment inclusions are present between pillows. Hammer for scale.

The hyaloclastite breccia-dominated foresets (Figure 4-16) also have a typical thickness of ~3 m, although the contact with the pillow-dominated foresets is gradational over ~50 cm. The hyaloclastite breccia foresets become thinner towards the passage zone and the sub-aerial lava (i.e. up-sequence). Basalt clasts in the hyaloclastite breccias are glassy, angular and small, ranging from 0.5 - 6 cm. Rare pillows, typically with sediment-filled cores, and pillow fragments range from 10 cm to 20 cm. The

hyaloclastite breccia foresets have a coarser matrix (>3 mm basalt clasts) than the pillow foresets. Sediment inclusions within the hyaloclastite breccia are less abundant than in the pillow-dominated foresets, and range in size from small blebs of ~1-2 cm to a maximum of 17 cm.

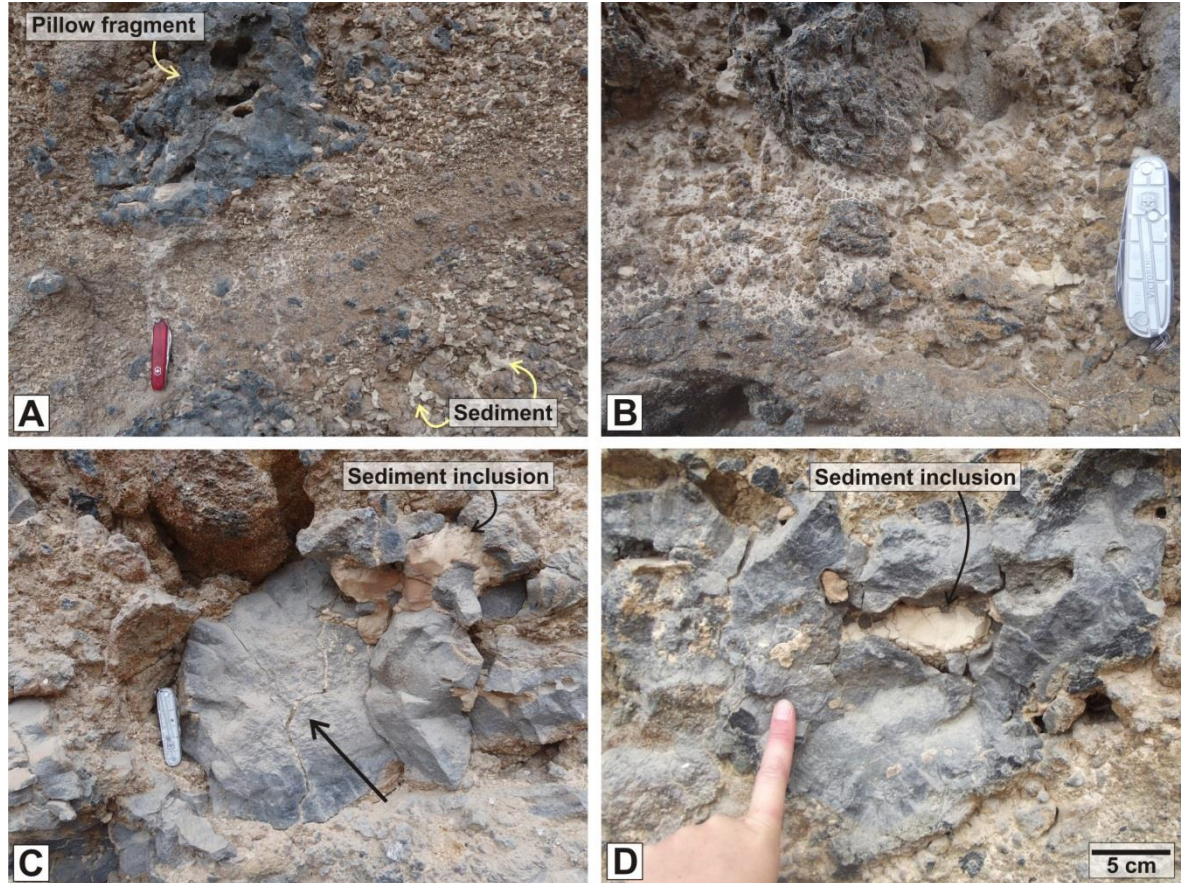


**Figure 4-17: Typical small scale features of the HPb.**

**A)** Hyaloclastite breccia within a hyaloclastite-dominated foreset. Pillow fragments are present within these foresets. **B)** A close-up of hyaloclastite breccia (grey and orange) with a high sedimentary content (pale cream). **C)** A sediment inclusion at the edge of a pillow, with sediment also filling the fracture through the centre of the pillow (arrow). **D)** Sedimentary inclusions within lava (this occurs in L3 and L2). Pen knife is ~8 cm.

#### 4.2.2.3 Sedimentary:

The sedimentary units (S3) of LSP3 are ~8 m thick and predominantly comprise white/grey siltstone to medium sandstone packages, with variable abundances of sub-rounded basalt clasts (Figure 4-18). S3 has a relatively high abundance of basaltic/volcaniclastic material compared to S1 and S2. The lower sedimentary units in S3 are typically massive, fine to medium sandstones with sub-rounded, vesicular, basaltic clasts ranging from 3 to 15 cm (Figure 4-18). Locally, massive pumice-rich siltstone beds (possibly tuffs) with basalt lithic clasts, 2 mm-4 cm across, are present. The lower units are locally observed in contact with the underlying L2 (Logs 20 and 22).

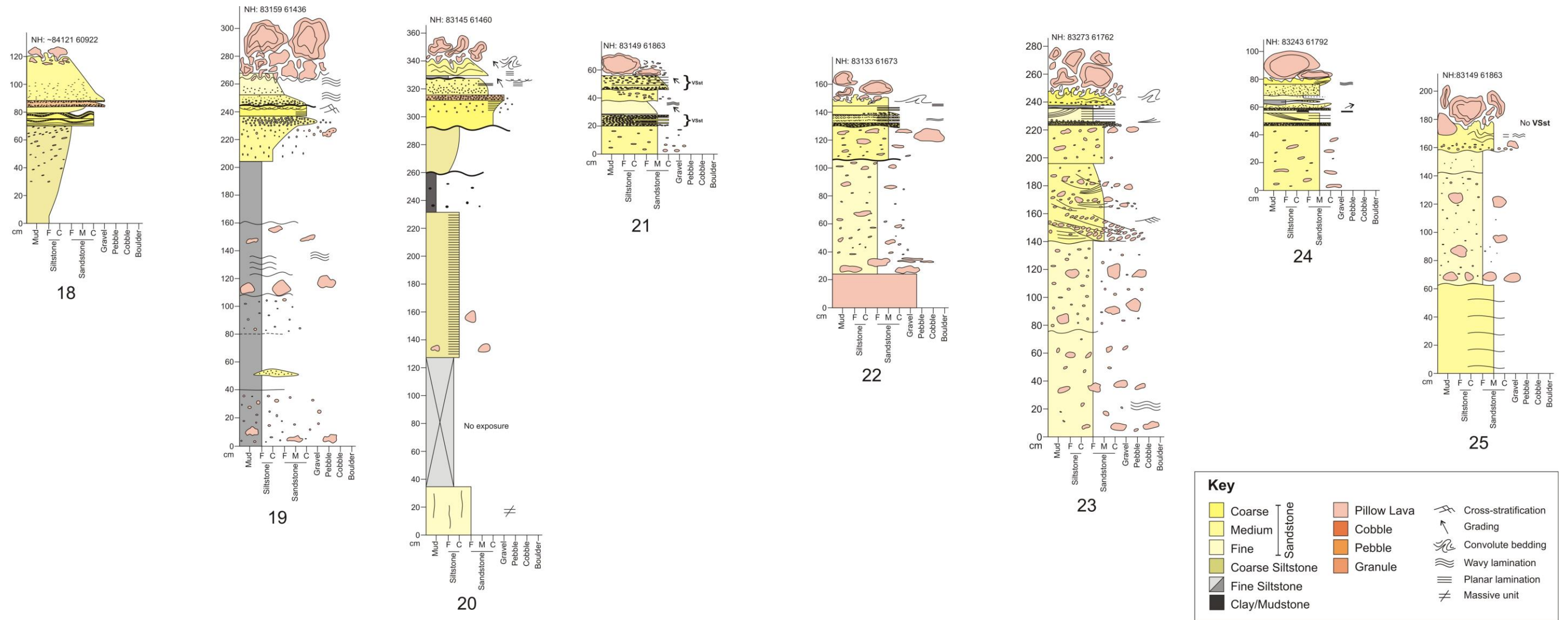
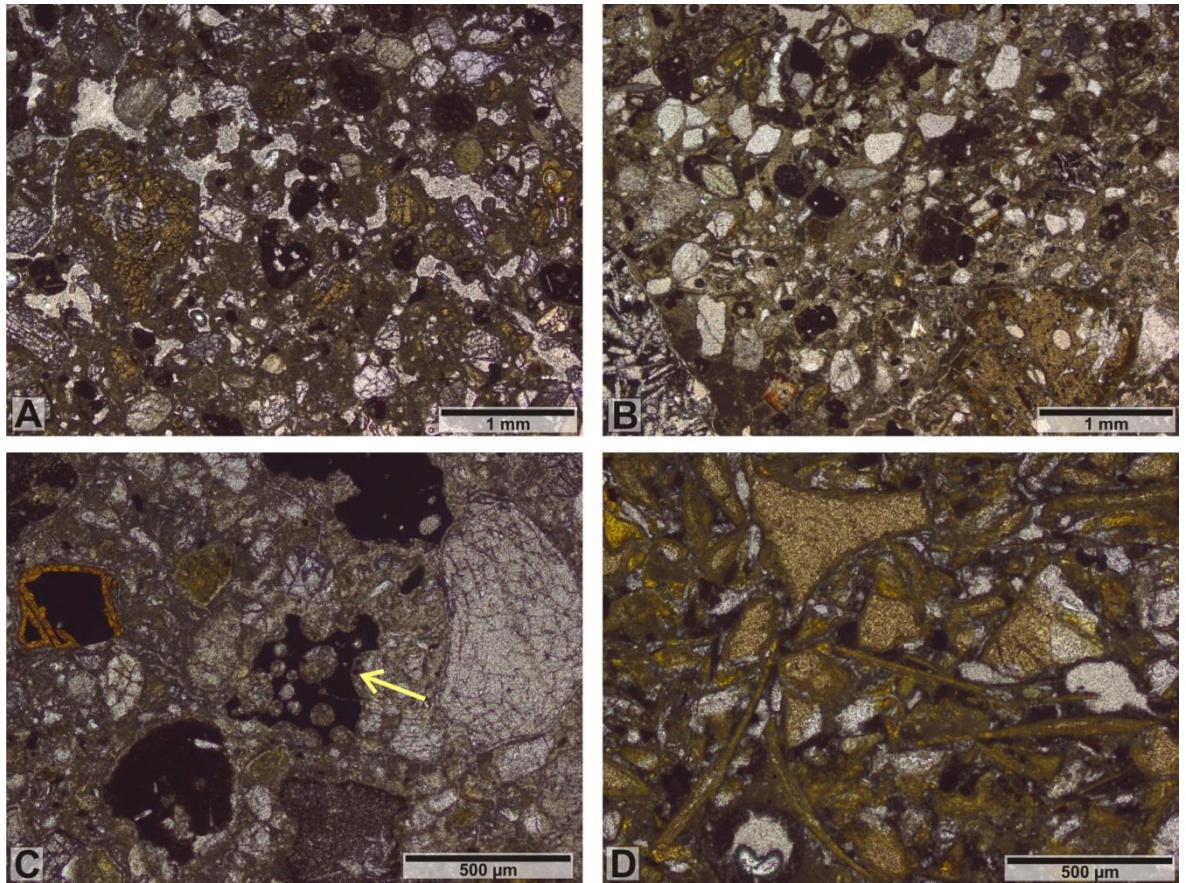


Figure 4-18: A correlation panel of the sedimentary logs of S3. These are hung from the VSst marker bed. See figure 2 for locations.

At locality 20 (Figure 4-2, Figure 4-18), the sediment is in direct contact with the upper surface of L2, and can be correlated across the canyon to locality 19. The unit comprises ~2.3 m of green-white coarse siltstone to fine sandstone (possibly reworked volcanoclastic material) with mm-size sub-angular lithics, and considerably larger basalt clasts, typically <10 cm. Faint, mm-scale lamination is present in the top 35 cm of this package. Overlying this is a 35 cm claystone unit with basalt clasts (5%) of <2 cm and a reverse graded fine siltstone to fine sandstone, 28-41 cm thick, which displays a wavy (erosional) top and base. These units are observed across the canyon, between the lobe geometries of L2. A white, hard, bedded tuff overlies L2, whereas a fissile, green/grey volcanoclastic sandstone with faint bedding and laminations, is at the same stratigraphic level as L2. Here, the sediment forms a flame structure at the lava-sediment contact. The sandstone is locally deformed with only rare mingling of basalt lava clasts with the sediment. This type of relationship/interaction is only observed at this location.

At log location 22, S3 is also in direct contact with L2. Here is 82 cm of massive, white fine sandstone, with large, sub-angular, vesicular clasts/lithics, 2-20 cm, concentrated at the base of the bed. Smaller lithics, 1-4 cm, are distributed throughout the unit. Grey/brown pumice clasts, 0.5-1 cm, are also present and are elongate but non-welded. This package is overlain by 22 cm of grey/yellow, massive, medium sandstone, with randomly distributed basalt clasts from 1 mm-4 cm. The basalt clasts coarsen (up to 25 cm) and become more abundant towards the top of the bed. Petrography of the units below the VSst is shown in (Figure 4-19.A and B), the sandstone, litharenite units, have a high abundance of basalt lithics and glassy shards (possibly reworked).

A mixture of the lower units is seen throughout the field area. Overlying them is a distinctive volcanoclastic sandstone package (VSst) observed throughout S3 exposures.



**Figure 4-19: Petrography of S3. All images PPL.**

**A) Volcaniclastic litharenite at the base of S3. The fine-grained sandstone comprises basalt lithic grains (possibly reworked), typically with irregular margins, crystals of plagioclase feldspar, olivine, pyroxene and quartz, which are held within a fine siltstone matrix. Grains show alteration, and open pore space is observed. B) Volcaniclastic litharenite directly below the VSst. Poorly sorted, medium-grained sandstone, with sub-rounded grains comprising basalt lithics and abundant plagioclase and olivine crystals. C) Sandstone litharenite directly overlying the VSst is similar to the sandstone below the VSst. It comprises basalt lithics, crystals, and scoriaceous, vesicular basalt clasts (yellow arrow). D) Orange-stained/palagonite glass shards representative of the discontinuous orange beds below and at the HPb-sediment contact. The shards are densely packed, and predominately confined to these beds.**

The VSst ranges in thickness from 12 to 22 cm and can be used as a marker when correlating the logs (Figure 4-18). The VSst typically comprises alternating dark grey and yellow, medium to coarse sandstone beds. The dark grey beds comprise clast supported, (reworked) scoriaceous basalt, with sub-rounded basalt clasts between 0.5-3 cm (Figure 4-21A and B). The yellow/orange beds comprise normally graded, matrix supported sandstone, with an abundance of basaltic clasts (Figure 4-21C). In the middle of the VSst, there is an ~8 mm thick, white fine siltstone (possibly reworked ash). It is wavy/hummocky and cross-cuts the dipping laminae of the underlying volcanoclastic unit, which is suggestive that it mantles and fills an irregular palaeo- topography. Petrographically, the fine siltstone comprises a fine-grained matrix with basalt fragments and glassy shards (Figure 4-21D).

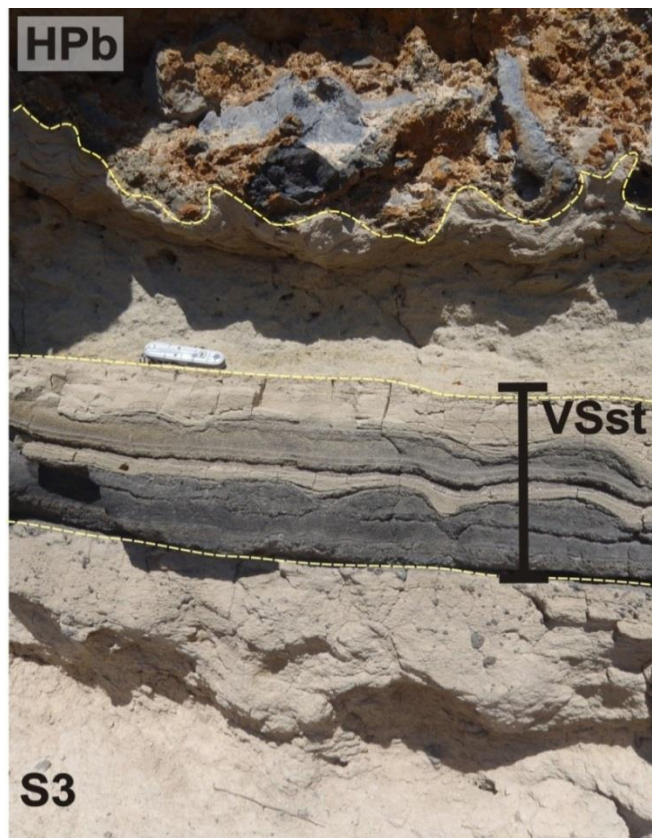


**Figure 4-20: Field view of the VSst unit of LSP3.**

The VSst unit provides a useful marker across the field area. It is situated near the top of S3, just below the contact with the overlying HPb, and comprises dark grey reworked scoria and volcanoclastic material. The central pale yellow layer comprises fine siltstone, likely reworked ash. Yellow dashed lines mark the VSst, and the overlying sediment-HPb contact.

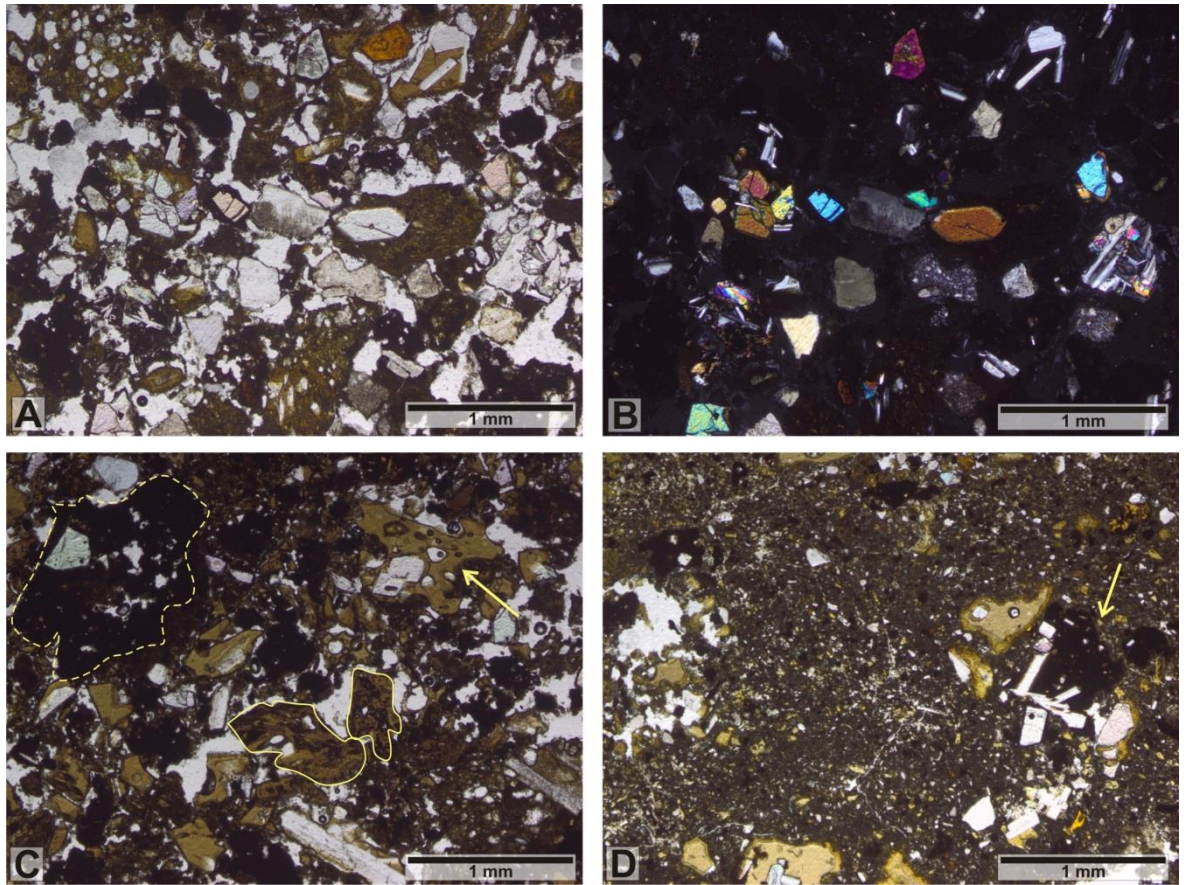


**Figure 4-21: Petrography of the VSst of LSP3.**

**A) PPL and B) XPL** represent the volcanic (basalt)-rich sandstone bed at the base of the VSst. **C) Coarse layer** within the VSst, with palagonite glass shards (yellow arrow) and basalt lithics (dashed yellow outline). (PPL) **D) Finer grained siltstone/claystone (tuff)** bed within the VSst (PPL). The siltstone matrix supports larger basalt fragments (yellow arrow) and glass shards.

Although the VSst is a correlatable marker, there is one location where it is absent (Log 25, Figure 4-22). This locality is the most northern exposure of S3 sediment; it is lens-shaped (Figure 4-22) as the overlying HPb comes into contact with the underlying L2. The S3 units here correlate with S3 units observed below the VSst at other locations (e.g. 22 and 23). These units are depicted within Log 25 (Figure 4-18) and include: an interbedded medium to coarse sandstone; white, fine sandstone with pumice and angular, vesicular basalt clasts (4 mm -15 cm); and a pumiceous massive tuff with basalt lithic lapilli (2-5 cm). The uppermost unit (in contact with the HPb) is a grey, fine to medium, wavy laminated sandstone with vesicular basalt clasts that has sediment-filled vesicles. The clasts are sub-angular to sub-rounded and range in size between 2-15 cm, with rare examples up to 23 cm. The largest clasts are typically at the contact with the HPb. Near to log locality 22 (Figure 4-18, Figure 4-23), the VSst varies in thickness (6-15 cm) around large, rounded, vesicular basalt cobbles (20 cm). These cobbles are situated at the top of the underlying white sandstone unit to the VSst, confirming the lack of VSst at locality 25.

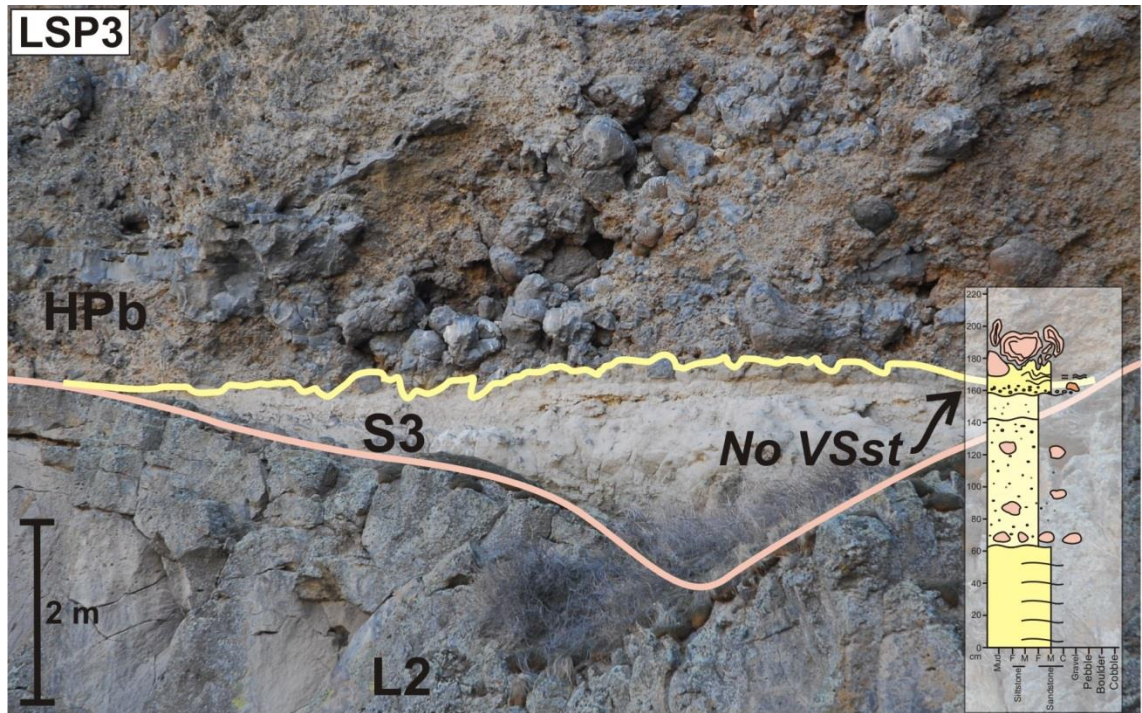


Figure 4-22: Field view of S3 and log 25, where the VSst is not recorded. At this locality (log 25) S3 sediment is a thin interval between the top of L2 and the base of the HPb. The VSst is not present, and the HPb has more abundant sediment inclusions.

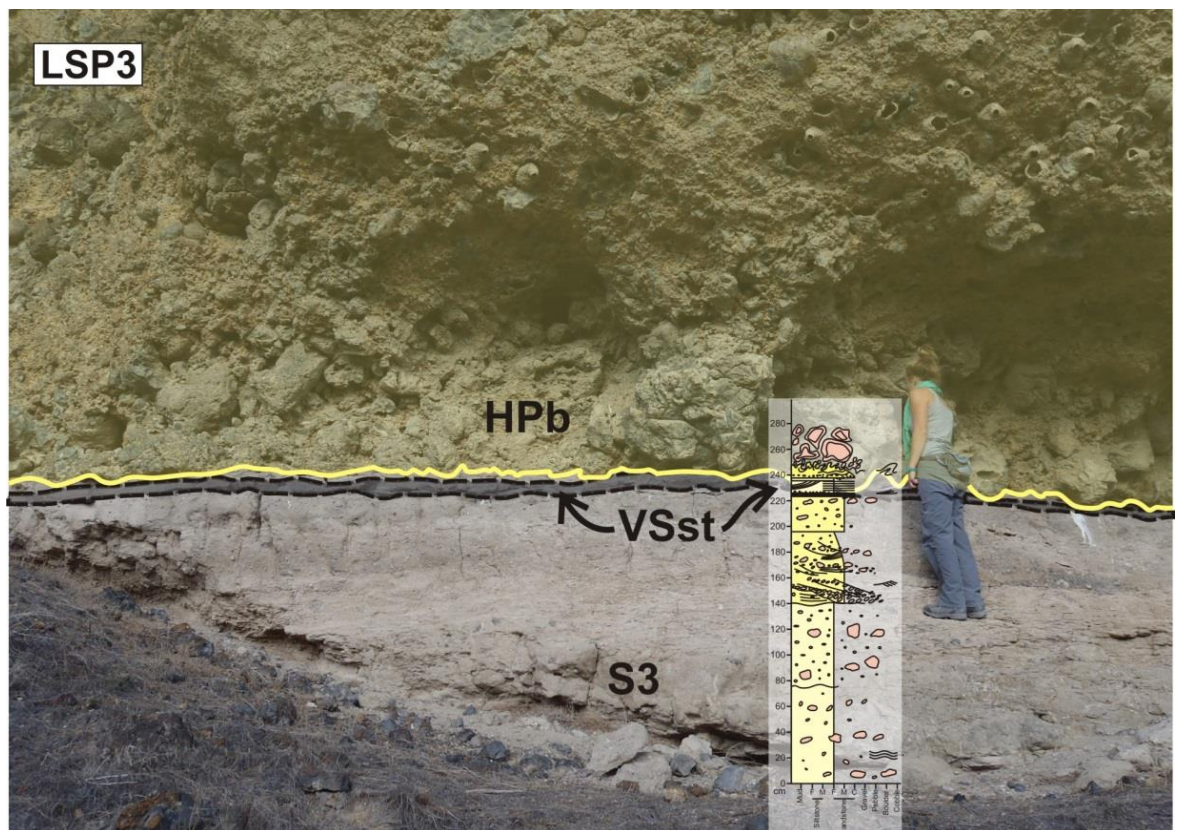
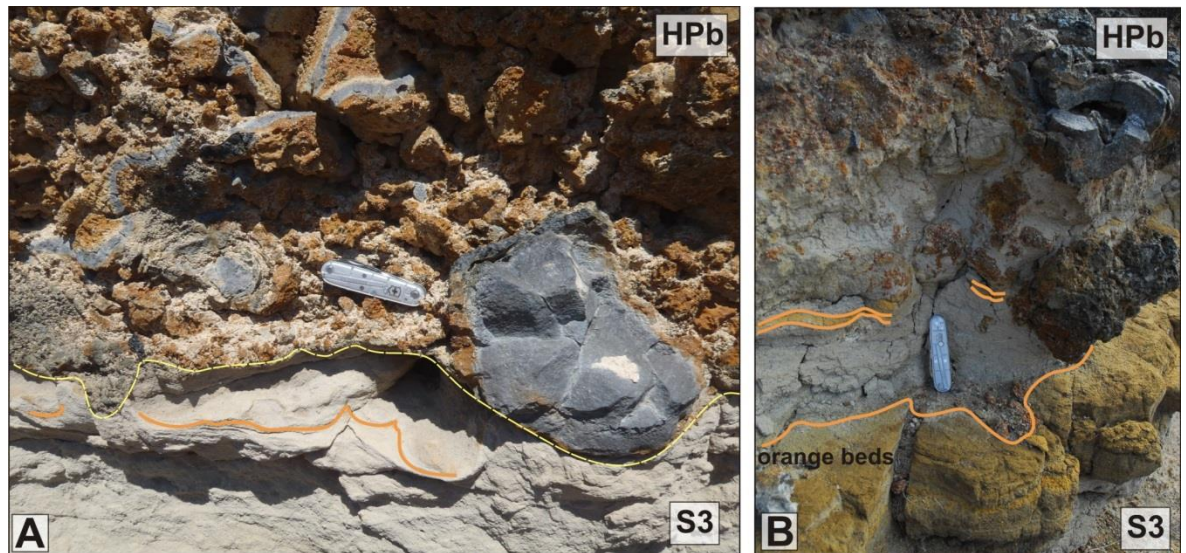


Figure 4-23: Field view of S3, showing the VSst marker bed and Log 23. Person for scale.

Above the VSst, the sedimentary unit is in direct contact with the HPb; it is a white, normally graded, coarse sandstone to fine siltstone, with wavy laminations and flame structures (Figure 4-20). The base of the unit is clast-rich with basalt clasts of 1-8 mm (Figure 4-19.C). Due to loading from the overlying HPb, the unit varies in thickness from 0-20 cm. Locally, the sediment is orange stained, in discontinuous layers/bands, especially where the unit is in contact with the HPb (Figure 4-24). Petrographically, these orange layers comprise abundant palagonite glassy shards (Figure 4-19.D).



**Figure 4-24: Discontinuous, orange-stained beds within the sedimentary units overlying the VSst and underlying the HPb.**

**A) The HPb is loading and deforming the underlying sediment, highlighted by the orange bed (orange line). B) Locally the orange beds are much thicker (~10 cm).**

In the southern part of the field area (log localities 14-17, Figure 4-2 and Figure 4-25), S3 is different to that in the rest of the field area. The VSst is much thicker, and the distinctive VSst is difficult to distinguish as the entire package is grey/black and volcanic dominated. Log 15 (Figure 4-25) potentially has a 65 cm thick VSst equivalent (between 25 and 90 cm on log).

The lower units are also different, with a relatively thick pebble unit overlain by medium sand to granule grade sandstone packages. In Log 17 (Figure 4-18), a trough cross-bedded granule grade sandstone unit with reworked, scoriaceous, glassy basalt clasts (<1 cm), is overlain by fine siltstone, which is heavily deformed and displays flame and dewatering structures.

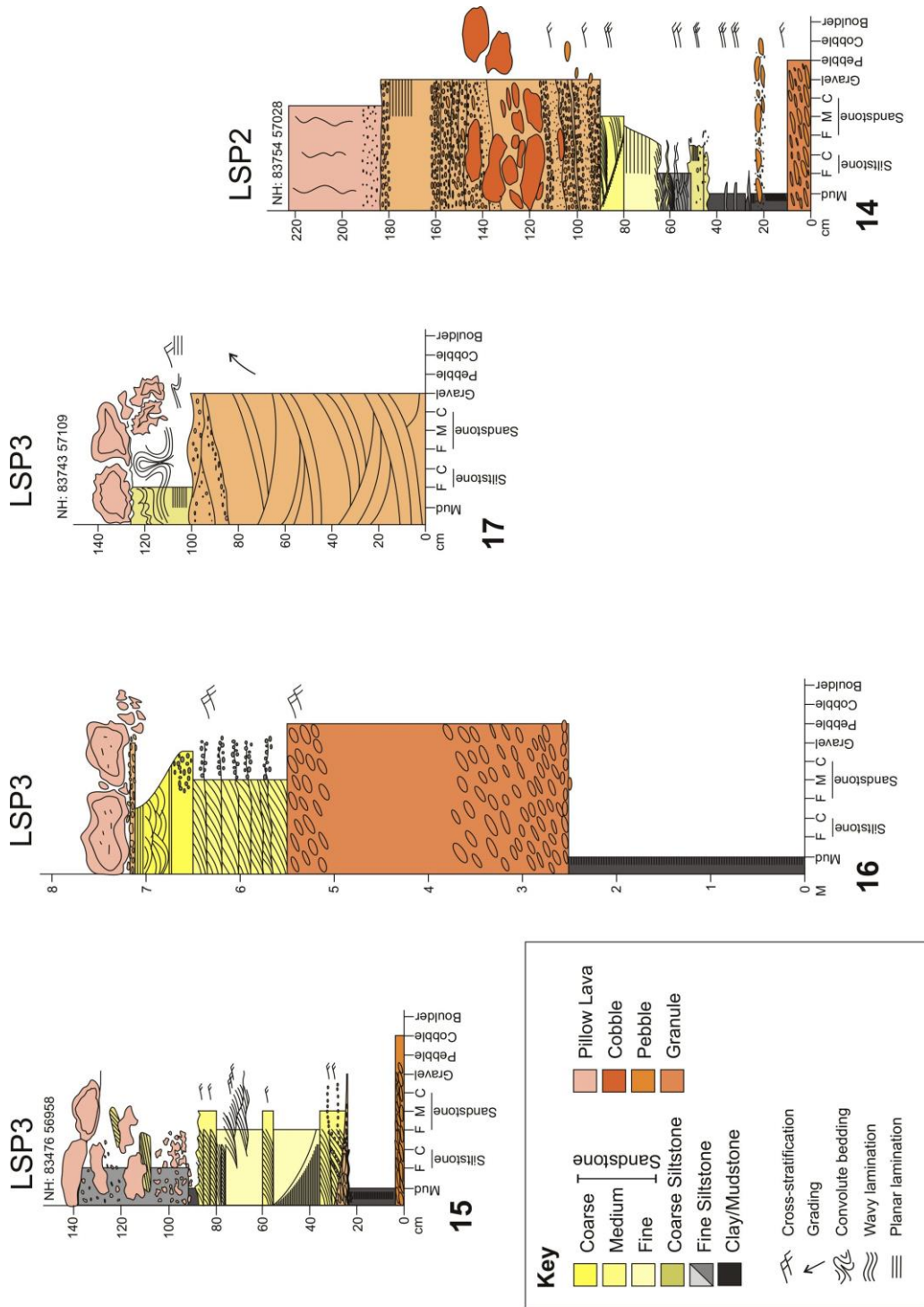
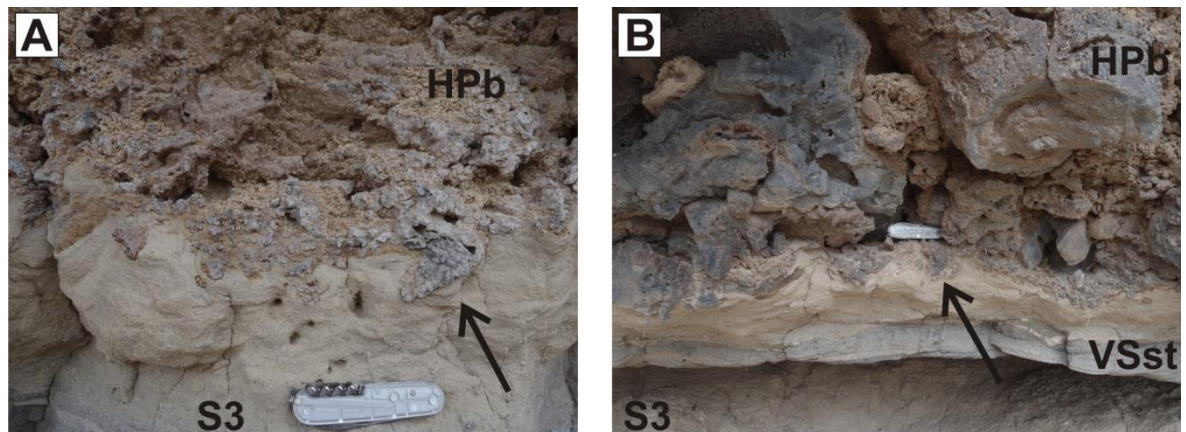


Figure 4-25: Logs depicting the sedimentary units observed at the road cut along CJ Strike Dam Reservoir, Mountain Home. LSP2 is shown here for comparison. Log colours simply denote grain size. Pink = lava nad/or HPb.

#### 4.2.2.4 HPb and S3 contact (sedimentary inclusions):

The nature of the contact between the S3 and the HPb is complex. Typically the contact is erosive or deformed and sharp, but locally it is gradational. The amount of white siltstone and sandstone that overlies the VSst varies, and it is this sediment that typically interacts with the HPb. Coherent sedimentary inclusions are abundant within the HPb (Figure 4-16 and Figure 4-17). This section outlines the range in contacts and interaction types observed.

The interaction and mingling between the pillow lava, hyaloclastite breccia and sediment is variable. In general, clasts penetrate into the underlying white fine siltstone for at least 8 cm (Figure 4-26). Clasts comprise glassy basalt ranging in size from mm to 15 cm, and display globular shapes, locally with micro-scale quenching and mingling at the edges (Figure 4-31). Larger pillows and spalled fragments tend to deform and load the sediment rather than mingle with it. The smaller basalt clasts (< 10 cm) however, mingle more with the surrounding HPb breccia and sediment. Finger-like invasions of basalt into the sediment, ~5-10 cm long, are common (Figure 4-26).



**Figure 4-26: Annotated field photographs of the LSP3 lava-sediment interface.**

**A) The arrow points towards a small basalt clast loading into the underlying sedimentary unit. B) The arrow points towards small basalt clasts (of hyaloclastite and pillow breccia) that load the (underlying) sediment, but do not come into contact with the VSst. In both images, the pen knife is ~ 8 cm long.**

At Locality 17 the pillow lava and hyaloclastite breccia is clast supported and there are no sediment inclusions or sediment-filled vesicles. At the base of the HPb there is an ~35 cm thick mingling zone between the pillow lava (HPb) and the underlying sediment (S3). Clasts, including pillow fragments and breccia, have fluidal and globular shapes. Larger clasts are elongate and up to ~65 cm, whereas small clasts are between 0.5 and

2.5 cm. The sediment is orange-weathered, due to the formation of palagonite, rather than white, around the clasts.

At Locality 24 the white, fine siltstone package overlying the VSst is considerably thicker, up to 30-40 cm in places. Many of the pillows and pillow tubes are large, with flat bases, and have multiple rinds that are striped (orange and grey due to preferential palagonitisation), and feature ropey textures. Where the bases of pillows are flat, the underlying white siltstone package is only 5-10 cm thick. Flame structures of the siltstone are present between the pillows, suggesting that the sediment has been 'squeezed' in between the pillows. Sediment inclusions here are large, some up to 80 cm across (Figure 4-27). Locally, the white siltstone is completely disrupted by the HPb, and is fluidised (no structure retained) and mingled with the HPb. A ~2-3 cm band of siltstone is preserved above the VSst, where mingling has not occurred. An orange-stained palagonitised band defines the contact (0.5 cm thick). Thin sections of this 'orange' band show that it comprises palagonitised glassy shards (Figure 4-19).

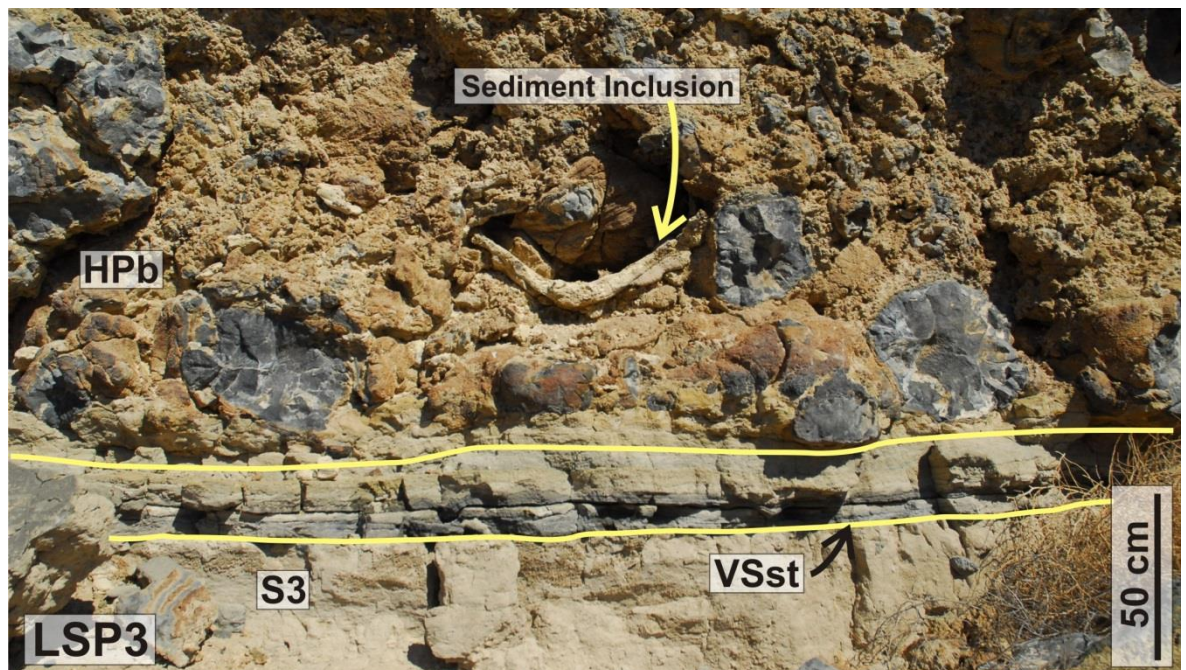


**Figure 4-27: The relationship between S3, the VSst and the HPb at Locality 24. Large sediment inclusions, comprising white, fine-grained siltstone, are found within the HPb, up to 80 cm. This image contains a sediment inclusion ~50 cm in diameter.**

At Locality 25 (where there is no VSst present), white, fine siltstone forms sedimentary inclusions, fills vesicles and dominates the matrix within the hyaloclastite breccia. Mingling of the HPb and sediment occurs on a mm - cm scale, and ranges from loading and deforming of the sediment to mingling of juvenile clasts and sediment (peperite) (Figure 4-31). Sediment structure is not retained at the contact. Whether the VSst is present, or not, the HPb interacts with fine-grained sediment.

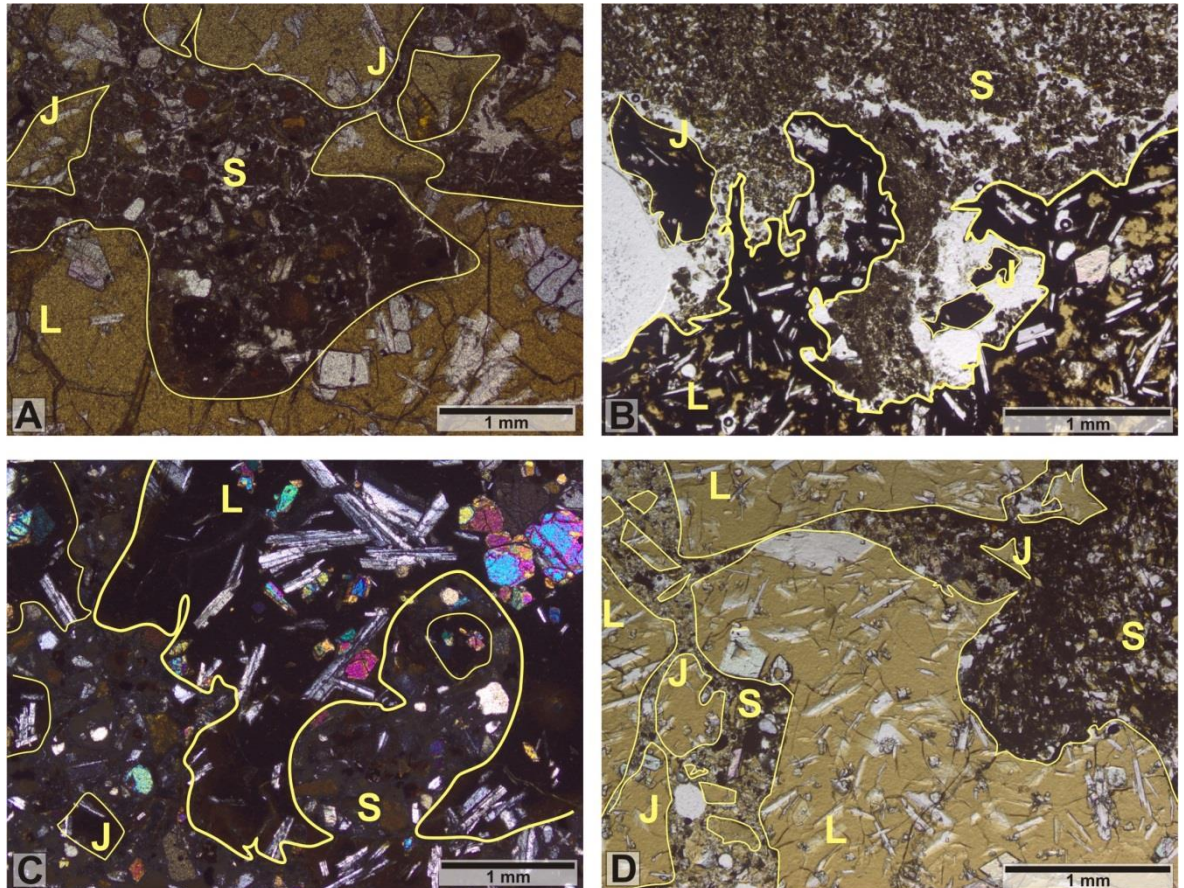


**Figure 4-28: Petrography of the HPb-sediment contact at LSP3.**

**A) Palagonitized basalt (L) with blocky irregular juvenile clasts (J) that have broken away from the main lava bleb (L). These are mingled with the volcaniclastic host sediment (S). PPL. B) Fluidal lava clast (L) has irregular margins in contact with the fine-grained siltstone host sediment. Fragmentation and mingling is represented by juvenile lava clasts (J) within the sediment. PPL. C) Globular embayment of a lava clast (L), with sediment (S) and juvenile blebs (J). XPL. D) As lava and sediment mingle the lava fragments produce juvenile lava clasts (J) within host volcaniclastic sediment (S). Juvenile clasts (J) are blocky and form a tight fragmentation zone between two larger lava clasts.**

---

#### 4.2.2.5 Interaction and penetration of the HPb with the VSst

Throughout most of the field area there is no interaction between the volcanoclastic siltstone unit (VSst) and the HPb. The VSst is commonly deformed and loaded (as noted above); however, locally, more complex interaction between pillow lava (the HPb) and the VSst is observed. Pillows in contact with the VSst range dramatically, and were measured systematically over the northern part of the field area.

From log locality 19 to 21, the contact between rubbly (pillow) lava and sediment is exposed. The VSst is laterally persistent for ~15 m and is commonly deformed, broken and breached by the overlying pillow lavas. Pillow lavas in contact with the VSst range in size, but are predominantly small (~20-50 cm). Flame structures, breached VSst, and broken and rafted blocks of VSst that are still *in situ*, are common.

A flame structure, involving the VSst, is observed deforming the original sedimentary layers (Figure 4-29). A large blocky, coherent sediment fragment, 20-30 cm in length, is included within the rubbly base of the pillow lava. The original lamination in the inclusion is preserved within its central part, but the outer margins are deformed due to mingling with the lava. Sediment also fills vesicles within breccia clasts of the HPb.

Further along the section (locality 19-21), the VSst is breached/broken by the overlying HPb. Figure 4-30 illustrates a typical example where a small pillow loads the VSst as it is broken and pushed up. Flame structures within the overlying fine white claystone are also observed (highlighted yellow).

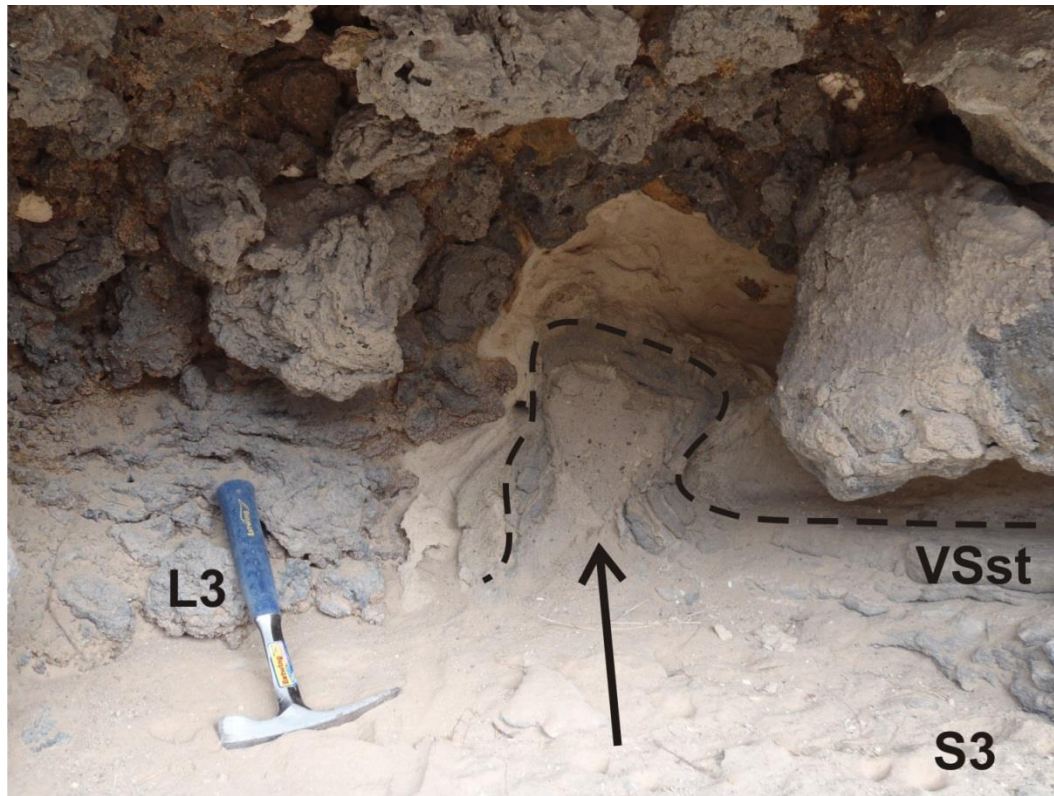


Figure 4-29: A flame structure of S3 sediment, including the VSst (dashed line). This deformation is a consequence of loading by the overlying HPb. Location south of log 19. Hammer is ~35 cm long. VSst = Volcaniclastic Sandstone; S3 = sedimentary unit 3; L3 = lava 3.

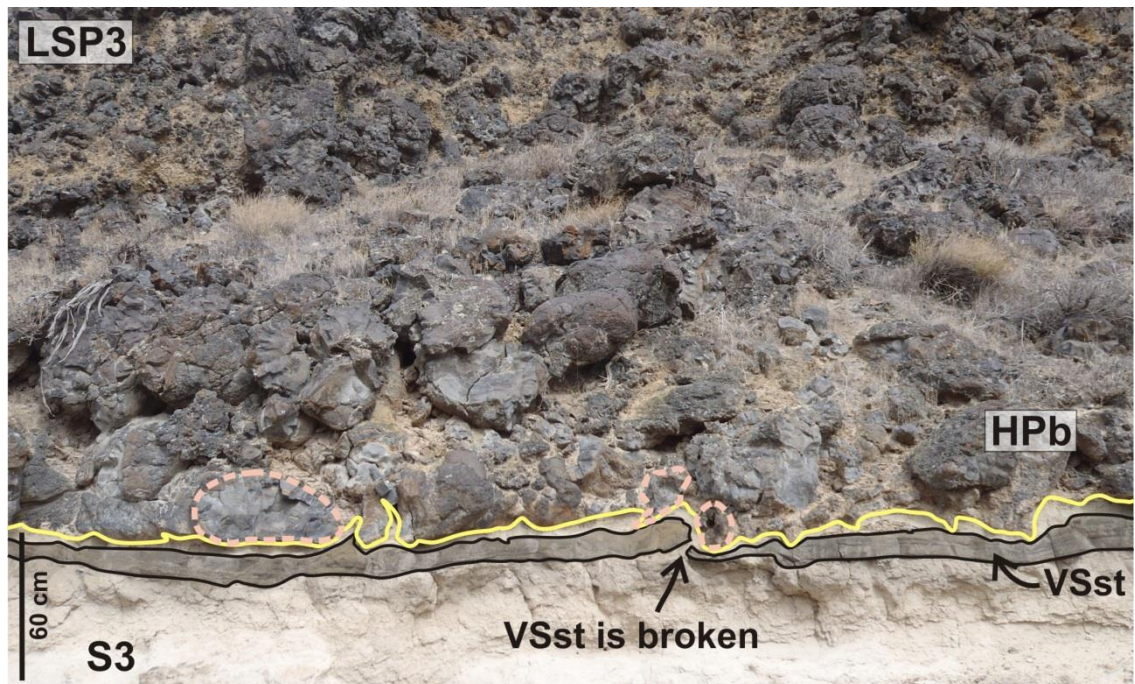


Figure 4-30: Interaction at the HPb and S3 interface at locality 19-21. The VSst (grey shading) is broken by overlying pillow lavas (dashed pink outline). The yellow line highlights the sediment-lava contact, showing loading and flame structures caused by the HPb.

At log locality 21 the VSst is observed twice due to a small isoclinal fold (Figure 4-31). Log 21 demonstrates that the second VSst layer is very similar to the first, and that therefore it is the same unit, rather than a repeated sequence. The VSst is broken and forms a flame-like structure, which is bent and curled over on itself (the small VSst unit that remains is upside down). The adjoining VSst (left of the figure) is observed to be pushed up over the first VSst, and although broken into chunks, forms this 'double' layer for ~3 m. The underlying sedimentary units and overlying HPb are typical of the rest of the field area. The sedimentary units still retain bedding, and the pillows are not particularly large or noticeably small (16-51 cm).

Near locality 21, an isolated, coherent block of sediment, ~90 cm across, which includes the VSst, is found within the HPb. The thickness of the VSst at this locality is 12 cm, and this thickness is preserved within the isolated block, along with the original sedimentary structures of the VSst and the surrounding alternating yellow and grey beds (Figure 4-32). Pillow lavas and hyaloclastite breccia surround the coherent sediment block, the edges of which mix and mingle with the breccia to form peperite. Sediment has been squeezed/injected into cracks and fractures within the surrounding pillows and hyaloclastite breccia.

Sedimentary inclusions within the HPb comprise hard, fine white claystone and siltstone, with desiccation cracks on their outer rim, where they have been in contact with pillow rinds. Thin sections show that they are very fine, structureless claystone.



Figure 4-31: The complex contact relationship between S3 and the HPb. The VSst is broken, deformed, and doubled over/repeated at locality 21. This is a consequence of the overlying pillow lavas and hyaloclastite breccia. Log 21 records the 'double' VSst. The pillows measure: i) 16 cm, ii) 40 cm, and iii) 51 cm across. Pen knife for scale in inset is 8 cm.

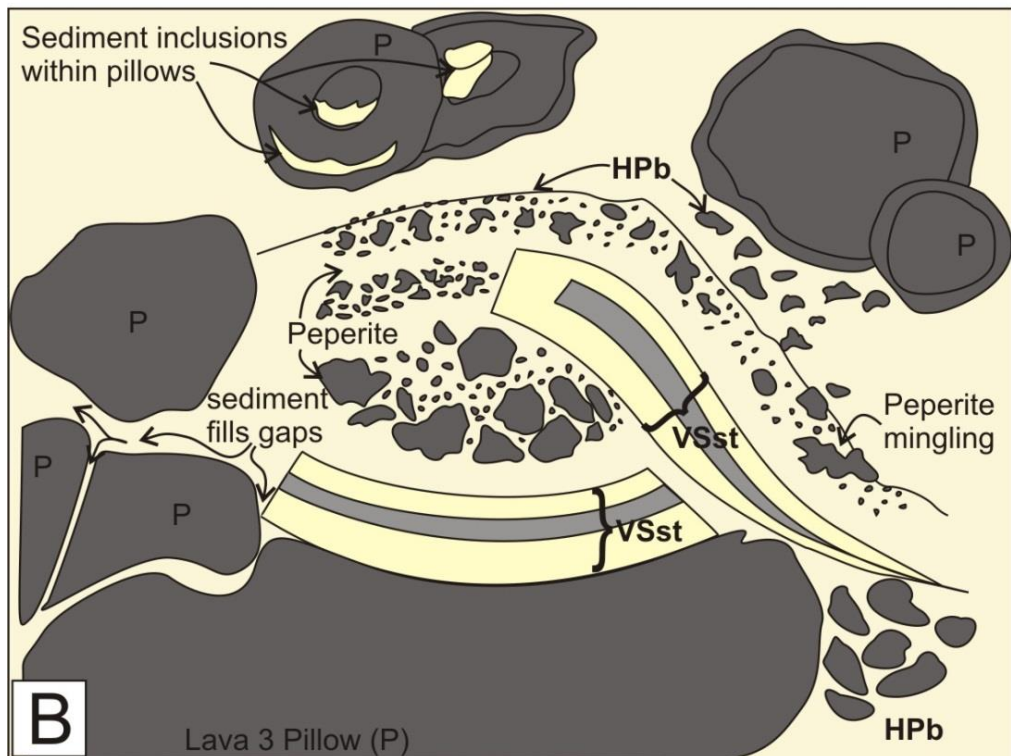
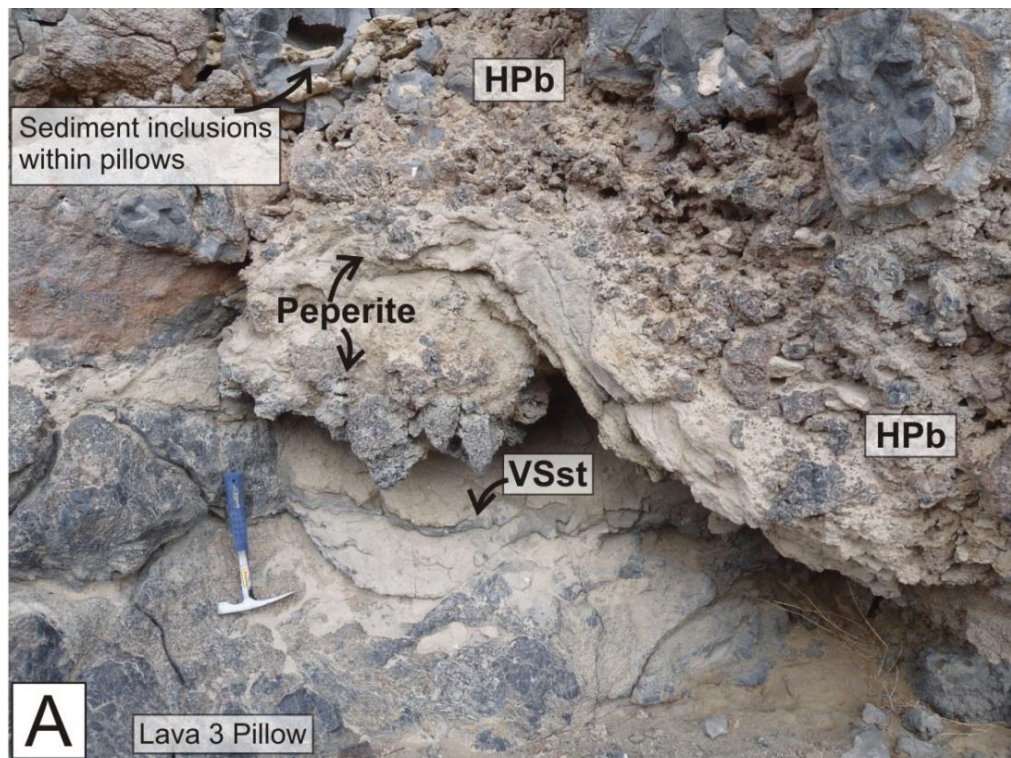


**Figure 4-32: Field view (A) and interpretative field sketch (B) depicting a large, isolated, coherent sediment block within the HPb.**

The coherent sedimentary block includes the VSst, with the original thickness and internal structure preserved in the coherent block. Peperite occurs at the contact between the sedimentary block and the HPb. Geological hammer is ~35 cm long.

### 4.2.3 LSP4

LSP4 is ~2.5 m thick and comprises a thin sub-aerial scoriaceous fall deposit and basalt lava (L4) (Figure 4-3).

#### 4.2.3.1 Lava:

Lava 4 (L4) is 1.9 m thick, but is likely thicker than this in other places; it is best observed at the top of the pipe road, which runs next to the water pipe shown in Figure 4-2 [11TNH 83402 58117]. L4 is dark grey, vesicular basalt lava with a ropey and slightly rubbly base. Small horizontal vesicles are present in the basal 75 cm, with a 2:1 aspect ratio, and the upper 60 cm. The core (~20-50 cm) is massive, with rare round vesicles. A rosette-type jointing pattern distinguishes it from L3. Petrography demonstrates that L4 is tholeiitic basalt (Figure 4-4).

#### 4.2.3.2 Sedimentary/Volcaniclastic:

A 50 cm dark grey scoriaceous unit underlies the L4. It is very coarse sandstone up to granule grade (0.5 - 4 mm; up to 2 cm) and clast supported. The package is laminated to diffusely bedded on a 2-8 cm scale. At the upper contact with L4, there is an ~5 cm thick erosional zone, cross-cutting the laminations.

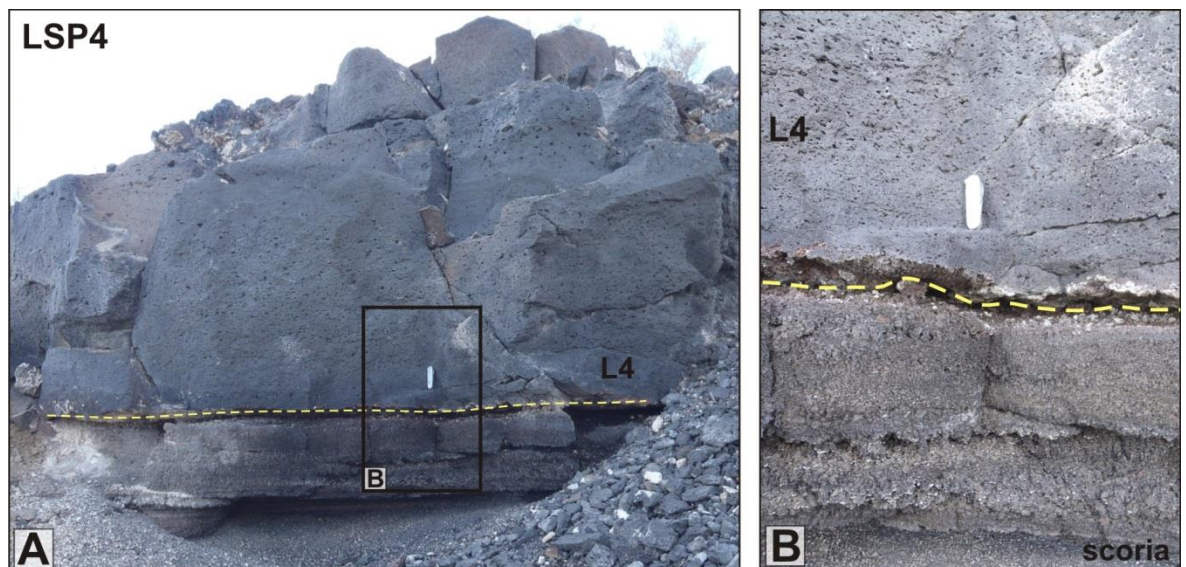


**Figure 4-33: Field photographs of L4 and LSP4.**

**Coarse sandstone to granular scoriaceous unit is overlain by sub-serial, vesicular basalt lava (L4). Yellow line marks the contact. B) The granular scoriaceous unit is clast-supported, ~50 cm thick, and diffusely bedded.**

## 4.3 Interpretation

Individual LSPs are discussed in detail below, but a brief summary is provided here. All of the lavas within the succession are wholly sub-aerial, with the exception of Lava 3, which was erupted sub-aerially but subsequently emplaced into a lake where it fragmented to form hyaloclastite and pillow breccia, building foresets as it prograded (into the lake). The dominance of sub-aerial lavas indicates that a standing body, or bodies, of water (lakes), present at the time of sediment deposition was shallowing, either due to filling of accommodation space, or drying out of the lake. This seems to have been cyclic, and perhaps more pronounced where close to the lake edge. The HPb in LSP3 is ~10-15 m thick, indicating the water depth at the time of its emplacement.

S1, S2 and S3 have increasing volcanic contents, up-sequence. Volcanic material ranges from reworked basalt (plus older material, such as e.g. rhyolite of Miocene age (Shervais et al. 2005) to pyroclastic material (reworked fall deposits and possible density current deposits). Reworking of the existing volcanic field, including material from vents, and cinder cones, by fluvial systems, provided the volcanoclastic material for deposition.

### 4.3.1 LSP1

#### 4.3.1.1 Lava:

L1 is inflated, pahoehoe lava, exposed within an area of faults (Figure 4-5). A graben-type structure is present within the lower canyon, perhaps explaining why L1 is not observed elsewhere. Ropey textures, abundant large elongate vesicles, the absence of cross-cutting relationships, and the general paucity of sheet intrusions in the area, indicate it was most likely a sub-aerial lava.

#### 4.3.1.2 Sedimentary units:

S1 comprises fine-grained lacustrine sedimentary rocks (claystone, siltstone and fine sandstone) with the rare addition of reworked volcanic material that increases up-sequence (Figure 4-6). Large thicknesses of claystone and siltstone in the basal units (Figure 4-7) were most likely deposited within a lake (Godchaux and Bonnicksen 2002; Shervais et al. 2002). Organic material observed in the lower units suggests pelagic sedimentation within a deep-water body, which is supported by petrographic analysis that reveals the presence of diatomaceous claystone. Trough-cross-bedded packages

and granular volcanic material in the lower part of the sequence may be a result of increased bedload and input at shallower depths, which is transported further into the lake, or collapse, slumping and reworking of previously deposited material up-shelf in shallower depths.

The 'upper' part of the S1 sequence (as defined by logs 1-4, (Figure 4-6 and Figure 4-9) records coarsening and reworking of volcanic material up sequence. This may have been through filling of the accommodation space, and/or drying up of the lake, but ultimately a higher energy fluvial input became dominant. Coarser sandstone units represent increased bedload, as rivers prograde into the lake. The presence of other clasts such as rhyolite and basalt, suggest erosion and transportation from the volcanic-dominated contemporaneous landscape by a fluvial system, with deposition within the fluvial/lacustrine environment. However, some deposits likely originated directly from coeval volcanic activity, (e.g. broken accretionary lapilli, which are unlikely to survive much fluvial reworking (Figure 4-8)), and which may have been relatively proximal (Brown et al. 2012). Phreatomagmatic eruptions were common at this time (Godchaux and Bonnicksen 2002; Shervais et al. 2002), and provided the increased input of volcanic material in the 'upper' sequence.

### **4.3.1.3 Interaction**

As the contact between L1 and S1 is not exposed, evidence for lava-sediment interaction is not observed. However, the lava is sub-aerial, which suggests that at the time of emplacement, the lake had shallowed, and/or the lava did not reach further than the edges of the lake/standing body of water.

## **4.3.2 LSP2**

### **4.3.2.1 Lava:**

L2 is a sub-aerial basaltic lava, comprising multiple lava packages. It displays hummocky, lobate geometries, and ropey textures, indicative of inflated pahoehoe lava (Macdonald 1953; Self et al. 1998). The pinching out of L2 towards the reservoir (southwards) suggests that this was the extent of the lava and it reached no further, and/or the flow field migrated in a different direction outwith the study area.

### 4.3.2.2 Sedimentary:

The white, fine grained claystone and siltstone units directly underlying L2 suggest a lacustrine depositional environment, with low energy sedimentary input into the lake. Petrographic analysis (Figure 4-13) records a volcanoclastic component, including reworked ash/tuff, in which glassy wispy shards are present. This suggests that low energy currents were transporting and depositing material within the water body. In the south of the field area S1 records a much higher energy environment, possibly fluvial to lacustrine. Pebbles of multiple lithologies are indicative of erosion of the landscape by a fluvial system, and their palaeo-flow direction records a north to south transportation, which agrees with the lava flow directions. The sequence in the South is also much more volcanic dominated and coarser (Figure 4-11), with volcanic material perhaps sourced from coeval volcanic activity (in the north) and transported within the fluvial system. It is likely that in the south of the field area the exposures were closer to the fluvial mouth/input into the lake, or that the water body was not present/had dried out, leaving only fluvial deposition. This explains the difference in sediment properties between the northern and southern exposures. Even if the lake was present in the south, the dominant fluvial deposition suggests that it was close to the mouth of the river at that time. The reddened material at the top of S2, in the south, suggests there was a slight pause in sedimentation as volcanic activity recommenced.

### 4.3.2.3 Interaction

The lack of pillow lavas, hyaloclastite and 'dynamic' peperite, is evidence that the water body that deposited the sediment of S2 was no longer present, or had significantly reduced in size, when L2 was emplaced.

Interaction between L2 and S2 is minimal, suggesting that the lava flowed over the sediment rather than nosed/bulldozed into it. Minor peperite and/or inclusion of sediment within the lava is observed (Figure 4-13), however, which suggests that sediment consolidation was localised. It is likely that the sediment was coherent, only partially saturated in places and relatively well compacted, apart from the upper few cm of the uppermost sedimentary unit (Figure 4-11). This would allow for minimal interaction of the upper sedimentary unit with the lava.

### 4.3.3 LSP3

#### 4.3.3.1 Lava:

Lava 3 comprises a hyaloclastite and pillow breccia (HPb) package overlain by sub-aerial pahoehoe lava (Figure 4-15). The HPb displays both pillow-dominated and hyaloclastite-dominated foresets (Figure 4-16) that record the aqueous/aerial transition from sheet-like pahoehoe lava into water body, likely a lake. This represents a lava-fed delta, similar to Gilbert-style deltas (Porębski and Gradziński 1990; Pedersen et al. 1998; Skilling 2002), deposits of which have been recorded in West Greenland (Pedersen et al. 1998), and Iceland (Watton et al. 2013). The exposure is ~15 m thick, indicating a relatively shallow water depth at the time of lava emplacement (Jones and Nelson 1970; Pedersen et al. 1998; Skilling 2002). The passage zone may be described as sheet-like (Self et al. 1998; Wright 2013), with a simple lava/hyaloclastite transition zone, suggesting lava flux was high, but accommodation space limited (Tucker and Scott 2009; Watton et al. 2013). However, closer inspection reveals a more complex HPb geometry.

The HPb foresets typically record multiple dip directions; although in the south the majority preserve a palaeoflow direction towards the south, supporting the interpretation that the volcanic source was likely to the north (Bonnichsen et al. 2004; Shervais et al. 2005). It is common for sub-aerial lava lobes to enter a lake in different directions, particularly along a sinuous shoreline and as a consequence of source switching between flow lobes (Wright et al. 2012; Watton et al. 2013). Source switching can be a major contributing factor in the creation of multi-direction hyaloclastite and pillow breccia foresets, particularly in primary hyaloclastite deposits (Wright et al. 2012; Watton et al. 2013). In part, this likely happened in Mountain Home, where flow lobes reached the lake shoreline at different entry points and angles to each other, but also at different times. These built breccia foresets and the delta prograded into the lake, eventually joining, coalescing, and perhaps overlapping, producing the chaotic deposits of the HPb.

Pillow-dominated foresets are interpreted as the products of the initial stages of lava tubes/feeders entering a water body, which then cool and break up. Upon cooling, quenched and spalled fragmental material (from the pillows) is produced and may act to insulate the pillows from further cooling and aggressive fragmentation (Skilling 2002; Watton et al. 2013). This allows further emplacement of lava through the tubes and channels, bypassing the upper transitional zone and reaching further downslope. The available water depth may have hindered this more complex process to some extent,

but does allow for the concentrated formation of pillow-dominated foresets and larger inflated and intact, pillow tubes, observed at the sediment interface.

The hyaloclastite-dominated foresets are the fragmental by-product of lava emplacement into water. They comprise the fragmental, broken, and quenched material spalled from the pillows and lava tubes (Figure 4-28), and a gradational boundary is observed with the pillow-dominated foresets (Figure 4-26). The material is further fragmented and likely reworked, through slumping and collapse of the foreset packages, as a consequence of the oversteepening lava pile, gravity-driven slumping, and lobe inflation (Skilling 2002; Watton et al. 2013). The cyclic nature of the pillow- and hyaloclastite-dominated foresets is likely a consequence of the cyclical pattern of lava emplacement. Multi-directional dipping foresets are typically associated with primary fragmented hyaloclastite systems in a near shore, shallow, environment (Watton et al. 2013).

#### **4.3.3.2 Sedimentary**

The sedimentary units of LSP3, S3, are predominantly volcanoclastic and have a larger volcanic component relative to S1 and S2. The lower units (i.e. those below the VSst, Figure 4-18) are interpreted as fluvial/lacustrine deposits, which comprise reworked material from the contemporaneous volcanic landscape. Exposures in the south (log localities 14-17, Figure 4-25) record much coarser units than elsewhere, with the presence of imbricated pebble-rich units, and higher energy bedding structures (e.g. trough cross bedding). These were most likely deposited within the fluvial system, and strengthen the interpretation that the fluvial input into the lake was focused around this area.

S3 is of variable thickness, dependant on the geometry of the underlying L2. It is likely that L2 overwhelmed the fluvial channel system (channel filling lavas are recorded in the WSRP (Bonnichsen and Godchaux 2002; Shervais et al. 2005), which then tried to re-establish itself. Towards the south, L2 pinches out, enabling the extended channel system to access more accommodation space.

The VSst marker is present throughout most of LSP3 and comprises scoriaceous, glassy volcanic material (most likely reworked), as well as reworked volcanoclastic strata. The basal black bed (Figure 4-20) has open pore space between angular grains (Figure 4-21) with minimal matrix. The central white, fine-grained middle package has an erosional base and cross-lamination (Figure 4-20), indicative of the erosion and/or filling of topography by reworked ash, rather than a mantling fall deposit. The VSst represents a

renewed volcanic pulse (explosive), which produced fresh volcanic material that blanketed the area. It achieves a consistent thickness in the north, but is much thicker in the south (Localities 14-17, Figure 4-2), where it is intermixed with fluvially deposited, potentially coeval, volcanic dominated sediments. This strengthens the evidence that palaeoflow direction was from the north towards the south (Godchaux and Bonnichsen 2002; Shervais et al. 2005). In places, the VSst is absent as it has been eroded and mingled with the HPb.

The overlying white claystone and siltstone that are typically in contact with the HPb are dominated by volcanoclastic material. These deposits are present in both the north and south of the field area. The orange-stained beds (Figure 4-24), comprising palagontised glassy shards likely represent an initial input of glass into the depositional system. Petrographical analysis of the orange beds (Figure 4-19) reveals reworked palaganotised volcanic shards, which are typically created during fragmental processes, such as phreatomagmatic explosions, hyaloclastite breccia generation and fuel-coolant Interactions (FCI's) (Wohletz 2002; Zimanowski and Büttner 2002; Schipper et al. 2011), at the lava-water interface.

The fluvial system feeding the lake was likely close to the south of the field area but it is probable that volcanic activity ultimately overwhelmed the sedimentary system as the two competed for space.

#### **4.3.3.3 Interaction**

The interaction between the HPb and the underlying S3 is complex. The HPb is mingled with sediment and suggests slumping and disruption of sediments (possibly nearshore) as the lava was emplaced into the lake. The HPb also thoroughly interacts with the volcanoclastic sediments in the south. The VSst provides a good marker bed to help visualise and characterise the interaction. It, itself, displays variable interaction with the overlying HPb. In places, there is no interaction, whereas in other areas the VSst is fragmented and incorporated into the HPb (Figure 4-32). Also, locally, the VSst is absent, having been obliterated by the bulldozing HPb (Figure 4-22) (Section 1.1.2.4).

The fluvial-lacustrine volcanoclastic sediment was wet, possibly water-saturated, and unconsolidated at the time of the emplacement of L3. As pillow lavas and hyaloclastite encroached upon the sediment, they load and deform it, finding weaknesses to bulldoze into it. The burrowing and nosing of the lava into the sediment causes interaction in the form of mingling to various degrees of complexity, as previously discussed. The top layers of sediment will be the most unconsolidated and (super)saturated, causing them

to act like a slurry when invaded by the pillows and hyaloclastite breccia. This sediment is fluidised and mingled with the HPb. Initial bulldozing takes energy out of the advancing pillows, and the ability of the pillows to bulldoze into the sediment weakens, due to energy and heat loss, increasing viscosity, and frictional shear stress with the sediment (Kokelaar 1982; Busby-Spera and White 1987; Dadd and Van Wagoner 2002; Zimanowski and Büttner 2002; Palinkaš et al. 2008). However, the underlying sediment (in particular the very fine-grained material), which is a little more consolidated and/or cohesive can be broken/fragmented/disrupted and incorporated into the HPb and pillow lavas as coherent sedimentary inclusions. These inclusions are extremely fine-grained and the pillows and breccia show evidence of quenching against them.

As interaction progresses deeper into S3 to the top of the VSst, it becomes more disruptive and dynamic. The fine-grained sediment is expelled, and/or squeezed and deformed round pillows and breccia, through fluidisation. Pillow sizes recorded at the VSst contact are wide ranging (dominantly 10 - 58 cm). The presence of a VSst block within the HPb (Figure 4-32) indicates that the VSst is not completely susceptible to breaching and invasion by the pillows. This may also explain the small section where the VSst is absent (Log locality 22, Figure 4-22), but most likely was deposited here before being incorporated into the HPb through planing and mingling.

The variability of the HPb-sediment interface across the area, from little interaction to complex mingling, suggests localised variations in both sediment properties and lava flux influence interaction.

#### **4.3.4 LSP4**

LSP4 comprises a locally deposited, thin, sub-aerial, scoriaceous fall deposit, and a sub-aerial tholeiitic basaltic lava (L4) (Figure 4-33). The glassy, clast supported nature of the scoria suggests a likely vent proximal accumulation, with little reworking and weathering before the overlying lava was emplaced. The vent is not preserved, but most likely belongs to the cluster of vents situated to the NW (Shervais et al. 2005). The absence of bombs indicates that the vent must be more than 200 m away (Brown et al. 2012; Williamson and Bell 2012). Lava 4 is of pahoehoe type, with indicative ropey textures, is thin, and pinches out to the south, indicating that this is the geographic limit of the flow unit, and that it was likely sourced from the north. The deposits associated with LSP4 indicate explosive vent and cinder cone type activity during the Pleistocene in the western SRP.

---

## 4.4 Discussion

This field study has highlighted a number of unique lava-sediment interaction features, which are discussed below.

### 4.4.1 Pillow Analysis

Data measurements were collected at key outcrops along the S3-L3 contact, which included pillow height and width (two longest axes in the vertical and horizontal), depth of the sediment from the base of the pillow to the top of the VSst, and total height of the sediment from top of the VSst upwards. The quantitative results illustrated in Figure 4-34 show little correlation between pillow size and penetration depth.

It is intuitive to suggest that larger pillows would penetrate further into sediment than smaller pillows. Conversely, it may be argued that larger pillows have a greater surface area on which to stabilise and rest upon the sediment interface (the reaching of terminal velocity when considering Stokes Law (Richardson and Zaki 1954)), rather than settling through the sediment. However, Figure 4-34 indicates that there is little to no correlation between the size of a pillow and the depth to which it penetrates the underlying sediment.

This also indicates the scale invariance of pillow penetration and therefore disruption of the sediment. Scale invariance suggests that sedimentary properties, such as grain size, cohesion, saturation etc. have a strong influence on the processes and products of lava-sediment interaction, as well as lava properties such as flux and viscosity.

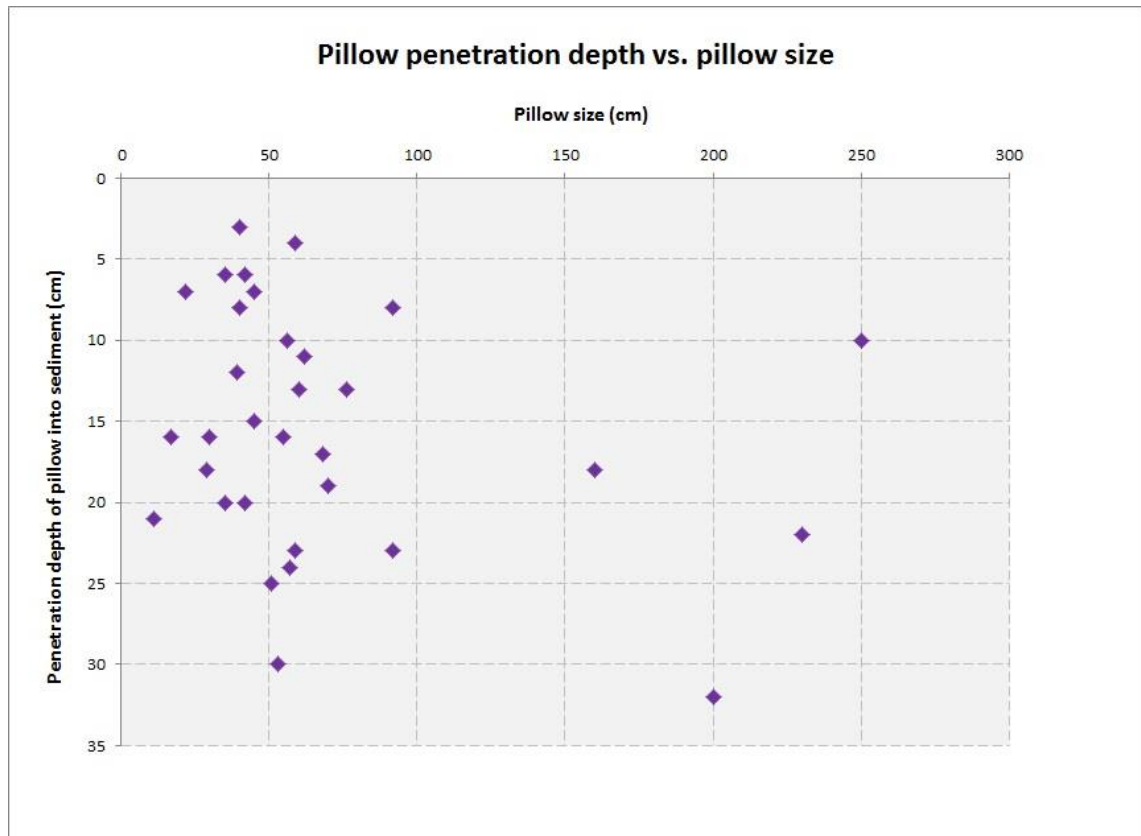


**Figure 4-34: Comparison of pillow lava size and penetration depth into the underlying sediment.**

**The data indicate that pillow penetration depth is scale invariant.**

### 4.4.2 Coherent sediment inclusions

Sediment occurs both at the interface with the HPb and throughout the unit. Entrained within the HPb are coherent fragments of sediment, ranging from 1 - 60 cm, incorporated from the underlying units (S3). Figure 4-35 illustrates how this may occur.

Pillow lava flows over and bulldozes into sediment, which is unconsolidated and saturated, or partially saturated, with pore water. The majority of the sediment becomes fluidised, facilitating the invasive character of the lava (Kokelaar 1982; Skilling et al. 2002); however more coherent masses of fine-grained, cohesive material are detached (Figure 4-35 A). The coherent fragments of sediment are churned and mingled with the HPb. Some likely fully disintegrate, and the majority decrease in size due to fracturing and disaggregation, with the excess material incorporated into the breccia matrix (Figure 4-35 B). The nature of the sediment is important in controlling its ability to form cohesive fragments. For example, an unconsolidated coarse-grained sediment has little internal cohesion, so would break up relatively easily, whereas fine-grained sediment with a significant clay content has a significant internal cohesion, and so, even when unconsolidated, has the ability to hold itself together (Owen 2003; Grabowski et al. 2011).

Pillow lavas may also envelop the coherent sediment fragments during (further) lava emplacement (Figure 4-35 C) leading to coherent inclusions within pillows (e.g. Figure 4-17). This process of interaction is progressive as the pillow lavas bud and continue to bulldoze into the sediment, synchronous with hyaloclastite formation.

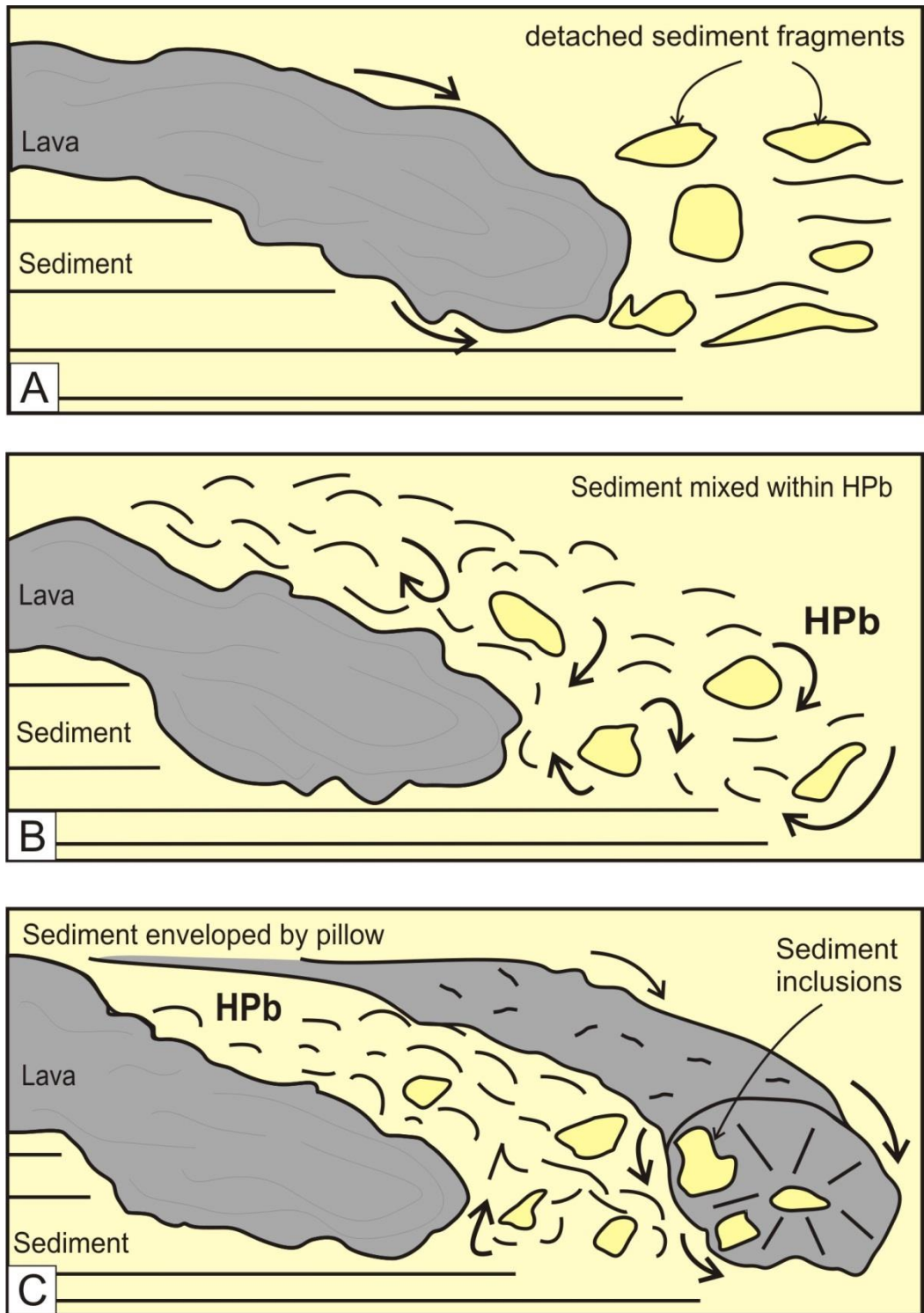


**Figure 4-35: Sketch showing bulldozing lava and sediment mingling within the HPb.**  
**A)** Lava bulldozes into unconsolidated sediment. Sediment is fluidized, but coherent fragments of fine, cohesive material are detached. **B)** The coherent fragments of sediment are incorporated within the HPb, mingled, broken and reworked. **C)** Sediment fragments are enveloped, forming sediment inclusions within the pillows.

### 4.4.3 Sedimentary Marker Bed and Barrier

This field study provides a case study of how a single sedimentary bed, within a sequence, can highlight, impede and possibly be a barrier to lava-sediment interaction. This is observed with the VSst marker bed in LSP3, and without this distinguishable unit, it would have been almost impossible to identify the locally variable interaction. Interaction occurs on a continuum from no interaction to dynamic mingling between lava and water-saturated sediment. Figure 4-36 illustrates some of the key lava-sediment interaction styles highlighted in the case study.

As the lava flows over the sediment it noses (down) and bulldozes into the sediment, whilst also deforming and mingling with it. In some instances very little to no interaction occurs, and the marker bed (VSst) remains intact and unmodified, and lava-sediment interaction only occurs above the VSst (Figure 4-36). Soft-sediment deformation and loading of the sediment column, including the VSst, may occur due to local changes in the sediment properties (Figure 4-36 B). If the sediment is more saturated (with pore water) and is less compacted, for example, this may facilitate the loading of the sediment by the invasive lava. Bulldozing and mingling of the sediment above the marker bed (VSst) occurs, and flame structures, including the VSst with sedimentary units above and below, are observed. The VSst is interpreted as a localised 'barrier' layer to invasive lava and deformation and mingling of sediment, as predominantly lava-sediment interaction occurs above this marker bed.

Locally, however, the invasive lava does break through and penetrate the VSst (Figure 4-36C). There is commonly some sediment remaining above the VSst, which is mingled, and sediment below the VSst becomes fluidised. Figure 4-36 D shows how lava-sediment interaction can be aggressive above the marker bed, whilst the underlying sediment units (below the VSst) remain intact. Peperite forms at the lava-sediment interface and sedimentary inclusions likely form throughout in all examples.

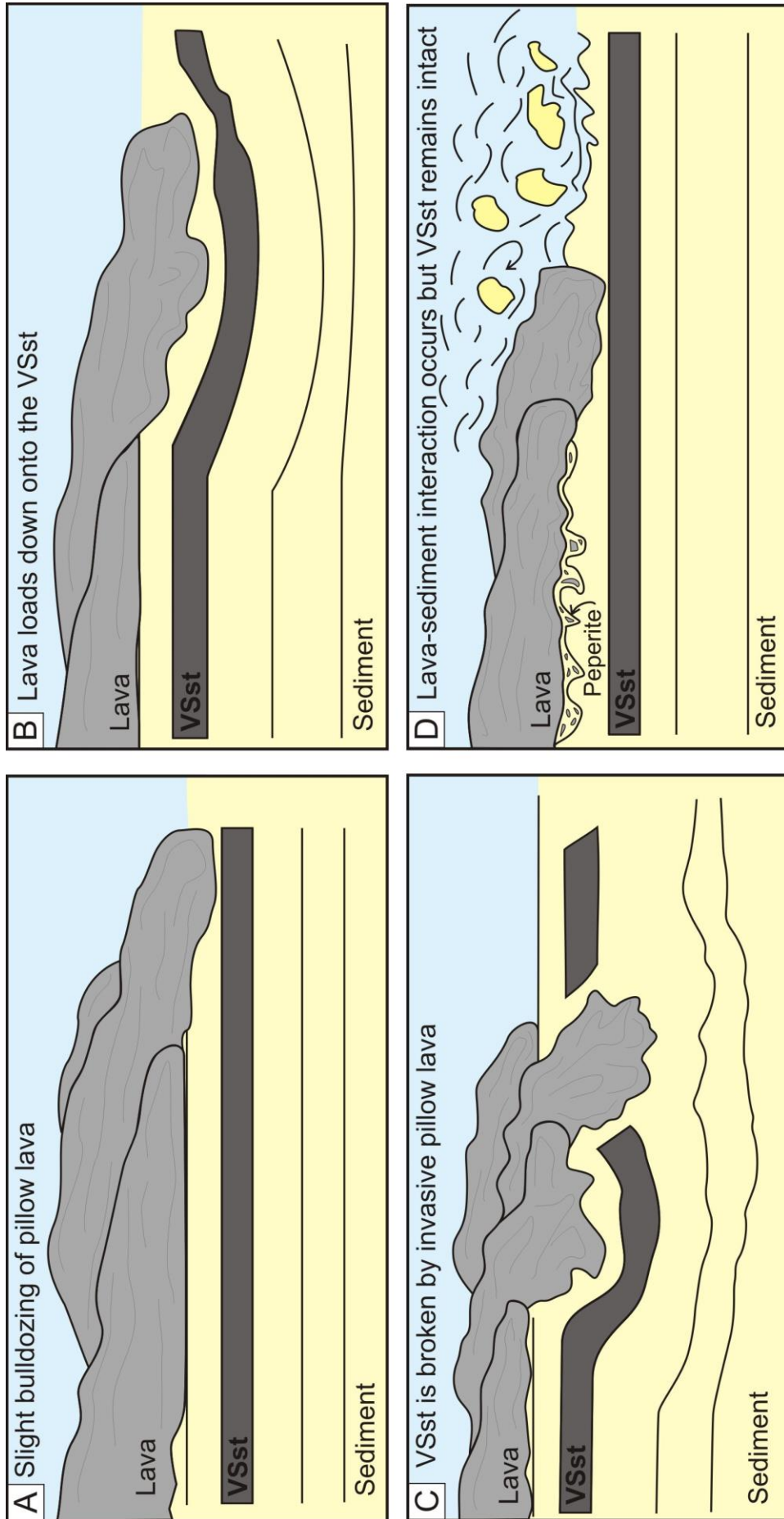


Figure 4-36: A series of schematic sketches depicting how invasive lava deforms and mingles with sediment. A) Lava penetrates sediments, but little interaction occurs. B) Soft-sediment deformation occurs as lava loads sediment. The VSst is loaded, but acts as a barrier between the lava and the underlying sediment. C) Locally, the VSst is disrupted and fragmented by the invasive lava. The sediment around the pillows is fluidised. D) Minimal loading occurs, but lava-sediment interaction occurs, forming peperite

This final scenario (Figure 4-36 D) may be of use when applying our knowledge of lava-sediment interaction to wider scientific/industry problems. For example, if a sedimentary column has the potential to be hydrocarbon bearing, but it is known that lava overlies it, it might typically be assumed that the lava and any lava-sediment interaction would have destroyed any reservoir potential. However, if only the upper part of the sediment column is affected, due to a single clastic unit forming an obstacle to lava penetration, then the underlying sediment units may still have hydrocarbon bearing potential. If this impeding unit has a regional distribution then this scenario would be plausible. Furthermore, it would be necessary to explore scenarios where such a barrier is found and assumed to be laterally constant and persistent, but in reality local variations inhibit its continuity.

#### 4.4.4 Emplacement Model

Sub-aerial lava emplacement into a lacustrine setting formed alternate pillow-dominated and hyaloclastite-dominated foresets that prograde and build a delta front (as illustrated in (Figure 4-37). The lava, whilst under a confining pressure (for pillow formation), likely flowed down-slope, providing an increase in lava flux and increasing the ability for pillows to bulldoze, plough and invade the underlying sediment (Skilling 2002). At the lava-sediment contact the lava mingles with the sediment causing further fragmentation of the lava, mingling with the sediment, mingling of the breccia and sediment, and sediment fluidisation. Further sub-aerial lava emplacement continued to build the lava pile.

This case study has revealed that lava-water-sediment interaction can occur over two different scales. These are illustrated in the 3D block diagram (Figure 4-37) that combines the models depicted in Figure 4-36 A-D, integrating the interpretations made from LSP3.

First, different units within a sediment pile respond differently to interaction with lava and, certain lithologies may impede the penetration and fragmentation of lava. This behaviour is most likely controlled by properties of the sediment such as composition, degree of cohesion, water content, and internal characteristics such as stratification etc. For example, the VSst most likely had properties that allowed it to withstand interaction for the most part (e.g. degree of compaction; cohesion), whereas the overlying white siltstone, was easily fluidised and mingled with the HPb, as it was most likely unconsolidated, uncompacted and highly saturated.

---

Second, individual sediment units behave differently on a smaller localised scale. For example, the VSst typically acted as a marker bed and possible obstacle to interaction, but displays localised, small-scale changes. Such changes include: breaching of the VSst by the penetration of overlying pillow lava; incorporation of the VSst into coherent sedimentary inclusions within the HPb; and the complete obliteration of the VSst by the overlying HPb.

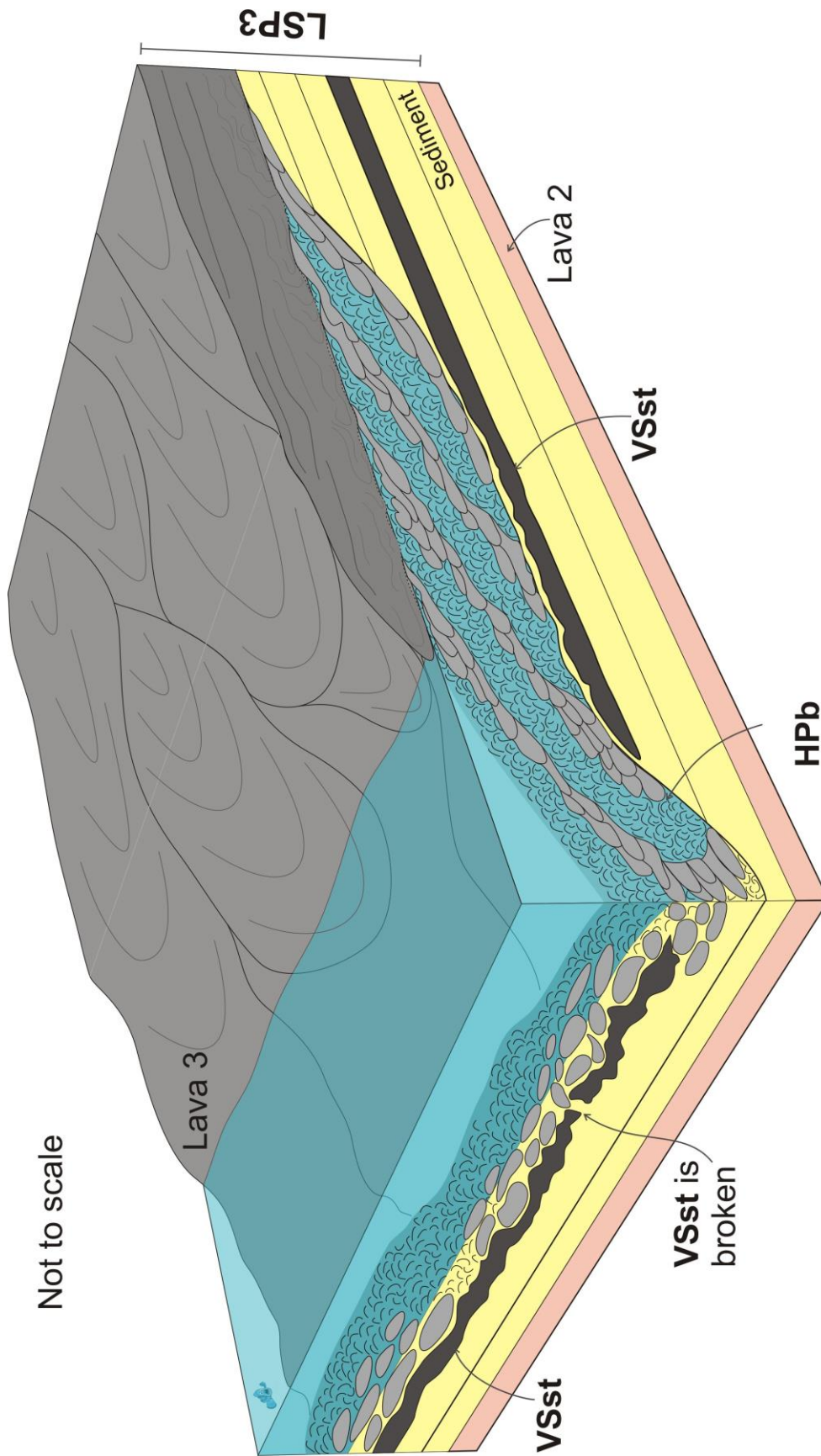


Figure 4-37. Schematic model showing the emplacement of the Mountain Home lavas of LSP3 into a large lake, and the relationships between lava, water and sediment. Pillow lava and hyaloclastite breccia (HPb) build foresets. Burrowing and penetration of the lava pillows into the sediment, results in complex mingling and interaction. The volcanoclastic sandstone (VSst) acts as a barrier, obstructing bulldozing and mingling between sediment and lava. Locally however, the VSst is disrupted and breached by the invasive lava, which mingles with the sediment.

---

## 4.5 Conclusions

This case study provides a regional scale analysis, both laterally and vertically through a lava-sedimentary succession, of the types of interaction that may typically occur at the interface between water-saturated unconsolidated sediment and lava. It demonstrates that the properties of the sediment into which lava is being emplaced can both facilitate *and* hinder lava-sediment interaction. Furthermore, sediment properties, as well as lava effusion rates/flux, and/or water combine to control the morphologies and scales of interaction.

The key findings from this case study are: a) quantitative data demonstrates lava-water-sediment interaction is scale invariant: the size of pillows in invasive lava, does not determine how penetrative they are into the sediment; b) individual sediment beds, which may be laterally continuous, can be an effective obstacle to lava bulldozing and mingling with sediment. The properties of a sediment unit within the sequence, allow it to withstand the disruption of invasive lava. The overlying sediment units are bulldozed, fluidised, and mingled, whereas the underlying units are protected by a 'barrier' layer; c) variations in a single bed of sediment can cause localised changes in the lava-sediment interface and interaction type (e.g. the VSst). The VSst provided a laterally continuous marker with which the different features can be recognised. The small variations in sedimentary properties, such as consolidation, cohesion, saturation, and grainsize, together with lava properties (e.g. effusion rate/flux and viscosity) highlight the complexities of lava-water-sediment interaction. D) Within this case study, the interface at which pillow lavas and hyaloclastite breccia interact with sediment is analysed, as well as sub-aerial lava and sediment. This provides a comparison between water depths, i.e. minimal surface water and/or pore water against ~15 m water, in which little difference is found between the types of interaction that occur.

## Chapter 5: Gran Canaria, Canary Islands, Spain

### 5.1 Introduction

A single lava-sedimentary package (LSP) is exposed within the deep ravine of Barranco de Tamaraciete, near Las Palmas, northern Gran Canaria (Figure 5-1). The LSP represents part of the island-building phases of the Miocene-Pliocene Gran Canaria volcanic sequence (Carracedo et al. 2002; Schneider et al. 2004; Perez-Torrado et al. 2014). The LSP comprises a basal sedimentary unit, which is sub-divided into an alluvial fan conglomerate and marine volcanoclastic deposits, and is overlain by basalt pillow lavas and a thick hyaloclastite breccia (HPb). The succession records the interaction between lava, sediment and water, enabling a comprehensive analysis and characterisation of the lava-sediment interface.

Detailed graphic logs, together with systematic measurements of pillow size and penetration depths into the sediment, were recorded along the length of a well-exposed roadside locality. Observed features include: 1) loading and flame structures; 2) inflated lava lobes; 3) small-scale development of peperite; 4) coherent sedimentary inclusions within the pillow and hyaloclastite breccia pile; and 5) fluidised sediment.

This field study recognises and provides supporting evidence for the variable nature of lava-water-sediment interaction. Sediment at the lava-sedimentary contact can undergo internal fluidisation (cm - m scale) as a consequence of invasive pillow lavas, in addition to being disrupted and incorporated into the overlying hyaloclastite pillow breccia as coherent sedimentary inclusions.

Statistical analysis from pillow measurement data demonstrates that penetration depth of the invasive pillow lava into the underlying sediment does not directly correlate with pillow size. Therefore, it is suggested that locally variable sedimentary and lava properties (e.g. lava effusion rates, sediment cohesion, saturation, grain size etc.) influence the style of lava-sediment interaction and the variable morphologies observed.

## 5.2 Geological Background

The island of Gran Canaria, is part of the Canary Islands archipelago (Spain), situated off the North West coast of Africa, at the coordinates N28° 7.489362', W15° 25.80039' (Figure 5-1 A), and is a classic ocean island volcano. There are currently a number of suggested models for ocean island formation, including the 'hotspot theory' (Carracedo et al. 1998; Schneider et al. 2004) and the 'propagating fracture model' (Fiske and Jackson 1972; Anguita and Hernán 2000), but as no model accurately explains every feature, they are not mutually exclusive. However, it is widely recognised that the Canary Island Archipelago formed over the last 15 million years (Schneider et al. 2004) as a consequence of the African plate moving ENE over a pulsating magmatic plume (Carracedo et al. 2002; Perez-Torrado et al. 2014).

Island development throughout the Canary Islands is characterised in a simplified 3 stage model: 1) an initial seamount and juvenile shield-forming stage; 2) a volcanic hiatus and erosional stage; and 3) renewed volcanism (Carracedo et al. 1998; Carracedo et al. 2002; Schneider et al. 2004; Perez-Torrado et al. 2014). Gran Canaria follows this model. The shield forming juvenile stage took place at c.14.5 - 8.5 Ma, the erosional stage is estimated at c.8.5 - 5.3 Ma, and the 'rejuvenated' volcanic stage at c.5.3 Ma to present day (Carracedo et al. 2002; Guillou et al. 2004; Schneider et al. 2004; Perez-Torrado et al. 2014). The north of the island is dominated by rejuvenated stage volcanism (Schneider et al. 2004; Perez-Torrado et al. 2014).

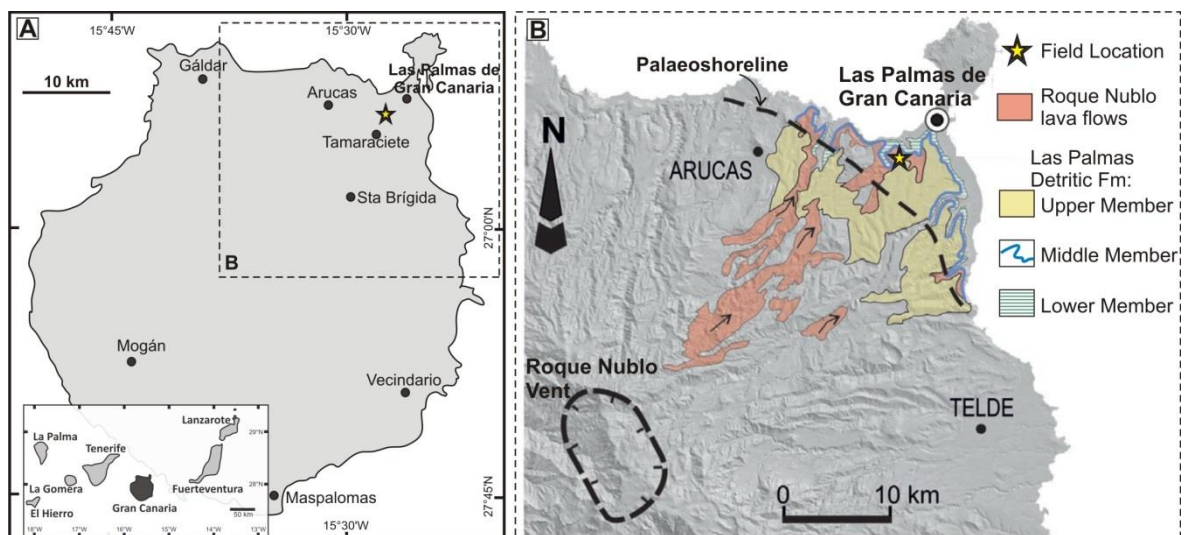


**Figure 5-1: Map of the Island of Gran Canaria, Canary Islands, Spain.**

**A) Gran Canaria is situated off the North West Coast of Africa. The star, near the town of Las Palmas, marks the field site, in the north of the island. B) Regional geological map of the surrounding area to the field site, adapted from Perez-Torrado et al. (2014).**

The volcano-sedimentary section discussed here belongs to the 'Las Palmas Detritic Formation' (LPDF) (Figure 5-2, Table 4), which was deposited during the late Miocene and Pliocene (Schneider et al. 2004; Perez-Torrado et al. 2014), contemporaneous with volcanic quiescence and the second island building stage of the Pliocene Roque Nublo stratovolcano (Perez-Torrado et al. 2014). The LPDF is split into three members: Lower, Middle and Upper. The Lower Member (late Miocene) comprises ~130 m of alluvial fan conglomerates (Schneider et al. 2004; Pérez Torrado et al. 2002), deposited during the main volcanic hiatus and erosional stage of island formation. Clasts are predominantly phonolitic composition (of the Fataga Volcanic Group), related to the underlying island-building stage. The Middle Member is composed of marine littoral deposits (~30 m thick) that host Pliocene fossils, which have been dated at ~4.9 - 2.9 Ma (Guillou et al. 2004; Schneider et al. 2004; Meco et al. 2007; Perez-Torrado et al. 2014), and currently crop out at altitudes of 50 - 100 m asl (Schneider et al. 2004; Perez-Torrado et al. 2014). The Middle Member represents a period of widespread transgression that occurred across the North Atlantic at the onset of Roque Nublo volcanic activity (Lietz and Schmincke 1975; Torrado 1992; Schneider et al. 2004; Cabrera et al. 2008). The Upper Member is dominated by numerous volcaniclastic units, which were deposited by alluvial, laharic and pyroclastic processes (Schneider et al. 2004). Deposition of both the Middle and Upper LPDF was contemporaneous with Roque Nublo volcanism (5.3 - 2.7 Ma) (Gabaldón 1989; Schneider et al. 2004). During Roque Nublo volcanism a complex stratovolcano, which produced basalt lavas and volcaniclastic deposits, developed in the central part of the island (Figure 5-1) (Pérez-Torrado et al. 1995; Pérez-Torrado et al. 1997; Schneider et al. 2004).

The studied succession belongs to the Lower and Middle members of the LPDF, which were deposited and preserved along a narrow marine shelf (Schneider et al. 2004; Carey and Schneider 2011). Lower Pliocene sub-aerial lavas (Roque Nublo) were emplaced along the shoreface and into the basin, forming pillow lavas and hyaloclastite, and the consequent lava-water-sediment interaction products described in this study. The pillow lavas at the lava-sediment contact in the Barranco de Tamaraceite have been dated at  $\sim 4.10 \pm 0.08$  Ma (Lietz and Schmincke 1975; Guillou et al. 2004; Schneider et al. 2004; Meco et al. 2007).



Figure 5-2: View of field locality across the Barranco de Tamaraciete, Gran Canaria, illustrating the stratigraphy of the Las Palmas Detritic Formation (LPDF). The labels refer to the Lower Member (LMLPDF), Middle Member (MMLPDF) and Upper Member (UMLPDF). PRN, post Roque Nublo Lavas. The UMLPDF is not present, as is typical around the island; however, an erosional unit and unconformity is present, inferring its presence between the MMLPDF and PRN. The sub-aqueous and sub-aerial portions of the MMLPDF are easily recognisable (grey dashed line).

LPDF Members	Thickness and Altitude	Lithology	Depositional Environment
Upper (C. 4-3 Ma)	-130 m thick >100m a.s.l	Dominated by conglomerates and volcaniclastic deposits, related to Pliocene Roque Nublo lava	Interbedded alluvial, laharcic and pyroclastic deposits, associated with Roque Nublo activity.
Middle (C. 5-4 Ma)	Up to 20 m thick -50 - 120 m a.s.l	Fine - coarse sandstones with siltstone and conglomerates. Pillow lavas. Mixed clast origin from both Miocene Phonolites and Pliocene Roque Nublo.	Near shoreface, marine littoral deposits, possibly sand and gravel beaches with littoral aeolian dunes. Slope likely 1-2°.
Lower (C. 8-5 Ma)	>130 m thick >10 m a.s.l	Conglomerates and finer grained sediments. Clasts predominately of Miocene Phonolitic origin.	Alluvial fans.

Table 4: Characteristics and depositional environments of the members of the LPDF as presented by Perez-Torrado et al. (2014).

---

## 5.3 Observations

The field locality is situated within the Barranco (meaning: gully/ravine) de Tamaraciete, close to the towns of Tamaraciete and Las Palmas, in northern Gran Canaria, Spain (Figure 5-1). The ~600 m long roadside exposure (Figure 5-3) displays a single lava-sedimentary package comprising a basal sedimentary unit, with both siliciclastic and volcanoclastic components, that is overlain by pillow lavas and a thick hyaloclastite breccia (HPb).

The HPb is unconformably overlain by a fluvial conglomerate, which in turn is overlain by a scoriaceous unit, and a sub-aerial lava with a basal breccia (locality B, Figure 5-3). The basal breccia is locally stratified, and comprises sub-rounded pebble-cobble size clasts of basalt and reddened stringers of fine sandstone. Locally, the breccia is stratified.

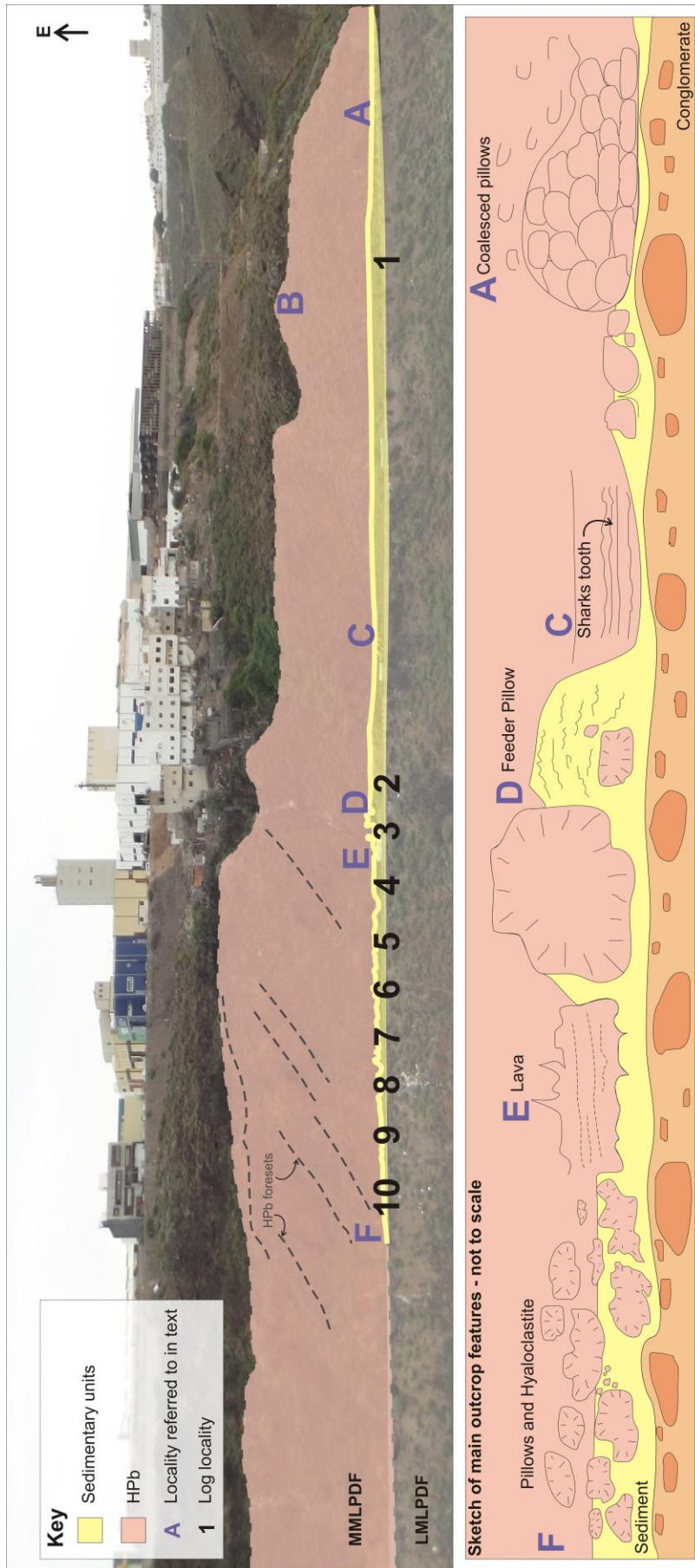
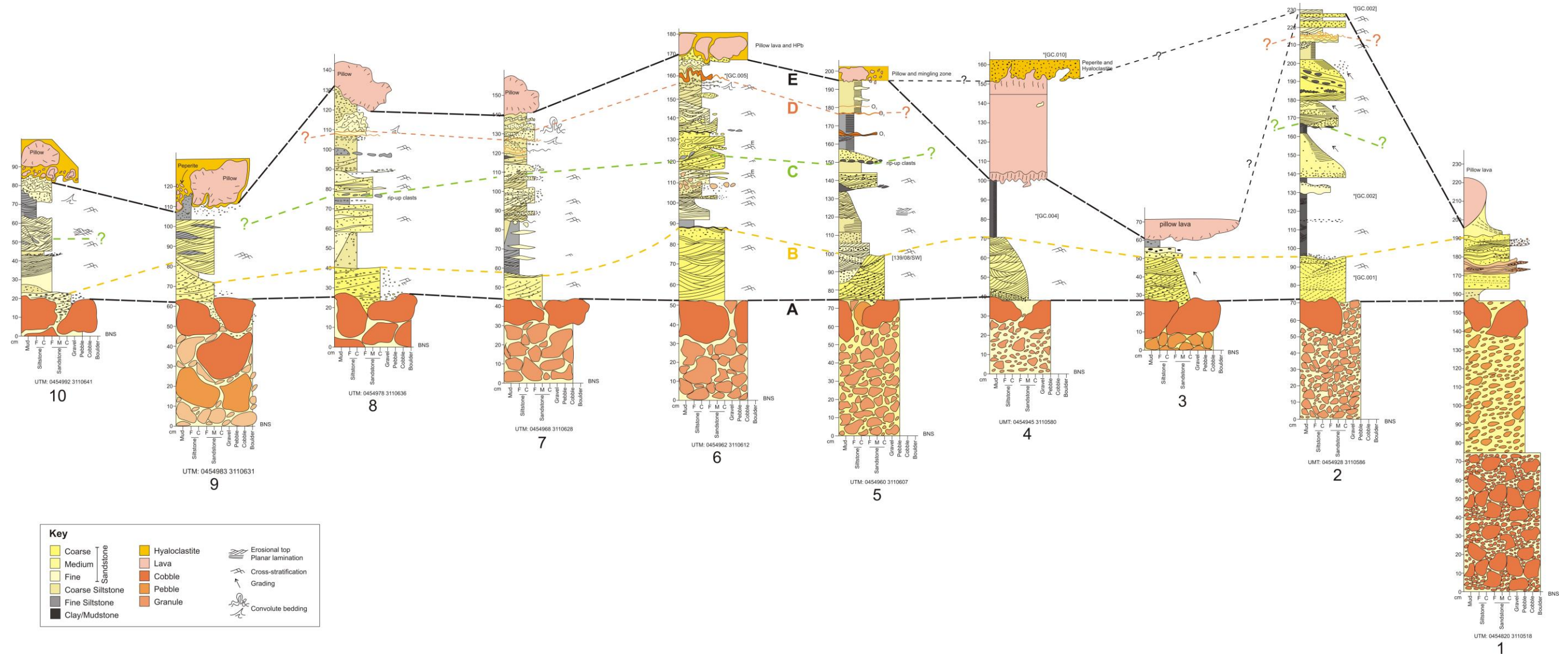


**Figure 5-3: Overview of the ~600 m long roadside exposure in Barranco de Tamaraciete, Las Palmas, Gran Canaria. The annotated photograph highlights the sedimentary units (yellow) at roadside level, and the overlying lava (pale pink). Numbers correspond to the log localities, and letters to other localities. LMLPDF – Lower Member Las Palmas Detritic Formation; MMLPDF – Middle Member Las Palmas Detritic Formation. The schematic sketch (enlarged and not to scale) illustrates the main features observed at the HPb-sedimentary contact along the exposure. Localities and log numbers are referred to throughout the chapter.**

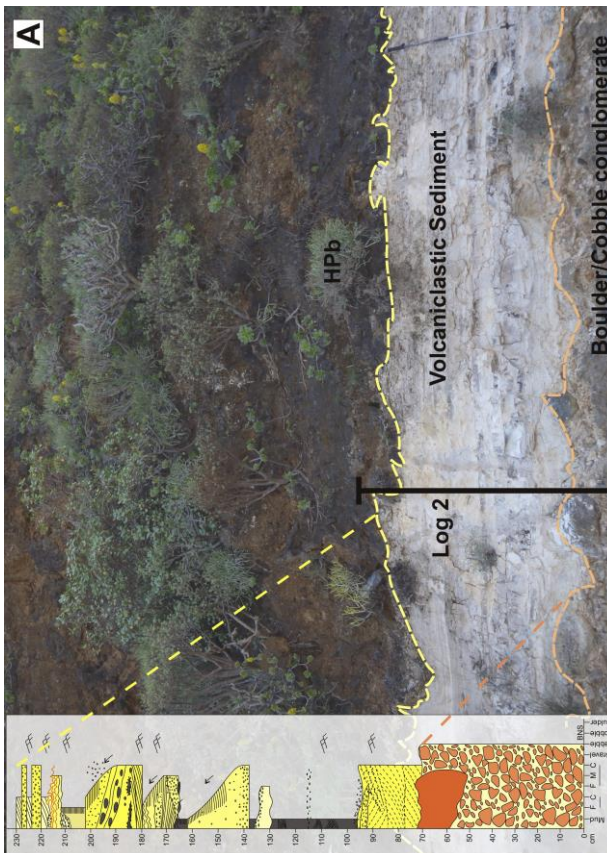
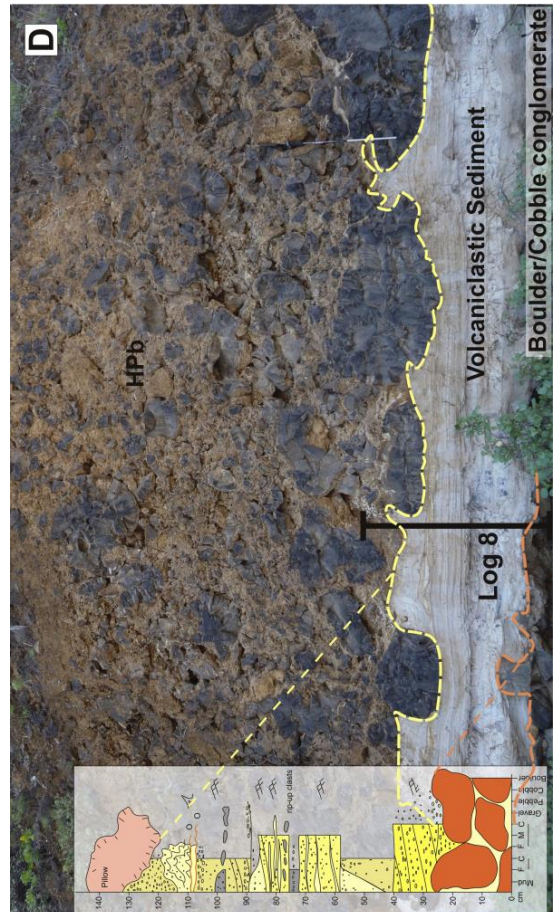
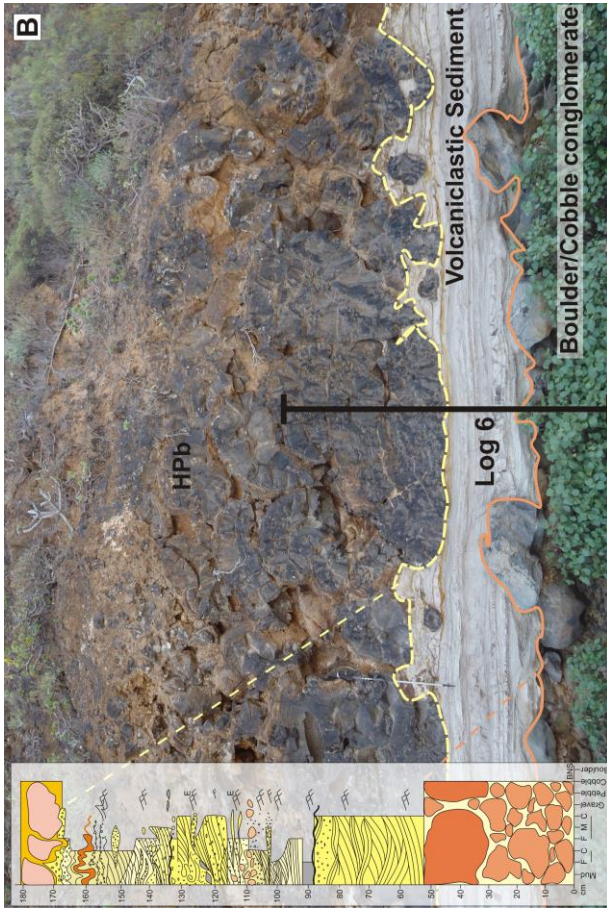
---

### 5.3.1 Sedimentary Units

A correlation panel of the individual logs along the section (Figure 5-4) illustrates the variability of the sedimentary unit, from a basal conglomerate, to a fine siltstone and sandstone unit, and into the overlying lava. The conglomerate unit has been used as a marker for correlation as it was preserved across the entire ~600 m long section (Figure 5-3). Field photographs at each of the log localities are given in, which provides examples of the lava-sediment interface that is discussed further below.



**Figure 5-4: Correlation panel of the sedimentary logs across the field section.** Log 1 is located at the south and Log 10 at the north of the section. Letters refer to correlation surfaces. A marks the top of the basal conglomerate unit, on which the correlation was based. B, yellow dashed line, marks the top of the sandstone unit that drapes the underlying conglomerate. C, green dashed line, marks a thin pumice-rich, cross-stratified sandstone, with imbricated fine siltstone, rip-up clasts at its base. D, orange dashed line, highlights the level at which discontinuous orange-stained siltstone beds occur. E marks the top of the sedimentary unit, and the lava-sediment contact.



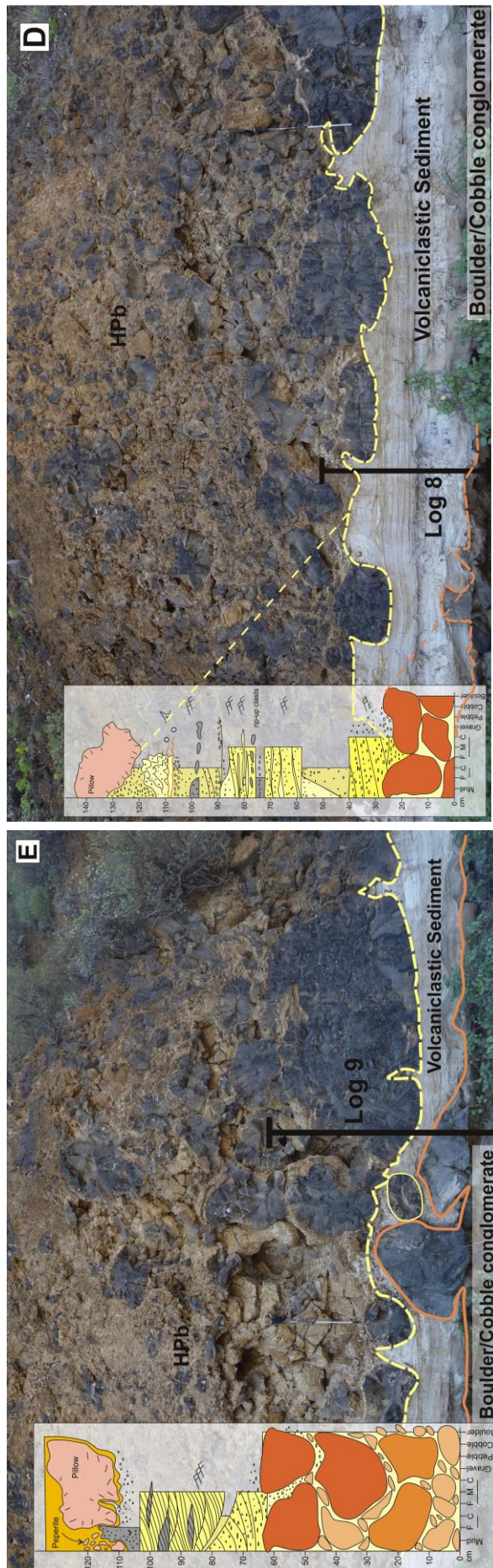


**Figure 5-5: Annotated field photographs and corresponding logs for the lava-sedimentary interface at a number of localities along the section.**  
 A) Log 2 near locality D. Here, the main sedimentary unit is at its thickest, ~160 cm. B) Log 6, a number of pillows from the HPb are isolated within the underlying sediment. Closer detail of this is shown in Figure 5-27. Internal fluidisation and disruption of the sediment (~130 cm in log) is at its greatest (though localised). C) Log 7. At the lava-sedimentary contact the sediment is locally fluidised around the invasive/penetrating pillow. Fluidised zones of sediment lack structure, are typically 'dirty' looking, and the boundary between coherent and disrupted sediment is sharp. D) Log 8 displays the lava-water-sediment contact, at which orange-stained sediment beds (O1 -O3) are observed. The image also highlights the difference in penetration depths between different sized pillows. E) Log 9. This illustrates the nature of the volcaniclastic unit, as it thickens and thins between the underlying conglomerate and the overlying HPb. Peperite is observed at the lava-sedimentary contact. F) Log 10, near locality F. Here the sedimentary unit is relatively thin and the boulders from the conglomerate are thinly draped by sediment. The pillow lavas are smaller, with more HPb common at the sedimentary contact. The HPb is normally graded. Walking pole is ~1 m.

The sedimentary sequence displays key features that are used to correlate the section. These are highlighted on the correlation panel (Figure 5-4) and described below.

The basal sedimentary unit (Surface A, Figure 5-4) is a clast-supported pebble- to cobble- grade conglomerate with a brown, fine sandstone and siltstone matrix. Pebbles and cobbles comprise a mixture of basalt, green welded ignimbrite, meta-sedimentary material and phonolite. Clast size ranges from 3 to 35 cm, with the majority of clasts belonging to the 3-10 cm range; they do not display imbrication (Figure 5-6). The unit has an irregular boulder top, comprising clasts 25-85 cm across, with the same composition as the underlying pebbles and cobbles, although a dominance of green welded ignimbrite. The overlying unit drapes the boulder-dominated top (Figure 5-7).

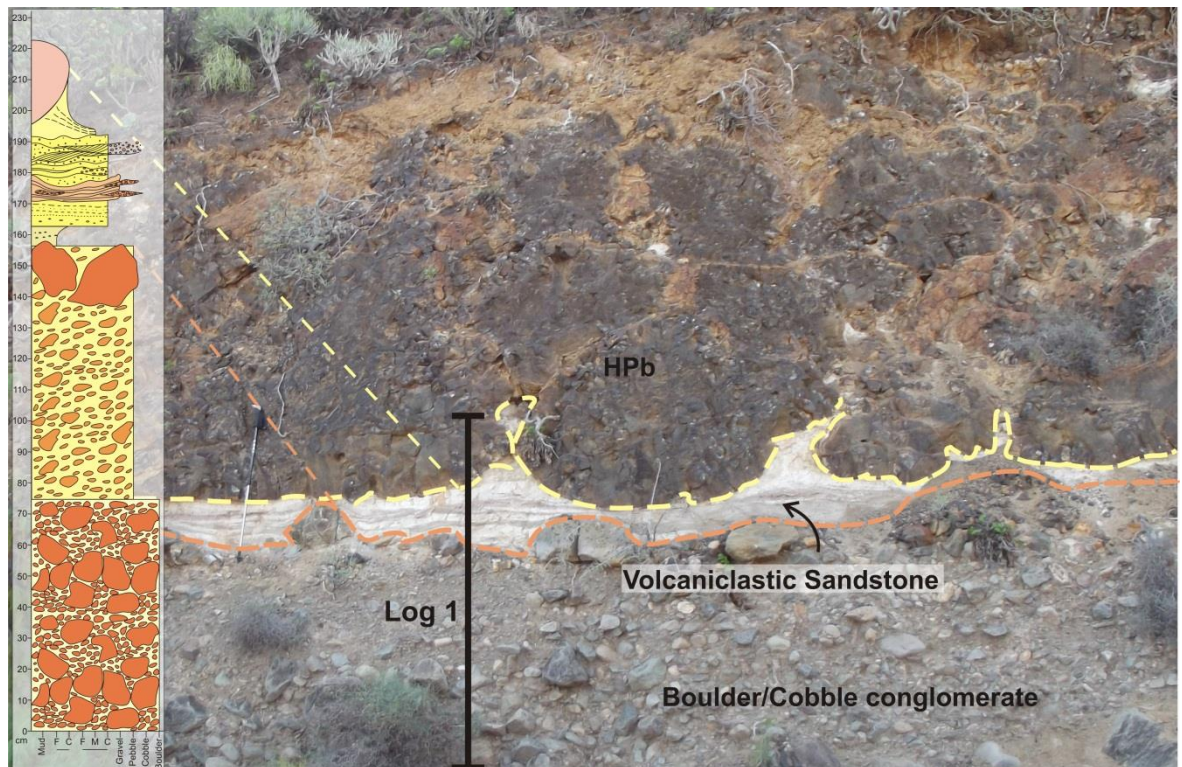


**Figure 5-6: Log 1 through the lava-sedimentary succession, where the cobble/boulder conglomerate is relatively thick.**

**The central sandstone/siltstone unit is relatively thin as it drapes the underlying conglomerate unit and is overlain by the HPb. Flame structures are created at the lava-sediment contact where sediment has been squeezed between pillows. Walking pole is ~1 m.**

The draping unit (Surface B, Figure 5-4) is a white/grey, 15 - 40 cm thick, medium to coarse volcanoclastic sandstone. Cross beds are ~10 cm, with mm-cm scale laminations that record a palaeocurrent direction of 139/08° SW. The package is lithic- and pumice-rich. Lithic-rich layers mostly define laminae with angular basalt lithics of <9 mm. Pumice-rich (~50 %) layers and/or lenses, are 3-10 cm thick, with mm pumice fragments (Figure 5-8). The unit typically has a wavy contact with the overlying unit (Figure 5-7).

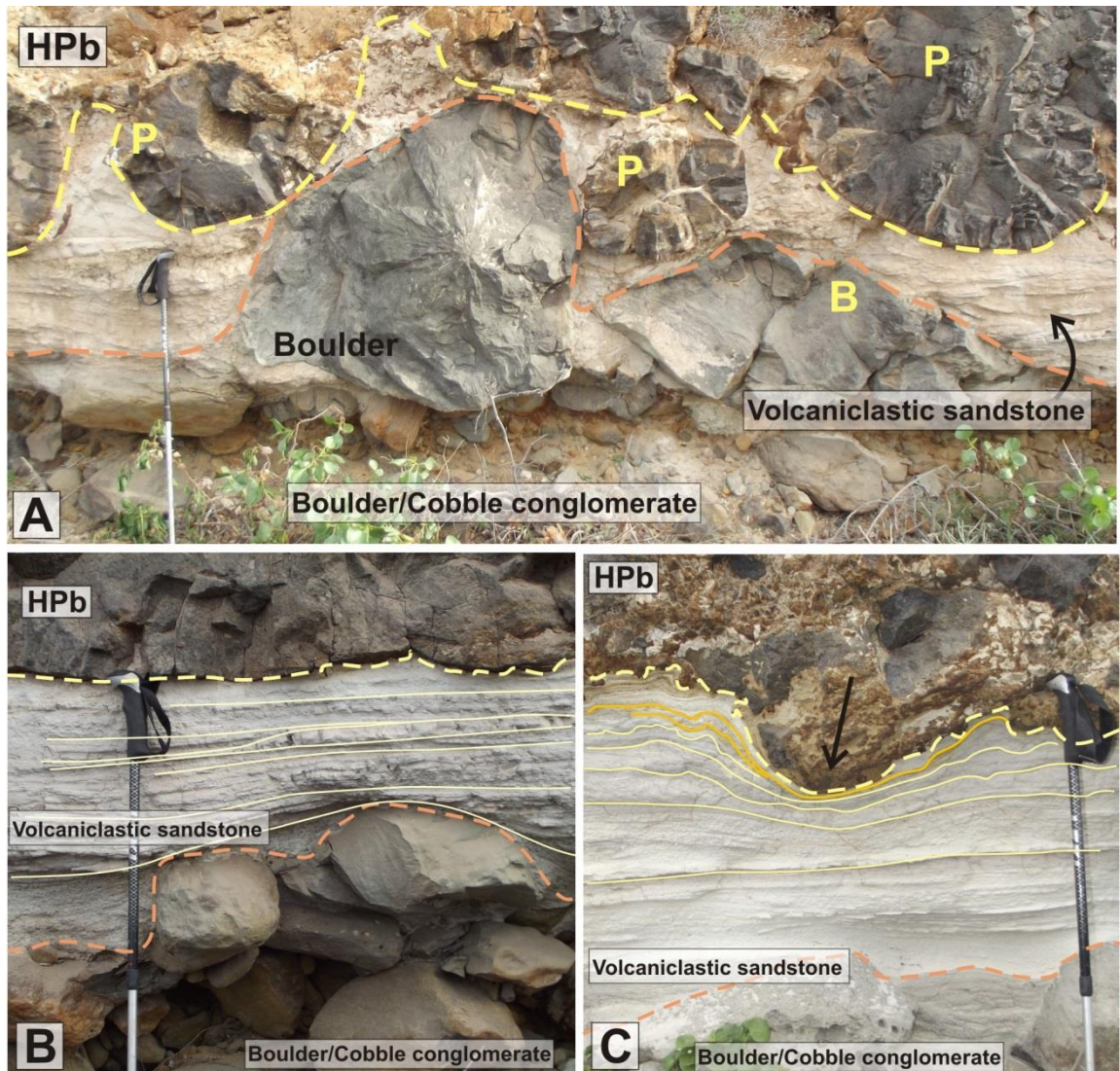


**Figure 5-7: The contact between the basal conglomerate unit, the volcanoclastic sandstone package, and the overlying HPb.**

**A) The volcanoclastic sandstone is very thin and drapes over the outsize boulders of the underlying conglomerate, whilst overlain by pillows and the HPb. B) The volcanoclastic sandstone (and siltstone) drapes the underlying conglomerate unit, and is thinly bedded with cross-stratification accentuated by lithics. C) The upper part of the volcanoclastic sandstone is loaded by the overlying hyaloclastite and peperite. Walking pole is ~1 m long.**

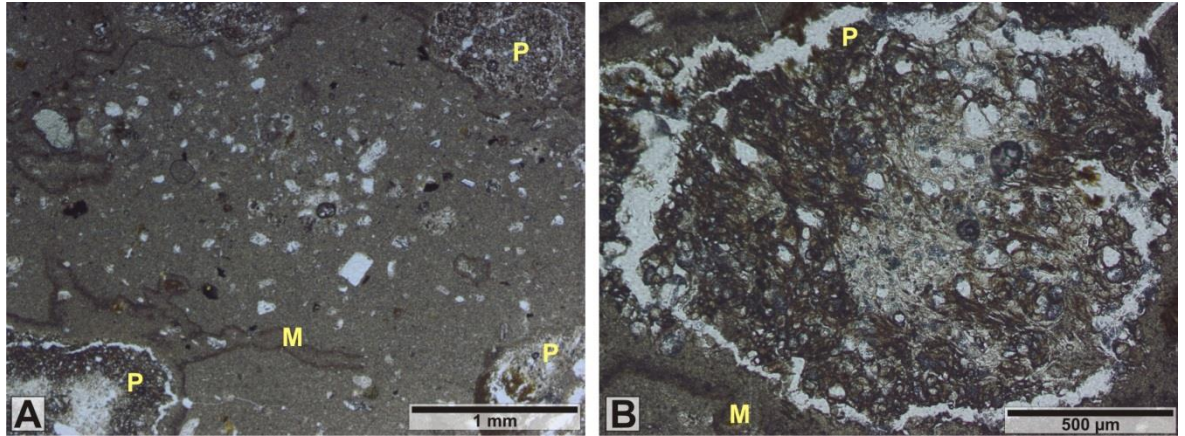


**Figure 5-8: Petrography of the volcaniclastic sandstone directly overlying the basal conglomerate (Sample GC.001), Log 2 (Figure 5-4).**

**Both images PPL. A) The volcaniclastic sediment (M), comprises a fine grained glassy siltstone, with crystals (predominantly feldspar, with some pyroxene) and lithic clasts (P), possibly reworked ash. B) Enlarged view of the rounded, vesicular lithic clasts (P) are abundant within a fine-grained volcaniclastic matrix (M). Some lithoclasts have aligned bubble-wall indentations, characteristic of tube pumice.**

The overlying sedimentary units range from volcaniclastic claystone to siltstone, and sandstone (Figure 5-9, Figure 5-10). Pumice is common and some individual packages are crystal- and lithic-rich (Figure 5-9A). The units are normally graded, and the majority are stratified and cross-stratified, with wave-ripple lamination and erosional surfaces (Figure 5-4 and Figure 5-9C). A small bivalve (~1 cm) was found in a 3-4 cm package of white, finely laminated, fine claystone/siltstone at the top of Log 3 (Figure 5-6 and Figure 5-9). This was the only fossil found within hand specimen. Petrographical analysis of the claystone underlying the lava at Log 4 (Figure 5-4) has revealed fossil algal material, that is likely diatomaceous (Figure 5-10).

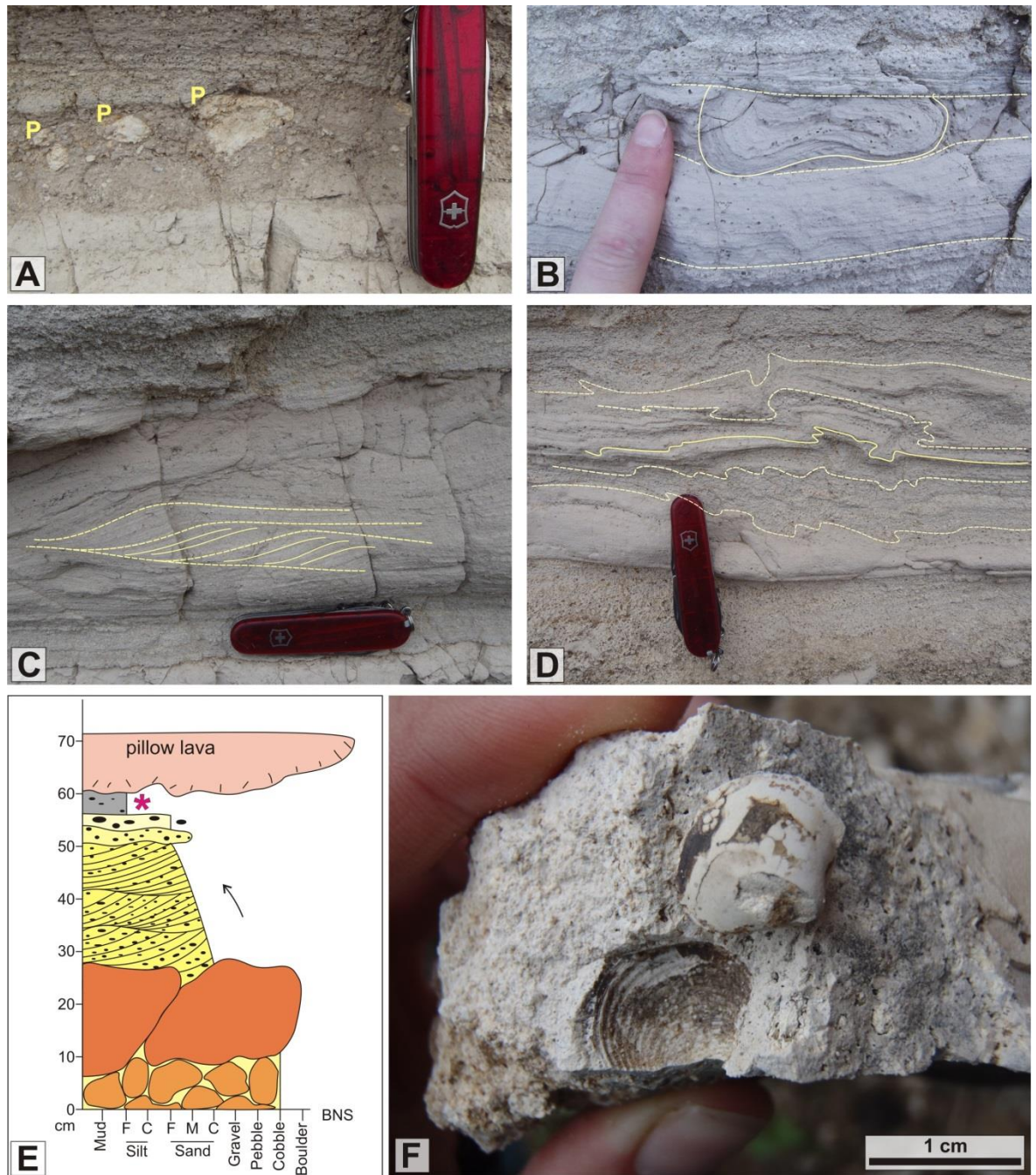


**Figure 5-9: Characteristic features and structures within the volcanoclastic units of the main sedimentary section.**

**A)** Beds dominated by pumice clasts (P), 0.5-3 cm across, are common. **B)** Dewatering and loading features are typical throughout the sedimentary beds. This dewatering structure is cut by the overlying siltstone. **C)** Cross-stratification within a volcanoclastic siltstone displays a paleocurrent to the SW. **D)** Loading, dewatering and fluidal sedimentary boundaries between individual beds are common. **E)** Log 3 through the sedimentary succession, at Locality D. **F)** A bivalve, ~1 cm, (pink \* on E) was found within the sedimentary unit directly underlying a large pillow lava. Pen knife is ~8 cm long; index finger, ~ 1.2 cm wide (B).

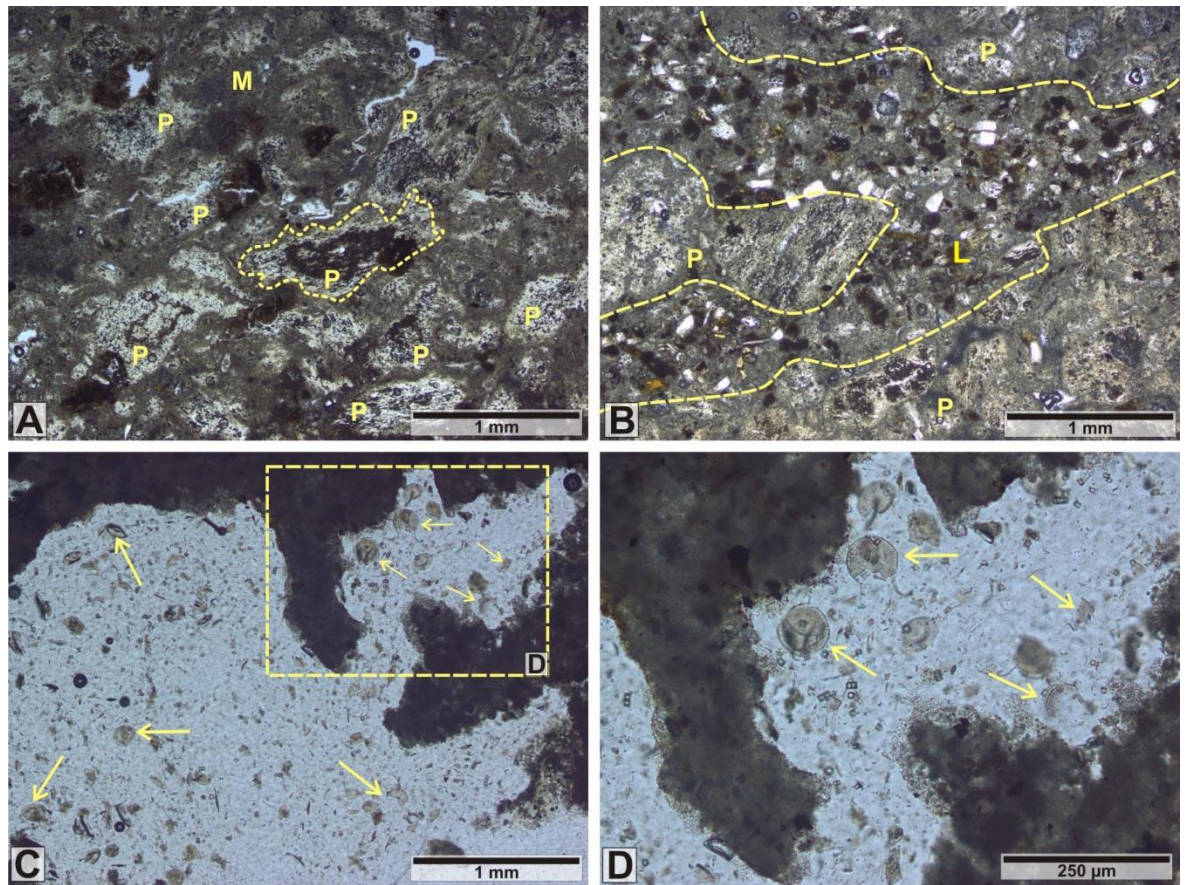


**Figure 5-10: Volcaniclastic siltstone (Sample GC.002) Log 2, (Figure 5-4), and fine grained claystone (Sample GC.011), underlying the lava in Log 4 (Figure 5-4).**

All images are PPL. A) A layer of lithic clasts of glassy, vesicular pumice (P, and yellow dashed outline example) within a fine-grained glassy volcaniclastic siltstone matrix. B) The pumice/lithic-rich layers are interbedded with, and have a sharp boundary with, layers comprising a crystal-rich sediment matrix (L) with larger lithoclasts (P). The sediment is more crystal-rich at the boundary, comprising subhedral, altered crystals of plagioclase, amphibole, clinopyroxene and lithics. Lapilli are predominantly pumice clasts, are elongated and appear slightly welded with irregular edges. C) Dominantly structureless claystone with no crystals or lithics, except for small ellipsoid fragments (yellow arrows), that are possibly algal. Yellow dashed box is D. D) Higher magnification showing the ellipsoid algal fragments, likely diatoms or coccoliths.

At Surface C (Figure 5-4), a thin, 5-12 cm, white, pumice-rich, low angle cross-stratified sandstone, contains rip-up clasts at its base. The rip-up clasts are purple/grey fine siltstone, 3.5 - 8 cm across, and are imbricated with a palaeo-flow towards the east. These have the same character as the underlying bed, confirming their origin. Other typical features of the sedimentary and volcaniclastic unit include soft-sediment deformation (Figure 5-9 B) and dewatering structures (Figure 5-9 D).

Near the top of the sedimentary unit, distinctive thin orange-stained beds, typically 1 - 3 cm thick, comprise tuffaceous siltstone and sandstone that are pumice and crystal-rich (Surface D, Figure 5-4; Figure 5-11). They are laminated and cross-stratified, and interbedded with packages of coarse tuffaceous, pumice-rich siltstone (Figure 5-12,

Figure 5-14). The beds show convolute stratification and are laterally discontinuous (Figure 5-12C, D), although they appear at a similar stratigraphic height and are correlated within the logs (Figure 5-4). Typically, multiple orange/yellow (-stained) beds are stacked together. Log 5 (Figure 5-11), illustrates three orange-stained beds (labelled O<sub>1</sub>, O<sub>2</sub> and O<sub>3</sub>) within a 15 -26 cm purple/grey finely laminated siltstone unit. The lowermost bed, O<sub>1</sub>, ~2 cm thick, is a coarse sandstone that is pumice-rich and displays wavy bedding. The upper two layers, O<sub>2</sub> and O<sub>3</sub>, are <1 cm thick, and comprise tuffaceous siltstone.

Petrographical analysis of the orange-stained beds at the top of Log 7 reveal that the colour is due to the high abundance of altered glassy basalt (palagonite) clasts. These clasts are vesicular and scoriaceous with cusped edges (Figure 5-13 A). Interbedded with these beds are laminated grey, crystal-rich fine siltstone and claystone that contain pumice (Figure 5-13 B). These are not stained. Paler orange and yellow beds, close to the orange-beds, are however, stained by the leaching of the glass and clay minerals from the glass-rich beds. Analysis of the white tuffaceous claystone and siltstone, reveals pumice-rich layers of pumice fragments and shards, interbedded with crystal-rich siltstone (Figure 5-14).

The top of the sedimentary unit is heavily deformed and displays convolute, wavy bedding, disruption of bedding (fluidisation) (Figure 5-12 B), flame structures, and dewatering structures at the lava-sediment contact (Surface E, Figure 5-4). In places, the fine-grained claystone-siltstone is mingled with the overlying pillow lava, hyaloclastite and juvenile basalt clasts, forming small-scale peperite (see Section 5.3.3), and forms inclusions within the HPB and pillow lavas.

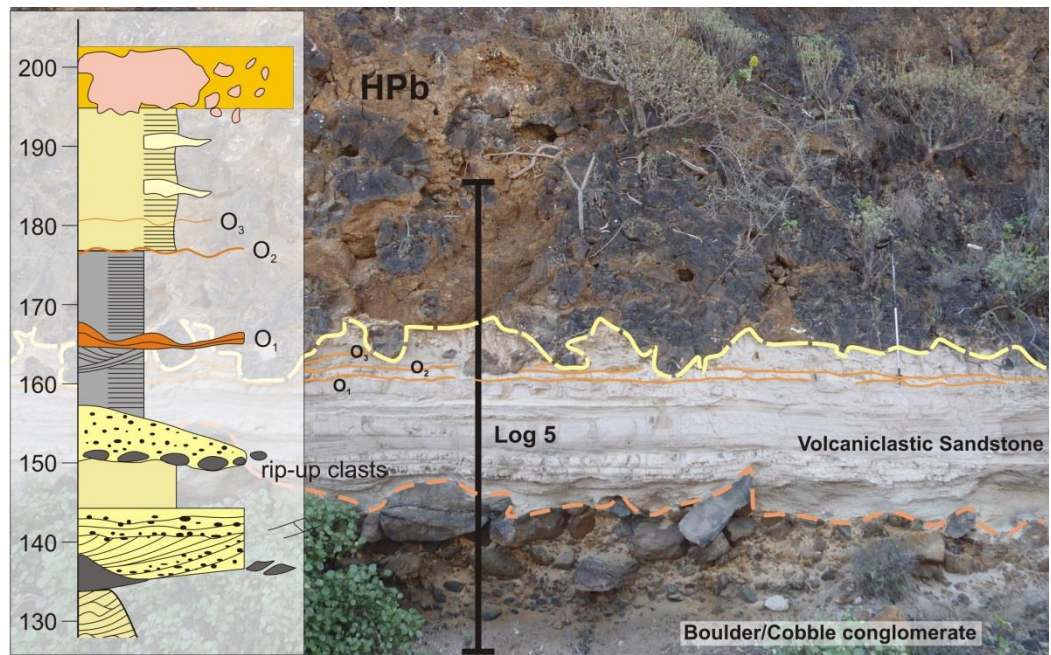


**Figure 5-11: Distinctive orange beds ( $O_{1-3}$ ) are observed close to the top of the sedimentary unit at the top of Log 5 (Figure 5-4). These units are laterally discontinuous and highlight the internal deformation of the sedimentary units at and below the lava-sediment contact. Walking pole is ~1 m.**

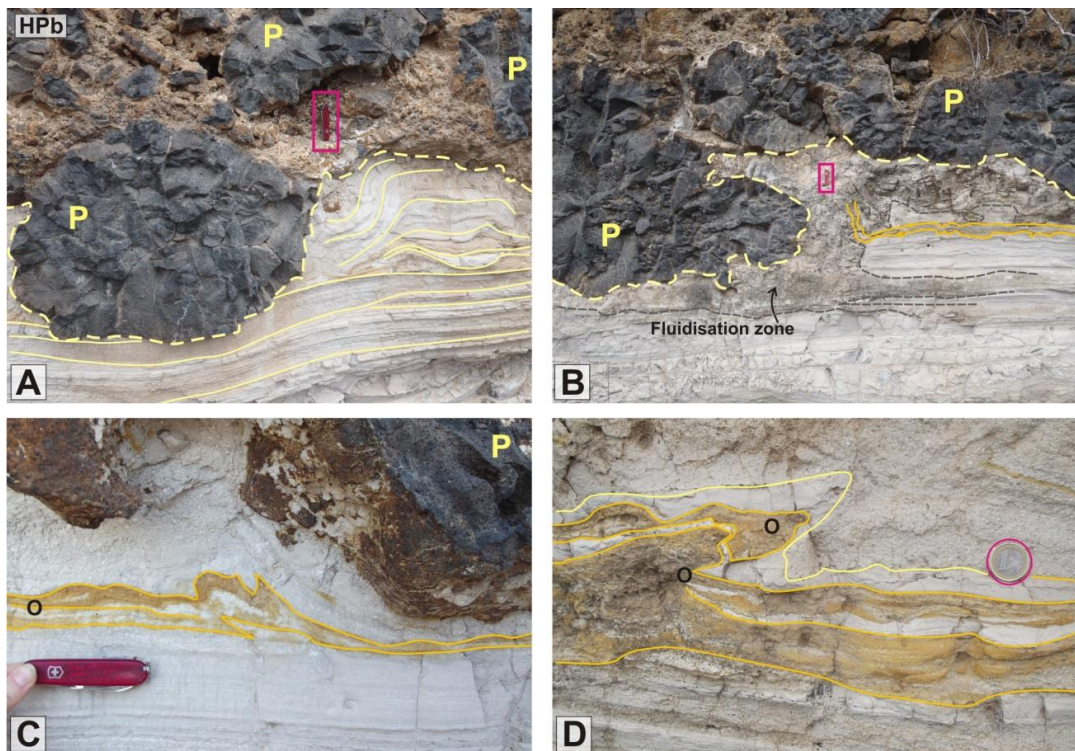


**Figure 5-12: Characteristic features at the lava-sedimentary contact.**

**A) Bedding of the sediments is deformed and loaded by pillow lava. B) Localised fluidisation of the sediment is present in a zone surrounding an invasive pillow. There is a relatively sharp contact between coherent sedimentary structures (not disrupted) and those that have undergone fluidisation. C) Orange stained beds and laminae are observed near the top of the sedimentary unit, close to the contact with the overlying HPb. These are depicted in logs 4-7 (Figure 5-4). These units have also been fluidised. D) The orange-stained units range in thickness and locally overlie each other, with interbedded “clean” white beds. Pen knife ~8cm long (Pink box) and 1 Euro coin is 2.3 cm diameter (Pink circle).**

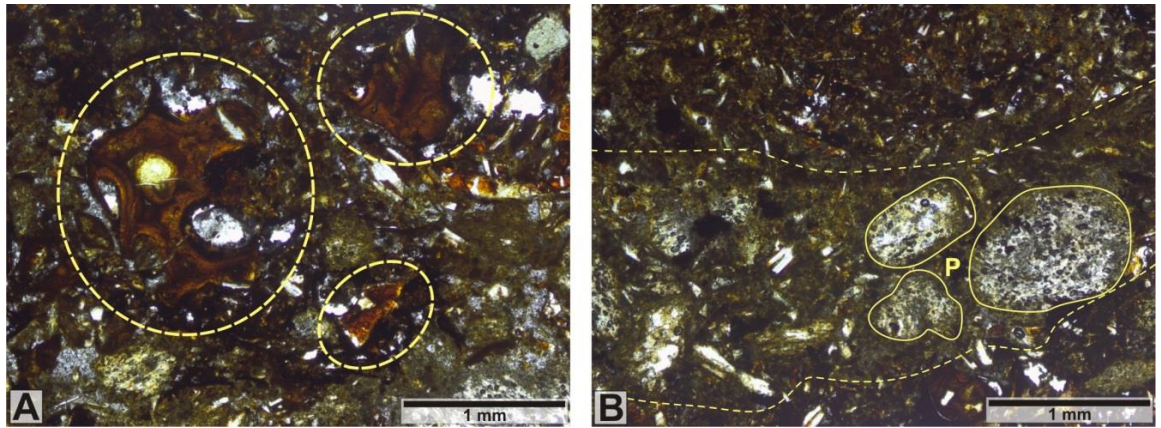


Figure 5-13: Petrography of orange-stained beds (Sample GC.006) collected from the top of Log 7 (Figure 5-3 and Figure 5-4).

Both images PPL. A) The orange staining is due to the high abundance of palagonitised scoriaceous basalt clasts (yellow dashed circles) concentrated within some beds. The scoriaceous clasts have cusped edges. B) Beds interbedded with the volcanic-dominated orange-beds are finer-grained, and laminated (dashed yellow lines), and comprise crystal rich siltstone with pumice clasts (P).

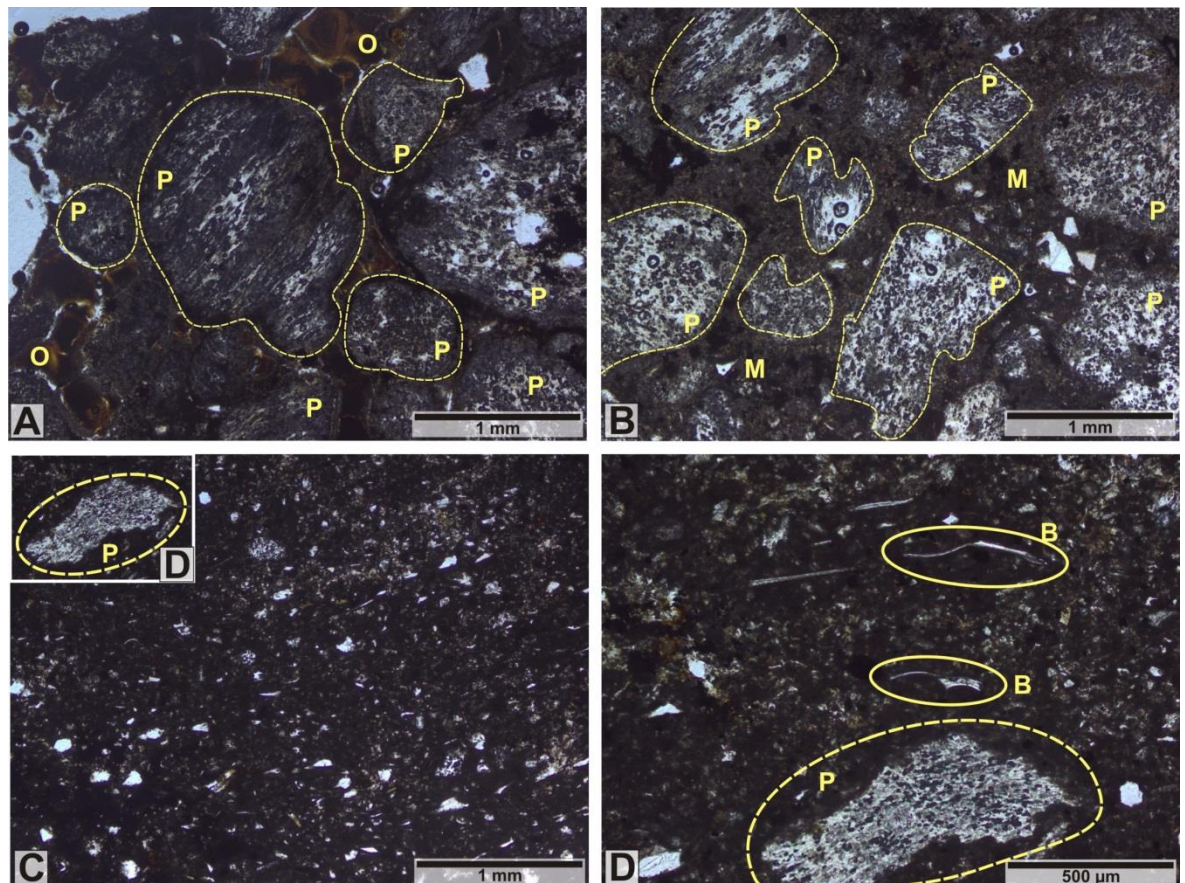


Figure 5-14: Interbedded claystone and siltstone with pumice-rich layers (Sample GC.007), top of Log 7 (Figure 5-4).

All images PPL. A) and B) show the abundance of pumice (P) within a glassy, crystal-rich matrix (M). Pumice are vesicular and some elongated, but welding and alignment is not apparent. C) The pumice-rich beds grade into finer siltstone, which is crystal-rich with rare pumice shards. D) A magnified image of C. Intact bubble-wall shards (B) are preserved.

---

## 5.3.2 Volcanic Units

The volcanic units of the LSP comprise a package of hyaloclastite pillow breccia, with graded foresets, and with a concentration of pillows and coalesced pillows/pillow tubes at the base.

### 5.3.2.1 Hyaloclastite Pillow breccia

The hyaloclastite pillow breccia (HPb) is an orange, medium to coarse-grained breccia, with large spalled pillow basalt clasts, of irregular shape and size, which have glassy rinds. Clasts are sub-angular, ranging from 3-50 cm, although typically are 5-15 cm. The HPb has a diffuse stratification, is normally graded (Figure 5-15), and contains isolated, cm size, pockets of white, fine grained siltstone (hard and chert-like), both within spalled lava fragments and adjacent to flame structures of the underlying sediment.

The HPb includes both pillow-dominated and hyaloclastite-dominated breccia facies that form foresets (Figure 5-15, Figure 5-16). Hyaloclastite breccia foresets are typically thicker than pillow foresets. Boundaries between facies are diffuse and show gradation from pillow-dominated to hyaloclastite and breccia dominated foresets, which provides evidence for reworking of the HPb.

At the base of the sequence, directly overlying the sedimentary units, a pillow breccia fines upwards into reworked pillow breccia/coarse sandstone. Angular basalt clasts are glassy, with rare oversized vesicular fragments, and abundant siltstone clasts. Overlying this package, at ~225 cm (Figure 5-16), a hyaloclastite-dominated breccia containing uncommon pillow tubes and spalled fragments displays normal grading. The package fines upwards from a coarse base to smaller glassy basalt fragments with less abundant vesicular fragments (as before). Above this basal section, the unit appears to give way to more typical alternating hyaloclastite- and pillow-dominated facies, although due to access difficulties, finer details of grading could not be determined.

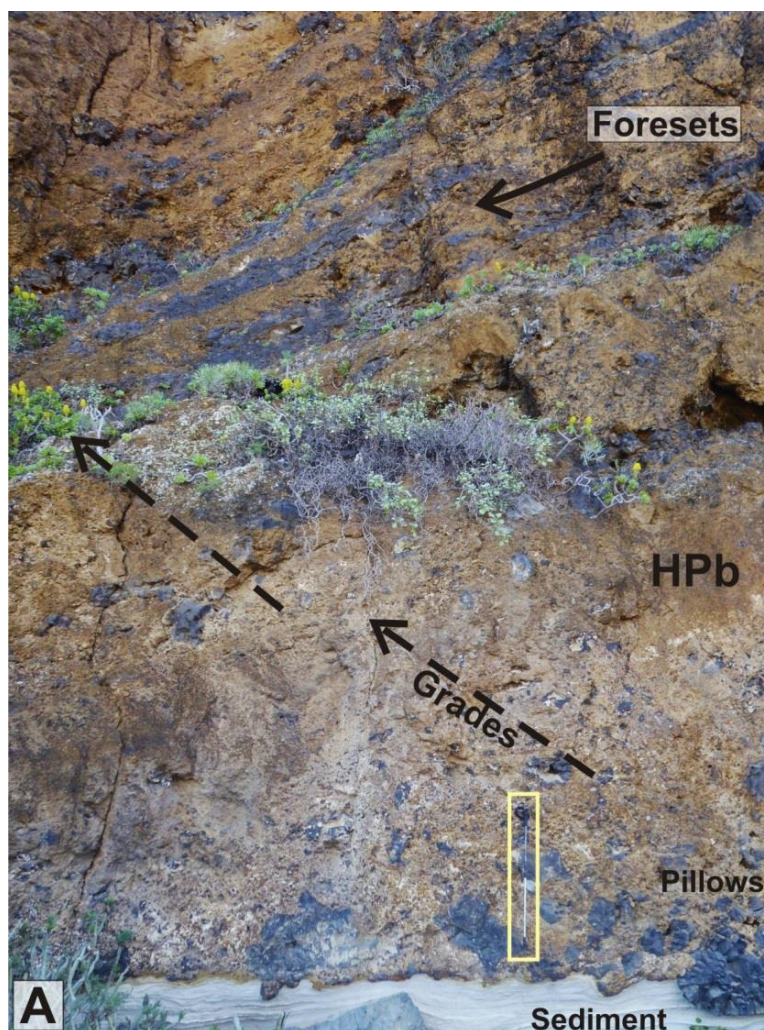


**Figure 5-15: The HPb at the northern part of the section (Locality F). The HPb has internal grading, and foresets are observed higher up the unit towards the passage zone. Walking pole is ~ 1m.**

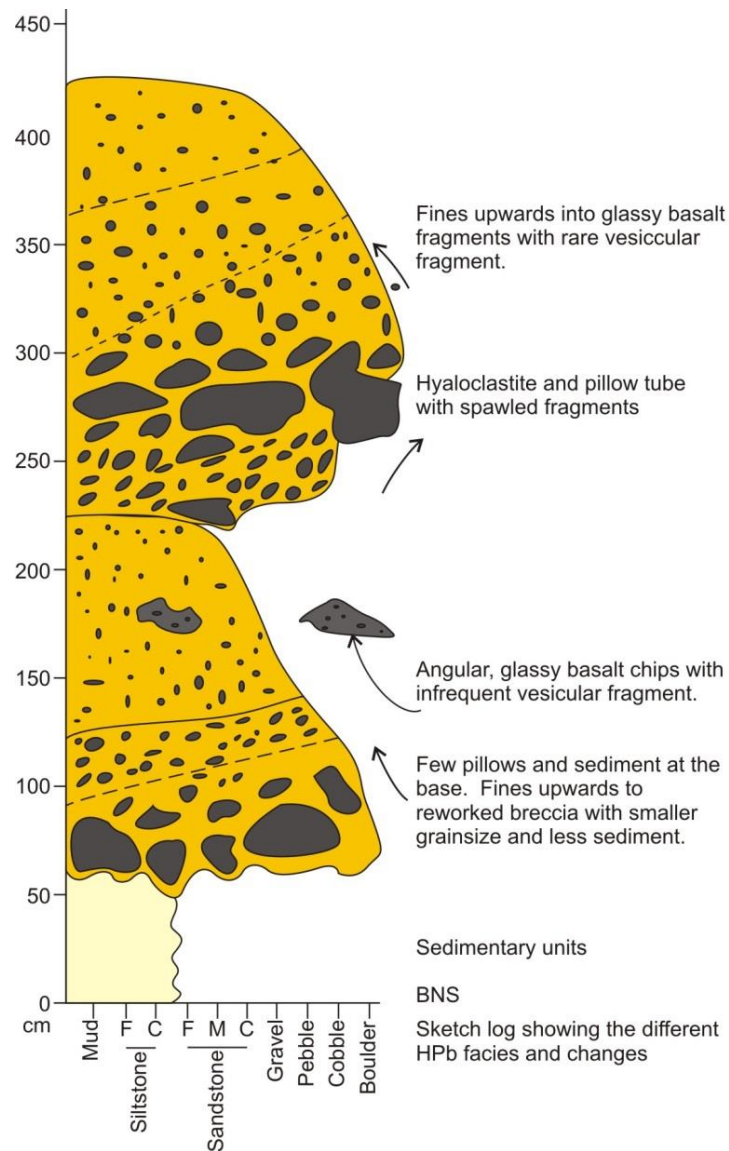


**Figure 5-16: Sketch log through the HPb, depicting the facies changes, and diffuse stratification within the hyaloclastite-dominated and pillow-dominated foresets. Colour changes denote grain size: pale yellow = fine sandstone/coarse siltstone, orange = hyaloclastite pillow breccia matrix of varying grain sizes (<pebble), and dark grey = pillow fragments of pebble-boulder size.**

### 5.3.2.2 Pillow lava

Pillow lavas are present throughout the section, forming graded foresets with the hyaloclastite breccia, and are abundant at the contact with the underlying sediment. The pillows range in size from <10 cm to ~280 cm across, and are typically sub-rounded with chilled margins and multiple glassy rinds (2-6 cm thick), which display orange-brown palagonite weathering. Large pillows, >80 cm diameter, typically have sharp, flattened bases, with chilled margins on the sides and upper surfaces, which give a more irregular shape (**Error! Reference source not found.** Systematic measurements of the pillows including height and width (a and b axis), penetration depth into the sediment, and sediment thickness (Figure 5-17), were recorded along the section for every pillow at the sediment contact. A typical measured section is shown in Figure 5-17, and Table 5 records the relevant measurement data.

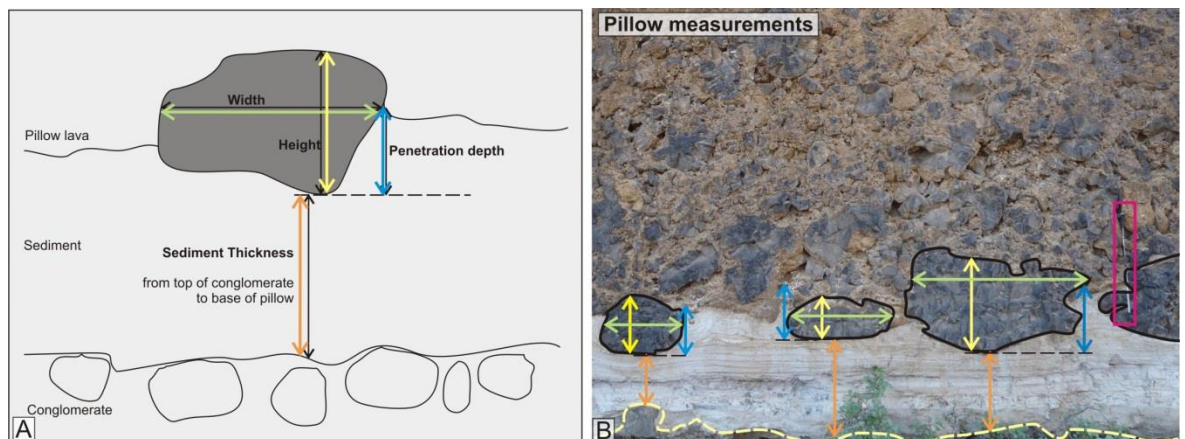


**Figure 5-17: Schematic illustration (A) and field view (B) of the different pillow measurements obtained along the section. Width and height correlate to the longest horizontal and vertical axis. Illustration is not to scale. Walking pole in B (pink box) is ~1 m.**

Width (cm)	Height (cm)	Penetration Depth (cm)	Sediment Thickness (cm)	Net Penetration Depth (cm)
2220	120 (variable)	33	11, 33	0
160	119	17	11	-102
143	105	0	0	-105
76	37	0	0	-37
179	88	0	0	-88
83	46	0	0	-46
71	42	0	0	-42
66	42	28	11	-14
59	34	47	12	13
143	65	0	7	-65
72	50	26	0	-24
159	72	25	9	-47
40	45	9	0	-36
74	45	49	11	4
182	120	49	19	-71
321	111, 198	94	24, 28	-17
102	42	110	8	68
361	91	95	18, 25	4
133	120	46	36	-74
62	59	33	71	-26
71	60	24	21	-36
160	82	33	39	-49
130	75	45	110	-30
200	115	15	120	-100
60	40	15	119	-25
185	80	36	93	-44
300	105	24	135	-81
127	62	20	127	-42
300	100	22	150	-78
144	60	40	110	-20
29	11	14	125	3
122	60	91	129	31
156	73	78, 39	136	5
119	78	210	0	132
30	53	183	0	130
174	162	40	0	-122
317	195	212	30	17
940	220, 68	0??	40, 63	68
104	72	52	73	-20
82	49	32	91	-17

Width (cm)	Height (cm)	Penetration Depth (cm)	Sediment Thickness (cm)	Net Penetration Depth (cm)
119	65	15	110	-50
71	59	29	70	-30
65, 42	68, 15	25, 45	82 & 77	-43
25	22	26	79	4
102	35	0	94	-35
57	99	45	50-90	-54
29	19	19	92	0
19	45	28	80	-17
31	32	38	44	6
89	64	50	72	-14
32	32	34	58	2
29	17	46	58	29
115	160	39	70	-121
208	58	44	71	-14
22	15	29	83	14
68	72	40	115	-32
221	159	90, 85	79	-74
155	108	107	88	-1
147	59	65	92	6
39	52	36	137	-16
79	49	67	135	18
196	120	128	80	8
306	145	134	89	-11
160	85	69	69	-16
105	35	74	83	39
71	95	92	100	-3
70	50	65	49, 62	15
61	32	36	112	4
35	23	28	100	5
59	50	43	92	-7
79	70	69	63	-1
132	84	57	63	-27
205	136	69, 108	43	-28
147	107	63	58	-44
261	219	100	33	-119
125	87	64, 47	68	-23
312	129	75	49	-54
49	41	66	30	25
27	24	32	38	8
79	103	33	59	-70

Width (cm)	Height (cm)	Penetration Depth (cm)	Sediment Thickness (cm)	Net Penetration Depth (cm)
64	46	46	46	0
85	53	57	43	4
102	52	38, 32	53	-14
214	55	29, 19	35	-26
40	125	22	46	-103
39	28	29	47	1
75	40	11	27	-29
70	28	25	30	-3
26	21	22	22	1
55	32	16	53	-16
85	42	34	30	-8
87	55	49	25	-6
127	61	35	25	-26
49	39	11	42	-28
13	16	20	33	4
20	23	24	40	1
21	21	15	32	-6
175	62	29	16	-33
66	32	0	60	-32
88	55	7	30	-48
830	130-160	0	0	-130
1310	95	0	0	-95
65	54	0	0	-54
89	38	0	0	-38

**Table 5: Pillow measurements, including width, height, penetration depth of the pillow into the underlying sediment and sediment thickness. See Figure 5-17 for details of pillow measurements.**

As well as pillow lavas, lava tubes of varying nature are observed, including coalesced pillow tubes, stacked hollow lava tubes and coherent lava body.

At the south of the section, Locality A, a bulbous lava body comprised of coalesced pillow lobes and/or lava tubes is present (Figure 5-18). There are no obvious rind structures to prove separate pillows; however, size and morphology of the exposure suggests multiple coalesced pillow tubes and/or pillows, which may have inflated. The upper contact with the overlying HPb is irregular, locally fluidal, and displays flame-like structures (Figure 5-18). The basal contact with the underlying sediment is typically planar, with minimal interaction (mm-cm scale) in the form of localised loading and deformation of sediment. Small, white, coherent clasts of sediment (~4 cm) occur at the margins of the coalesced lava body and within the overlying HPb. Within the

overlying graded HPb, a ‘foreset’ of pillows, which vary in size, is present. The pillows appear to stack against the bulbous part of the underlying lava tube/coalesced pillows, which is likely a function of the exposure angle.

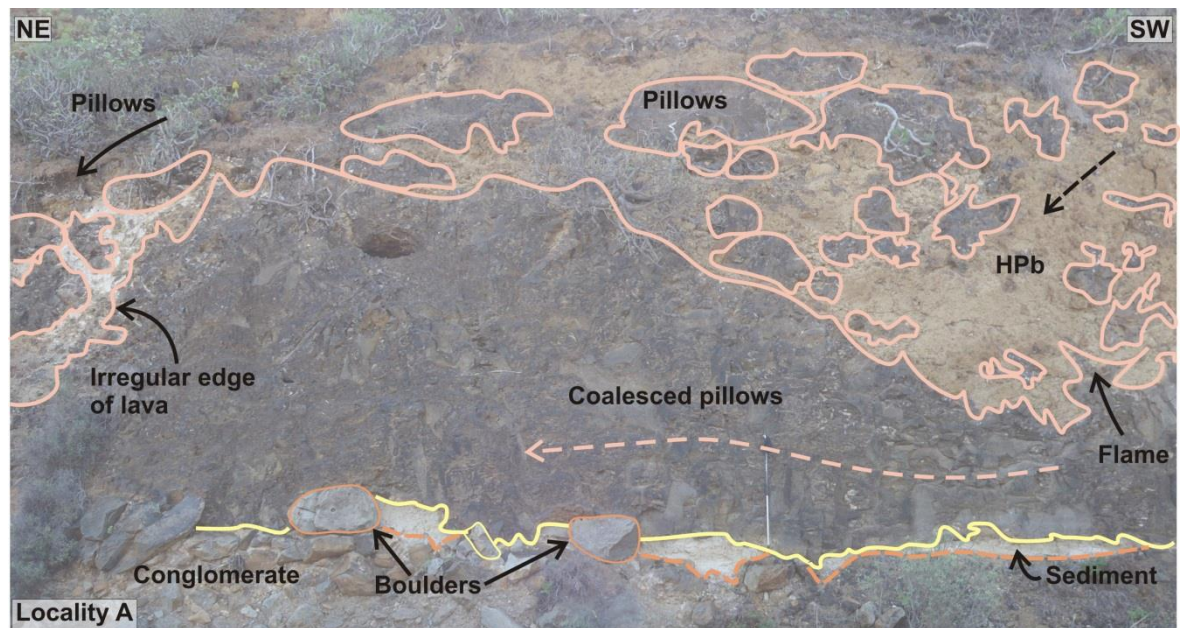


**Figure 5-18: Field view of locality A (Figure 5-3).**

**A bulbous lava body comprised of coalesced pillow lobes and pillow tubes overlies the sedimentary units. The underlying volcanoclastic sandstone is thin, <10 cm thick, where it drapes the boulder conglomerate. The basal contact of the lava has minimal interaction with the sediment, whereas the upper contact has flames into the overlying HPb. The margin of the lava/pillows is irregular and brecciated. The HPb displays grading between pillows and breccia.**

At Locality C (Figure 5-3), a series of stacked hollow, pillow lava tubes underlie coalesced pillow lobes (Figure 5-19). The outer crusts of the pillow lava tubes display ropey textures, whilst internally the tubes are hollow. A ‘shark’s tooth’ texture is observed within the hollow cavities of the tubes. Petrography of the lava confirms their basaltic composition (Figure 5-20).

At locality E (Figure 5-3) a coherent body of lava (possibly inflated) is observed, the top margin of which has an irregular upper surface that ‘fingers’ upwards, into the overlying, sediment-rich HPb (Figure 5-21). This contact is fluidal, and displays flame structure margins. Quenched rinds and spalled fragments within the HPb are present close to the fluidal lava contact.

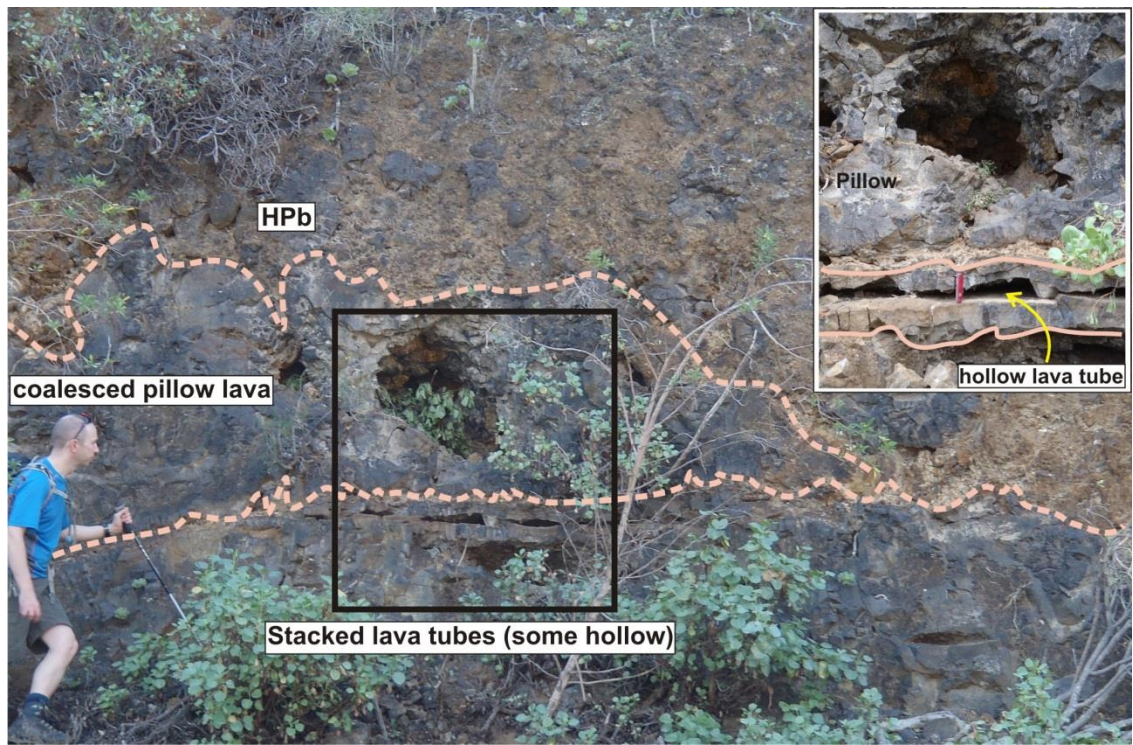


**Figure 5-19: Field view of lava tubes at Locality C.** The inset shows the thin pahoehoe lava tubes, which display shark's tooth texture in the hollows. Person for scale; pen knife (inset) is ~8 cm.

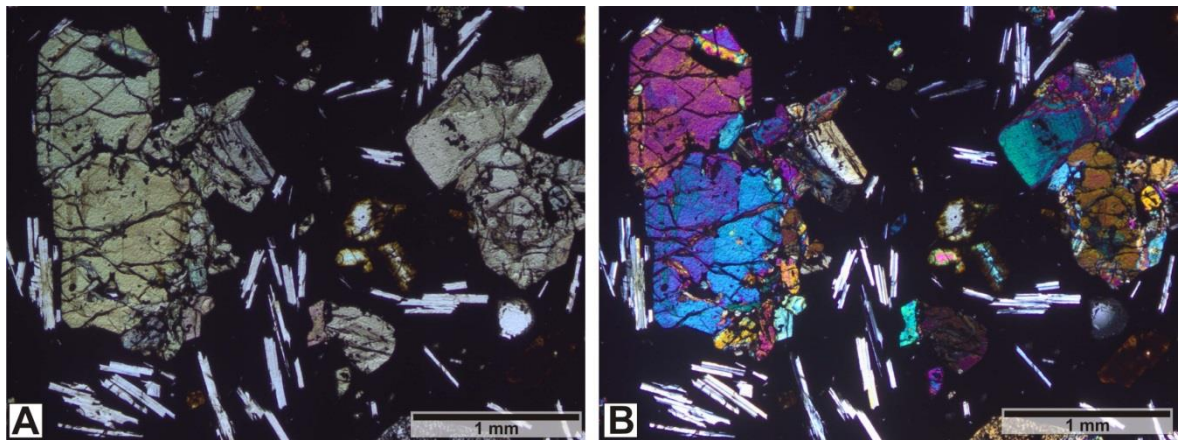


**Figure 5-20: Photomicrographs of the shark's tooth lava at Locality C (Figure 5-3).** A) PPL. B) XPL. Basalt lava comprising large phenocrysts of pyroxene/olivine are present within a glassy aphanitic groundmass containing microphenocrysts of plagioclase (sub mm).

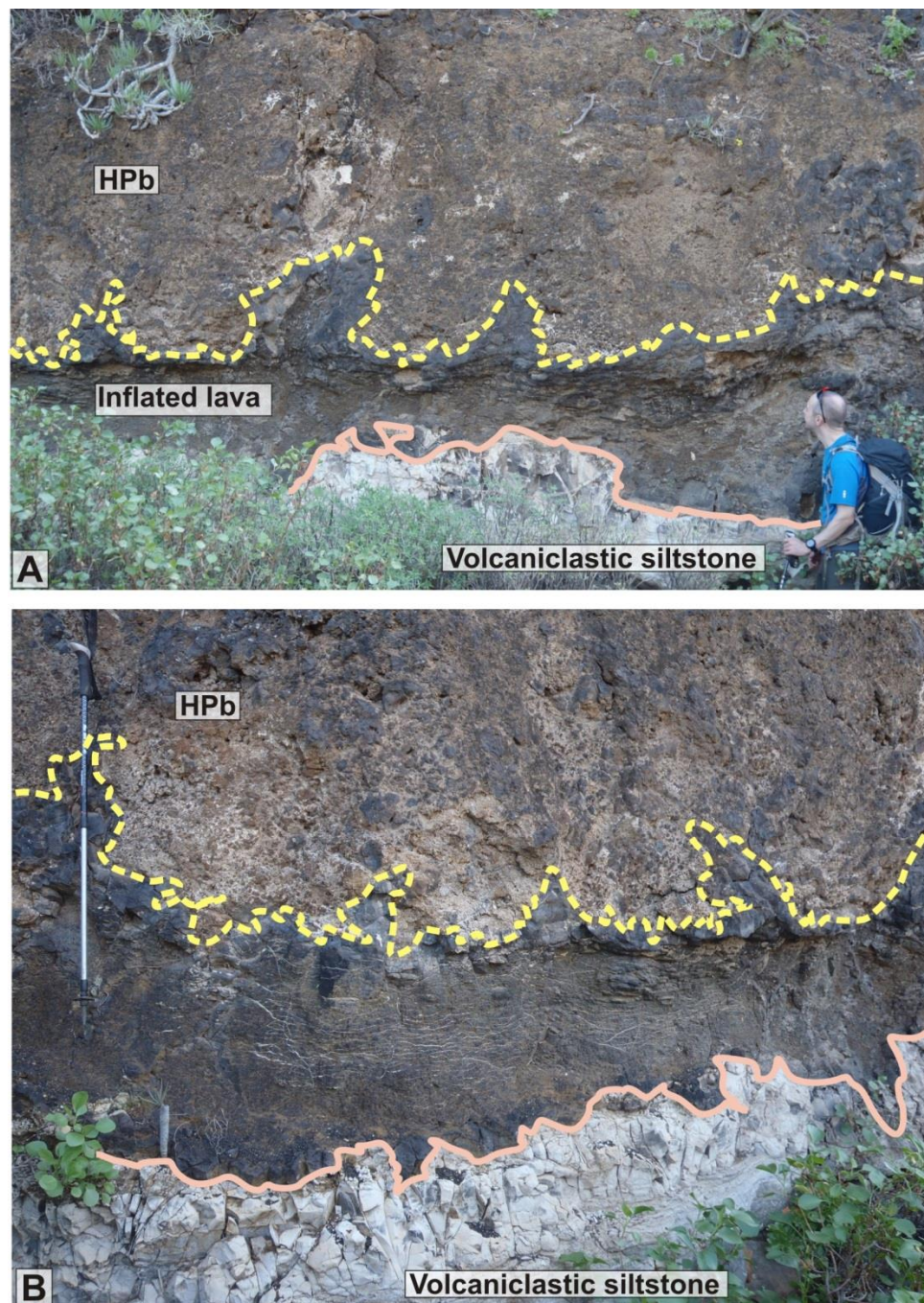


**Figure 5-21:** Field view at Locality E, where a coherent lava sheet is present between the sedimentary unit (pink solid line) and the overlying HPb (yellow dashed line). A and B show the irregular basal and upper contacts that finger away from the main lava body into the volcaniclastic siltstone and/or HPb. A) Person for scale; B) Walking pole is ~1 m.

---

### 5.3.3 Lava-Sediment Interface

Throughout the section, a variety of lava-sediment interaction features are preserved including loading of sediment by pillows, sediment fluidisation, coherent sediment inclusions within the HPb and minor peperite. These are described from key examples below. Throughout the section mingling and fluidisation zones are locally restricted.

At Locality A (Figure 5-3) the contact between the basal margin of the lava (coalesced pillow body) and the underlying sedimentary units is restricted to loading and soft sediment interaction on a mm-cm scale. The sedimentary units are thin, and have no internal structure preserved as the lava cuts down into them (potentially fluidised). The lava-sediment contact is very close to the underlying conglomerate unit (Figure 5-18).

Well-formed pillow lavas rest on top of fine-grained white sedimentary units, displaying a relatively sharp contact with minimal to no interaction at the base of the pillows. However, at the edges of the pillows, sediment is found between them and forms flame-like structures (Figure 5-22). Bedding and laminae within the sediment are disrupted and the white siltstone and sandstone is fluidized into the flame structure. A small amount of sediment is present within fractures of the pillow rinds. Flame-like features occur at almost every pillow edge in this part of the section.

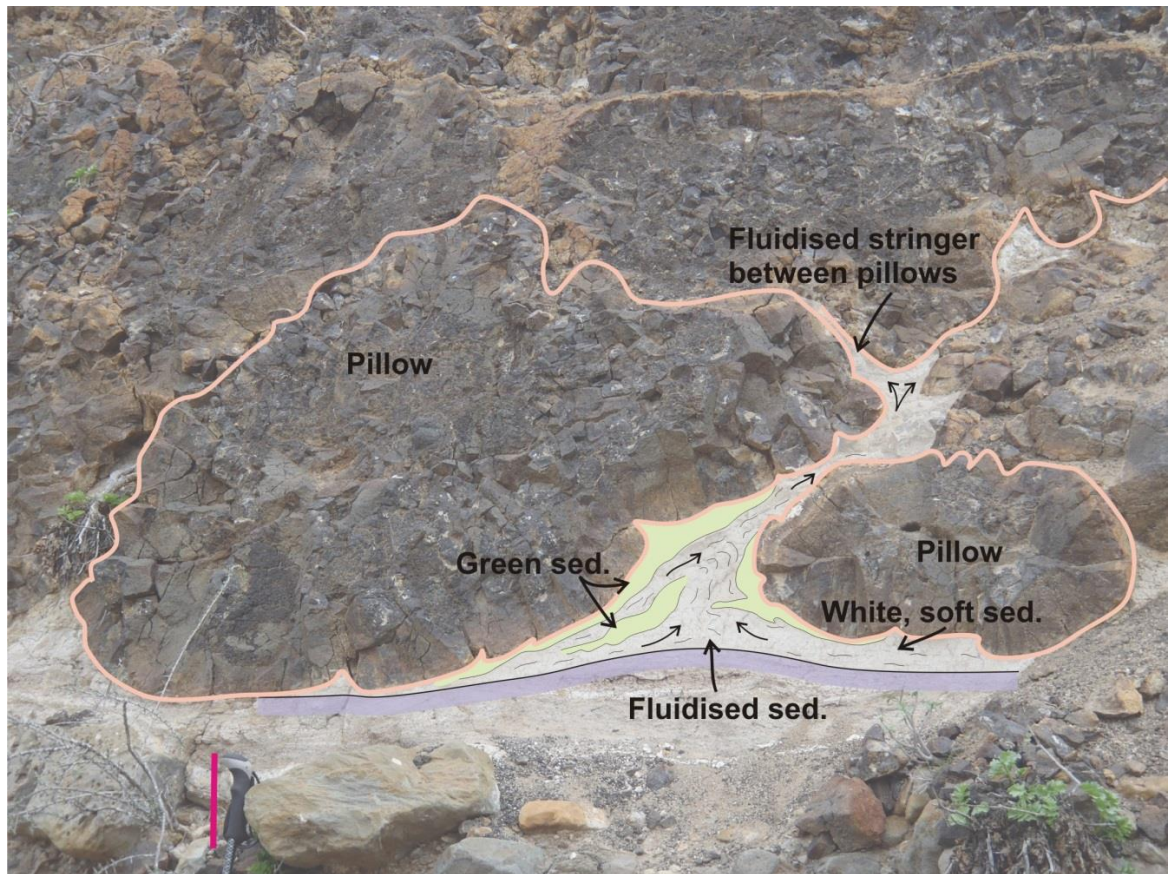


**Figure 5-22: Annotated field view depicting the flame structure produced as sediment (sed.) is fluidised and squeezed between two overlying pillow lavas. Arrows show the interpreted direction of sediment movement. This feature sits almost directly on top of the basal conglomerate unit of the sequence, between logs 1 and 2. Small pillow is ~30 cm, walking pole handle (pink bar) is ~10 cm long.**

At Locality D, (Log 3, Figure 5-4, Figure 5-23) the largest pillow in the section is observed. Only 30 cm of fine siltstone remains between the top of the conglomerate unit and the base of the pillow (Figure 5-23). At the lateral margins of the pillow, sediment is fluidised and sediment structure is not preserved. This pillow is surrounded by a ~20 -25 cm wide zone of fluidised sediment; however, to the right of the pillow, the fluidisation zone extends to a distance of 150 cm. Mingling of small spalled chunks (1-10 cm) of pillow lava and sediment is observed at the edges. Mingling at the basal margin of the pillow with underlying sediment is present, but minimal.

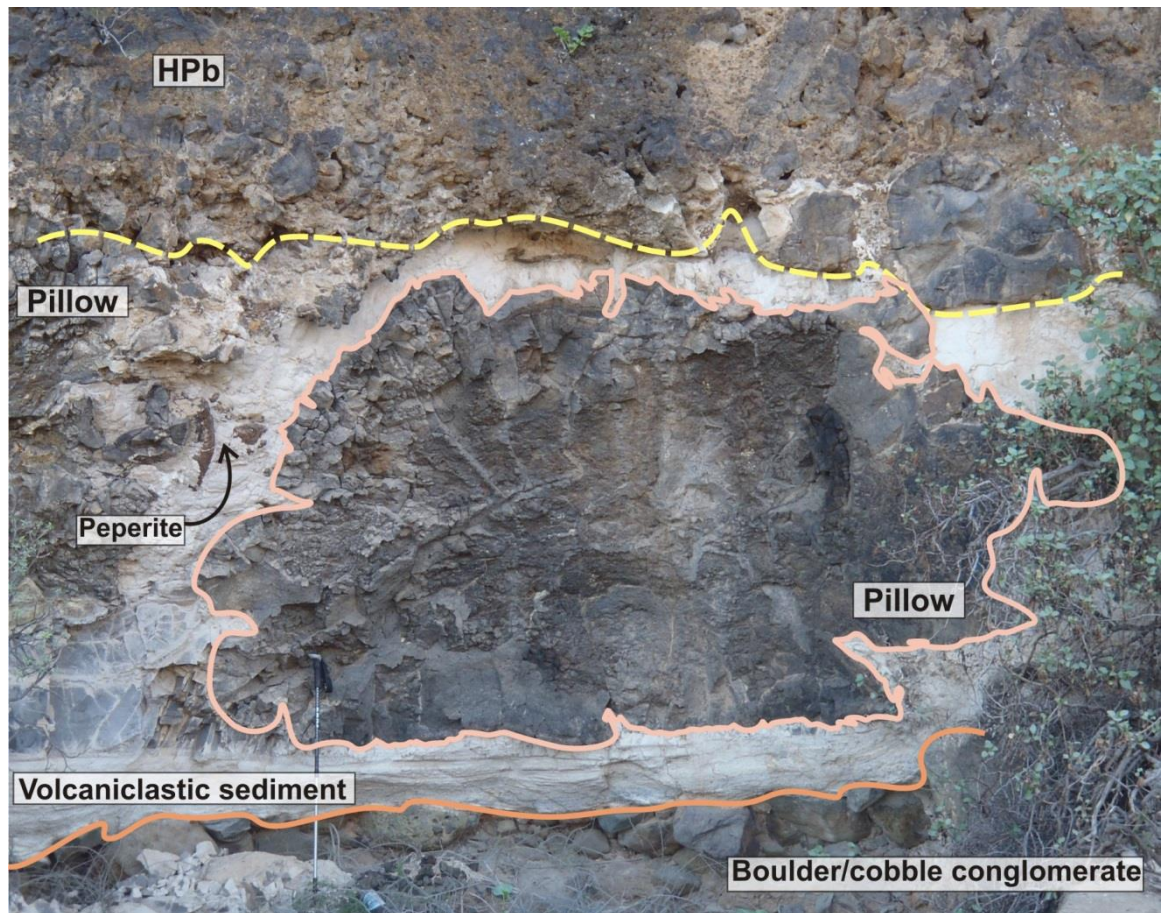


**Figure 5-23: The largest pillow in the section, possibly a feeder pillow, at locality D. The pillow margins are quenched and micro-scale mingling with sediment (peperite) is observed. Walking pole is ~1 m.**

Throughout the section peperite is preserved in ‘pockets’, rather than within a laterally continuous layer. Sediment mingling at the top of Log 6 (Figure 5-6) is interpreted as peperite. The (preserved) sediment is predominantly white, fine silt and clay grade, and in places pumice rich. The entire unit is deformed and disrupted by the lava, and mingled with it (Figure 5-24). Some sediment is also found within chilled rinds of the pillows. The sequence above Log 2 (Figure 5-4 and **Error! Reference source not found.**), between the pillow and sediment, comprises ~25 cm of diffuse peperite, which thins to 4 cm and is then only visible in small (2 cm) lenses. Clasts (juvenile?) comprise glassy basalt with quenched rims (Figure 5-25) and range in size and shape; small clasts, ~ 1-2 cm, are blocky, whereas larger clasts, ~ 5-28 cm, have fluidal margins. The sediment is pumice-rich, white, fine siltstone. It appears fluidised and displays orange weathering. The lower margin of the peperite zone extends into the underlying sedimentary units.

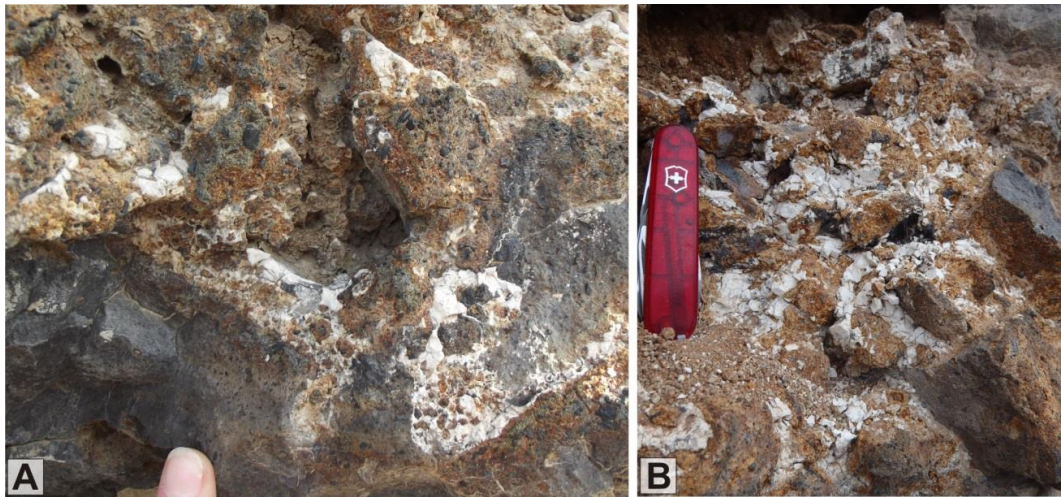


Figure 5-24: Lava-sediment mingling at Log locality 9 (Figure 5-3) occurs between the pillows, HPb and the sediment.

Peperite is observed in a number of log localities along the section at the lava-sediment interface. Finger nail 1 cm wide, Pen knife is ~ 8 cm.

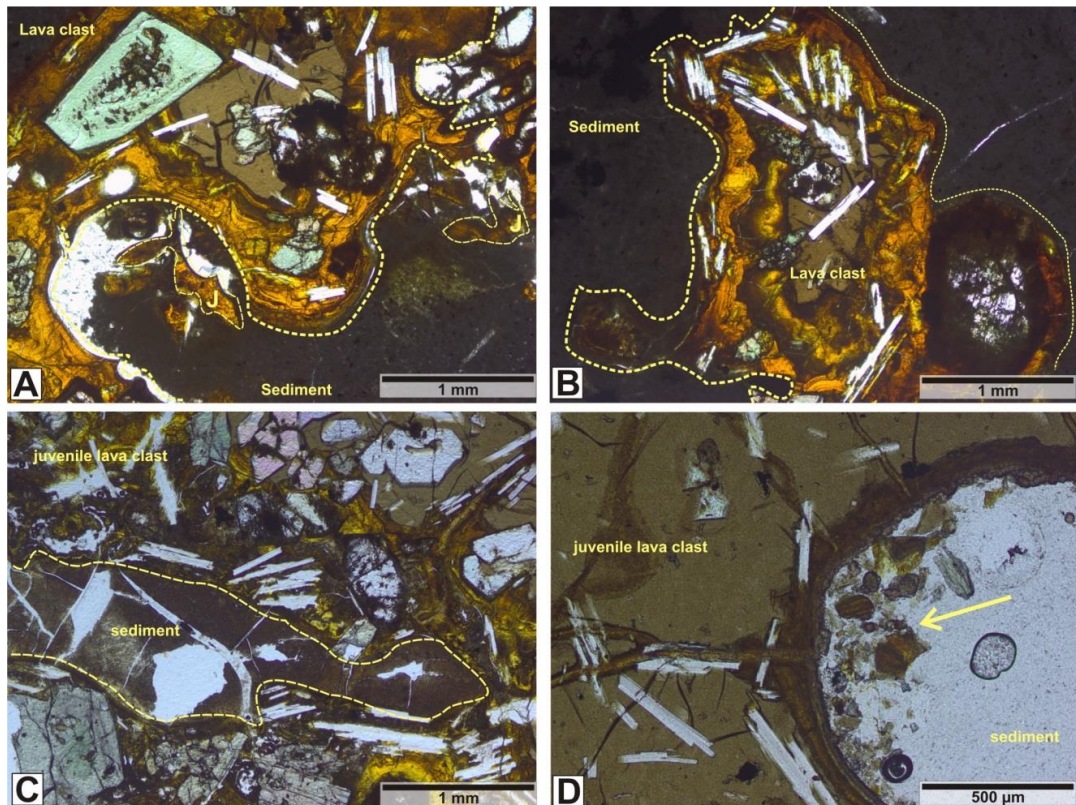


Figure 5-25: Photomicrographs of basalt juvenile lava clasts within a volcaniclastic matrix at the lava-sediment boundary (XPL).

A and B) sample GC.003 collected at the top of Log 2, close to Locality D (and Figure 5-4), C and D) sample GC.005, top of Log 5 (Locality E), Figure 5-4). A) The fluidal, amoeboid edge of a juvenile lava clast (dotted yellow line, J), which displays minor-scale peperite within the clast 'hollow'. The small fragmented juvenile clasts (dashed yellow lines) are likely fragmented from the larger juvenile clast. B) A fluidal/globular juvenile lava clast (dashed yellow outline) within fine-grained volcaniclastic siltstone. The clast displays alteration of the basalt glass (sideromelane) to gel palagonite (orange) (Stroncik and Schminke 2002). C) Juvenile lava clast with phenocrysts of plagioclase, olivine and pyroxene, with zoned apatites, within a glassy matrix. D) Micro-scale glass shards (arrow) are found within the sedimentary matrix, suggesting an explosive clast generation process.

The volcanoclastic units recorded in Log 2, Locality D (Figure 5-4), are thoroughly disrupted and fluidised around, and below, several pillows (Figure 5-26). The sketch in Figure 5-26.B illustrates how the original bedding and clearly defined units (observed in Log 2, **Error! Reference source not found.**) are abruptly ‘cut’ by the pillow lava and fluidisation zone. This zone directly overlies a single isolated pillow (71 cm tall by 130 cm wide), and lies beneath two other pillows. The size of the pillows varies between 53 and 174 cm (height) by 30 and 162 cm (wide). The isolated pillow (71x130 cm) lies deep within the sedimentary succession (in comparison to pillows within the rest of the succession), almost at the top of the conglomerate unit. All original bedding has been fluidized and lost directly above this pillow. Despite the ‘invasive’ nature of this pillow, lava-sediment interaction is minimal; although several spalled lava fragments are observed surrounding the pillow; peperite is not present. Rather, it is the sedimentary units that are mingled and fluidised together, and with each other.

The volcanoclastic siltstone and sandstone units have been fluidised and mixed together, with some textural homogenisation, however, this zone has its own characteristics. These include elutriation pipes of vesiculated sediment, discontinuous, convolute laminations, and small coherent fragments of very fine-grained claystone and siltstone. Remnants of the orange-banded siltstone (e.g. Figure 5-11) are also observed, and these too are disrupted and fluidised (Figure 5-26).

Disruption and fluidisation of the sediment at the lava-sediment interface is a common feature, and especially highlighted by the orange, scoriaceous beds, which appear more susceptible to deformation. Whilst this is purely a function of colour, it acts to highlight the amount, and extent of internal mixing of the sedimentary beds. Figure 5-27 shows fluidization and consequent mingling of sedimentary units around invasive pillow lavas, highlighted by the orange scoriaceous layers and purple pumice-rich layers. The beds thicken and thin, and appear discontinuous as a consequence of deformation and internal fluidisation caused by invasive pillow lavas.

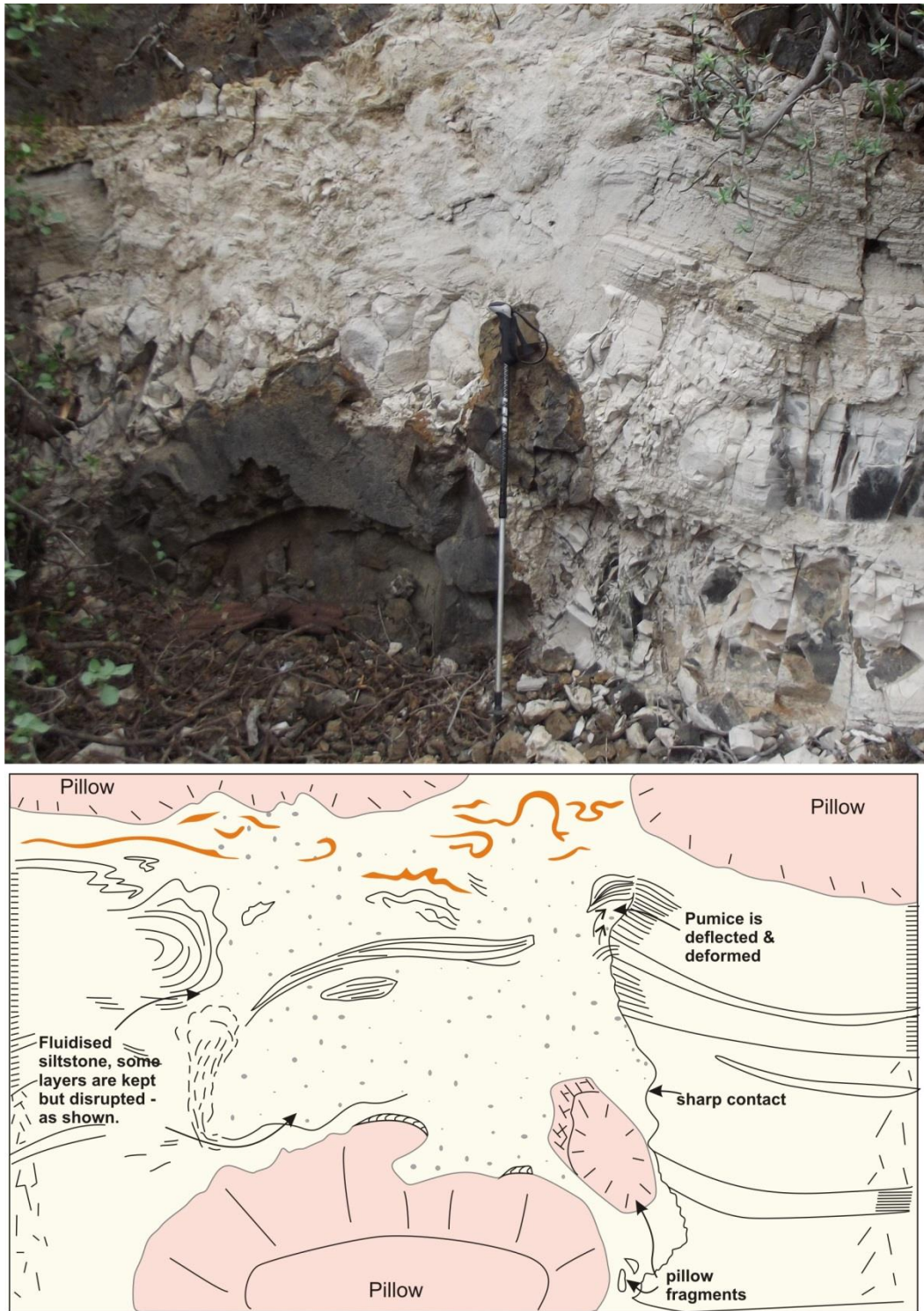


**Figure 5-26: Field view (A) and sketch (B, slightly oblique to photograph) showing the features of a heavily fluidised zone, at Locality D.**

The fluidised zone is observed above a pillow lava that appears to have burrowed into and under the sedimentary units. The sketch highlights the isolated pillow, the heavily disrupted zone of sediment and the convolute orange-stained beds. Walking pole is ~1 m.

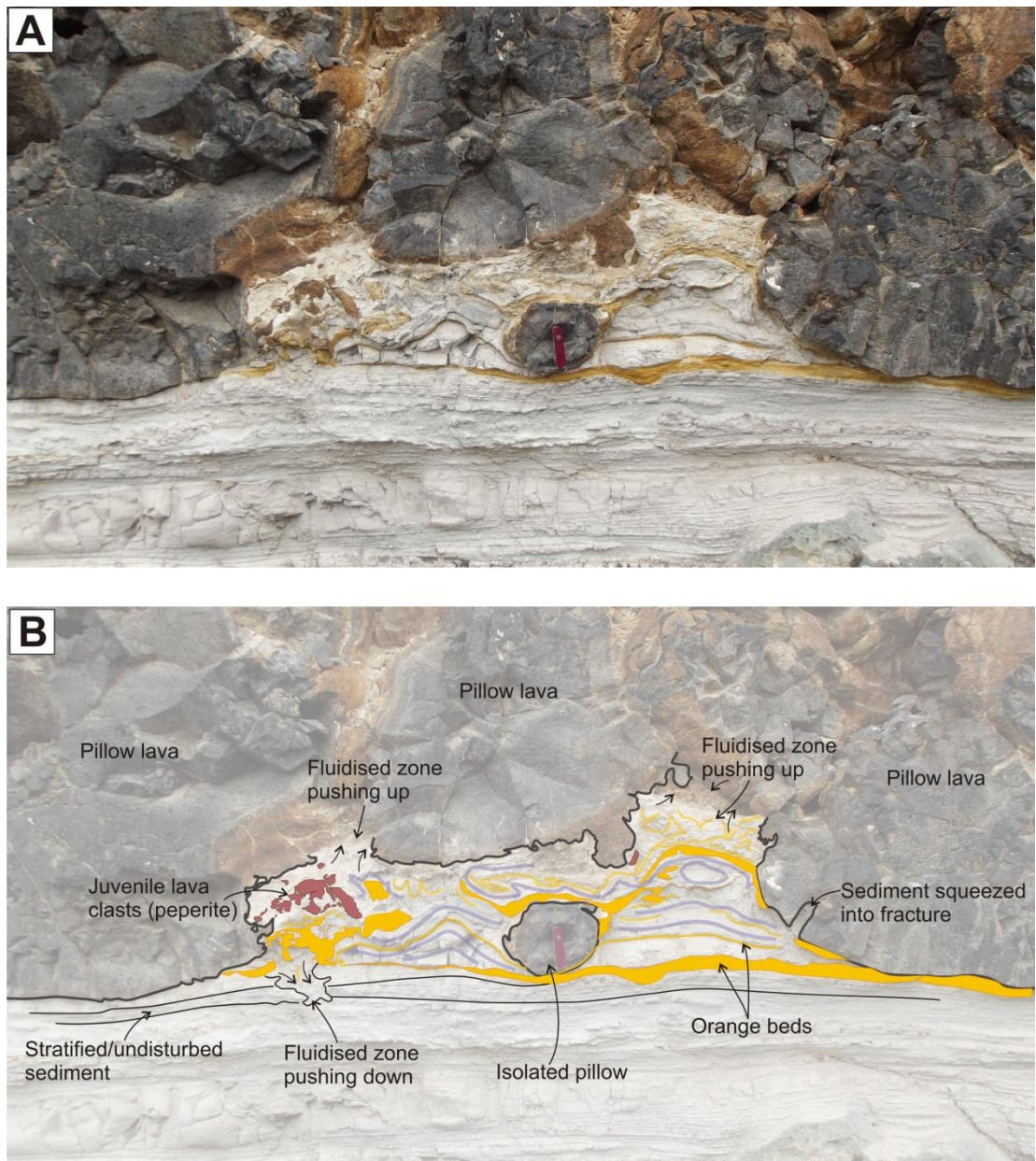


**Figure 5-27: The lava-sedimentary contact between localities E and F, near log 6, (Figure 5-3).**

**Orange scoriaceous beds (yellow) and fine-grained pale purple beds (lilac) highlight fluidisation and consequent mingling of volcanoclastic units around pillow lavas. Juvenile lava clasts, detached from the pillows (brown) are hosted within the sediment, close to the pillow contact. Pen knife in central pillow (red) is ~8 cm.**

## 5.4 Interpretation

The succession, described above, provides an insight into magma-sediment interaction involving shallow marine sedimentation and lava emplacement. The sequence records alluvial fan to shoreface marine volcanoclastic sediment deposition, overlain by a basaltic pillow lava and hyaloclastite breccia pile. These units represent the Lower and Middle Members of the LPDF, deposited during the Miocene-Pliocene.

### 5.4.1 Sedimentary Units

The basal cobble-boulder conglomerate unit (Figure 5-4), which has a fine sandstone matrix, is interpreted as an alluvial fan conglomerate (Pérez Torrado et al. 2002; Schneider et al. 2004). The clasts of mixed lithologies, predominantly phonolite, represent the erosion and reworking of the pre-existing volcanic deposits on the island, emplaced during the initial island building stages, >8 Ma (Carracedo et al. 2002; Schneider et al. 2004). This supports the pre-existing evidence for the Lower Member LPDF representing the volcanic hiatus and erosional stages of the volcanic ocean island (Carracedo et al. 2002; Guillou et al. 2004; Schneider et al. 2004; Perez-Torrado et al. 2014).

The main sedimentary unit (Figure 5-4) comprises volcanoclastic claystones siltstones and sandstones, dominated by pumice and reworked basalt lithics, recording the reworking of volcanic material. Cross-stratification, wave-ripple lamination and erosional surfaces, suggest a high-energy depositional environment, likely of near-shoreface to shallow marine. The presence of a bivalve fossil (Figure 5-9), and algal material (Figure 5-10) supports this, indicating a tropical, shallow marine environment. Known fossil records across Gran Canaria and the Canary Islands are widely reported and have dated these strata, of the Middle Member of the LPDF, as being of Pliocene age, 4.9-2.9 Ma (Guillou et al. 2004; Schneider et al. 2004; Meco et al. 2007; Perez-Torrado et al. 2014; Meco et al. 2015).

The orange-stained basalt-lithic dominated beds (Figure 5-11 and Figure 5-13), interbedded with pumice-rich layers (Figure 5-14), record the reworking of basalt glass and the likely renewed onset of effusive volcanic activity and input into the depositional system. As the beds are quite close to the lava-sediment contact, they may also represent the initial stages of lava entering the basin, producing glassy hyaloclastite breccia, up-slope, which is reworked and deposited near the shelf-edge/down slope. Previous studies have suggested a narrow marine shelf depositional environment for these deposits (Lietz and Schmincke 1975; Balcells et al. 1992; Schneider et al. 2004; Cabrera et al. 2008).

## 5.4.2 Volcanic Component

### 5.4.2.1 HPb

The HPb displays both pillow- and hyaloclastite-dominated foresets (Figure 5-15) that record the sub-aqueous emplacement of pahoehoe lava into a marine basin. This represents a progradational lava-fed delta, similar to Gilbert-style deltas (Porębski and Gradziński 1990; Pedersen et al. 1998; Skilling 2002), as previously described in Chapter 4. The HPb is diffusely stratified and gradational between pillow-dominated and hyaloclastite-dominated foresets, which provides evidence of reworking, likely by tidal wave-currents, due to near-shore processes and depositional environment.

Pillow lavas and pillow-dominated foresets are the products of the emplacement of lava, subaqueously. Multiple quenched rinds are produced due to quenching and rapid cooling of the lava as it enters the water. Water penetrates fractures in the rind, which leads to rapid cooling and quenching of the interior and formation of second, and multiple rinds. Occasionally, the (initial) rind will fracture and break away, sometimes due to pillow growth and expansion, but may also remain attached to the pillow (Walker, 1971; Moore, 1975; Self 1998; Bear 2007). Within the pillow pile, the quenched and spalled fragmented pillow material may insulate the pillows from further cooling (Watton et al. 2013), allowing the pillows to grow, forming mega pillows (as observed at Locality D, Figure 5-23), and bypassing the upper transitional zone, progressing further downslope through feeder tubes, and reaching the sediment interface in concentrated pillow-dominated foresets.

The hyaloclastite-dominated foresets are the fragmental by-product of lava emplacement into water, comprising the fragmental, broken, and quenched material spalled from the pillows and lava tubes. The material is further fragmented and reworked, through slumping and collapse of the foreset packages, as a consequence of the oversteepening lava pile, gravity-driven slumping, and lobe inflation (Skilling 2002; Watton et al. 2013).

### 5.4.2.2 Sheet lava

The presence of ropey textures and multiple tubes and flow lobes indicate that this lava is most likely of basaltic pahoehoe type. The 'sharks tooth' texture displayed within hollow pahoehoe lava tubes at Locality E (Figure 5-19) is evidence for active lava inflation and drainage during emplacement. This process involves the cooled, quenched rinds insulating the inner lava and enabling inflation of the lava (Walker 1971; Rowland and Walker 1990; Self et al. 1998). The 'sharks tooth' texture is created when the lava

tube drains and remaining molten lava drips from the solidified ceiling rind of the tube (Kauahikaua et al. 1998).

Whilst the pillows and hollow flow tubes provide evidence for pahoehoe lava, there is also evidence for slabby pahoehoe-type flows. The sheet-like lava, observed at Locality E (Figure 5-3), is a coherent lava body that has an irregular, fluidal and flame-like upper margin in contact with overlying HPb (Figure 5-21). The sheet may represent a passive lava, that burrows into the underlying sediment and hyaloclastite breccia, and then inflates.

Previous studies of submarine basalt lavas and Gilbert-style lava deltas deduce that effusion rates of the lava, coupled with the slope angle, determine the morphology of lava that progrades or aggrades into the basin. Typically, low effusion rates,  $\sim 5\text{-}10\text{ m}^3/\text{s}$  (Ramalho et al. 2013), of sub-aerial pahoehoe-type lavas, will result in hyaloclastite and pillow breccia, due to quenching and fragmentation, and foresets prograde in Gilbert-style deltas (as previously discussed in Chapter 4). However, as effusion rates increase above this threshold ( $>5\text{-}10\text{ m}^3/\text{s}$ ) (Rowland and Walker 1990; Griffiths and Fink 1992; Gregg and Smith 2003), to medium-high rates, typically associated with slabby-pahoehoe and 'a'a flows, lobate lavas, mega-pillows, coalesced mega-pillows and sheet flows are produced (Ramalho et al. 2013). Little quenching and fragmentation occurs subaqueously, and the lava retains coherence (Ramalho et al. 2013). Morphological changes are also a consequence of slope angle, and these features may also be linked to slope angles of between  $10\text{-}25^\circ$  (Gregg and Fink 2000; Gregg and Smith 2003; Ramalho et al. 2013). Therefore, on Gran Canaria, there is evidence for development of the effusion rate, slope angle and lava flow-type, from slabby-pahoehoe sheet lavas with high effusion rates, to pahoehoe-type flows that produce hyaloclastite pillow breccias.

### 5.4.3 Lava-sediment interaction

At the lava-sediment contact variable features are observed from minimal interaction, with planar contacts, to peperitic margins and sediment fluidisation. During lava emplacement the sedimentary units were saturated with varying degrees of consolidation and compaction.

With pillow lavas, the lava-sediment interface is dominantly sharp, with the exception of sedimentary loading and flame structures between pillows. Flame structures (Figure 5-22) within the sediment are interpreted as a consequence of loading of the partially consolidated and compacted sediment. Fluidisation of the sediment is interpreted from the disrupted internal structures of the sediment within flames, and at pillow margins.

Brecciation, and therefore peperite formation, of the pillows is limited, a likely consequence of the already quenched and cooled chilled margins of the pillow lavas.

Typically peperite formation requires saturated, unconsolidated sediment with which lava can mingle. Here, juvenile lava clasts typically comprise spalled fragments, with occasional juvenile clasts and peperite zones created at the newly formed margins of an invasive pillow bud. This explains the discrete zones of peperite. Whilst there is a mixture of juvenile clast morphologies, they are typically fluidal, which indicates a ductile, rather brittle, fragmentation regime (Skilling et al 2000). The host sediment is fine grained siltstone, and is also present as inclusions within the HPb. Sedimentary inclusions are interpreted to form as the sedimentary units are bulldozed and invaded by pillow lavas, with more cohesive, typically more fine-grained sediment entrained within the pillow lavas and/or HPb, as coherent fragments (see also Chapters 4 and 6).

The internal structure of the sedimentary package and individual units is typically lost at the lava-sediment contact, however, locally, individual units display more complex disruption. Fluidisation occurs on a cm to m scale, and is localised. Internal sediment fluidisation requires the invasion of a fluid or heating of the pore fluids in which sediment grains can be entrained (Kokelaar 1982; Lorenz 1984; Skilling et al. 2002; Zimanowski and Büttner 2002). Fluidisation of the sediment causes mingling between bedding and layers, resulting in the convolute and disrupted sedimentary units. Bedding and structures are lost; however, textural homogenisation is not thorough, and structures such as elutriation pipes of vesiculated sediment are preserved, as seen at Locality D (Figure 5-26). The fluidisation and internal mixing of the sediment is interpreted as a consequence of the invasion of pillow lavas, which cause the superheating of pore-water, and the movement of sediment grains (Figure 5-26). Heating of the sediment, and therefore movement, is a continual process until an equilibrium is reached, with the pillow lava sufficiently cooled, and the pore fluids driven off. Further emplacement of lava directly on top of the disrupted sedimentary pile may cause further loading and disruption, or may have little effect. The order of pillow emplacement, such as those at Locality D is not determined. The scale of disruption and internal fluidisation is observed on a cm to m scale, and is highly localised, which suggests that disruption is independent of the size of the pillow, and thus related to the internal sedimentary properties such as grain size, porosity, and permeability.

## 5.5 Discussion

This field study is a detailed analysis of the lava-sediment interface within a sub-aqueous environment, focusing in particular on pillows and fluidisation of sediment.

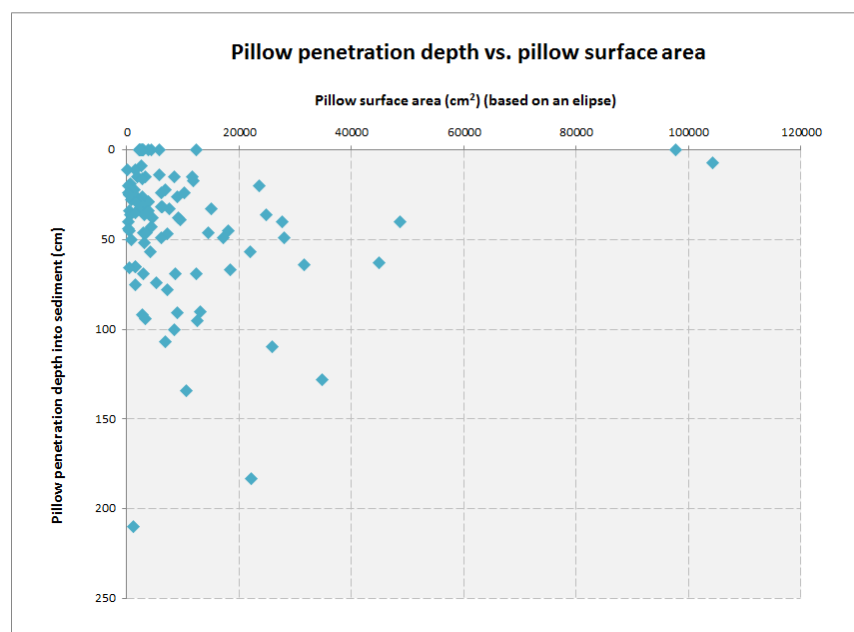
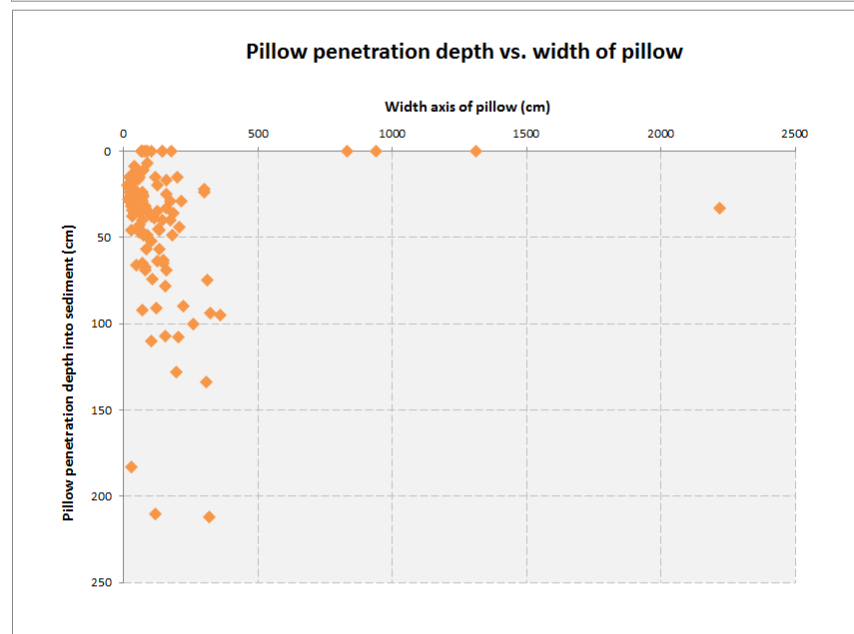
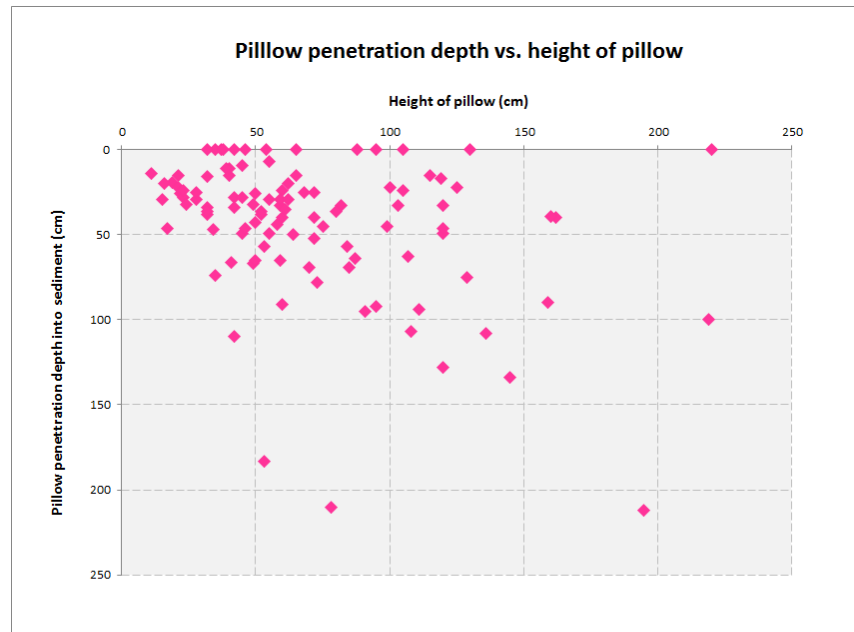
### 5.5.1 Pillow measurements

The statistical data collected from measurements of pillow size and penetration depth indicate that pillow size does not correlate with depth of penetration into the underlying sediment (i.e. larger pillows do not necessarily penetrate further than smaller pillows).

The data (Figure 5-17 and Table 5) provide an insight into the effect of pillow shape and size at the lava-sedimentary interface. In the field study at Mountain Home (Chapter 4), limited data indicate that pillow shape and size does not correlate with the depth to which the pillow may penetrate into the sediment. In this study, the more systematic sampling of every pillow along the well-exposed locality allows a more accurate and detailed insight into a single sequence and the behaviour of the pillow lava and sediment. The penetration depth of the pillows into the sediment is plotted against the height (vertical axis) of the pillow, the width (horizontal axis) of the pillow and, the surface area of the pillow. The three plots (Figure 5-28) highlight little correlation between pillow shape and size and penetration depth.

Plot A, pillow penetration depth vs. pillow height, displays a large spread of data, with little to no trend (Figure 5-28). Both large and small pillows record penetration depths from 0 - 200 cm. Plot B displays a small spread of data. Note the change in scale from the height of pillows (Plot A), to the width (Plot B) (Figure 5-28). Plot B, like Plot A shows pillow width has little correlation with penetration depth.

Plot C, pillow penetration depth vs. pillow surface area displays a wide spread of data (Figure 5-28). Pillow surface area was based on the assumption that the pillow formed an ellipse; however, as many of the pillows are irregular in shape there is some error in the data. Nonetheless, Plot C supports the other data in demonstrating that penetration into the underlying sediment is independent of pillow size, and that pillows may penetrate a small amount, a large amount, or not at all, irrespective of their size.



---

**Figure 5-28 (previous page): Scatter plots illustrating the relationship between pillow size and the depth to which the pillows penetrate into the sediment. There is little to no correlation between the size of a pillow and the depth to which it penetrates the underlying sediment. A) Pillow penetration depth against height of the pillow; B) pillow penetration depth against width of the pillow; C) pillow penetration depth against surface area of the pillow. The surface area was calculated based on the assumption that the pillows were ellipsoids. All measurements are in cm, surface area in cm<sup>2</sup>.**

Analysis from pillow measurements demonstrates that penetration depth of the invasive pillow lava into the underlying sediment does not directly correlate with pillow size or shape. Therefore, it is suggested that sediment properties (e.g. sediment cohesion, saturation, grain size etc.), rather than lava effusion rates/pillow size, strongly influence the style of interaction between lava and sediment, and the variable morphologies observed at the interface. Pillow size and shape variability also indicates the scale invariance of pillow penetration and sediment disruption, supporting the evidence presented in Chapter 4 (Mountain Home). This is illustrated in Figure 5-29, which compares the data from Mountain Home and Gran Canaria. This study also recognises how the sediment behaves locally due to pillow lava (+/- HPb) emplacement.

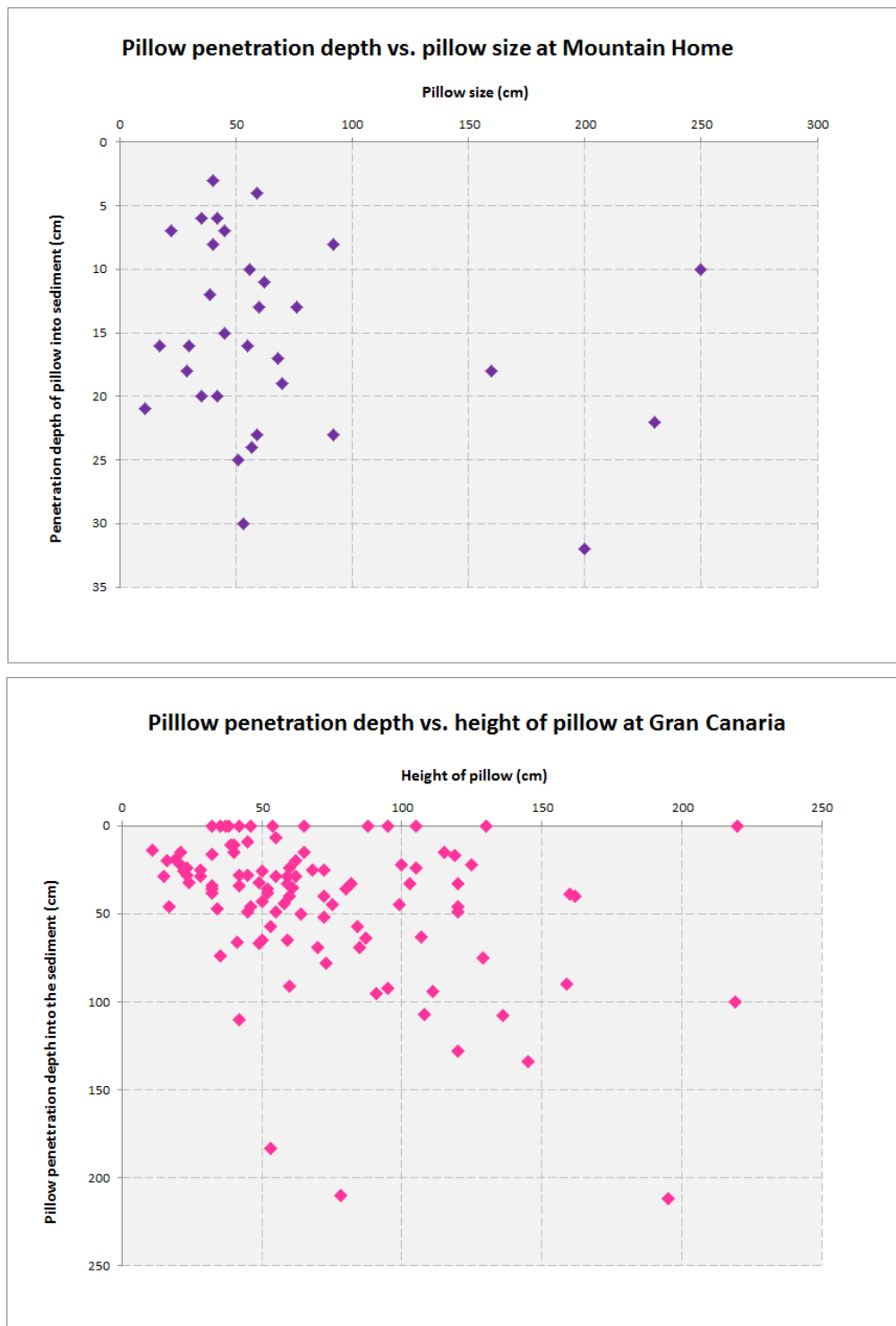


**Figure 5-29: A comparison of pillow measurement data between Mountain Home and Gran Canaria filed sites.**

**Both plots show similar patterns, that the depth of penetration of pillow lavas into underlying sediment is scale invariant.**

## 5.5.2 Fluidisation

Internal structure of the sediment at the lava-sediment contact can be greatly significantly affected by lava invasion, which can greatly change the sediment characteristics in terms of physical characteristics and porosity and permeability (e.g. a neatly stratified sediment with open pore space but capped by a closed impermeable layer may now be fluidised with discontinuous permeable and impermeable layers and poor porosity). Pillow analysis suggests that sediment disruption and invasion is not a function of pillow size, and is therefore related to localised variations in internal sedimentary properties.

Figure 5-30 is a schematic 2D model that illustrates the variety of lava-sediment interactions that occur as a consequence of pillow lavas loading, disrupting, and invading sedimentary units. These features do not always appear together, but occur as a consequence of localised variations in sedimentary properties, with changes in lava properties also likely. The model shows a single invasive pillow, with a coherent sedimentary inclusion, that has invaded the sediment (S, Figure 5-30). Loading and flames occur at the sides of, and between pillows. Bedding, and marker beds highlight the degree of sediment disruption, fluidisation and textural homogenisation. Complete disruption of the sediment is not limited to the sides and upper margins of the pillow, but is more common.

Sediment fluidisation is widely recognised as a process that is associated with peperite formation (Kokelaar 1982; Skilling et al. 2002; Owen 2003); however, here it is described as a consequence of invasive pillow lava emplacement. The features previously recognised, such as textural homogenisation and elutriation pipes do occur here. Theoretically, the pillow acts as a large, lava apophysis, or juvenile clast that remains coherent rather than fragmenting into peperite, apart from in minor cases. Small peperite domains are recognised at the margins of some pillows, but notably not all.

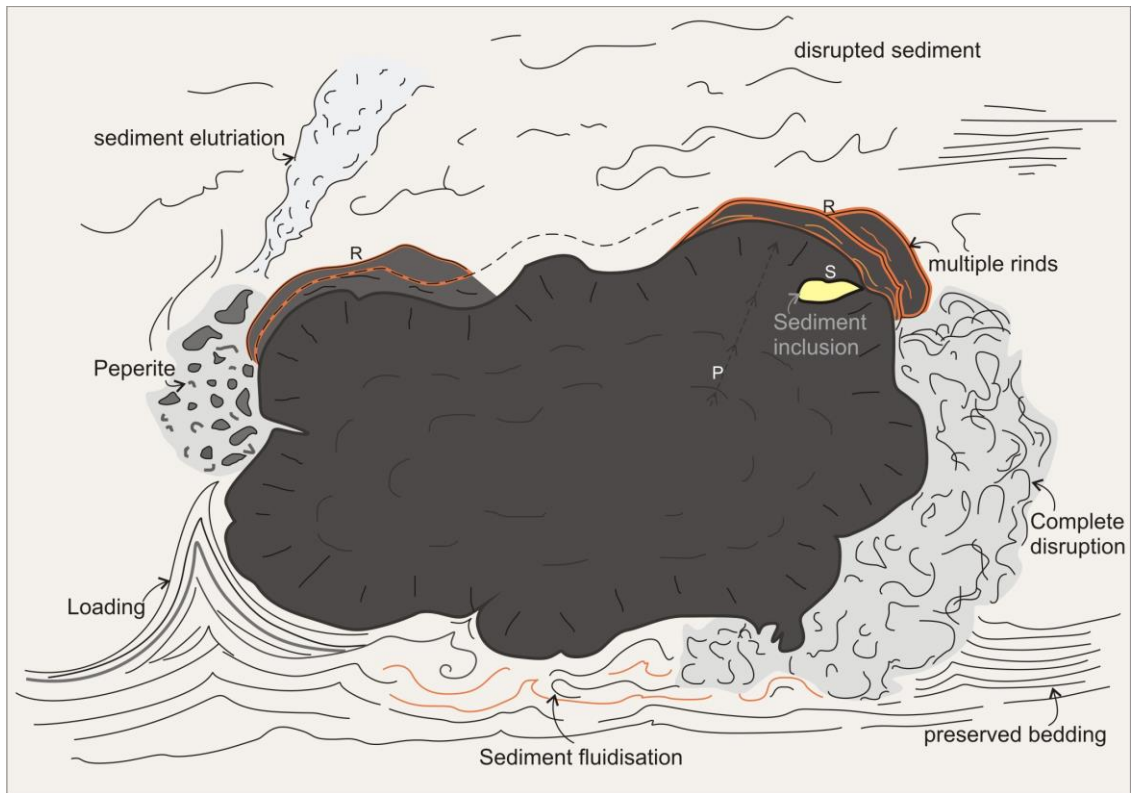


**Figure 5-30: Schematic diagram of an invasive pillow lava (P) and the variety of sedimentary products that may form as a consequence of lava-water-sediment interaction.**

The observed interactions range from minimal interaction, where bedding is preserved and loading and flame structures are produced, to sediment fluidisation, peperite, and the complete disruption of the sedimentary units. P = pillow; R = rind; S = sediment.

## 5.6 Conclusions

This study provides a comprehensive field study focused on the lava-water-sediment interface along a lateral contact on the island of Gran Canaria. Mio-Pliocene volcanoclastic sedimentary units record the fluvial-shallow marine transition, and reworking of the emerging volcanic landscape. The overlying pillow lavas and hyaloclastite pile record sub-aerial lava emplacement into the marine basin and subsequent interaction with the underlying sediments.

The excellent exposure of the lava-sedimentary contact enables the characterisation of various changes in lava-water-sediment interaction at the interface from minimal to passive interaction and invasion of the sedimentary pile by pillow lavas. The lava-sedimentary contact is not limited to pillow lavas, with evidence for coherent sheet lavas of pahoehoe to slabby-pahoehoe flows, also present. Previous work has only a limited assessment of the direct lava-sediment contact, and the effects of pillow lava on underlying sediments.

This study has provided a detailed analysis of the pillow lavas, including pillow size and penetration depth. Pillow measurements build on the work from Mountain Home (Chapter 4) demonstrating and supporting evidence that penetration depth, and invasion into the sediment, is independent of pillow size (i.e. large pillows do not necessarily invade further into the sediment compared to smaller pillows).

A consequence of pillow invasion and lava-sediment interaction, recorded here, is the disruption and internal fluidisation of sedimentary units. The scale and styles of fluidisation are similar to those recorded at peperitic margins of sub-aerial basalt lava flows. Small-scale peperite is observed at some pillow margins. Sediment disruption is localised, likely as a result of localised variations in sedimentary properties, such as cohesion, consolidation, saturation (pore-fluid) and grain size.

## Chapter 6: St. Cyrus, Scotland, UK

### 6.1 Introduction

A series of intercalated basaltic lavas and sedimentary rocks are exposed at St. Cyrus, Angus, located on the east coast of Scotland, south of Aberdeen (Figure 6-1). The ~120 m thick succession represents the Montrose Volcanic Formation of the Arbuthnott Group of Lower Devonian age, part of the Lower Old Red Sandstone (ORS) depositional sequence in the Midland Valley of Scotland (MVS) (Bluck 2000; Browne et al. 2002). The succession records the intricate interactions between lava, sediment and water, from which a series of variable processes and products are characterised.

Five types of mixed lava-sedimentary domains are identified, each of which record localised changes and variability in sedimentary properties at the time of lava emplacement. These are: i) sedimentary inclusions within lava, indicating passive interaction with partially consolidated, dry to semi-saturated sediment; ii) isolated lava lobes, indicating passive interaction with partially consolidated sediment; iii) isolated sedimentary units with localised peperite, indicating passive interaction with unconsolidated to partially consolidated, semi-saturated sediment; iv) stacked lava lobes with sediment layers, indicating passive emplacement of lava into unconsolidated sediment and; v) peperite, indicating aggressive and dynamic interaction of lava with unconsolidated, saturated sediment.

The mixed lava-sedimentary domains demonstrate the complex relationship between volcanic and sedimentary drainage systems. The lavas most likely exploited fluvial channels during emplacement, whilst the drainage system recovered and fluvial channels re-established during volcanic hiatuses. This study provides evidence that localised variations in sedimentary and lava properties (e.g. sediment cohesion, saturation and lava effusion rates), influence the style and morphology of the processes and products of lava-water-sediment interaction.

## 6.2 Geological Setting

St. Cyrus, Angus, is located on the east coast of Scotland, south of Aberdeen (Figure 6-1). It lies within the northern part of the Midland Valley of Scotland (MVS) (Figure 6-1), which is dominated by Old Red Sandstone (ORS) rocks. Sedimentation and deposition of ORS strata occurred during the Late Silurian to early Carboniferous, on the newly formed continent of Laurentia. An unconformity, during the Devonian, separates the Lower from the Upper ORS sequences (Figure 6-2) (Bluck 2000; Browne et al. 2002; Woodcock and Strachan 2008), and represents a period of Mid-Devonian uplift, which led to large scale topographic changes (Woodcock and Strachan 2008). Within the MVS, ORS strata are preserved within two depositional centres, the Strathmore Basin and the Lanark Basin, the axes of which run parallel to the Highland Boundary and Southern Uplands faults (Figure 6-1).

The ORS succession is characterised by terrestrial fluvial conglomerates intercalated with volcanic rocks at its base, and fluvial and alluvial fan sandstones and mudstones at its top (Bluck 2000; Browne et al. 2002; Woodcock and Strachan 2008; Hole et al. 2013). The lithostratigraphy of the MVS during ORS deposition is presented in Figure 6-2. Sediment was derived from local sources along both the northern and southern flanks of the Strathmore Basin (Haughton 1989; Bluck 2000; Trewin and Thirlwall 2002), as well as through the reworking of contemporaneous volcanic material (Hole et al. 2013). Volcanism within the MVS comprises basalt and basaltic andesite lavas (Thirlwall 1981, 1982; Woodcock and Strachan 2008), erupted from a chain of volcanoes situated in the central MVS along the axis of the Ayr-Ochil-Sidlaw Anticline (north-east to south-west). Eruptions from the various centres took place over a period of 15 My during the Early Devonian (Trewin and Thirlwall 2002).

The intercalated lava-sediment succession at St. Cyrus belongs to the Montrose Volcanic Formation of the Arbuthnott Group (Figure 6-1 and Figure 6-2) of the Lower ORS. The Arbuthnott Group comprises ~2000 m of conglomerates and sandstones that grade into sandstones and shale towards the south (Bluck 2000; Browne et al. 2002). The lavas of the Montrose Volcanic Formation comprise basalt and basaltic andesite erupted from the northern flank of the Montrose Volcanic Centre (Armstrong and Paterson 1970; Trewin and Thirlwall 2002; Woodcock and Strachan 2008). The Upper ORS is faulted against the Lower ORS to the north of St. Cyrus.

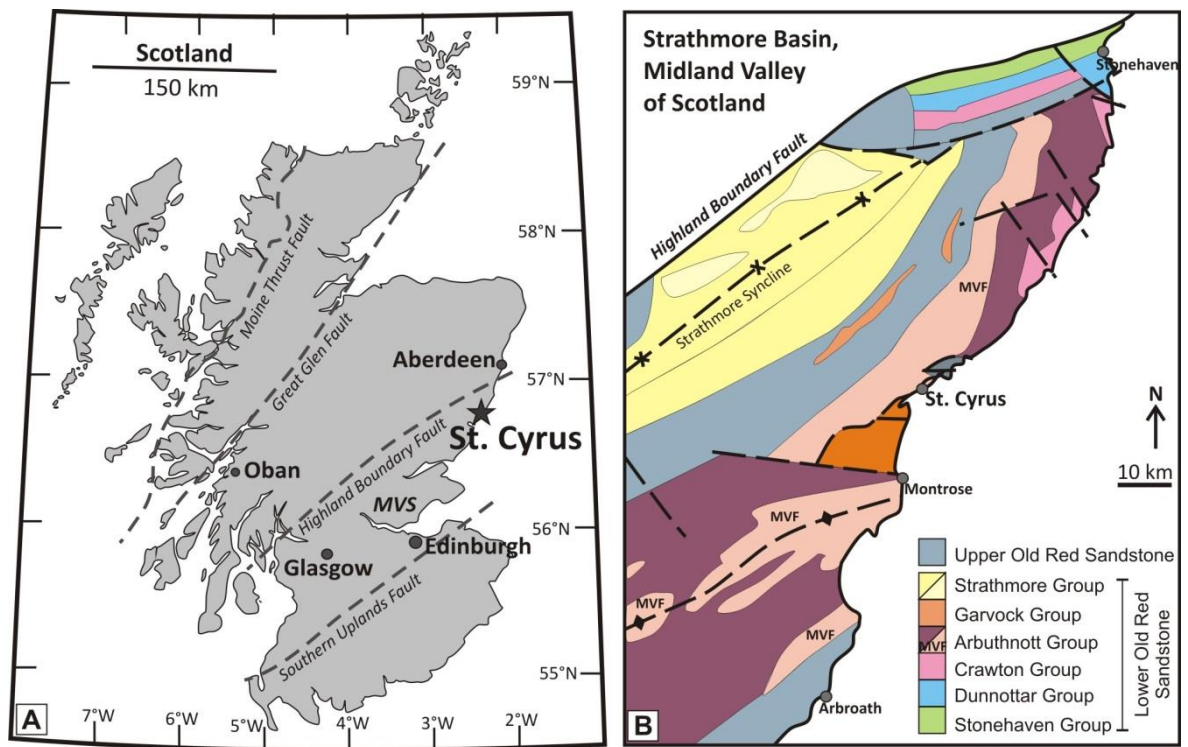


**Figure 6-1: A) Location map of St. Cyrus, and the Midland Valley of Scotland (MVS) (adapted from Macdonald and Fettes 2007). B) Regional geological map of the Strathmore Basin, north east MVS (adapted from Haughton 1989; Browne et al. 2002; Hole et al. 2013).**

**MVF= Montrose Volcanic Formation (faded pink), part of the Arbutthott Group.**

Period	Epoch	Stage	Lithostratigraphic Classification		
			Groups		
DEVONIAN	UPPER	Famennian	Stratheden Group		Upper Old Red Sandstone
		Frasnian			
	MIDDLE	Givetian	<i>Unconformity</i>		
		Eifelian			
	LOWER	Emsian	Strathmore Group	Lanark Group (southern MVS)	Lower Old Red Sandstone
		Pragian	Garvock Group		
		LOCHKAVIAN	MVF		
			Crawton Group		
SILURIAN	PERIDOLI	Pridolian - Wenlockian	Dunnottar Group		
	LUDLOW		Stonehaven Group		
	WENLOCK				

**Figure 6-2: Lithostratigraphy of the Midland Valley of Scotland (MVS) during Old Red Sandstone deposition of the Silurian and Devonian (Browne et al. 2002; Hole et al. 2013). MVF: Montrose Volcanic Formation.**

---

## 6.3 Field Relationships

The field area is situated at the north of St. Cyrus beach, Angus (Figure 6-1), covering an ~1.5 km coastal stretch. The main field localities, shown in Figure 6-3, are detailed in a series of annotated panoramas (Figure 6-4 and Figure 6-5). The succession is dominated by sub-aerial lavas, siliciclastic sedimentary units, and mixed lava-sedimentary domains; the various lithofacies are detailed below.

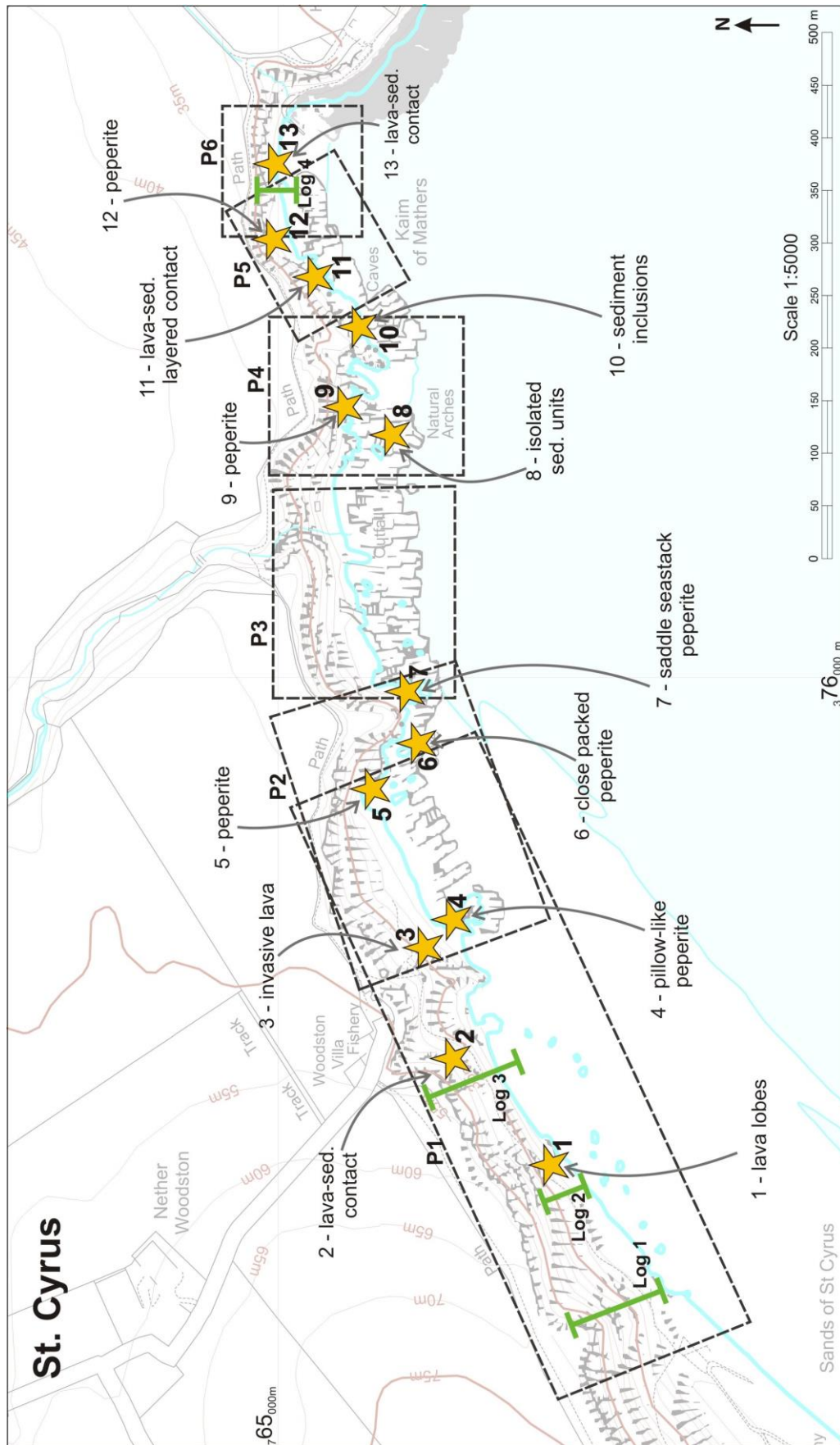


Figure 6-3: Map of the St. Cyrus succession, detailing the locations of the panorama photographs (P1-6). Yellow stars (\*) denote key outcrop locations and green bars are locations of sedimentary logs, referred to in the text.

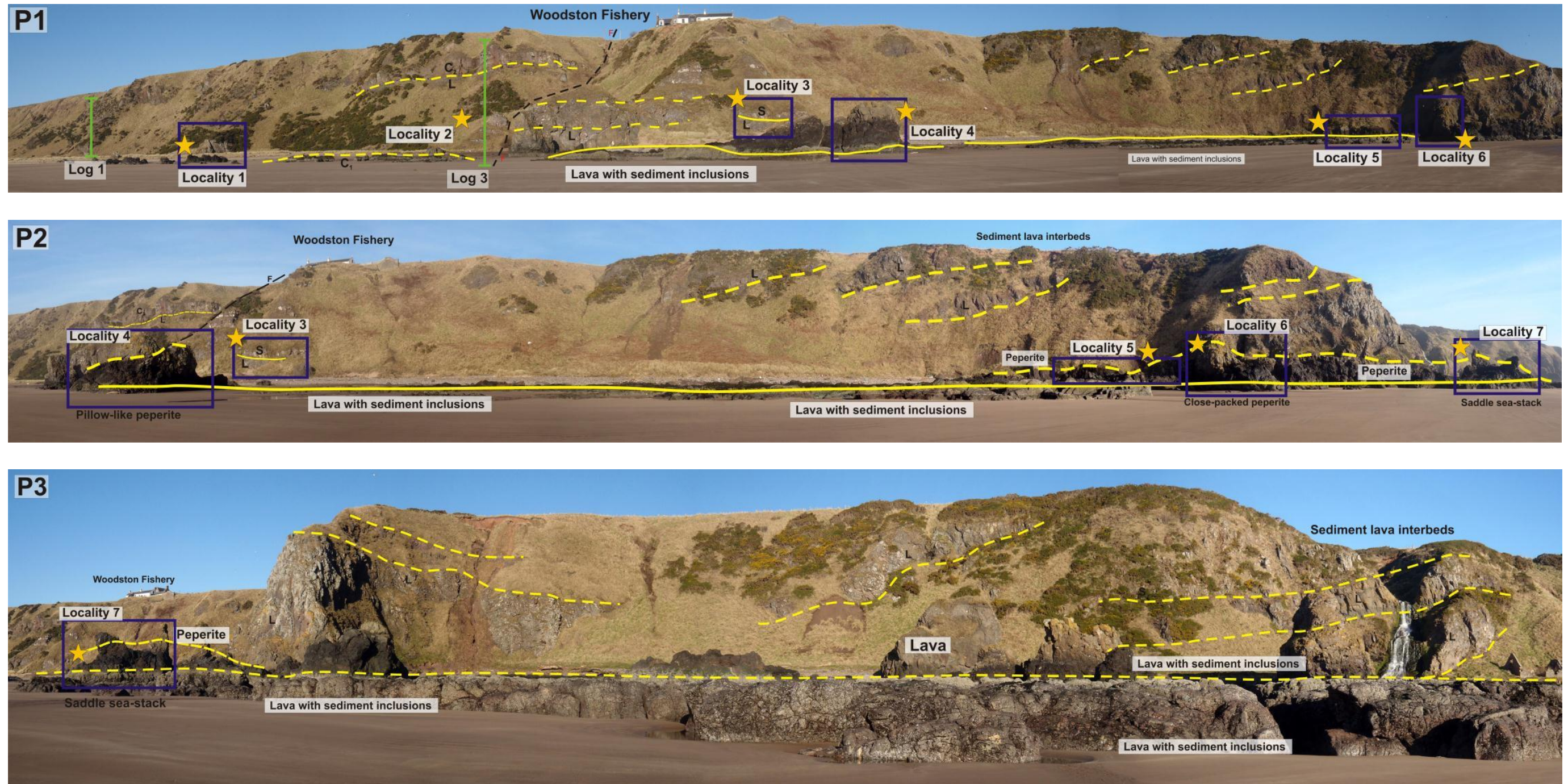


Figure 6-4: Panoramas, P1, P2, and P3 (see Figure 6-3), of the western part of the field area at St. Cyrus Beach. Locality numbers are referred to in text. The images show the larger scale geology of the field area, which is dominated by pahoehoe lavas, interbedded with sandstone and conglomerate sedimentary units. Many of the lavas show interaction with the sediment, e.g. peperite.





**Figure 6-5: Panoramas of the northern part of the field area at St. Cyrus (P4-7).** Locality numbers are referred to in text. The images show the larger scale geology of the field area, which is dominated by pahoehoe lavas, interbedded with sandstone and conglomerate sedimentary units. Many of the lavas show interaction with the sediment (e.g. peperite).

### 6.3.1 Lavas

The lavas at St. Cyrus are reddish-brown to dark grey, prismatic jointed, basalts and basaltic andesite (Figure 6-6). Petrographic analysis shows the lavas range from aphyric to plagioclase micro-porphyrific, with phenocrysts <1 cm across (Figure 6-6.A). The lavas are typically amygdaloidal (and vesicular), with amygdales, 0.3 cm to 2 cm across, of calcite, chlorite and quartz (Figure 6-6.B). Pipe amygdales, 2-8 cm long, are found at the base of some lava (and indicate a NE-SW palaeoflow direction). Vesicular layers, ~<2 cm thick, are also present, spaced between massive aphyric lava (Figure 6-6.C). Lava with small-scale (cm) ropey textures (Figure 6-6.D), typical of pahoehoe type lava, is observed. The majority of the lavas contain sedimentary clasts or inclusions, which are discussed below in Section 6.3.3.1. Peperite occurs at the margins of, and between, many of the lavas, and these domains are also discussed below (6.3.3.4). Hyaloclastite and pillows are not observed.

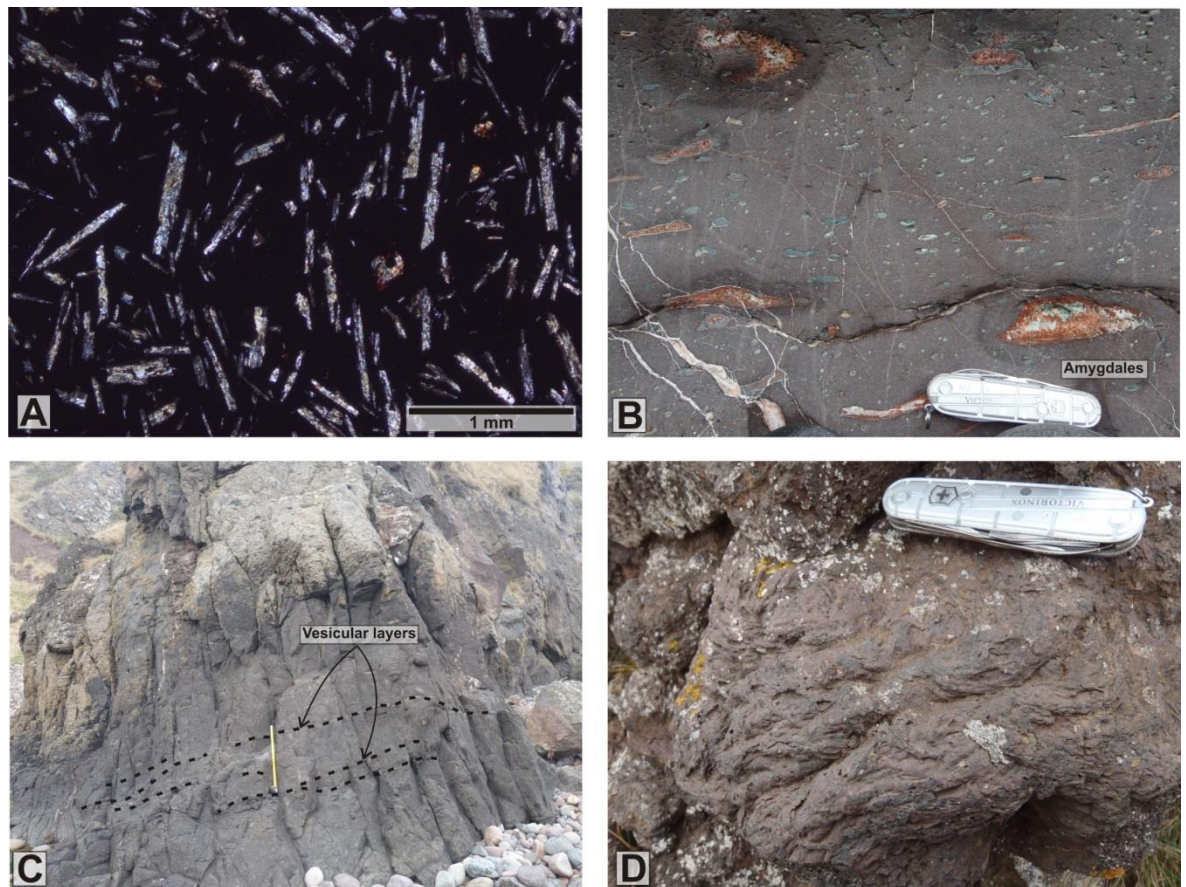


**Figure 6-6: Features of the lava at St. Cyrus.**

**A)** Photomicrograph of basaltic andesite lava, showing microphenocrysts of plagioclase feldspar within a glassy groundmass. **B)** Typical basalt lava with amygdales of chlorite and calcite. Pen knife is ~8 cm. **C)** Massive, prismatic jointed, basalt andesite lava, with vesicular intervals. Yellow tape measure is 50 cm. **D)** Small-scale ropey textures of the top surface of a lava, typical of pahoehoe type lava flow.

---

### 6.3.2 Sedimentary Units

The sedimentary rocks at St. Cyrus comprise various conglomerates, sandstones, and siltstones, which are typically laterally discontinuous. Conglomerate units dominate the base and top of the sequence whereas finely laminated siltstone and sandstone units are interbedded with the lava in the middle part of the sequence. Those units interbedded with the lavas typically display lensoid geometries. Contacts between the lavas and sedimentary rocks range from planar to irregular.

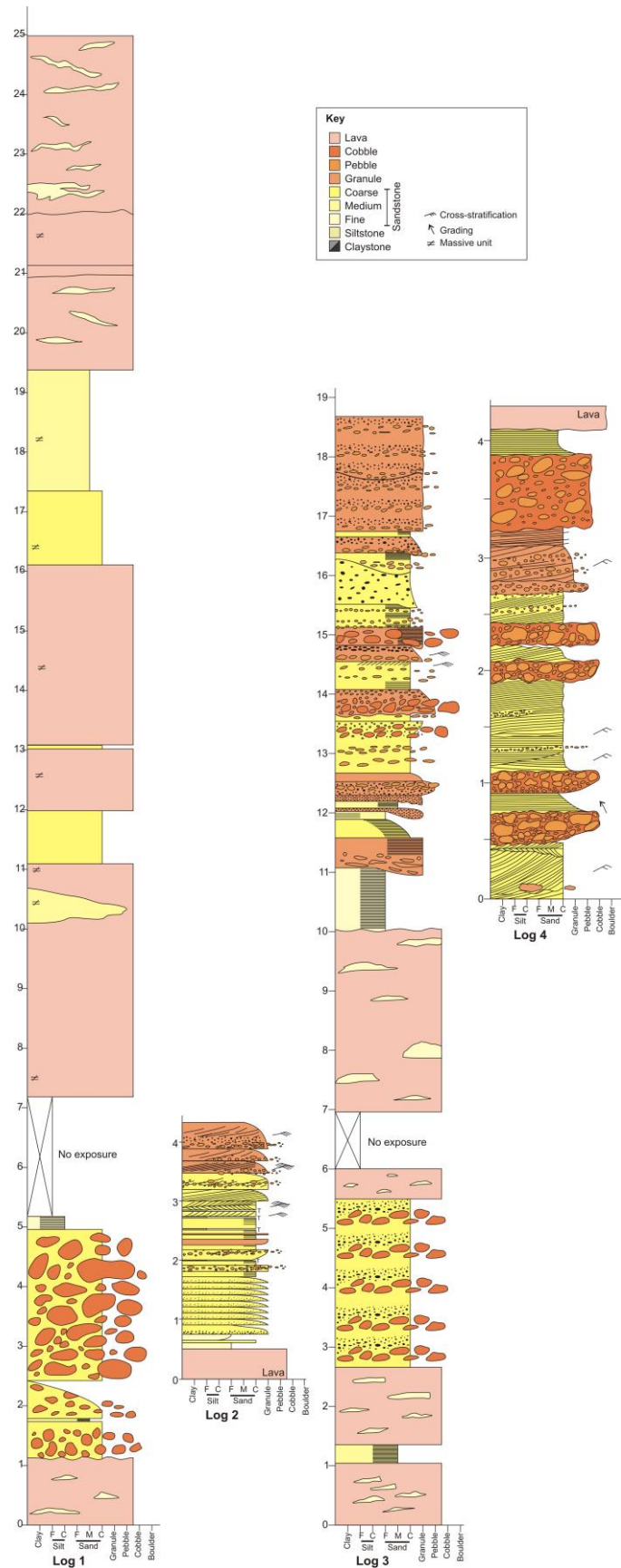


**Figure 6-7: Representative sedimentary logs at St. Cyrus (locations on Figure 6-3). Log 1) Sketch log through the succession in the west of the section. Log 2) Sedimentary units at Locality 1 mostly comprise coarse sandstone units with granular beds and thin interbedded tuff beds (<1 cm thick). Log 3) The lava-sedimentary succession at Locality 2 is dominated by lavas in the lower portion, and by sedimentary units in the upper portion. Log 4) Sedimentary log through the conglomerate unit at Locality 13 (Panorama 5 and 6, Figure 6-5).**

### 6.3.2.1 Conglomerate

Conglomerates are observed in both the east and west sections at St. Cyrus, at Localities 2 and 13 (Figure 6-3 and Figure 6-8). The reddish brown conglomerates comprise pebbles and cobbles within a coarse sand and granule grade matrix. The cobbles are well rounded, typically range from 8-15 cm across, and are of a range of volcanic lithologies including basalt and basaltic andesite (Figure 6-8 A). Beds of well rounded, <2 cm, pebbles within a coarse-grained sandstone matrix are also present.

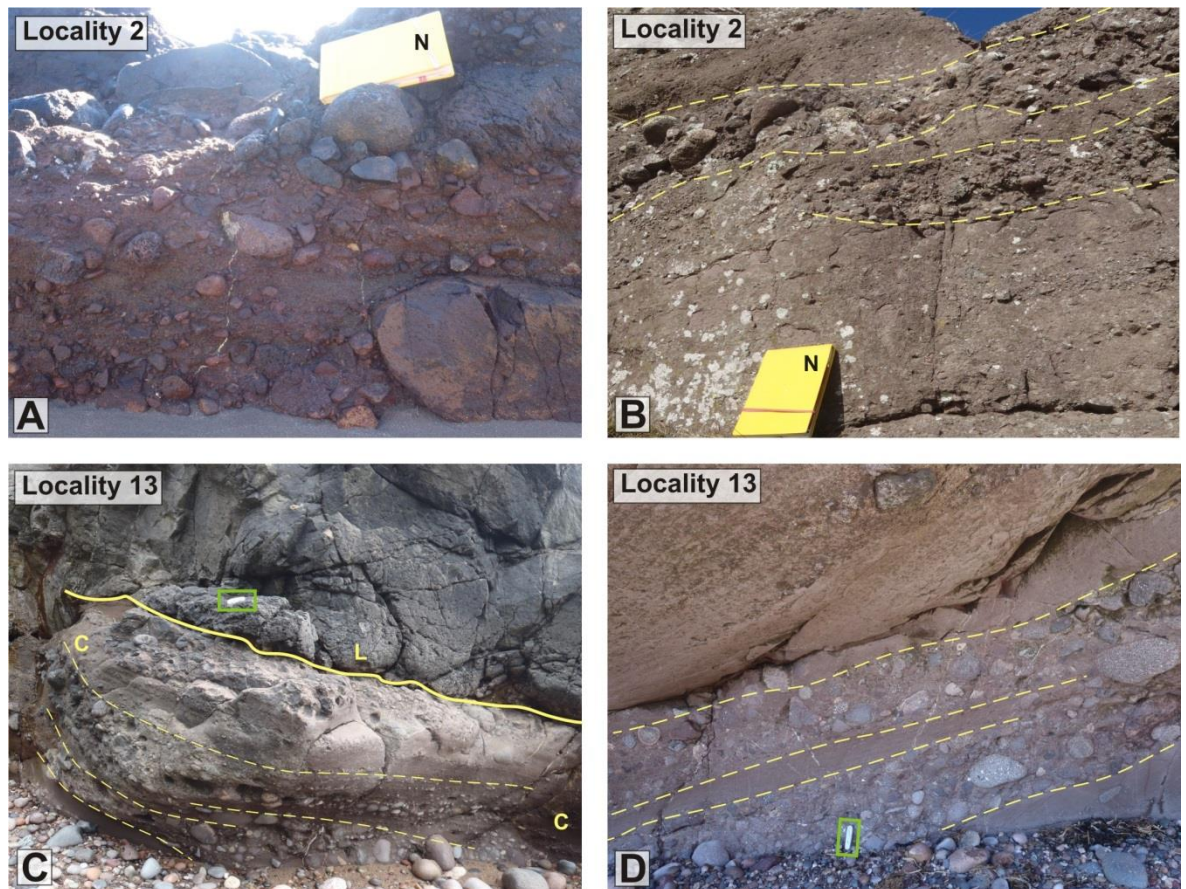


**Figure 6-8: Conglomerates at St. Cyrus.**

**A) Lower conglomerate unit at Locality 2, Log 3, comprising poorly sorted sub-rounded to rounded clasts. B) Upper conglomerate unit that caps the sequence at Locality 2 (C<sub>3</sub>), Log 3. C) The lava-sedimentary contact at Locality 13. Here the lava (L) directly overlies the conglomerate (C) units, having invaded the overlying sandstone units (not seen). D) The lower part of the conglomerate unit at Locality 13 where pebbles and cobbles form distinct packages with erosional contacts. Yellow notebook (N) in A and B is 20 cm long; pen knife (green box) in C and D is ~ 8 cm long.**

The conglomerate unit, C<sub>3</sub>, that caps the sequence at Locality 2 (Figure 6-9) unconformably overlies lava, and comprises coarse-grained sandstone that grades upwards into beds of granule- and cobble-grade conglomerate (Figure 6-7.3, Figure 6-9).

At the base of the upper conglomerate unit, at 10 m in Log 3 (Figure 6-7.3), a fine-medium grained sandstone, directly overlying the lava, is planar laminated and ranges in thickness laterally from 15-35 cm. Locally, the lava-sediment contact is irregular (Figure 6-10), and the sediment colour changes from red to pale green (this may be a 'baked' contact). The lava has sedimentary inclusions (xenoliths) within it, and the sediment contains small (possibly juvenile) lava clasts at the contact (Figure 6-10). Above this contact and the fine-medium sandstone, there is a ~ 5 cm thick coarse-grained sandstone, which has mm to cm thick pale beds of fine silt grade material that is possibly tuffaceous. This is overlain by red, finely laminated fine-grained sandstone. The remainder of the logged section comprises granule, pebble and cobble-rich conglomerates (Figure 6-7.3).

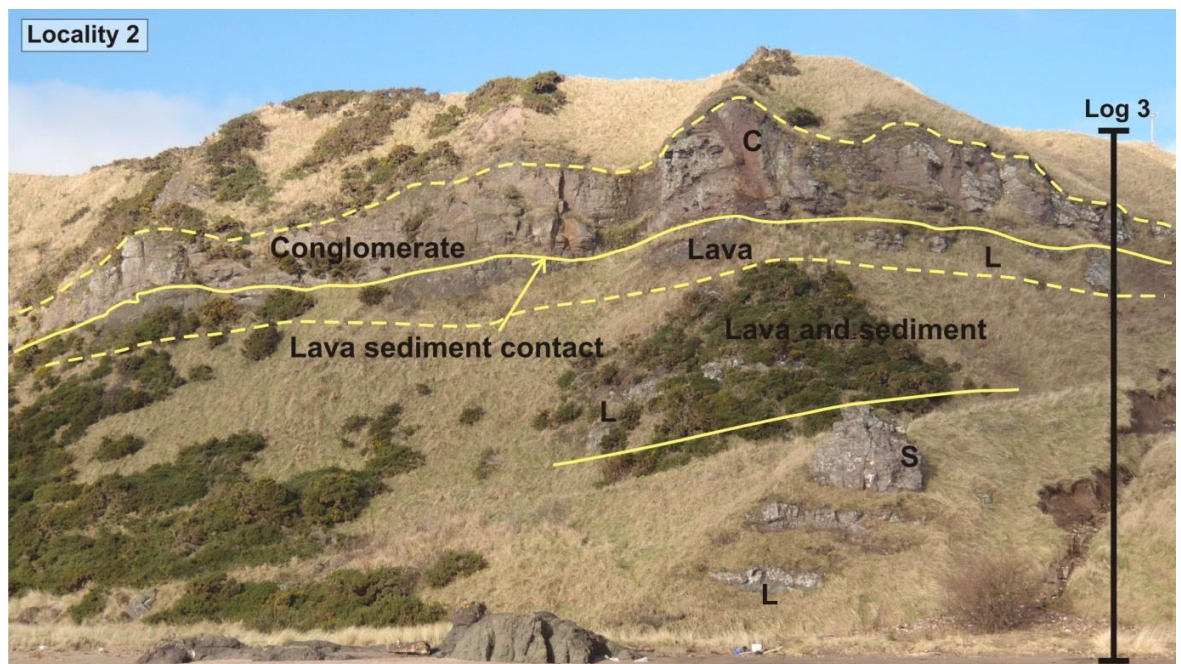


**Figure 6-9: Cliff section, Locality 2 (P1, Figure 6-4) and location of Log 3 (Figure 6-7). Log cuts through the interbedded lavas (L) and sedimentary units (S); conglomerate (C) caps the succession.**

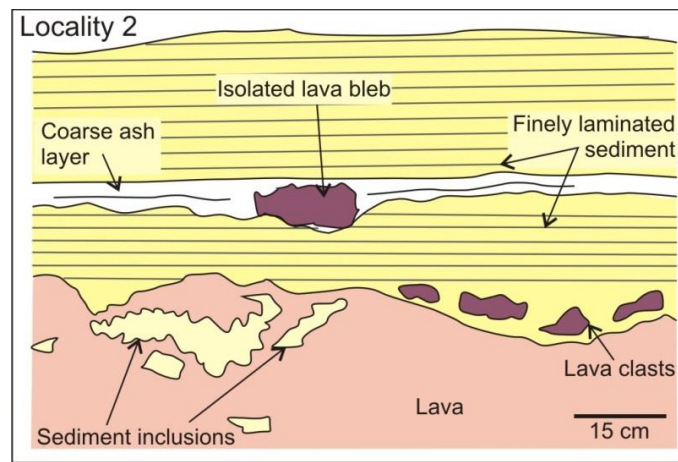


**Figure 6-10: Sketch of the lava-sedimentary contact at the top of Log 3, Locality 2 (Figure 6-3).**

**Sedimentary inclusions (xenoliths) are present within the lava, and clasts of lava occur within the sedimentary units.**

The conglomerate unit at Locality 13 (Figure 6-4) comprises granule- and pebble-grade conglomerate interbedded with laminated fine to coarse sandstone, and is overlain by lava (Figure 6-5 and Figure 6-7.4). The conglomerate comprises multiple distinct pebble- and cobble-rich packages, typically with erosional bases, and with coarse sand and granule grade matrices (Figure 6-8). Most packages show cross stratification, commonly tabular cross-lamination, although herringbone cross bedding is also present at the base of the unit. The pebbles and cobbles are poorly sorted, sub-rounded to rounded, 2-20 cm across, and comprise basalt and basaltic andesite. They are typically aligned along their long axis (SW) but do not show imbrication. A 25-40 cm thick finely laminated coarse sandstone caps the conglomerate (Figure 6-7.4). The unit is overlain by lava and locally has a direct contact with the conglomerate. Peperite is locally preserved (discussed in Section 6.3.3.5).

### 6.3.2.2 Sandstone and siltstone

The sandstones and siltstones in the St. Cyrus sequence are typically red and locally interbedded with the lavas (Figure 6-11 and Figure 6-12). They range from fine siltstone to coarse sandstone and are planar to ripple laminated with some intervals displaying small (cm scale) cross-laminae. At Locality 1 (Figure 6-3 and Figure 6-4), a fine grained red sandstone is cross-cut by lava (Figure 6-11). Desiccation cracks are present in a ~20 cm thick, finely bedded, fine siltstone and sandstone bed (Figure 6-11). Fine sandstone beds overlying this, grade upward over 3 m into interbedded medium-coarse sandstone and granule conglomerate, with uncommon pebble beds (Figure 6-7.2). Pebbles, 3- 5 cm across, are sub-rounded and rounded. Bed thickness ranges from 4-20 cm. Several of the coarse sandstone and gravel conglomerate units are cross-

bedded, including ripple laminations and herringbone cross-bedding. At Locality 13 (Figure 6-3 and Figure 6-5), the sedimentary units at the base of the conglomerate, contain small igneous clasts (Figure 6-13). The igneous clasts are sub-rounded and lenticular, <3 cm, and are held within a volcanic-dominated siltstone and sandstone unit. This unit is overlain by siltstone, sandstone and conglomerate units, detailed above (Section 6.3.2.1). Petrographically, the siltstone and sandstone units are quartz dominated, with some volcanoclastic material (Figure 6-12). There are slight differences between red and green sedimentary inclusions, however, this is predominantly colour change and in some cases grain size, rather than composition.

The majority of sandstone and siltstone units are found in association with the lavas and form complex lava-sedimentary domains, described below (Section 6.3.3).

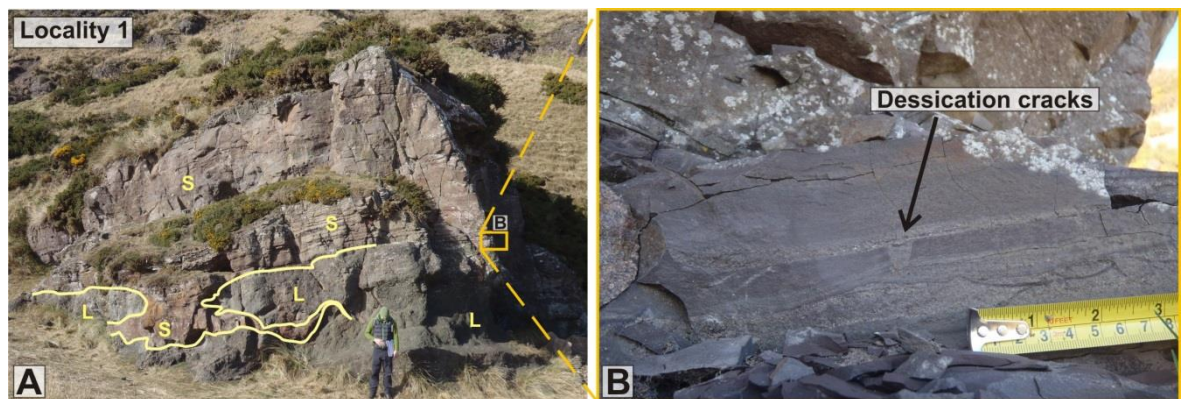


**Figure 6-11: The lava-sedimentary relationship at Locality 1 (Figure 6-4).**  
**A)** fluvial lacustrine sandstones/siltstones (S) are interdigitated with lava (L). Inset shows location of B. Person for scale. **B)** Desiccation/mud cracks within siltstone and sandstone beds above the lava. Mud cracks (<1 cm thick) are indicative of the wet environment drying out, and then later being covered by coarse sandstone and gravel deposits during flooding events.

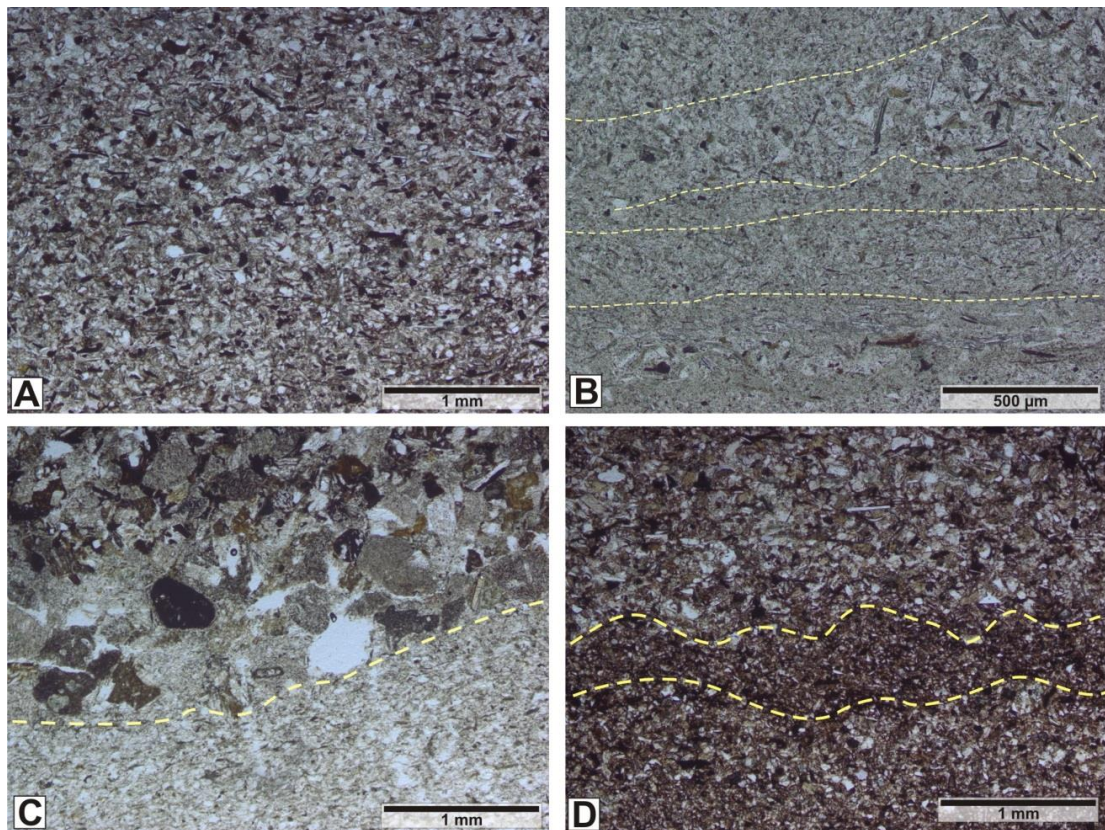


**Figure 6-12:** Photomicrographs of typical sandstone and siltstone units observed at St. Cyrus.

All PPL. A) Red fine-grained siltstone litharenite, typical of the sedimentary units and red sedimentary inclusions. Locality 8, sample SC.063.B. B) Green siltstone sediment inclusion, preserved within a peperite domain. The siltstone has retained some lamination between fine and coarser laminae. Locality 9, sample SC.058. C) Contact between a coarser sandstone and finer, green, siltstone. Locality 1, log 2, sample SC.051. D) Red fine sandstone from the base of the siltstone-sandstone unit at Locality 1. Fine-scale grading is observed. Locality 1, sample SC.053.



**Figure 6-13:** The base of the sedimentary section at Locality 13.

Sedimentary beds comprise fine-grained red siltstone and sandstone with packages of reworked igneous clasts. Lava blebs are detached from an invasive, lava body. Yellow tape measure is 50 cm long.

### 6.3.3 Mixed lava-sedimentary domains

Complex relationships between lavas and sedimentary units occur throughout the succession at St. Cyrus. The features and facies observed at lava-sedimentary contacts may be regarded collectively as “mixed lava-sedimentary domains”; however, the variability between them demands individual descriptions. The key features observed, described below, are: 1) sedimentary inclusions within lava; 2) isolated lava lobes; 3) isolated sedimentary units; 4) stacked lava lobes with sediment, and 5) peperite, which is also sub-divided (see below).

#### 6.3.3.1 Sedimentary inclusions within lava

Sedimentary inclusions are a common feature of the lavas at St. Cyrus (Figure 6-14). They are highly variable in size and shape, ranging from mm to m (horizontally and vertically orientated), and from small, curvilinear lenses to larger sub-angular, coherent blocks (Figure 6-14). Lensoid inclusions are typically small, <20 cm across, whereas larger blocks can be up to 1 m in length, and have deformed margins (Figure 6-14C). The inclusions are typically randomly dispersed throughout the lava, and both small lenses and large blocks are observed together. Inclusions comprise red and green, fine to medium sandstone and siltstone. Fine, planar, laminae are commonly seen in larger coherent block-like inclusions, but typically not in smaller lenses. At Locality 5 (Figure 6-3 and Figure 6-4) closely packed similarly oriented inclusions are preserved. The fine laminae can be “traced” from inclusion to inclusion, indicative of a remnant stratigraphy.

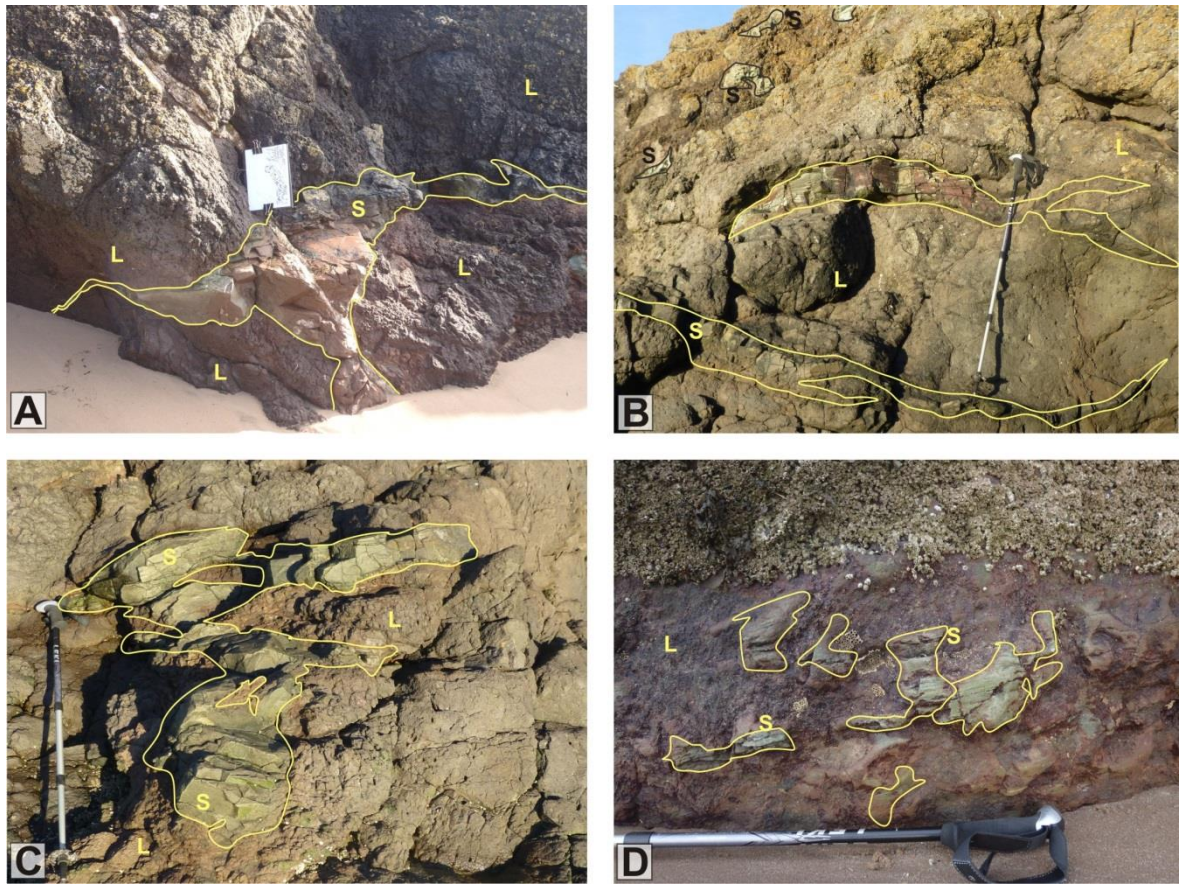


**Figure 6-14: Sediment inclusions (S) within the lava (L) at St. Cyrus.**

**A) A large sedimentary inclusion within the lava. The large, central portion contains sedimentary laminations and bedding. The edges are fluidal and taper into lenticular lenses in the lava. White map board is A4 (~30 cm long). B) Lenticular sediment inclusions within lava. Walking pole is ~1 m. C) A blocky sedimentary inclusion (S yellow outline) within lava. Walking pole is ~1 m. D) Small green sedimentary inclusions (S-yellow outline) are present within a lava and peperite domain. The inclusions show faint “remnant” stratigraphy that can be traced between the inclusions. Walking pole handle is ~10 cm long.**

Sedimentary inclusions are also associated with peperite domains, where coherent inclusions are observed within the host sediment matrix alongside juvenile lava clasts (see Section 6.3.3.5). At Locality 10 (Figure 6-3 and Figure 6-5) the lavas contain multiple sediment inclusions and peperite domains of varying size and shape (Figure 6-15). The sedimentary inclusions vary in size from 2 to 80 cm, and display irregular shapes, although in 2D most appear blocky. Also at this locality, amygdales comprise red fine grained siltstone, which is petrographically similar to the sedimentary inclusions also found within the lava. Locality 10 is complex, with boundaries between lavas difficult to determine. As is shown in the sketch log (Figure 6-15) sedimentary inclusions are encased within the lava, and are associated with peperite domains. They are observed both within the peperite, as smaller <10 cm fragments, and as larger coherent inclusions at the edges of the peperite and lava contact.

Petrographical analysis of both red and green inclusions (Figure 6-12) indicates that they are of similar composition, comprising litharenites with sub-rounded grains of basalt, basaltic andesite and crystals, and that their colour is likely an artefact of weathering. Red inclusions are slightly coarser and contain red, Fe-rich material; whereas green inclusions typically comprise finer sedimentary material (likely with more chlorite - weathering green).

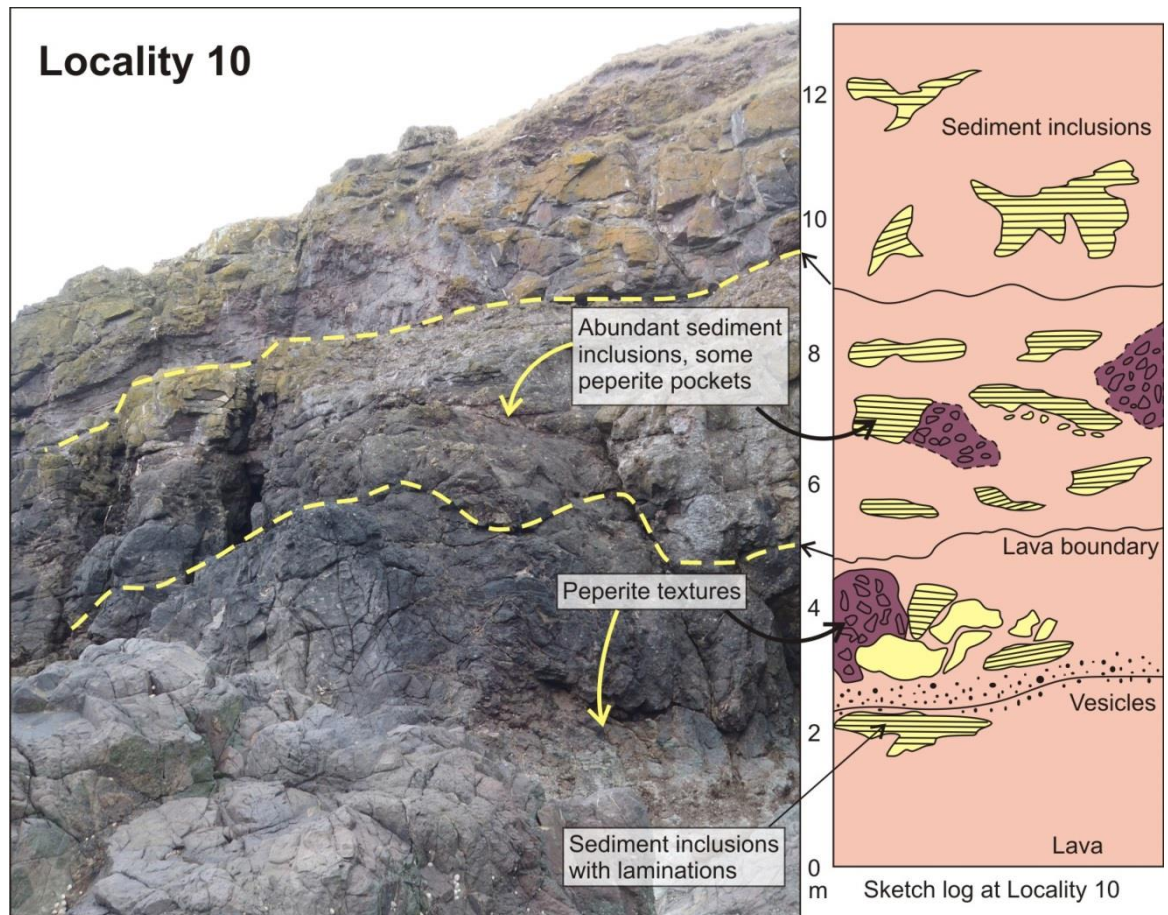


**Figure 6-15: Field view and sketch log at Locality 10.**

The lava (pale pink) is intermingled with peperite domains (purple) and coherent sediment inclusions (yellow) of varying sizes and shapes. Exposure is ~12 m high.

### 6.3.3.2 Isolated lava lobes

At Locality 1 (Figure 6-4) basal lava and lava 'toes' (the edges or tip of a flow lobe) interdigitate with finely laminated, red-weathered, fine to medium sandstone (Figure 6-16). The sandstone forms long (<1 m) lenticular tendrils away from the main central sedimentary body, which are deformed around the lava toes and pinch out. In these deformed lenses, the sediment has no lamination or internal structure. At the base of the sandstone body, there is peperite (Figure 6-16), with lava clasts supported within

the red host sediment. Small scale, minor mingling has occurred in places along the upper and lower margins of the lava lobes. The lava lobes are overlain by a thin layer of sediment that is correlated to the central sandstone body between the lava lobes (S, Figure 6-16). This is overlain by ~20 cm of finely bedded, fine sandstone and siltstone, in which desiccation cracks are present (Figure 6-11 A and B).

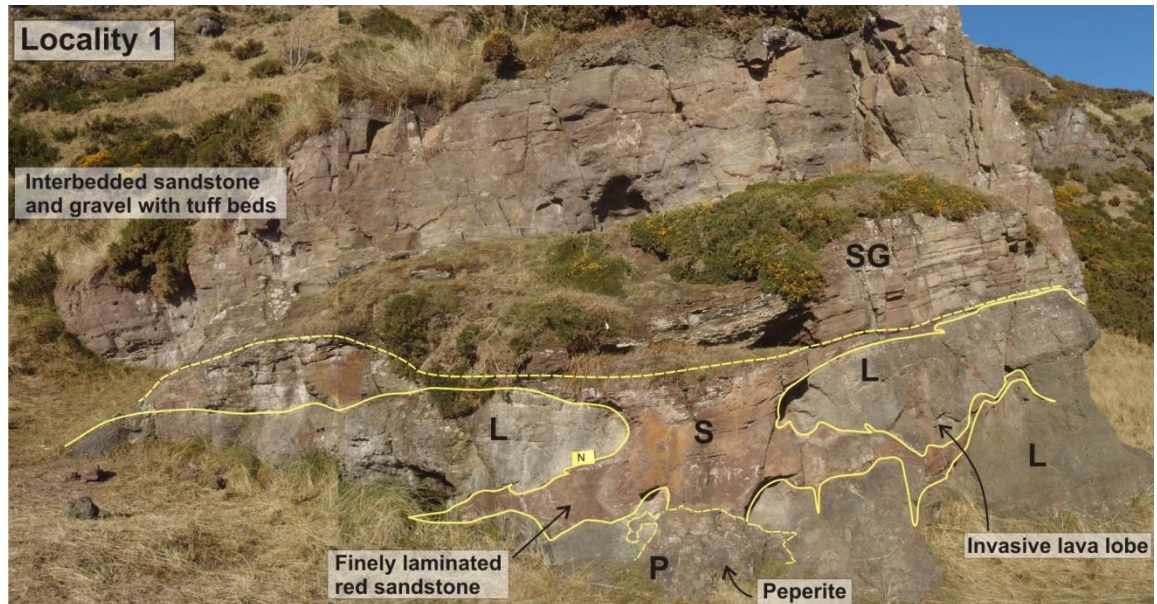


**Figure 6-16: Lava-sediment interaction at Locality 1 (P1 Figure 6-4).** Lava (L) lobes or toes are interdigitated with a unit of finely laminated lacustrine sandstone (S). Small-scale peperite (P) is observed at the lava-sedimentary contact. The lavas have invaded into the underlying sediment causing the lenticular wisps of sediment to deform against the lava, and peperite to form. The overlying unit comprises interbedded sandstone and gravel beds (SG). Yellow notebook (N) is ~20 cm.

### 6.3.3.3 Isolated sedimentary units with localised peperite

There are several individual, massive sandstone units, interbedded with the lavas at Locality 9 (Figure 6-5). These units of fine-grained sandstone range in thickness from 20-30 cm (Figure 6-17) and are typically finely laminated. At their upper and lower margins, in contact with lava, peperite has developed, and the sandstone units lose their internal structure. The peperite domains, 0.5-1.5 m thick, comprise globular to amoeboid clasts of basalt, 1-12 cm across, within a fine sandstone matrix. 'Pods' and interconnected lobes, rather than continuous lateral sheets across the sandstone unit, are present. At Locality 3, (Figure 6-4), a red laminated, medium to coarse sandstone unit is under- and overlain by a rubbly, vesicular lava that contains multiple green-weathered sedimentary inclusions. The lava-sedimentary contact is peperitic, with a 10-15 cm thick discontinuous peperite zone (Figure 6-18). Lava clasts are ~2-10 cm across and are hosted within a red sandstone matrix.

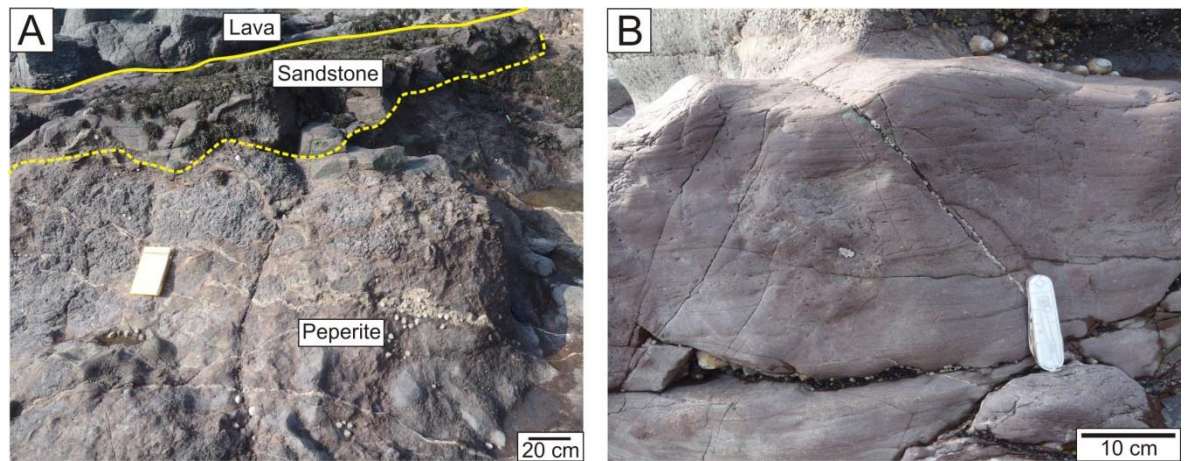


**Figure 6-17: Isolated sedimentary units (see Panorama 4) near Locality 9.**

**A) Relationship between an isolated sandstone unit and the overlying lava and underlying peperite. B) The sandstone units between the lavas are finely laminated and commonly the surrounding lava has interacted with their lower and upper parts.**

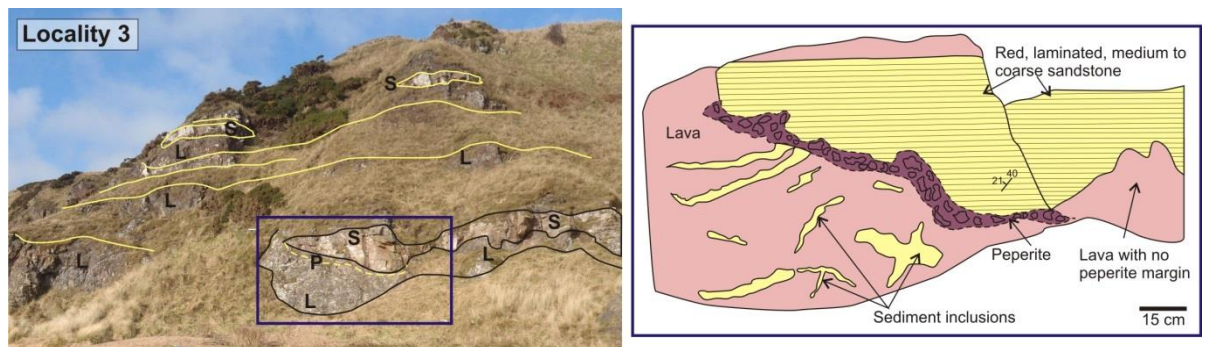


**Figure 6-18: Annotated field view and sketch of the lava-sedimentary contact at Locality 3. The lava has an upper peperitic margin with the overlying large sedimentary body, which indicates the lava was likely invasive.**

#### 6.3.3.4 Stacked lava lobes with sediment

At localities 7 and 12 (Figure 6-3 and Figure 6-5) there are a series of lava-sedimentary ‘layers’, ranging in length from 0.3 to 2 m long (Figure 6-19 and Figure 6-20). Vesicular basalt lava contains multiple discontinuous, sedimentary layers, typically 6 to 8 in a single locality, comprising red fine-grained siltstone and sandstone (Figure 6-19). The siltstone ‘layers’ are 0.5-3 cm thick, and display an irregular and fragmented contact with the lava 5- 10 cm thick (Figure 6-20). Micro-scale (mm) mingling, and rare larger coherent sediment inclusions (3-10 cm) (Figure 6-20), are preserved within the layers. Samples were taken systematically at Locality 12 (Figure 6-20) to understand the micro-scale relationship between the lava and sediment.

Petrographical analysis of the samples indicates vesicular basalt lava, typical of the field area, intercalated with red, fine grained siltstone litharenite. The siltstone comprises quartz grains and volcanic lithics, and is similar to the sedimentary units observed across the field area (Figure 6-12). The lava-sediment contacts are fluidal and peperitic, with juvenile lava clasts mingled with the host sediment (Figure 6-21). Juvenile lava clasts have irregular and fluidal morphologies (Figure 6-21), and micro-scale peperite is observed (Figure 6-21.C).

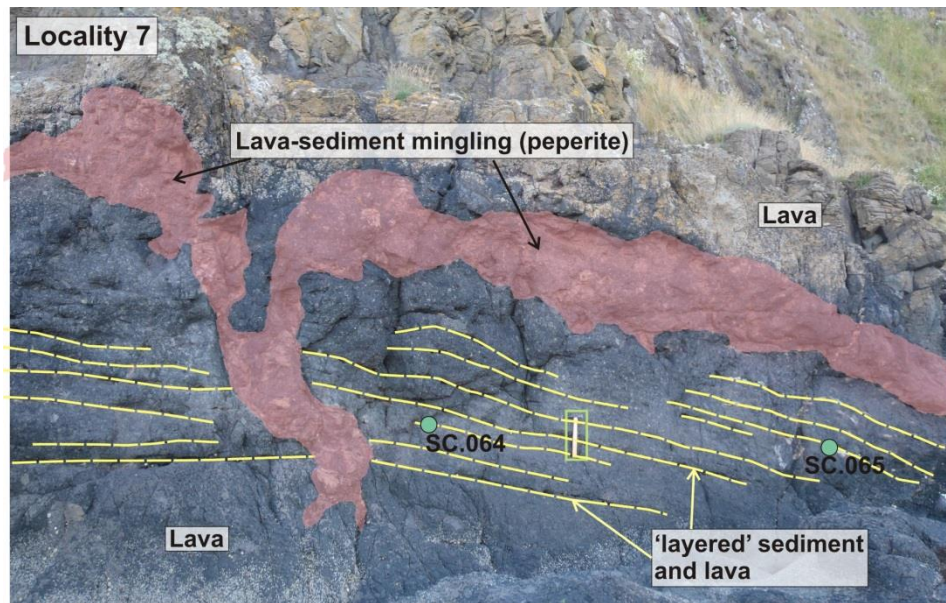


**Figure 6-19: Lava-sedimentary relationships at Locality 7 (Figure 6-3).** Rock hammer (green box) is ~35 cm long. Lava lobes are interbedded or “layered” with sediment (yellow dashed lines). Overlying this is a discontinuous peperite domain of mingled juvenile lava clasts and a sedimentary host matrix.

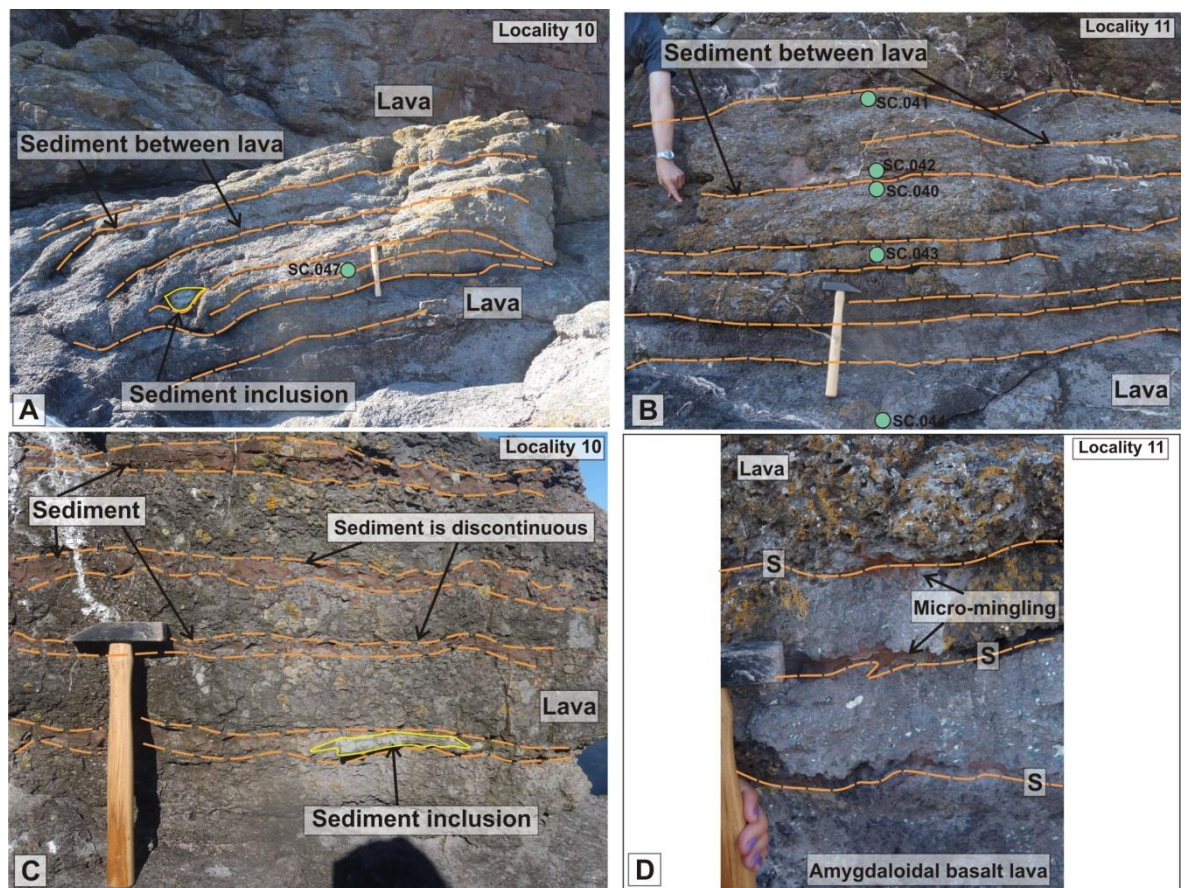


**Figure 6-20: Stacked lava lobes at Localities 10 and 11.**

**A) and B** Thin sedimentary layers (orange dashed lines) are found between thin, pahoehoe lava lobes at locality 10 and 11 (Green dots are samples). **C)** Close up of the interbedded lava-sediment layers which highlights the discontinuous nature of the sediment layers. A more coherent sediment inclusion (yellow outline) is also present within these layers. **D)** Close up of the stacked/incrementally emplaced lava and sediment layers. The lava is vesicular and amygdaloidal. Micro-scale lava-sediment mingling is observed at the contact. Rock hammer is ~35 cm long, and hammer head is 2.5 cm thick.

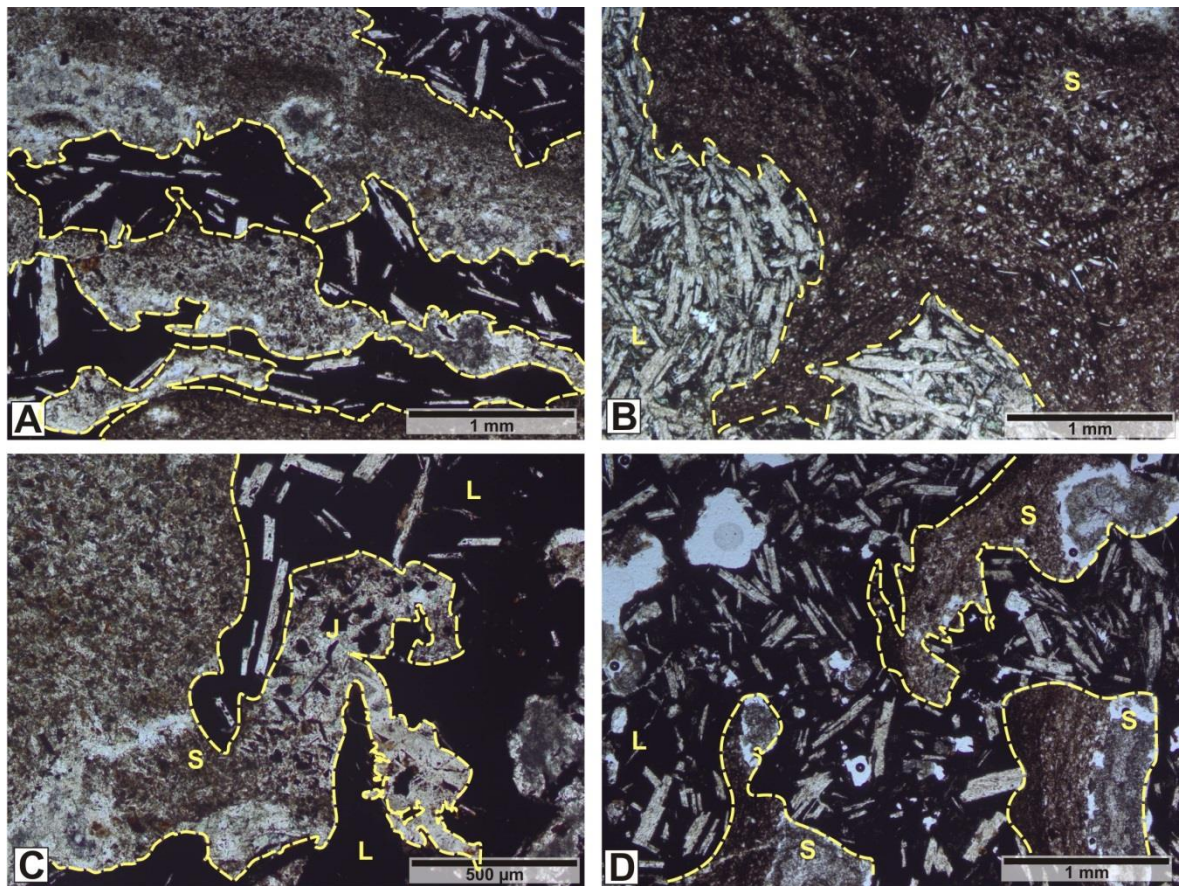


**Figure 6-21: Photomicrographs of the lava-sediment interface between stacked lava lobes and intercalated sediment layers.**

The samples show irregular fluidal and amoeboid geometries of the lava and sediment contact. All images PPL. A) Micro-scale layering of irregular and fluidal lava blebs and fine-grained red siltstone. Sample S.C045.A, Locality 11. B) Red-green, fine-grained sediment (S) intercalated with lava (L). The lava has a fluidal margin. Away from the lava margin, the sediment is vesiculated. Sample S.C064, taken from Locality 7. C) The intricate fluidal contact between invasive lava (L) and sediment (S). Micro-scale peperite is preserved as juvenile clasts (J) are detached from the main lava bleb (L) within the sediment (S). Sample S.C045.A, Locality 11. D) Sediment (S) also fills vesicles within the invasive lava (L), which appears to grade from dark to pale brown across the vesicle. Sample S.C045.B, Locality 11.

### 6.3.3.5 Peperite

In addition to minor peperite at the basal margins of lavas and invasive lobes (described above), a wide range of peperite morphologies are observed within the rock sequence at St. Cyrus, including: 1) close-packed 'regular' peperite; 2) 'pillow-like' peperite; and 3) 'rootless' peperite. Types 1-3 are defined here as 'dynamic peperite' and occurs in isolated pods and lobes, which are rarely interconnected, rather than forming discrete beds or sheets across the succession.

Characteristically, the peperite comprises juvenile basalt lava clasts, of differing size and shape, within a fine-grained, structureless, red to green siltstone and sandstone matrix. Juvenile clasts are vesicular and typically display mixed morphologies of fluidal with sub-planar margins, amoeboid and globular (Figure 6-22. B, C, D). Jigsaw fit textures are also present (Figure 6-22.D). Clasts range in size from mm to dm, but are typically 5-20 cm. These peperite morphologies tend to vary over a couple of metres, and all grade into lava.

The majority of the described peperite domains at St. Cyrus contain consolidated sedimentary inclusions in conjunction with lava clasts, within a sedimentary matrix (Figure 6-23). The coherent fine-grained siltstone and sandstone inclusions range in size from 6 to 20 cm, with larger blocks from 20 cm to 1.5 m. They are typically green, in contrast to the more typical red sedimentary matrix, with blocky to irregular shapes, in some cases distorted by the surrounding lava clasts. The inclusions are randomly dispersed within the peperite domains: some are abundant and well dispersed with the juvenile lava clasts, whereas other domains contain very few. Inclusions display fine laminae, which are distorted, especially at inclusion margins. Sedimentary inclusions within peperite are synonymous with those displayed and described within lava (Section 6.3.3.1).

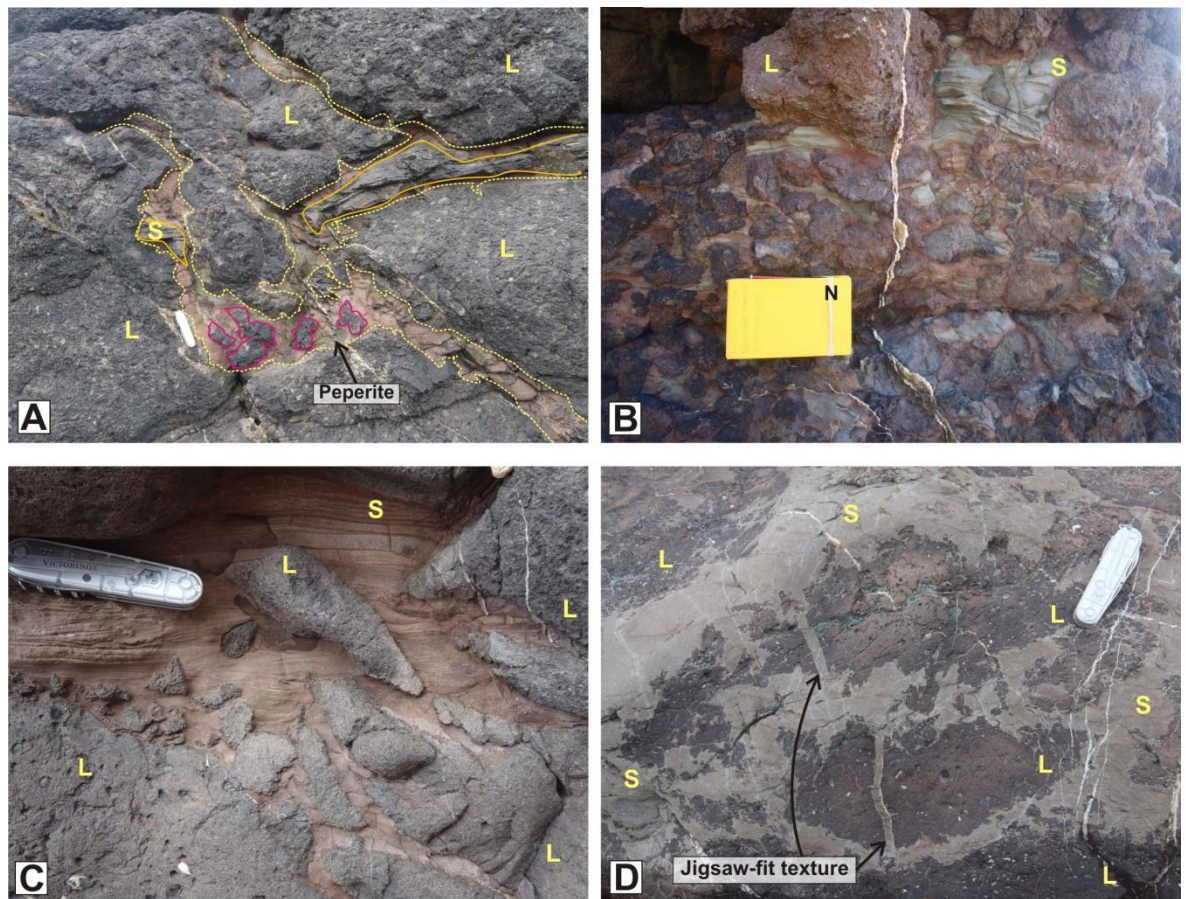


**Figure 6-22: Variations in peperite textures at St. Cyrus.**

**A)** A small peperite domain (dashed yellow outline) within lava (L). The peperite has a red sandstone matrix with juvenile basalt clasts (pink outline). Coherent sediment inclusions are also preserved (yellow outline, S). **B)** A peperite domain comprising evenly spaced, irregular, juvenile lava clasts within a red, fine-grained sandstone matrix. Green, blocky to irregular coherent sediment inclusions (S) are preserved. **C)** Peperite at locality 12. The lava (L) fingers into fine-grained, laminated, sandstone matrix (S), but laminae are lost around the juvenile clasts, due to fluidisation. The juvenile lava clasts are irregular to blocky and range in size from <1 cm to ~60 cm. **D)** Fluidal juvenile lava clasts (L) display jigsaw fit texture, within a fine grained sandstone matrix (S). Pen knife is ~8 cm long, and notebook (N) is ~20 cm long.

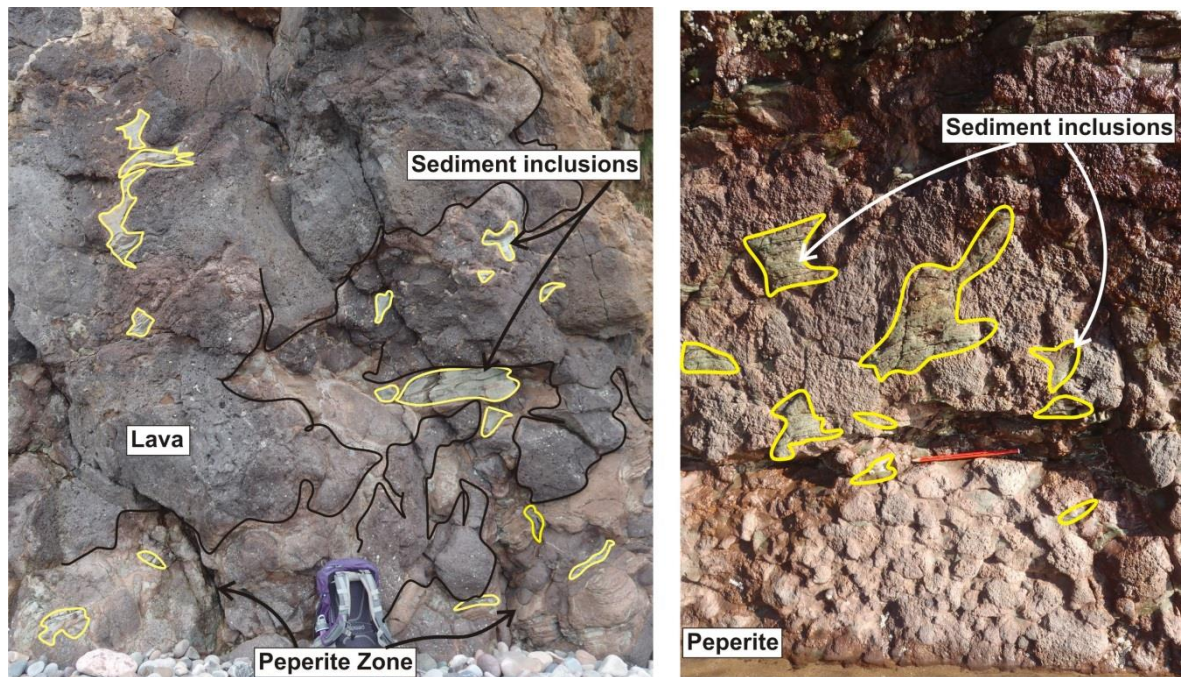


**Figure 6-23: Sediment inclusions within peperite domains are a common feature at St. Cyrus.**

**A) Locality 12, sedimentary inclusions, ~30-80 cm, of irregular, blocky and globular morphologies, mingled with juvenile lava clasts in a peperite domain. B) Sediment inclusions at Locality 5 are ~3-10 cm and typically display irregular –blocky morphologies. Rucksack is ~80 cm; pencil is ~15 cm long.**

### 1) Close-packed ‘regular’ peperite

Close-packed ‘regular’ peperite (Hanson and Wilson 1993) occurs at Locality 6 (Figure 6-4) where the peperite is well sorted with similarly sized and evenly spaced juvenile clasts (Figure 6-24). This is in contrast to other zones of peperite that are “poorly sorted” with randomly sized, shaped, and spaced clasts. Clasts range in size from 2 to 5 cm, are typically sub-rounded to rounded, and display globular and amoeboid morphologies. The sedimentary matrix is fine-grained red siltstone with little internal structure or laminations. Figure 6-24 illustrates how the clasts grade inward from the lava, into large, angular and irregular lava clasts (size and shape), towards the close-packed ‘regular’ peperite pod. Also within the peperite domain there are green, fine grained coherent sediment inclusions, 5-10 cm, that display blocky irregular shapes and are randomly dispersed by the surrounding lava clasts.

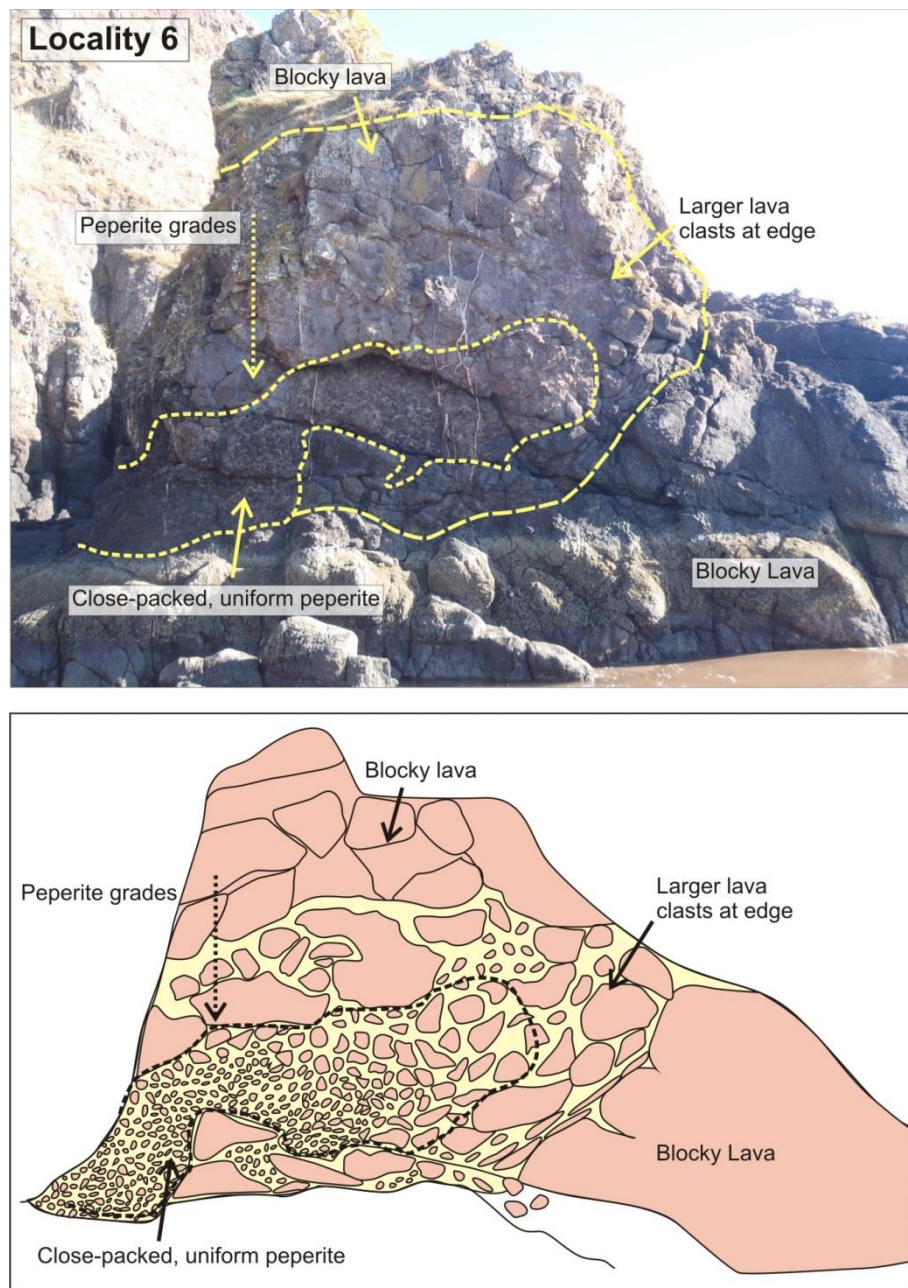


**Figure 6-24: Close-packed peperite at locality 6 (P1 and P2, Figure 6-4).** A variety of textures within the peperite are observed as the peperite grades from small, closely packed juvenile clasts to large, irregular shaped clasts at the edges of the peperite domain. Exposure is ~ 5 m high.

## 2) 'Pillow-like' peperite

At Locality 4 (Figure 6-4) the peperite displays 'pillow-like' structures within a red sandstone matrix (Figure 6-25). The large juvenile clasts, 20-50 cm, are rounded and resemble pillows (however, typical pillow rinds are absent) and display small mm-scale peperitic margins (Figure 6-25). Green, fine-grained siltstone inclusions, 2-10 cm, with deformed laminae are also present within the fragmented lava and peperite domain (Figure 6-25). The inclusions are sub-angular and deformed around the juvenile clasts adjacent to them.

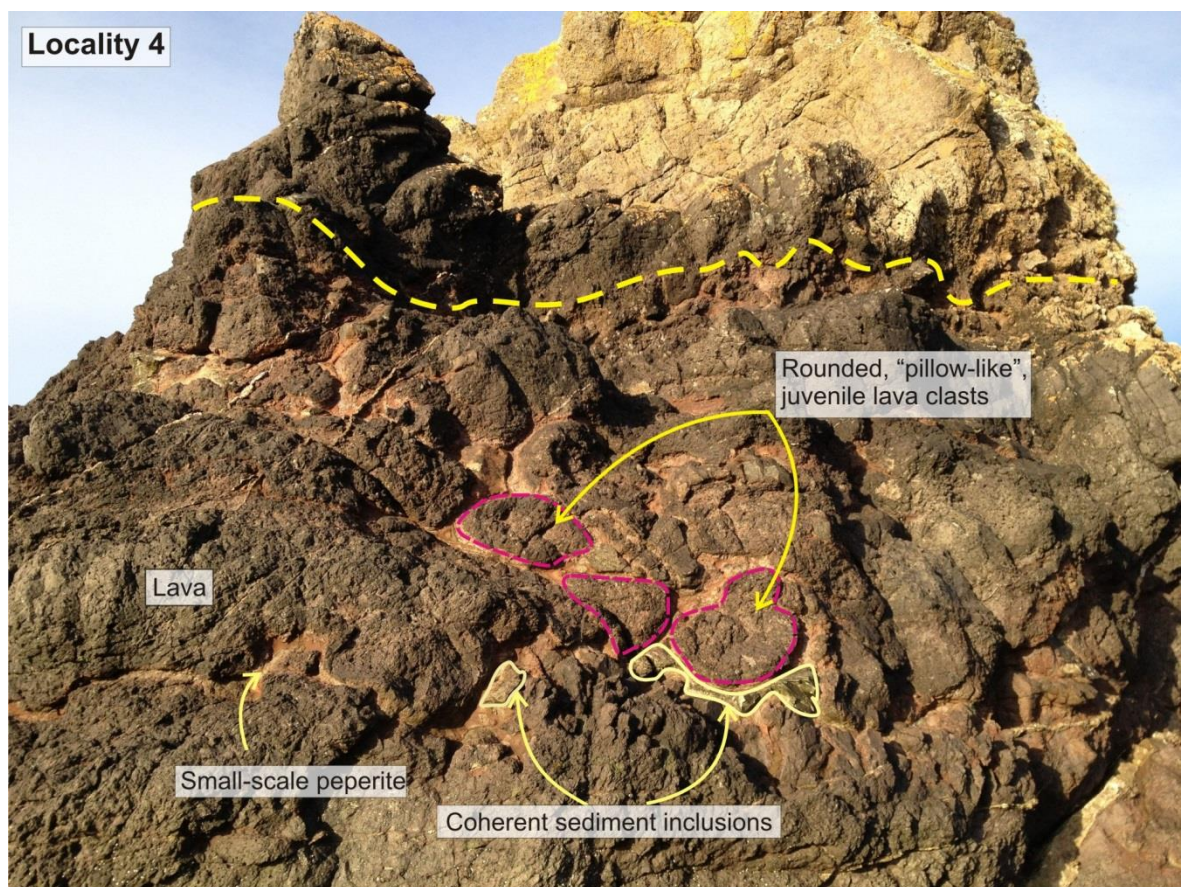


**Figure 6-25: Pillow-like peperite at Locality 4, (P1 and P2, Figure 6-4).**

Blocks of coherent sediment (outlined in yellow) are incorporated and preserved within the peperite, and are locally deformed by the lava clasts. The juvenile clasts of peperite are large and resemble rounded pillow structures (outlined in purple). The clasts do not have chilled margins, and most form mm scale peperite at their edges. Exposure is ~ 2 m.

### 3) 'Rootless' peperite

Rootless peperite encompasses the peperite domains that display variable juvenile clast sizes and morphologies, and a thorough disaggregation of the host sediment, as seen at Locality 5 (Figure 6-4). Connections from these domains to associated overlying and underlying lava are extremely difficult to determine, with only rare connected apophyses of lava observed invading the sediment, as well as abundant juvenile lava clasts (Figure 6-26). The domains are typically large, >2 m. The host sediment is fine grained red-green siltstone and sandstone. Sedimentary bedding and structure is very poorly preserved within the host sediment, but is retained in coherent sedimentary inclusions. Juvenile lava clasts display irregular, fluidal and globular morphologies, typically ranging in size from 2 to 10 cm, although this is not absolute. Petrography of the peperite shows a fine-grained litharenite host sediment with plagioclase-phyric basalt juvenile lava clasts, that have fluidal contacts and display micro-scale peperite.

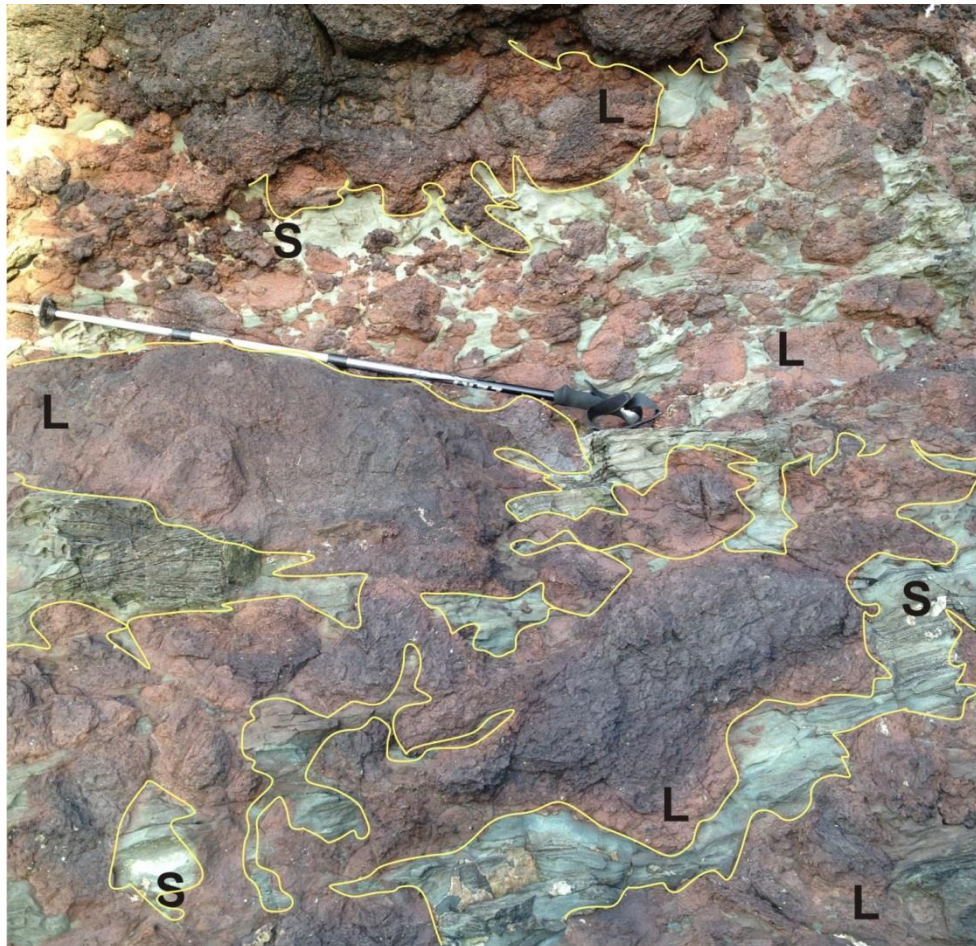


**Figure 6-26: Rootless peperite observed at Locality 5.**  
Note the thorough disruption and disaggregation of the green, siltstone host sediment (S) by the purple/red juvenile lava clasts (L). Walking pole is 1 m long.

---

## 6.4 Interpretation

### 6.4.1 Lava

The basaltic lavas of the Montrose Volcanic Formation are interpreted as sub-aerial pahoehoe lavas with characteristic ropey textures and pipe vesicles/amygdales (Macdonald 1953; Walker 1987). Vesicular intervals mark crusts of individual inflating lava lobes (Figure 6-6). Eruption of the sub-aerial lavas most likely occurred during a single sustained volcanic event, with several periods of lava effusion and quiescence. The presence of peperite and sedimentary units interbedded with the lavas suggests that the lavas were emplaced within an active drainage system, which provided surface water and sedimentary substrate with which the lava could actively mingle (Hole et al. 2013). These mixed lava-sediment domains are discussed below (Section 6.4.3). Exploitation of pre-existing fluvial channels by the lava(s), possibly on an alluvial plain, is likely. The absence of hyaloclastite and pillows suggests that large, deeper, bodies of water (i.e. lakes) were not present within this part of the flow field.

### 6.4.2 Sedimentary Units

#### 6.4.2.1 Conglomerate

The conglomerate units, with a coarse sandstone matrix and rounded pebbles and cobbles, are interpreted as fluvial, possibly flood, deposits, and mark a return to siliciclastic deposition after, or during a hiatus in, effusive volcanism. The conglomerates most likely represent deposits from a fluvial system that was trying to re-establish channels previously overwhelmed by lava. The rounded clasts suggest a long travel distance within a mature fluvial system (Hole et al. 2013), yet the unsorted nature to some sedimentary packages suggests an intermittent increase of energy in the transport system.

#### 6.4.2.2 Sandstone and Siltstone

The finely laminated, graded siltstone and sandstone units are interpreted as fluvial flood plain, and possibly lacustrine margin/ephemeral lake deposits, indicated by the gradual coarsening of sedimentary input from siltstone to granules and pebbles. Desiccation cracks at Locality 1 (Figure 6-9) are an indication that the depositional environment underwent periods of drying and flooding between sediment depositional periods. This supports the interpretation of Hole et al. (2013). The sedimentary units, red and green, are predominantly siliciclastic-volcaniclastic. Evidence for tuffaceous

material is limited; however, thin, fine-grained tuffaceous beds may represent fluvial reworked air-fall deposits (Hole et al. 2013).

The igneous clasts within sedimentary units at Locality 13 (Figure 6-5) are interpreted as reworked basalt material from (freshly emplaced?) lava. As the lava flow(s) encountered the fluvial drainage system, but did not block it, the lava, and loose material, were reworked by the water. This produces clasts that are reworked, transported, and deposited within the fluvial system, likely in pulses, producing the observed beds.

### 6.4.3 Mixed lava-sediment domains

#### 6.4.3.1 Sedimentary inclusions within lava:

The sedimentary inclusions in the lavas are unlikely to represent simple “xenoliths” entrained from vent walls and/or the substrate, primarily due to their quantity, size and shape. The deformation of some inclusions and the localised development of peperite, indicates that some inclusions were most likely formed due to passive emplacement of lava into unconsolidated/partially consolidated, possibly wet, sediment. As the lava flows over and bulldozes down into the sediment, depending on the consolidation and water saturation of the sediment, the sediment breaks up into coherent fragments/blocks. These fragments may form levee type deposits on the surface as the lava bulldozes through the sediment. These levees can then be incorporated into the lava as flow lobes inflate and grow, and new lobes breakout, consuming the sediment. This model explains the typical random orientation and dispersal of inclusions within the lavas. Later flows could also flow over and/or entrain the sediment, although the inclusions do not necessarily coincide with any obvious flow boundaries. Locally, however, a ‘remnant’ stratigraphy is recorded by the sediment inclusions, so that the original bedding and structure of the sediments, into which the lava has bulldozed, has been preserved. This may occur as the lava bulldozes into sediment, splitting into lava toes that passively “inject” into the sediment, possibly exploiting bedding planes/laminae. Although disrupted, the sediment remains essentially *in situ* and the original structure and stratigraphy is preserved as disaggregated inclusions within the lava. The retention of a remnant stratigraphy, rather than more thorough disaggregation of sediment to form randomly oriented inclusions, is most likely controlled by the host sediment properties; indicating at least partial consolidation of the sediment at the time of the lava emplacement. The variable size, morphologies and scale of the sedimentary inclusions within this single succession, shows the scale invariance of such lava-sedimentary features.

### **6.4.3.2 Isolated lava lobes:**

This succession (Figure 6-16) is interpreted to be on a fluvial or lacustrine margin, possibly an overbank setting, with deposition of fine-grained sediment. Desiccation cracks denote that the environment was not always fully water saturated, and was able to dry out, before further deposition of sediment. The fine, planar laminated sandstone is interpreted as having been deposited first, and then locally invaded and fluidised by the lava. Figure 6-16 (Locality 1) illustrates how the lava toes have not coalesced. Invasion of the lobes into the sediment has caused localised deformation of the sediment and some fluidisation, with localised mingling and peperite formation. The lenticular sedimentary wisps deformed around the lava toes and attached to the main sedimentary body, together with small zones of peperite, are evidence of passive intrusion of sub-aerial lava into sediment that was unconsolidated-partially consolidated and had minimal pore water. After lava emplacement, further deposition of sediment continued. The observed features could not have formed during periods of later sediment deposition or infilling of gaps between the lava lobes, as they form as a consequence of molten lava interacting with sediment.

### **6.4.3.3 Isolated sedimentary units with localised peperite**

These isolated units (Figure 6-17) are interpreted as lenses of sediment that have been isolated by invasive lava. As lava flows over and bulldozes through unconsolidated to partially consolidated, semi-saturated sediment, the lenses of sediment are uplifted and isolated, with peperite forming at the base and/or top of the isolated sedimentary unit. The peperitic lava-sedimentary contact at Locality 3 (Figure 6-18), which is observed at the basal margin of the sediment, suggests that the sediment was unconsolidated to partially consolidated, and most likely contained pore water that facilitated peperite formation. The sediment is interpreted to have been intruded by sub-aerial lava, and possibly rafted within, on top, or at the margins of a lava lobe, leading to its isolation, as above (Figure 6-27). The lava also contains coherent sedimentary inclusions, providing further evidence of the envelopment of sediment by invasive lava.

Shallow bulldozing of lava into poorly consolidated, wet sediment

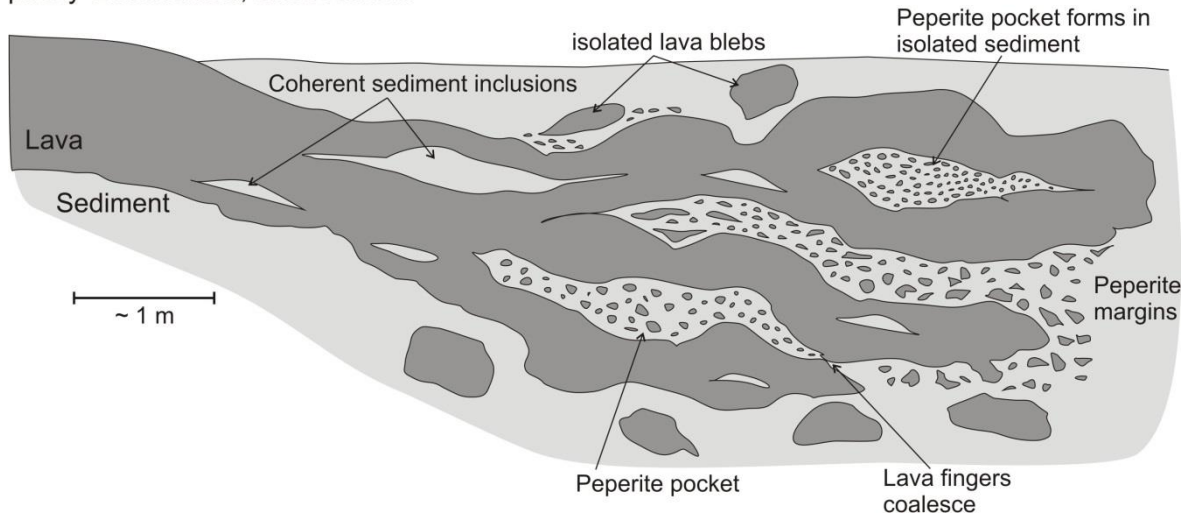


**Figure 6-27: Schematic diagram showing various features and morphologies of lava-water-sediment interaction, as observed at St. Cyrus.**

An invasive lava, with multiple lobes/toes has coherent sedimentary inclusions and peperite margins. Isolated lava blebs are within the host sediment. As lava lobes/fingers coalesce they isolate pockets of sediment and enclose peperite domains. These products are typically produced as sub-aerial lava bulldozes into poorly consolidated, semi-saturated sediment.

#### 6.4.3.4 Stacked lava lobes with sediment

The interstratified lava and sediment domains, which are present across the field area, comprise sub-aerial vesicular basalt lava, likely of pahoehoe flow type, with discontinuous layers of fine-grained fluvial/lacustrine sandstone (Figure 6-19 and Figure 6-20). The lava-sediment contacts are irregular, with micro-scale peperite present (Figure 6-20 and Figure 6-21). This feature is interpreted as multiple lava lobes or toes that have thin sedimentary layers between them. As the lava was emplaced in the characteristic pahoehoe flow style (Rowland and Walker 1990), it shallowly invaded the underlying sediment, which produced a thin layer of sediment at the upper surface of the lava lobe. Further incremental lava emplacement and breakout of new toes/lobes, repeated this process, with lobes overlapping and coalescing. The end result is a lava pile, with intermittent/trapped sedimentary layers, that is observed in cross-section as stacked lava lobes. Sediment was likely unconsolidated to slightly consolidated with minimal pore-water content, allowing the lava to exploit any weakness in the strata, and for micro-scale mingling between lava and sediment to occur. Petrographical analysis reveals that the basalt lava is intermingled with fine-grained fluvial/lacustrine sediment, as with the rest of the field area. There is no textural evidence for agglutinated spatter, which contradicts the previous interpretation by Hole et al. (2013) that these facies are spatter ramparts with the inter-layering of tuffaceous siltstone and

agglutinated lava spatter. The presence of coherent sedimentary inclusions within the sedimentary inter-layers also disproves their interpretation.

#### 6.4.3.5 Peperite

The range of peperite morphologies seen at St. Cyrus suggests that diverse sediment conditions (e.g. consolidation, saturation and compaction) were present at the time of lava emplacement. The peperite at St. Cyrus is not a linear or laterally continuous feature; rather it appears in isolated pockets and domains, depicting the localised variations in lava and sedimentary properties (present) during peperite formation. The shallow invasion and bulldozing of lava occurs within fine-grained siliciclastic siltstone and sandstone. There is no mingling between lava and conglomerates. This is likely a function of grain size on mingling, as previously suggested by Busby-Spera and White (1987) and Skilling et al. (2002).

The abundant consolidated sedimentary inclusions, in addition to the sedimentary matrix and lava clasts within peperite domains are thought to represent more compacted, consolidated, less water-saturated sediment into which magma has bulldozed and mingled. A typical sediment column, even just a few metres thick, will still likely display diverse properties (e.g. differences in saturation, possibly grain size, and consolidation, which will likely vary the most). Although an oversimplification, it can be assumed, or expected, that a sedimentary column in a dynamic environment is more compacted and consolidated at its base, whilst more saturated (with pore water) and potentially aerated (in some cases) at the top. As lava bulldozes into and mingles with the sediment, the sedimentary column is disrupted and thoroughly mixed internally (Figure 6-28). The super-saturated sediment at the top of the column is first to be fluidised and mingled with the lava, potentially facilitating further invasion, whilst the more compacted and consolidated layers are planed and entrained, as coherent fragments, into the lava body and invasion process (Figure 6-28). Sediment that is very fine grained (claystone and siltstone) is also typically more cohesive (Winterwerp and van Kesteren 2004; Grabowski et al. 2011), which enables coherent sediment inclusions to form and be incorporated within the lava facies. The mixing of the sediment occurs simultaneously with lava-sediment mingling, which forms the peperite, with the end result a peperite with coherent inclusions of sediment distinct from the fluidised host sediment.

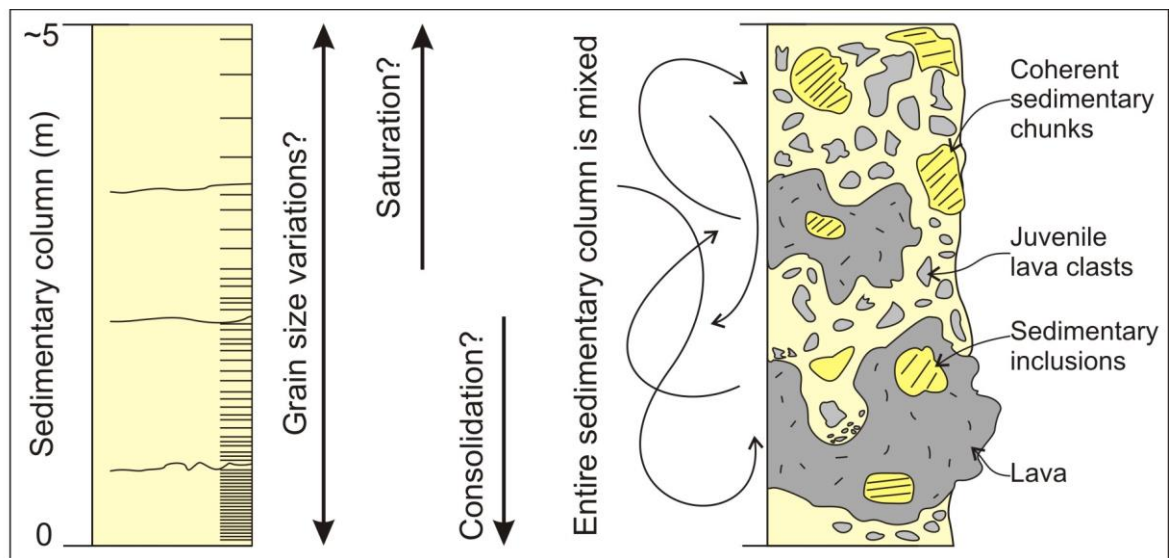


**Figure 6-28: A simplified, schematic diagram of the characteristic features of lava-water-sediment interaction within a small sedimentary column.**

**This highlights the relationship between some of the influencing factors of the sediment (i.e. variability of sediment grain size, saturation and consolidation) and the products produced during mingling.**

The close-packed peperite pods represent sedimentary bodies that have been completely disrupted and overwhelmed by juvenile lava clasts during lava-sediment mingling, and illustrate a transition from the lava into the peperite domain (Figure 6-24). Globular clast shapes suggest ductile processes (Busby-Spera and White 1987), such as fluid instabilities, which occur during clast generation (Skilling et al. 2002). It is thought that forceful magma intrusion and sediment fluidisation (Skilling et al. 2002) are key mingling processes during peperite formation. The grading of the lava clasts into the close-packed pod from the overlying massive lava, suggests that processes involved in the initial peperite-forming stages were not sustainable, and other processes, such as brittle quenching, may have taken over (Skilling et al. 2002). It is interpreted that close-packed peperite forms in domains where the sediment is highly unconsolidated and possibly more evenly saturated with pore water.

The “pillow-like” peperite at Locality 4 (Figure 6-25) is interpreted to have formed as lava flows over and mingles with the underlying sediment, which was mostly unconsolidated and supersaturated with pore water. As lava toes protrude and invade the saturated, unconsolidated sediment, large pillow-like clasts form and detach from the main magma body (Figure 6-29). The coherent sedimentary inclusions within the peperite most likely originate from more consolidated sedimentary beds, potentially underlying the upper unconsolidated, saturated layers. As the magma bulldozes into the sediment, coherent fragments remain, and mingle with the juvenile lava clasts, and are locally deformed by them (Figure 6-29).

The “rootless” peperite, such as that at Locality 5 (Figure 6-26), is representative of the thorough disaggregation of a sedimentary unit by invasive sub-aerial lava, but from which the transition between lava and peperite is unclear. There may only be apophyses of lava that penetrate the peperite, or none at all, as is the case with peperite domains within thick lava piles (Figure 6-15). Sedimentary properties that facilitate “rootless” dynamic peperite are similar to the close-packed peperite morphology (i.e. unconsolidated and saturated sediment).

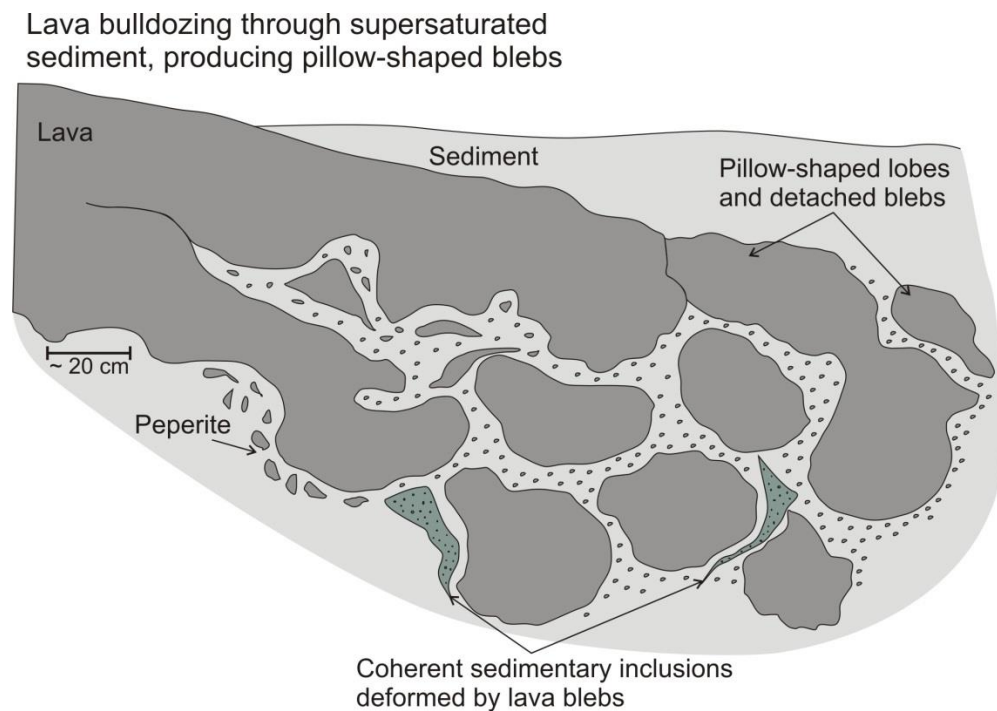


**Figure 6-29: A schematic model of the interpretation of pillow-like peperite and sediment inclusions.**

Lava is emplaced and bulldozes into super-saturated sediment. Large globular juvenile clasts and lobes are produced as a function of lava-sediment mingling. Small-scale peperite also occurs at the margins of some lava lobes and clasts. Coherent sedimentary inclusions are also observed within the peperite domain, and are deformed around the juvenile clasts.

## 6.5 Discussion

The succession at St. Cyrus records five types of mixed lava-sedimentary domains: i) sedimentary inclusions within lava, ii) isolated lava lobes, iii) isolated sedimentary units with localised peperite, iv) stacked lava lobes with sediment layers, and; v) peperite, which is subdivided. These domains range from passive invasion of lava into sediment, to peperite zones that exhibit evidence of extensive mingling and dynamic disaggregation of the host sediment. These mixed lava-sedimentary domains are summarised in Table 6 along with the interpreted sediment properties that influenced lava-sediment interaction.

Mixed Lava-Sedimentary Domains	Sediment Properties
Sediment Inclusions	Passive interaction Partially consolidated, dry to semi-saturated
Isolated lava lobes	Passive interaction Partially consolidated, minimal porewater
Isolated sedimentary units with localised peperite	Passive interaction Unconsolidated to partially consolidated, semi-saturated
Stacked lava lobes with sediment	Passive emplacement Unconsolidated sediment
Dynamic Peperite: <ul style="list-style-type: none"> <li>• Close-packed peperite</li> <li>• “Pillow-like” peperite</li> <li>• “Rootless” peperite</li> </ul>	Dynamic interaction Unconsolidated, saturated to super-saturated

**Table 6: A summary table of the mixed lava-sediment domains identified at St. Cyrus and the interpreted sediment properties that facilitate the interaction.**

### 6.5.1 Sediment Properties

At St. Cyrus, the mixed lava-sedimentary domains are much more complex than those reported in the previous case studies (chapters 3-5), and highlight the dynamic mingling of lava and host sediment. The lavas bulldoze, invade (essentially intrude) and mingle with sediment in a variety of ways, which is dependent on the properties of both the lava and the sediment. The properties of the sedimentary units (e.g. consolidation, grain size, saturation, and compaction) combined with properties of the lava (e.g. effusion rate and composition) are interpreted as influential controls on the products and processes involved at the lava-water-sediment interface. Slight changes in one or

more of the properties may considerably change the product that is produced as a function of lava-sediment mingling.

Density and viscosity contrasts between lava and sediment have been suggested as the most dominant factors for interaction (Hole et al. 2013), although the amount and distribution of pore water also likely plays a fundamental role (Zimanowski and Büttner 2002). Magma properties, such as density, are affected by vesicularity (Hanson and Maltman, 2003), thus this should be taken into consideration, as well as the sediment density affected by porosity (Maltman and Bolton 2003; Owen 2003). Previous studies at St. Cyrus suggest that the viscosity of sediment decreases as a consequence of lava penetration, and thus affects further magma penetration and movement within the sediment (Hole et al. 2013). Sediment densities are highly variable, but estimated for both a fine grained slurry,  $\sim 1230 \text{ kgm}^{-3}$ , and a partially consolidated sandstone,  $\sim 1800 \text{ kgm}^{-3}$  (Hole et al. 2013). Basalt magma density at St. Cyrus is estimated at  $\sim 2620 \text{ kgm}^{-3}$ , with an eruption temperature of  $\sim 1000^\circ\text{C}$  (Thirlwall 1982; Hole et al. 2013), and  $\sim 2000 \text{ kgm}^{-3}$  with  $\sim 20\%$  vesicularity (Hole et al. 2013). These figures provide a lava-sediment density contrast of  $\sim 200\text{-}800 \text{ kgm}^{-3}$ . For comparison, analysis of sand-grade sediment producing load structures within a clay-rich sediment forms with a density contrast of  $\sim 400 \text{ kgm}^{-3}$  (Owen 2003). The larger margin for lava-sediment density contrasts potentially implies that lower density contrasts may produce simple loading, with higher density contrasts possibly resulting in passive and dynamic lava-sediment mingling.

Sedimentary properties influencing lava-water-sediment interaction are previously discussed, in Chapters 3-5, within simple layer-cake style stratigraphic sequences. However, at St. Cyrus, the complexity and the spatial differences in distribution of the mixed-sedimentary domains, are developed within a dynamic depositional environment. The effects of depositional environment on the processes and products of lava-water-sediment interaction are discussed below.

### 6.5.2 Depositional Environment

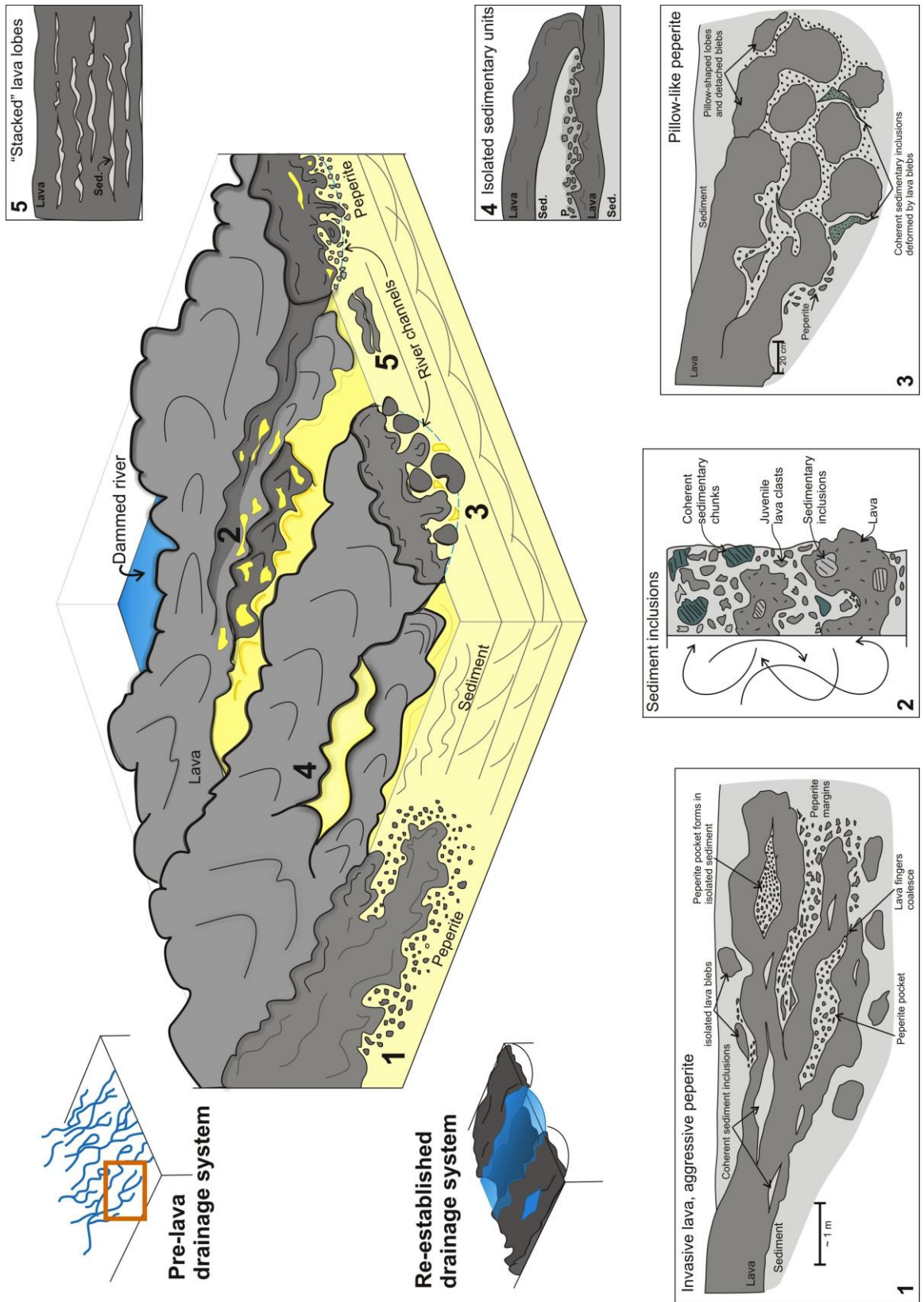
The inter-lava lithologies at St. Cyrus record the development of a typical lava flow field over/within a pre-existing fluvial drainage system, which was likely emplaced during a prolonged period of effusive volcanism. The processes and distribution of the products of the lava-sediment interaction are directly linked to the spatial and temporal controls of the pre-existing landforms, combined with the competing fluvial and volcanic systems (Figure 6-30).

Figure 6-30 illustrates the geometries of a fluvial, possibly braided, system (as described by Hole et al 2013, and Schofield et al 2012), and how it is overwhelmed by sub-aerial lava effusion. Initial emplacement of lava, will exploit the pre-existing topography, flowing into rivers, blocking and damming part(s) of the river system (Figure 6-30), and re-directing drainage (Dohrenwend et al. 1987; Tiercelin and Lezzar 2002; Ely et al. 2012; Hole et al. 2013; Schofield and Jolley 2013). In the case of St. Cyrus, a pahoehoe flow field developed (Hole et al. 2013) with different flow lobes active and inflating at different times. This creates new topographic lows for further lava flows to exploit, which may include the floodplains and overbank deposits, as seen at locality 2 (Figure 6-11 and Figure 6-16), eventually leading to an inverted topography, where the lava-filled channels become the topographic highs. During this period the complex array of lava-sedimentary domains are formed, from the passive emplacement of lava into partially consolidated, relatively unsaturated sediment, to the shallow bulldozing of unconsolidated, saturated sediment that forms peperite domains and coherent sedimentary inclusions (as described in section 6.4.3). Dynamic style peperite forms as the lava invades super-saturated, unconsolidated sediment (e.g. sediment close to, or within, river channels) (Figure 6-30), which allows the lava to easily exploit and disrupt the sediment through fragmentation and mingling.

During volcanic hiatuses the fluvial system re-establishes, exploiting the newly formed topography on top of the lava flow field. New sedimentary packages are deposited, possibly in new channels and/or in small lakes, which creates new sedimentary units that can be exploited by the next outburst of volcanic activity, if timing permits. It is clear at St. Cyrus that substantial water bodies did not develop during lava effusion as there are no preserved hyaloclastite, pillow or phreatomagmatic deposits. The distribution of mixed lava-sediment domains, therefore, is not only a function of 'vertical'/temporal changes through a succession, but also, and possibly more significantly, a function of the lateral/spatial variation and geometries of the sedimentary depositional system.

**Figure 6-30: (next page) A schematic model illustrating the development of a lava-flow field within a braided river drainage system, and the associated lava-water-sediment interactions that occur.**

**Lava typically exploits topographical lows, such as river channels, which causes blocking and re-directing of the drainage system. Lava-sedimentary domains are created as lava shallowly invades and bulldozes the sediment. Aggressive peperite (1) forms as lava invades saturated and unconsolidated sediment. The bulldozing of sediment by lava creates coherent sediment inclusions (2), which are found within lavas, and peperite domains. Invasion of super-saturated sediment creates pillow-like peperite (3). Isolated sedimentary units (4) can occur between flow lobes. Passive emplacement of lava into sediment may create "stacked" lava lobes with sediment and peperite trapped between each lobe (5). After lava emplacement, the drainage system re-establishes, exploiting the newly formed topography.**



---

## 6.6 Conclusions

The lava-sedimentary sequence at St. Cyrus provides an excellent case study of the processes and products of lava-sediment interaction. Fluvial to lacustrine siltstone, sandstone and conglomerate units are intercalated with sub-aerial basalt lavas, emplaced during a sustained volcanic event with several periods of lava effusion. Lavas are interpreted to have exploited fluvial channels and topographic lows within an active sedimentary drainage system, which resulted in the variety of mixed lava-sedimentary (peperite) domains that dominate the sequence. The products of lava-water-sediment interaction observed are: sedimentary inclusions, isolated lava lobes, isolated sedimentary units with localised peperite, stacked lava lobes with sediment layers and, aggressive/dynamic peperite.

Coherent sedimentary inclusions, both within lava and peperite domains, have been described here for the first time. They range in size (cm - decimetre scale) and shape (blocky to lenticular), and typically comprise fine-grained siltstone and claystone. They are interpreted to form as lava invades partially consolidated, cohesive sediment, which fragments and is entrained within the lava or mingled within the peperite domain.

The prevalence of mixed lava-sedimentary domains, and coherent sedimentary inclusions within lava, highlight the aggressive nature of lava and disruption of sediment. The style and products of lava-water-sediment interaction is influenced by localised variations in sedimentary properties including consolidation, saturation, and cohesion, as well as properties of the lava, as previously discussed. A dynamic depositional environment is inferred for the development of complex geometries and spatial differences in distribution of the mixed lava-sedimentary domains. This depositional setting explains the more aggressive nature of peperite formation and distribution of peperite, compared to those described in chapters 3-5.

# Chapter 7: Discussion and Application to Petroleum Systems

## 7.1 Introduction

Lava-water-sediment interaction is an encompassing term, used to describe a wide range of interactions and products, including pillow lava/breccia, hyaloclastite and peperite. The research presented here demonstrates that lava-water-sediment interaction is a complex yet common occurrence within landscapes that encounter competing volcanic and siliciclastic systems. Within these systems a wide range of products beyond simple pillow breccia, hyaloclastite and peperite are identified, and it has been determined that fragmentation at the interface of various materials/components is strongly influenced by sediment properties and depth of emplacement into the sediment column.

In Chapter 3 (Kinghorn, Fife), the relationship between thin, isolated sediment bodies intercalated between lavas is described. A basic model of lava-water-sediment interaction is established, and a continuum from little to no interaction, to passive and, dynamic interaction between lava and the host sediment is developed.

Chapter 4 (Mountain Home, Idaho) is a large-scale, field study of a succession with multiple lava-sedimentary packages, one of which records the emplacement of lava into a substantial body of non-marine water. A unique view of the products of three types of lava-water-sediment interaction is observed along the same interface, providing insights regarding the importance of localised changes in the nature, geometries and scale of sedimentary units.

Chapter 5 (Gran Canaria, Canary Islands) is an investigation of the interaction and effects of invasive pillow lavas and hyaloclastite with underlying sediment. It focuses on the interactions that occur as pillows are emplaced into, and fluidise sediment, building upon the observations and conclusions presented in Chapter 4.

Chapter 6 (St. Cyrus, Angus) is focused on the “dynamic” style of lava-water-sediment interaction, and the intricate features that are produced. This links with the continuum established in Chapter 3 (Kinghorn); however, it explains why the complex geometries develop, in the context of the depositional environment and lava-sedimentary architecture.

This discussion includes a synthesis of findings from all of the field studies, combining the features into a set of models that may be used in future investigative work. Having done this, the relevance and importance of the wider implications of this research, in particular to the hydrocarbon industry, is discussed.

## 7.2 Field Synthesis: Fundamental Concepts

Chapters 3-6 address in detail the interaction of lava with sediment and water. A number of features have been recognised previously (e.g. peperite), but this study provides new insights through a more focused analysis of the textures and geometries of interaction. Features and products, such as coherent sediment inclusions, stacked lava lobes within sediment, and sediment within hyaloclastite and pillow lavas, have been described and interpreted in detail.

Table 7 is a summary table of several lava-water-sediment interaction characteristics that are found across the study sites. Similarities and differences are apparent; however, this essentially demonstrates that characteristic features of lava-water-sediment interaction remain the same irrespective of tectonic and environmental setting (e.g. from rifted margins to ocean islands, and fluvial-lacustrine to marine environments). It is acknowledged, however, that pillow lavas and hyaloclastite require the availability of larger bodies of water in order to form, and thus, these are somewhat environmentally controlled.

Based on the observed features of lava-water-sediment interaction (Table 7), this research has established a continuum from passive to dynamic interaction (Section 7.2.1, Figure 7-1 and Figure 7-2). The continuum highlights the many intermediate products and processes, and consequence of (host) sedimentary properties that enabled, or induced, such interactions between lava, sediment, and/or water (Figure 7-1).

Features	Kinghorn	Mtn. Home	Gran Canaria	St. Cyrus
Loading	X	X	X	X
Flame structures	X	X	X	X
Pillow lava	X	X	X	
Hyaloclastite	X	X	X	
Passive peperite	X	X	X	X
Dynamic peperite	X			X
Sedimentary inclusions	X	X	X	X
Siliciclastic sediment	X			X
Volcaniclastic sediment	X	X	X	X
Lava tubes		X	X	X
Lava tubes filled with sediment		X		X
Sediment fluidisation		X	X	

**Table 7: A summary of the main features of lava-water-sediment interaction observed at each field locality (chapters 3-6).**

## 7.2.1 Lava-water-sediment Continuum

For the purposes of this research the lava properties (effusion rates/flux, composition, temperature, viscosity, shear strength etc.) were considered essentially the same, and a constant across individual field studies, to allow a primary focus on sediment properties. Whilst it is fully acknowledged that lava properties locally vary, in all areas the lavas were subaerial (at least initially), of pahoehoe type, and of similar composition (basaltic or variants thereof) and thus mineralogy, viscosity (low effusion rates  $\sim 5\text{-}10\text{ m}^3\text{s}^{-1}$ ) and density (typically  $\sim 2.8\text{-}3\text{ g/cm}^3$ ). Lava flux is considered a key constraint on the emplacement of pahoehoe lava into water (Stevenson et al. 2012; Watton et al. 2013), but the extent to which this is critical to sediment interaction is uncertain. It has not been possible to determine effusion rates of the lavas at the field sites, but regardless, it appears that sediment properties exert a fundamental control on fragmentation.

The sediment properties considered in this research included: grain size, composition, degree of compaction, degree of consolidation, and water content (surface water vs. pore water). The way in which sediments influence lava-sediment interaction has previously been speculated upon, particularly grain size of the host sediment, water content, porosity and consolidation (Busby-Spera and White 1987; White et al. 2000; Jerram and Stollhofen 2002; Skilling et al. 2002). Field and petrographic observations

---

allow the distinction and categorisation of the different interaction products and how these are likely influenced by the sedimentary components and properties. These interactions are represented in a schematic diagram (Figure 7-1) and a conceptual flow diagram (Figure 7-2), which illustrate and explain the continuum of lava-water-sediment interactions, from no interaction, to minimal and passive interactions, to dynamic and complex interactions. The main findings of which are:

- When sediment is partially consolidated and compacted, with relatively little to no water content, loading and passive interaction occurs.
- When sediment is supersaturated, unconsolidated, and uncompact, aggressive/dynamic peperite and sediment fluidisation occurs.

When sediment is very fine grained, compacted, saturated and only slightly consolidated, it is typically more cohesive and produces coherent sedimentary inclusions.

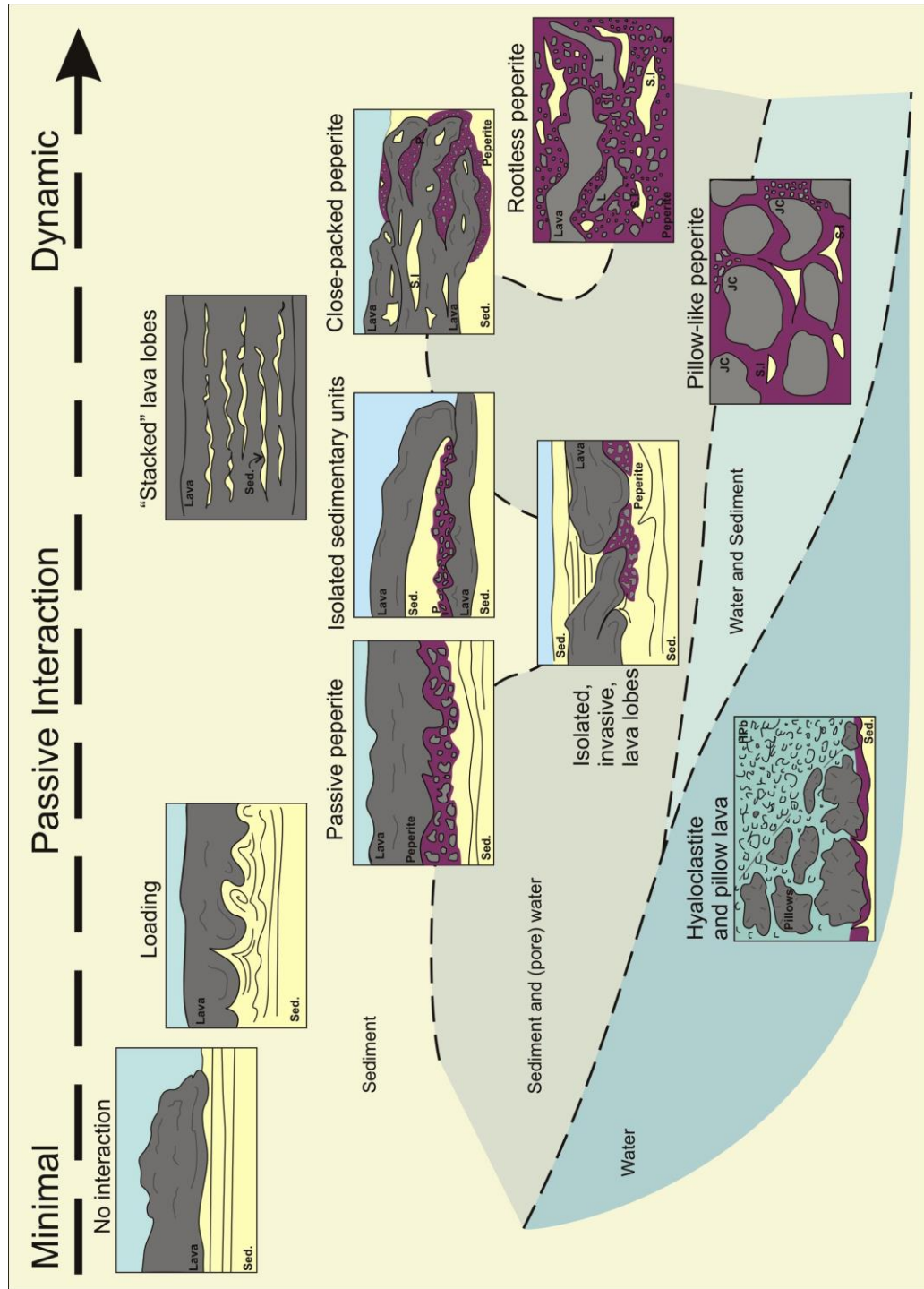


Figure 7-1: Diagrammatic representation of the main types of lava-water-sediment interaction documented within this research. The interactions form a continuum from minimal, to passive, to dynamic interaction of lava and sediment, with varying amounts of water saturation. Key: Sed. = sediment; SI = sediment inclusion; JC = juvenile clast.



The conceptual flow diagram (Figure 7-2) has a series of simple yes/no ‘questions’. It attempts to simplify the interaction features into products and sediment properties, highlighting the differences and links. It is important to note that subtle changes in the sediment properties (e.g. water saturation) can lead to significant differences in process and type of interaction. Each of the key products is discussed further, below:

- Pillow lava and hyaloclastite, with or without sediment inclusions, are the products of quenching and fragmentation of lava that has been emplaced into a body of water. If sediment is present, it is likely that there will be some interaction between fragmenting lava and underlying sedimentary units (see also coherent sedimentary inclusions, below).
- Loading (passive interaction) occurs as sediment is loaded by lava (including pillow lava), with minimal interaction. Load structures, such as sediment flames, indicate a passive style of interaction, with the underlying sediment unit, which was most likely slightly compacted and/or consolidated, with minimal porewater. This enables the sediment to be compressed and moulded, bearing the weight of the overlying lava, but not succumbing to, or inducing, interaction. It may be argued, however, that the lava properties may play a role here, perhaps as significant as the sediment properties. Low viscosity lava flows are potentially more likely to induce loading, rather than an aggressive interaction, as they are typically thin and flow more easily over sediment rather than bulldozing into it. Conversely, higher viscosity lava, may potentially be more aggressive. An example of the interaction between sediments and thick rhyolite lavas is observed in Owyhee County, Western Snake River Plain (WSRP), USA. Here, the rhyolite lavas induce extensive disruption of the underlying volcanoclastic sedimentary units, including loading, fluidisation and liquefaction; invasion of the lava into the sediment produces peperitic margins (McLean et al. 2016, *in press*). The scale of this interaction is much greater than that observed with basaltic lavas, with lava thickness ~20 m. Therefore, interaction of high viscosity magmas and sediment is more dynamic, but similar interactions are observed.
- ‘Passive peperite’ appears isolated in the conceptual model, as the product of mingling and interaction with sediment at the base and sides of a lava body only, such that it cannot be classified as invasive or burrowing. The lava is emplaced on top of the sediment body, and interaction may be extensive, but restricted to the base and/or edges of the lava body. Sedimentary properties, however, are

likely similar to those of an ‘dynamic peperite’: unconsolidated, uncompacted and typically water-saturated, as widely stated in the literature (White et al. 2000; Skilling et al. 2002). It is important to note, however, that peperites may also occur in arid, aeolian environments (Jerram and Stollhofen 2002). Nonetheless, within the case studies of this research the environmental evidence indicates that the sediment was typically saturated with water at the time of lava emplacement and interaction.

- If lava becomes invasive, and noses into the sediment, it can, in some cases, remain as a coherent body. As it is continuously emplaced (the lava flow/flux remains high and sediment properties allow), stacked lava lobes may form. As the invading lava exploits weaknesses in the sedimentary strata, thin lava lobes are incrementally emplaced trapping thin layers of sediment between them. In cross section this gives a vertically stacked lava lobe appearance with trapped sediment layers in between. This will cause small- and micro-scale mingling at the contacts. In this situation, sediment is most likely unconsolidated with minimal pore water content (i.e. not super-saturated).
- If lava is not continuously emplaced into the sediment, this can result in isolated lava lobes, whereby the lava bulldozes into sediment that is partially consolidated and has minimal pore water, or is dry, and thus, little interaction takes place. The examples presented here, demonstrate that the lava lobes are inflated with peperitic margins and cause deformation/fluidisation of the sediment. It may also be argued that a lack, or loss, of (mechanical and thermal) energy inhibits the lava in its ability to dynamically interact with the sediment, highlighting the intimate interplay of lava and sediment properties.
- ‘Dynamic’ peperite (as defined by this thesis) is the complete disruption and mingling of the sedimentary domain by and with the lava. A variety of morphologies are included, showing the range of different interaction styles; these sub-types are outlined below and in Figure 7-2.
  - Pillow-like, close-packed and, rootless peperite are described in detail in Chapter 6 (St. Cyrus). They can occur above, below, and at the sides of the lava body. The term “pillow-like” peperite describes the rounded, large, bulbous and globular juvenile blebs that are detached from the main invasive lava body within the sediment. They form as the lava bulldozes into and interacts with super-saturated, unconsolidated sediment. The water content

allows a sustained vapour film (Kokelaar 1982; Busby-Spera and White 1987) to form around the lava bud, enabling it to grow larger before detaching. The 'regular' close-packed peperite is akin to peperite previously described within the literature (Hanson and Wilson 1993). This style forms as lava bulldozes into domains where the sediment is unconsolidated and evenly saturated with pore water, enabling an even (or homogeneous) mix of juvenile clasts and host sediment, and showing a gradation and transition into the main lava body. Rootless peperite describes complex peperite domains where no clear relationship to the main feeder lava body is observed.

- Isolated sediment units are present either because there was deposition during volcanic quiescence or because the invading lava has not mingled with parts of the sediment body. Typically, a large portion of the sedimentary domain remains as a single, un-invaded body, and becomes isolated. This is potentially due to passive interaction as lava mingles with partially consolidated sediment that is dry (or has minimal pore water), at the upper margins of the sediment body. The scale and geometries of these isolated sedimentary domains could have wider implications for the hydrocarbon industry, when considering their size, and how they are connected to other sedimentary domains as well as connection to the peperite (see section 7.3 below).
- Coherent sediment inclusions, can occur in a number of instances, and are distinct from the host sediment. Sediment that is very fine grained, compacted, water-saturated and only slightly consolidated, is typically more cohesive and more likely to produce coherent sedimentary inclusions. These inclusions are produced as the lava bulldozes the sediment and can be incorporated into lava lobes, within hyaloclastite and pillow breccias, and within peperite domains. Passive interaction with the sediment may incorporate sedimentary inclusions into the lava base, whereas a more aggressive bulldozing and interaction may incorporate inclusions throughout the lava body. In some instances, coherent sediment inclusions within peperite domains may retain stratigraphy, which may suggest that the lava passively "injects" into and envelopes the host sediment, leading to inclusions remaining *in situ*, producing a "ghost stratigraphy".

How plausible is the nosing and bulldozing of lava through sediment? Recent research highlights how lava bulldozes, melts, and interacts with thick ice sheets. Edwards et al.

(2014) demonstrate through a series of field experiments and illustrations the activity that occurs at the lava-ice interface. This thesis research supports such findings, in that lava can and will actively bulldoze through sediment (and water), and that the by-products will be produced. A key example includes, blocky fragments of sediment, which are produced as the lava bulldozes down and through the sediment. These are rafted on top of the lava, and either incorporated during inflation, or incorporated by later lava emplacement (Figure 7-1). This process has also been mimicked in small-scale hydrodynamic mingling experiments, which observe vesicular particles incorporated into the melt as the invasive body passes the air/coolant interface (Schipper et al. 2011).

Quantifying the processes that occur during lava-sediment interaction is difficult, principally because calculating the sediment characteristics prior to interaction (e.g. porosity and water saturation) is almost impossible (Waichel et al. 2007). The variability of sediment properties also influence the water/melt ratio that is used to infer magma-sediment mingling (Zimanowski and Büttner 2002; Waichel et al. 2007). Experimental data available within the literature (e.g. Lorenz et al. 2002; Wohletz 2002; Zimanowski and Büttner 2002; Schipper et al. 2011) has attempted to address these questions, but limitations are still present.

Thermodynamic and fluid properties of magma and water are relatively well constrained and tested within explosive MFCI experiments (Wohletz 2002; Zimanowski and Büttner 2002) however, complexities occur when extending these results to include sediment or 'particle impurities' (Schipper et al. 2011). Engineering literature also does not consider inherent heterogeneities within sedimentary bodies, sediment slurries or granular flows (Schipper et al. 2011). However, experiments focused on hydrodynamic mingling, the non-explosive fragmentation of one liquid within another (Zimanowski and Büttner 2002; Schipper et al. 2011), have attempted to analyse and quantify peperite formation processes. These experiments exemplify the current understanding of peperite textures, including how blocky and fluidal textures form, whilst also proving the theory of hydrodynamic mingling for a more passive, non-explosive mingling process between lava, water and sediment (Schipper et al. 2011). Hydrodynamic mingling occurs in four regimes, with experiments showing that mingling is most effective/enhanced during tests with high sediment content, ~10-30 %, within the 'coolant' (Schipper et al. 2011). This is related to slower heat transfer and matched viscosities between the melt (lava) and the coolant (water/sediment slurry) (Schipper et al. 2011); processes that need to occur to promote mingling (Zimanowski and Büttner

2002). Thermal granulation is interpreted to be controlled by the type and abundance of sediment in the coolant (Schipper et al. 2011).

These types of experiments provide evidence for a single, passive, process of lava-water-sediment mingling, by which the sediment content, granularity and heterogeneity affect the mingling process and products. Further work looking at higher sediment content, along with systematic changes in sediment type, grain size, and compaction may provide additional insight.

## 7.3 Industry Application of Field Analogues

The interaction of lava with water and sediment and its effects are becoming increasingly acknowledged within the petroleum industry, especially within companies who work within volcanic-rifted margins, such as the North Atlantic Margins and its basins, particularly the Faroe-Shetland Basin (FSB). The Rosebank Field (see Chapter 1) is a key example of a prospect that has been developed from a volcanic-dominated sequence within the FSB. As a consequence, research is ongoing to better understand how and why lava-sediment interaction has occurred. However, there are still uncertainties that govern and/or restrict geoscience exploration and, recognition, awareness and understanding are often lacking. Nonetheless, there is a desire within the petroleum industry to know more about volcanic-sedimentary systems and their potential.

Through time spent at OMV UK, as part of a placement during this research, field data from this thesis has been integrated with well log data acquired from the FSB. This integration allows for a more simplified understanding of the array of lava-sediment-water products and processes and the application of these findings to industry projects, especially where data and/or expertise may be lacking.

### 7.3.1 Borehole Imaging

The data used in this study were resistive borehole images, obtained from formation micro-resistivity imaging (FMI) (©Schlumberger). These provide a detailed, flattened 3D image of the borehole, to be used alongside the wireline logs (gamma, resistivity, neutron porosity, bulk density, velocity etc.) (see Chapter 2). FMI is becoming increasingly popular within the industry as it is far cheaper than collecting core, but provides a much clearer image than traditional wireline log and point data. This is

particularly useful as core is commonly not collected in volcanic sequences, and, where it has been collected, the interface between lava and sediment is usually lost.

Interpretation of the borehole image data is comparable to many of the interpretations and findings across the four field sites of this study, especially Kinghorn (Chapter 3) and St. Cyrus (Chapter 6). The borehole image data can also be used in conjunction with the interpretative conceptual models from the field case studies to provide further understanding in recognising lava-water-sediment interaction features. This application is key to providing a quick and comprehensive “guide” and awareness of lava-water-sediment interactions within basin-scale examples (i.e. small wireline/borehole data within a large basin, for those unfamiliar with lava-water-sediment interactions and their interpretation).

### **7.3.2 Combining borehole images with field analogues**

Lithofacies such as hyaloclastite, lava tubes and peperite have recently been recognised within FMI studies featuring data from the Rosebank Field, FSB (e.g. Figure 2-10, Watton et al. 2014), which aided the work presented here, an analysis of data from the Cambo Field, FSB (see Chapter 2). In summary the Cambo FMI logs reveal similar lithofacies, together with complex lava-sediment-water interaction features including: loading, sediment inclusions, invasive lava, and more complex peperite features. Linking these features to a large scale, field example is important to gain an understanding of the true scale and geometries of these features where only a single borehole image (~8 inch; 20 cm, resistive flat or 3D image) interpretation is available.

In FMI data analysis, the resistivity of the different units controls the images produced. In this study, resistive facies, such as lava and other volcanic lithologies, show a bright response (white or pale yellow), whereas conductive facies, such as siliciclastic sediments, show a dark response (dark brown or orange) (see Chapter 2, and Figure 7-3). Volcaniclastic facies blur the lines, as in other wireline log data, but analysing the combination of wireline and FMI data together can increase the accuracy of interpretation (Figure 7-3). The wireline logs and the static FMI images provide useful data of broad lithological variations and larger scale interpretation (Figure 7-3), however, the distinguishing feature of FMI logs is the high-resolution data (bedding fine-scale facies variations) gained from the dynamic FMI image. Four key FMI images with wireline log data (i.e. bulk density, neutron porosity, gamma ray and velocity) and corresponding interpretation are presented below (Figure 7-5-7).

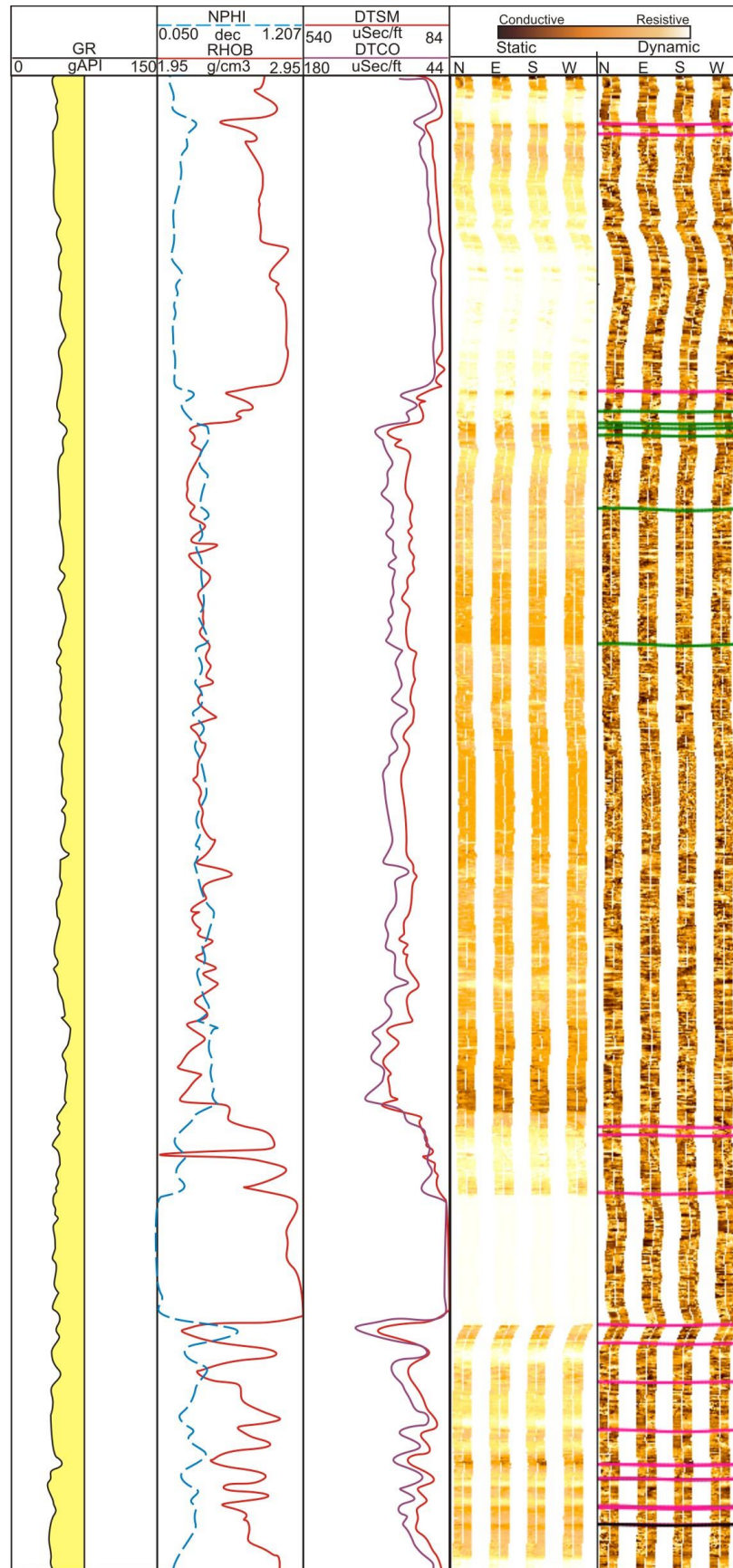


**Figure 7-3: Large scale FMI and wireline logs of lava and interlava lithofacies. At this resolution the lava is clearly identifiable both within the FMI (bright white static FMI response) and within the wireline logs (transit times are slow, with lower porosity and higher densities). With the gamma response, the inter-lava facies can be interpreted as volcanoclastic, which show mixed wireline responses also.**

Within FMI images, and wireline, a distinction can be made between coherent, massive lava cores (brightest resistive signal, higher bulk density, lower porosity) and vesicular and rubbly bases. Figure 7-4 shows a typical lava lobe that has a massive core with a vesicular rubbly base and a vesicular top. The upper lava-sediment contact is irregular, but there are no visible detached juvenile clasts of lava in the overlying sediment. The basal lava-sediment contact is also irregular and has been interpreted as a thin mingling zone between the lava and sediment. Zones of contrasting brightness can be seen, suggesting lava clasts are juxtaposed against sediment within this mingling zone. The nature of the upper contact suggests that the lava was sub-aerial and that it may have shallowly invaded the sediment; for example, small irregularities and contacts similar to this are observed in the lava-sediment contacts at St. Cyrus (Chapter 6, Figure 6). However, the upper lava-sediment contact could also be interpreted as the result of weathering or irregularities in the lava's surface, later in-filled by sediment, and therefore a wholly sub-aerial lava. The basal contact can be interpreted as a small-scale peperite (passive) zone, developing at the base of sub-aerial lava as it flowed over wet, unconsolidated sediment. However, the basal contact of the lava could also be interpreted as a rubbly base that is simply loading onto the underlying sediment.

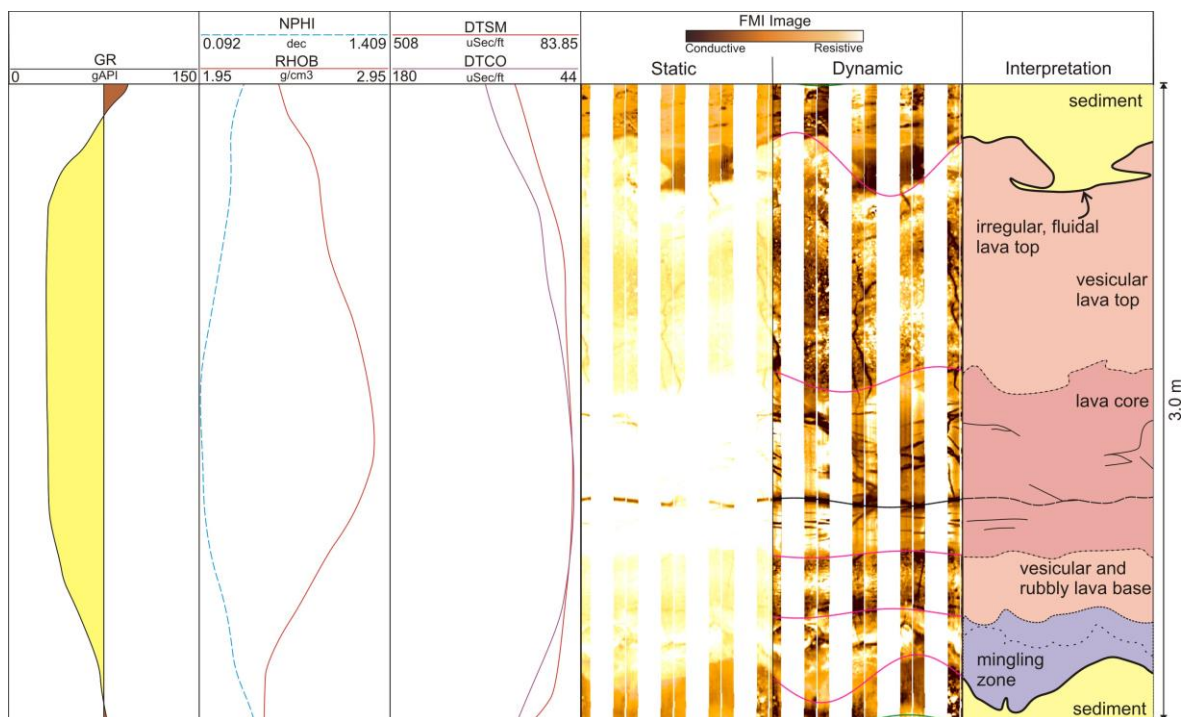


**Figure 7-4: Flattened FMI images, wireline data and interpretation of a pahoehoe lava with irregular lava-sediment contacts.**

The lava core shows the highest resistivity, with the vesicular and rubbly base and top showing less resistivity. The lava-sediment contact is irregular both at the base and top. A higher gamma (GR) response at the base and top of the lava is interpreted as a sedimentary (clastic) contact. Key: GR = Gamma Ray; NPHI = Neutron Porosity; RHOB = Bulk Density; DTSM = Shear wave transit time (sonic velocity); DTCO = compressional wave transit time (sonic velocity).

Figure 7-5 shows an example and interpretation of a peperite formed at the base of a lava. The lava appears to protrude down into the sedimentary domain and lava clasts and fragments of higher resistivity material are seen within a conductive matrix. This zone is bound at the base by sediment and another lava, the latter displaying a vesicular and rubbly top, and a massive core. The wireline supports this interpretation. It is almost impossible to determine the geometry of this peperite zone just from the borehole image. Examples of small isolated peperite pockets within lavas are observed at St. Cyrus (Chapter 6, Figure 15), but equally, laterally extensive peperite zones (tens of metres) are also feasible.

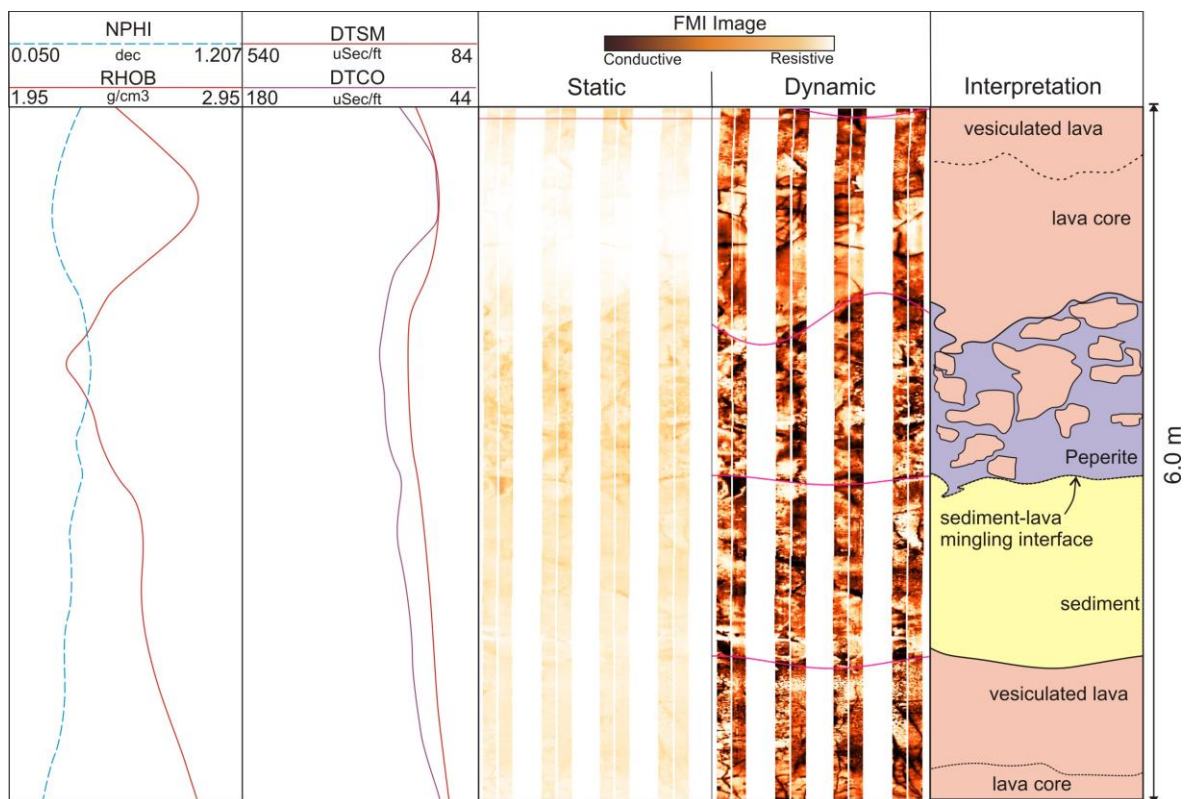


**Figure 7-5: FMI images, wireline data, and interpretation of peperite at the base of a lava. The interpreted lava-sedimentary contact occurs where clasts of higher resistivity (indicating lava) are surrounded by a conductive matrix (indicating sediment). Key: GR = Gamma Ray; NPHI = Neutron Porosity; RHOB = Bulk Density; DTSM = Shear wave transit time (sonic velocity); DTCO = compressional wave transit time (sonic velocity).**

The FMI data are remarkable for highlighting the complex interface between lava and sediment. Figure 7-6 shows sediment inclusions within the base of a lava that has loaded the underlying sediment. The image shows sediment, possibly volcanoclastic, overlain by vesiculated lava. The lava-sediment contact is irregular, with flame/fluidal type geometries, where the lava is interpreted to have loaded onto the sediment. The dark, detached, rounded bleb is interpreted as a sediment inclusion within the base of



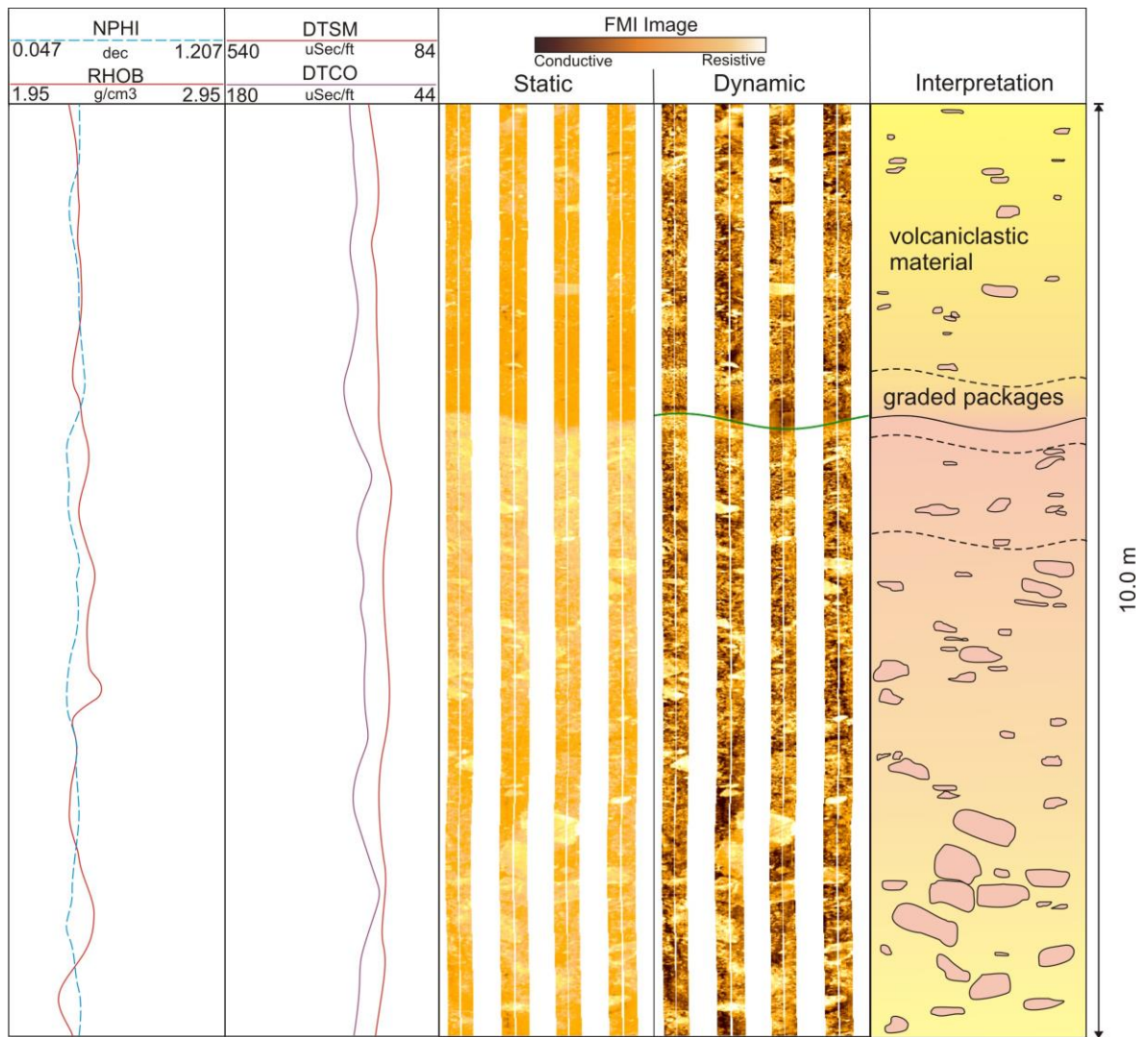


**Figure 7-7: FMI images, wireline logs and interpretation of graded hyaloclastite packages observed within the Cambo Field data.**

**Clasts of high resistivity are indicative of volcanic clasts. Key: GR = Gamma Ray; NPHI = Neutron Porosity; RHOB = Bulk Density; DTSM = Shear wave transit time (sonic velocity); DTCO = compressional wave transit time (sonic velocity).**

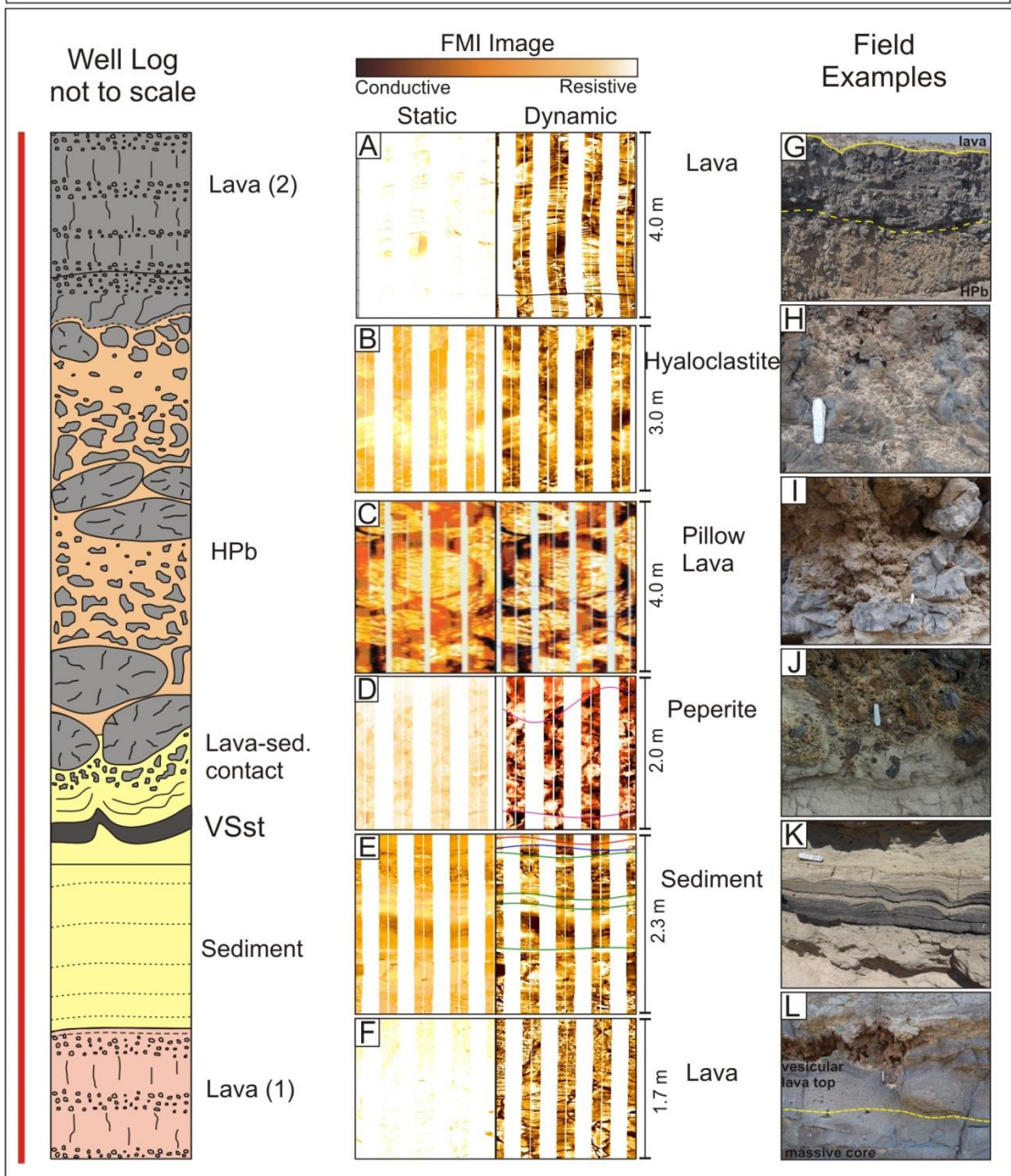
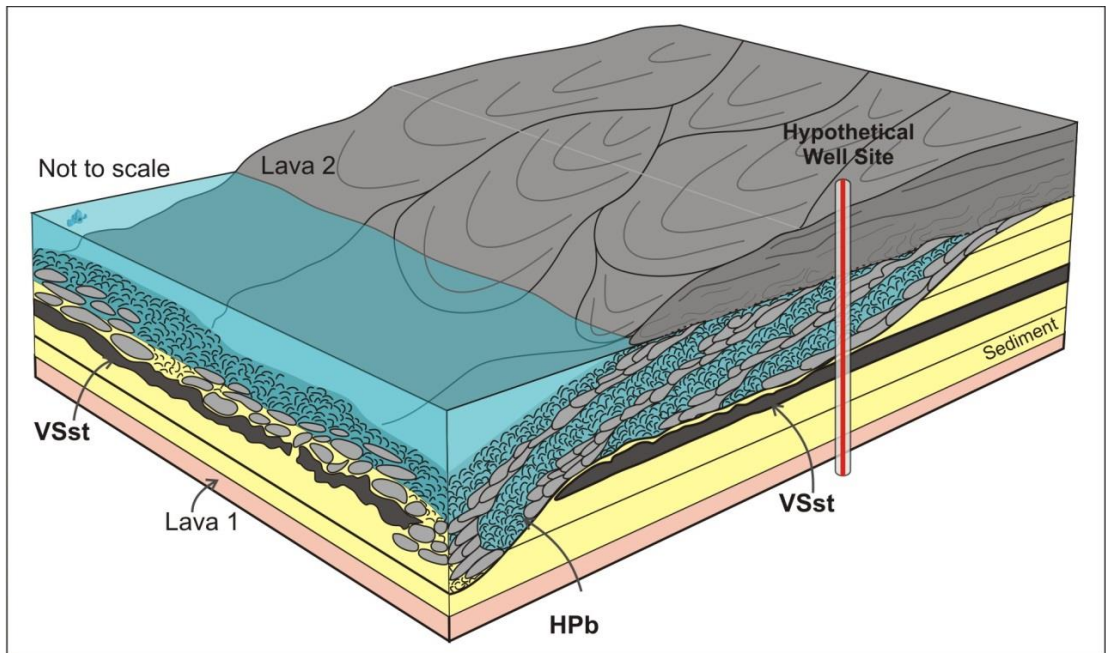
The uncertainties with the interpretations of each of the above examples highlight the complexities of limited datasets and the unknowns of lava-sediment interaction. Where there is uncertainty, other accompanying well data and examples can be used to inform the interpretation further (e.g. well logs, core samples). By acknowledging that lava-sediment interactions are likely to have occurred, it also aids the interpretation of the local and regional geology. For example, the nature of lava-water-sediment interactions has implications for environments and timescales of deposition in the basin.

Figure 7-8 is a schematic model of a conceptual field locality and log, populated with representative FMI images, and actual field examples of characteristic lithofacies. The

3D model is reconfigured from Chapter 4, Mountain Home, and an arbitrary log location has been picked, with the likely lithofacies highlighted in the logs below. The hypothetical well log is a sketch log through the main lithofacies, including the lava-sediment contact. The FMI log images are examples of each of the facies observed within the Cambo wells (except the pillow lava, C). Both images A and E are lava packages and show high resistivity within the static images. Individual lava lobes can typically be identified, with a contrast between coherent lava cores and vesicular margins. Rubbly tops and bases are also observed. B is representative of hyaloclastite (as above). Image C is a representation of pillow lavas (from the Rosebank Field; (Watton et al. 2014) within a sequence; however, pillow lavas were not observed within the Cambo data. Image D is of peperite (as above), where high resistivity juvenile clasts are surrounded by conductive sediment. Image E is part of a sedimentary sequence in which bedding is clearly visible. This is possibly volcanoclastic sediment, as some beds show a higher resistivity. The field examples show each feature as seen in Mountain Home.

This conceptual model plus the hypothetical graphical log, FMI images, and field images provide a basis for recognising key features within the lithostratigraphy of a lava-dominated sequence. Whilst these responses do not cover every eventuality, they illustrate the value of, and necessity for, knowledge of field analogues in addition to the direct well information. The significance of linking the borehole image data to field examples is to understand the scales and, where possible, geometries of these features in order to accurately understand and make correlations (e.g. between wells). In challenging areas of exploration, such as the NAIP, it is just as crucial to eliminate possibilities, as it is to define them, on a number of scales. It is proposed that this model serves as an 'atlas' to those in the industry investigating complex lava-sedimentary sequences.

**Figure 7-8: (next page): A 3D model through an interbedded lava-sedimentary succession, with a sketch log, FMI responses and field examples through a hypothetical well site. The top section is a 3D model, reconfigured from the Mountain Home case study (Chapter 4) with a hypothetical well site overlain. The bottom section shows a schematic sketch log through the hypothetical well, indicating the likely features that would be seen. In the middle (A-F), examples of likely FMI images are shown to correlate with the features on the sketch log. The colour scale bar indicates resistivity and conductivity. Image C shows pillow lavas, but this is not from the Cambo Field as no pillows were observed (image adapted from Watton et al. (2014)). The third column (G-L) shows field examples (from Mountain Home, Idaho) of each of these features.**



### 7.3.3 Basin-scale implications of lava-water-sediment interaction

Possibly the largest unanswered question surrounding the products of lava-water-sediment interaction (described within this thesis), is what affect do these lithofacies have on reservoir potential and petroleum systems? Volcanic rocks are capable of acting as source rocks, traps, reservoirs, seals, and migration pathways for hydrocarbons, yet the effects of volcanic rocks at basin scale are poorly constrained. Regions where flood basalts blanket sedimentary basins, without intrusions in the direct subsurface, are likely the most prospective (Halford et al 2012). Recent studies have shown how intrusions cause compartmentalisation of the petroleum system, and act as barriers and baffles to fluid movements, and are associated with hydrothermal fluids (see: Schutter 2003; Planke et al. 2005; Rohrman 2007; Halford et al. 2012; Schofield and Jolley 2013). Compartmentalisation is defined as the segregation of a petroleum accumulation in to multiple individual fluid/pressure compartments (Jolley et al. 2010). Little discussion however, is given to the lava-sediment interface and lava-sedimentary geometries.

Hyaloclastite and pillow breccias are reported to be good reservoir and stratigraphic traps (Schutter 2003) if emplaced into favourable conditions (e.g. a lacustrine setting, that has underlying organic-rich sediment, acting as the source rock, and overlying sub-aerial lavas and lacustrine sediments acting as lateral and top seals) (Schutter 2003). Peperites, associated with maar diatremes, have also been described as reservoir rocks, due to associated lacustrine deposits that likely provide both a source and seal (Barrabe 1932; Schutter 2003). However, these facies also occur in other depositional environments.

This research has shown that the lava-sediment interface can be extremely variable in thickness, lateral extent, and 3D geometry, providing challenges in understanding complex offshore sequences. Limited mingling and/or passive contacts, like at Kinghorn (Chapter 3), cause little effect on the sedimentary domain, and are most similar to the layer cake geometries of blanketing flood basalts. Invasive lavas, however, cause highly disruptive interfaces, as seen at St. Cyrus (Chapter 6), and extensively disrupt the sedimentary domain. Accurately predicting the lateral extent of these features on a large-scale is difficult, and may always remain a challenge. However, a conceptual well-log correlation is presented (Figure 7-9), which illustrates a range of lava-sediment interfaces associated with the interplay of sub-aerial lava, volcanoclastic, and siliciclastic systems. The aim of the diagram is to highlight the possible geometries of

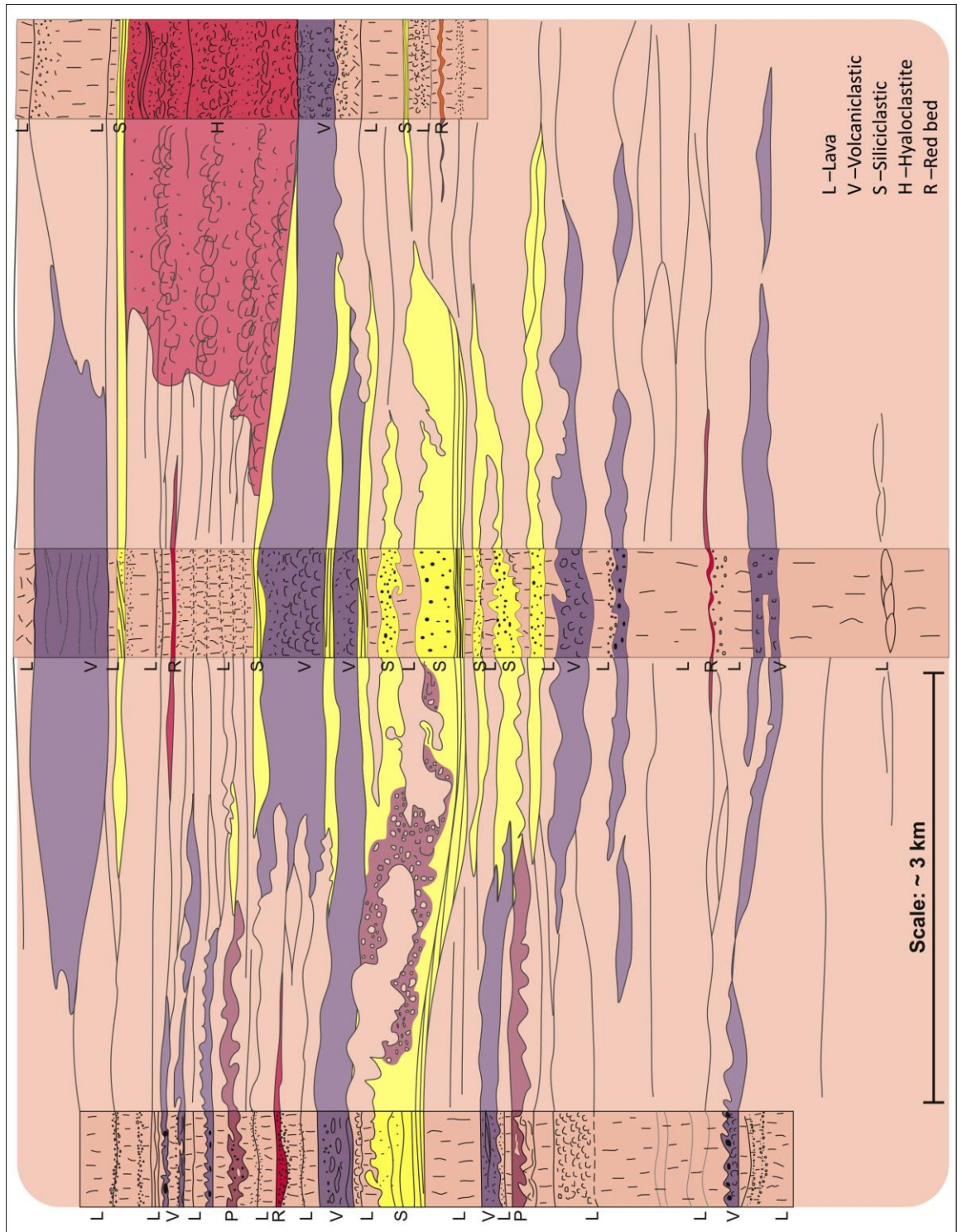
lava-water-sediment interactions, to aid recognition of their impact on petroleum systems.

The model shows the invasion of lava into a siliciclastic body, and a large peperite domain (Figure 7-9). If peperite is considered a good reservoir rock (Schutter 2003) then this domain may have limited effect on the migration and storage of hydrocarbons. However, considering the peperite as a seal, possibly due to diagenetic effects and geometry of the interface, then the domain could cause compartmentalisation of the siliciclastic body, which would provide problems during predictions of lateral continuity, thickness, connectivity, and likely accumulations within the potential reservoir.

The lava-sediment interface can no longer be considered a simple layer-cake geometry at basin-scale. Not only are intra-lava flow field geometries complex, but the interface between lava and sediment can also be highly variable. Disruption of sedimentary bodies is not restricted to igneous intrusions. Consideration of the presence and likely effects of lava-water-sediment interactions at basin-scale is important for more accurate delineation of the subsurface and hydrocarbon exploration.

**Figure 7-9: (next page) Hypothetical well log interpretation and correlation of a lava-dominated sequence (~175 m thick) at basin scale (km).**

The log data has been interpreted from FMI images from the Cambo field, and hypothetical correlations have been inferred. Note the disruption of the siliciclastic sedimentary bodies by the lava, forming peperite. This figure shows how lava-sediment interfaces can be interpreted, and illustrates the potential problems that cause difficulties for petroleum exploration within lava-dominated sequences. Key: L = lava, V = volcanoclastic sediments, S = siliciclastic sediments, P = peperite, H = hyaloclastite and pillow breccia, R = red bed.



---

## 7.4 Further work

Future work arising from the findings of this thesis could include the following:

- The prevalence of sedimentary inclusions within lava-water-sediment interfaces poses questions surrounding the effects of these within the lava. For example, what effect do the inclusions have on the porosity and permeability of the lavas in which they are contained?
- Computer based models could be created to test the range and scale of sedimentary properties and how they are affected by lava. This could also be expanded to involve a range of lava types (e.g. morphological and compositional differences - rhyolite and 'a'a vs. basalt and pahoehoe), as well as sedimentary types, such as carbonates and evaporates. This would widen the breadth of knowledge surrounding lava-sediment interactions, as well as providing interactive models that can be utilised within academia and industry.
- Future use and application of the conceptual model and field analogues to other industry led projects would increase the knowledge base of lava-water-sediment interactions. This could be aided by field-testing of the gamma responses from the newly identified facies recognised in this work, together with generating synthetic seismic cubes to demonstrate the architecture hypothesised in Figure 7-9.

## Chapter 8: Conclusions

This research has demonstrated that sedimentary properties (e.g. water content, consolidation and grain size) are critical in controlling the processes and products of lava-water-sediment interaction, and that the properties of the lava (e.g. effusion rates/flux) are not the dominant factor, as previously assumed. Although the role of sediment had always been inferred, it is much more influential in lava-water, and lava-water-sediment interactions, than was previously recognised. This research accurately, and for the first time, recognises the array of textures that can be produced, on both the macro- and micro-scale, between basaltic lavas and siliciclastic sediments, and explains how their formation is controlled by the sediment properties.

This research has demonstrated the scale at which lava-water-sediment interaction occurs and the complexity of the interfaces between lavas and sedimentary rocks. The geometries of lava-water-sediment domains may be further complicated, as a consequence of the depositional environment, such as dynamic fluvial floodplains, as demonstrated in Chapter 6 (St. Cyrus). These results are important to the petroleum industry as they: 1) provide greater understanding of how potential reservoir units may be disrupted by lavas (both physically and by “compartmentalization” of the reservoir); and 2) how lavas, which can be petroleum seals/traps, have the potential to considerably fragment on interaction with sediment and/or water (e.g. St Cyrus). Together, these data will help to develop petroleum plays in volcanic rifted margins, and de-risk exploration in these areas.

The results of this thesis/research have a strong applicability to the petroleum industry in aiding exploration within volcanic-rifted margins. The use of detailed field analogues aids the interpretation of industry acquired well data, and informs our understanding of the interplay of volcanic and sedimentary systems.

## References

- ALLEN, J.R., 1982, Sedimentary structures, their character and physical basis, Elsevier.
- ANGUITA, F., and HERNÁN, F., 2000, The Canary Islands origin: a unifying model: *Journal of Volcanology and Geothermal Research*, **103**, 1-26.
- ARMSTRONG, M., and PATERSON, I.B., 1970, The Lower Old Red Sandstone of the Strathmore Region, HM Stationery Office.
- ASQUITH, G.B., KRYGOWSKI, D., and GIBSON, C.R., 2004, Basic well log analysis, American association of petroleum geologists Tulsa.
- BALCELLS, R., BARRERA, J., and GÓMEZ, J., 1992, Geological map 21-21/21-22 Isla de Gran Canaria: *Geological Map of Spain. IGME, Madrid*.
- BARRABE, L., 1932, Oil in Limagne Area, France: *AAPG Bulletin*, **16**, 825-832.
- BATIZA, R., and WHITE, J.D., 2000, Submarine lavas and hyaloclastite: *Encyclopedia of volcanoes*, 361-381.
- BEAR, A.N., and CAS, R.A.F., 2007, The complex facies architecture and emplacement sequence of a Miocene submarine mega-pillow lava flow system, Muriwai, North Island, New Zealand: *Journal of Volcanology and Geothermal Research*, **160**, 1-22.
- BELL, B., and BUTCHER, H., 2002, On the emplacement of sill complexes: evidence from the Faroe-Shetland Basin: *Geological Society, London, Special Publications*, **197**, 307-329.
- BERANEK, L.P., LINK, P.K., and FANNING, C.M., 2006, Miocene to Holocene landscape evolution of the western Snake River Plain region, Idaho: Using the SHRIMP detrital zircon provenance record to track eastward migration of the Yellowstone hotspot: *Geological Society of America Bulletin*, **118**, 1027-1050.
- BERGER, A., GIER, S., and KROIS, P., 2009, Porosity-preserving chlorite cements in shallow-marine volcanoclastic sandstones: Evidence from Cretaceous sandstones of the Sawan gas field, Pakistan: *AAPG bulletin*, **93**, 595-615.
- BLAIR, T.C., and MCPHERSON, J.G., 1999, Grain-size and textural classification of coarse sedimentary particles: *Journal of Sedimentary Research*, **69**.
- BLUCK, B.J., 2000, Old Red Sandstone basins and alluvial systems of Midland Scotland, in Friend, P.F.W.B.P.J., ed., *New Perspectives on the Old Red Sandstone*, Volume 180: Geological Society Special Publication, p. 417-437.
- BOLDREEL, L.O., 2006, Wire-line log-based stratigraphy of flood basalts from the Lopra-1/1A well, Faroe Islands: *Geological Survey of Denmark and Greenland Bulletin*, **9**, 7-22.
- BONNICHSEN, B., and GODCHAUX, M., 2002, Late Miocene, Pliocene, and Pleistocene geology of southwestern Idaho with emphasis on basalts in the Bruneau-Jarbidge, Twin Falls, and western Snake River Plain regions: *Tectonic and Magmatic Evolution of the Snake River Plain Volcanic Province: Idaho Geological Survey Bulletin*, **30**, 233-312.
- BONNICHSEN, B., LEEMAN, W., HONJO, N., MCINTOSH, W., and GODCHAUX, M., 2008, Miocene silicic volcanism in southwestern Idaho: geochronology, geochemistry, and evolution of the central Snake River Plain: *Bulletin of Volcanology*, **70**, 315-342.
- BONNICHSEN, B., MCCURRY, M., and GODCHAUX, M.M., 2004, Miocene Snake River Plain rhyolites of the Owyhee Front, Owyhee County, Idaho: *Geological field trips in southern Idaho, eastern Oregon, and northern Nevada. Boise State University, Boise*, 154-173.

- BRANNEY, M., BONNICHSEN, B., ANDREWS, G., ELLIS, B., BARRY, T., and MCCURRY, M., 2008, 'Snake River (SR)-type'volcanism at the Yellowstone hotspot track: distinctive products from unusual, high-temperature silicic super-eruptions: *Bulletin of Volcanology*, **70**, 293-314.
- BRANNEY, M.J., and KOKELAAR, B.P., 2002, Pyroclastic density currents and the sedimentation of ignimbrites, Geological Society of London.
- BROOKS, E.R., 1995, Paleozoic fluidization, folding, and peperite formation, northern Sierra Nevada, California: *Canadian Journal of Earth Sciences*, **32**, 314-324.
- BROWN, D.J., and BELL, B.R., 2007, How do you grade peperites?: *Journal of Volcanology and Geothermal Research*, **159**, 409-420.
- BROWN, R., BLAKE, S., BONDRE, N., PHADNIS, V., and SELF, S., 2011, 'A'ā lava flows in the Deccan Volcanic Province, India, and their significance for the nature of continental flood basalt eruptions: *Bulletin of Volcanology*, **73**, 737-752.
- BROWN, R., BONADONNA, C., and DURANT, A., 2012, A review of volcanic ash aggregation: *Physics and Chemistry of the Earth, Parts A/B/C*, **45**, 65-78.
- BROWN, R., BRANNEY, M., MAHER, C., and DÁVILA-HARRIS, P., 2010, Origin of accretionary lapilli within ground-hugging density currents: evidence from pyroclastic couplets on Tenerife: *Geological Society of America Bulletin*, **122**, 305-320.
- BROWNE, M., DEAN, M., HALL, I.H., MCADAM, A., MONRO, S., and CHISHOLM, J., 1999, A lithostratigraphical framework for the Carboniferous rocks of the Midland Valley of Scotland. Version 2.
- BROWNE, M., SMITH, R., and AITKEN, A.M., 2002, Stratigraphical framework for the Devonian (Old Red Sandstone) rocks of Scotland south of a line from Fort William to Aberdeen.
- BUSBY-SPERA, C., and WHITE, J.L., 1987, Variation in peperite textures associated with differing host-sediment properties: *Bulletin of Volcanology*, **49**, 765-776.
- CABRERA, M., GIMENO TORRENTE, D., and PEREZ-TORRADO, F.-J., 2008, Vulcanismo y sedimentación: interrelación en ambientes costeros.
- CAREY, S.N., and SCHNEIDER, J.-L., 2011, Chapter 7 - Volcaniclastic Processes and Deposits in the Deep-Sea, in Heiko, H., and Thierry, M., eds., *Developments in Sedimentology*, Volume Volume 63, Elsevier, p. 457-515.
- CARRACEDO, J.C., DAY, S., GUILLOU, H., RODRÍGUEZ BADIOLA, E., CANAS, J., and PÉREZ TORRADO, F., 1998, Hotspot volcanism close to a passive continental margin: the Canary Islands: *Geological Magazine*, **135**, 591-604.
- CARRACEDO, J.C., PÉREZ TORRADO, F., ANCOCHEA, E., MECO, J., HERNÁN, F., CUBAS, C.R., CASILLAS, R., RODRÍGUEZ-BADIOLA, E., and AHIJADO, A., 2002, Cenozoic volcanism II: the Canary islands. In: Gibbons, F.A.W. & Moreno, T. (eds) *The Geology of Spain.*, Geological Society of London.
- CAS, R.A.F., EDGAR, C., ALLEN, R.L., BULL, S., CLIFFORD, B.A., GIORDANO, G., and WRIGHT, J.V., 2001, Influence of Magmatism and Tectonics on Sedimentation in an Extensional Lake Basin: The Upper Devonian Bunga Beds, Boyd Volcanic Complex, South-Eastern Australia, in White, J.D.L., and Riggs, N.R., eds., *Volcaniclastic Sedimentation in Lacustrine Settings*, Int. Assoc. Sediment. Spec. Publ., Blackwell Publishing Ltd., p. 81-108.
- CAS, R.F., and WRIGHT, J.V., 1987, *Volcanic Succession: Modern and ancient*: London, Allen & Unwin, 528 p.

- CLEMENS, D., and WOOD, S., 1993, Radiometric dating, volcanic stratigraphy, and sedimentation in the Boise foothills, northeastern margin of the western Snake River Plain: *Ada County, Idaho: Isochron/West*, **59**, 3-10.
- CRISP, J., and BALOGA, S., 1994, Influence of crystallization and entrainment of cooler material on the emplacement of basaltic aa lava flows: *Journal of Geophysical Research-Solid Earth*, **99**, 11819-11831.
- CUKUR, D., HOROZAL, S., KIM, D.C., LEE, G.H., HAN, H.C., and KANG, M.H., 2010, The distribution and characteristics of the igneous complexes in the northern East China Sea Shelf Basin and their implications for hydrocarbon potential: *Marine Geophysical Researches*, **31**, 299-313.
- DADD, K.A., and VAN WAGONER, N.A., 2002, Magma composition and viscosity as controls on peperite texture: an example from Passamaquoddy Bay, southeastern Canada: *Journal of Volcanology and Geothermal Research*, **114**, 63-80.
- DOHRENWEND, J.C., ABRAHAMS, A.D., and TURRIN, B.D., 1987, Drainage development on basaltic lava flows, Cima volcanic field, southeast California, and Lunar Crater volcanic field, south-central Nevada: *Geological Society of America Bulletin*, **99**, 405-413.
- DORÉ, A., LUNDIN, E., JENSEN, L., BIRKELAND, Ø., ELIASSEN, P., and FICHLER, C., 1999, Principal tectonic events in the evolution of the northwest European Atlantic margin, Geological Society, London, Petroleum Geology Conference series, Volume 5, Geological Society of London, p. 41-61.
- DOS ANJOS, S.M., DE ROS, L.F., DE SOUZA, R.S., DE ASSIS SILVA, C.M., and SOMBRA, C.L., 2000, Depositional and diagenetic controls on the reservoir quality of Lower Cretaceous Pendencia sandstones, Potiguar rift basin, Brazil: *AAPG bulletin*, **84**, 1719-1742.
- DOYLE, M.G., 2000, Clast shape and textural associations in peperite as a guide to hydromagmatic interactions: Upper Permian basaltic and basaltic andesite examples from Kiama, Australia: *Australian Journal of Earth Science*, **47**, 167-177.
- DUNCAN, L., HELLAND-HANSEN, D., and DENNEHY, C., 2009, The Rosebank Discovery A new play type in intra basalt reservoirs of the North Atlantic volcanic province, Devex Conference.
- DURANT, A., SHAW, R., ROSE, W., MI, Y., and ERNST, G., 2008, Ice nucleation and over seeding of ice in volcanic clouds: *Journal of Geophysical Research: Atmospheres (1984-2012)*, **113**.
- DURANT, A.J., and ROSE, W.I., 2009, Sedimentological constraints on hydrometeor-enhanced particle deposition: 1992 Eruptions of Crater Peak, Alaska: *Journal of Volcanology and Geothermal Research*, **186**, 40-59.
- EBINGHAUS, A., HARTLEY, A.J., JOLLEY, D.W., HOLE, M., and MILLETT, J., 2014, Lava-Sediment Interaction and Drainage-System Development In A Large Igneous Province: Columbia River Flood Basalt Province, Washington State, USA: *Journal of Sedimentary Research*, **84**, 1041-1063.
- EDWARDS, B.R., BELOUSOV, A., and BELOUSOVA, M., 2014, Propagation style controls lava-snow interactions: *Nat Commun*, **5**.
- ELLIS, D., PASSEY, S., JOLLEY, D., and BELL, B., 2009, Transfer zones: The application of new geological information from the Faroe Islands applied to the offshore exploration of intra basalt and sub-basalt strata, Faroe Islands Exploration Conference: Proceedings of the 2nd Conference. *Annales Societatis Scientiarum Færoensis, Tórshavn*, Volume 50, p. 205-226.
- ELY, L.L., BROSSY, C.C., HOUSE, P.K., SAFRAN, E.B., O'CONNOR, J.E., CHAMPION, D.E., FENTON, C.R., BONDRE, N.R., OREM, C.A., GRANT, G.E.,

- HENRY, C.D., and TURRIN, B.D., 2012, Owyhee River intracanyon lava flows: Does the river give a dam?: *Geological Society of America Bulletin*.
- FISHER, R.V., 1961, Proposed classification of volcanoclastic sediments and rocks: *Geological Society of America Bulletin*, **72**, 1409-1414.
- FISHER, R.V., 1966, Rocks composed of volcanic fragments and their classification: *Earth-Science Reviews*, **1**, 287-298.
- FISKE, R., and JACKSON, E., 1972, Orientation and growth of Hawaiian volcanic rifts: the effect of regional structure and gravitational stresses, *Proceedings of the Royal Society of London A: Mathematical, Physical and Engineering Sciences*, Volume 329, The Royal Society, p. 299-326.
- FURNES, H., and FRIDLEIFSSON, I.B., 1974, Tidal Effects on the Formation of Pillow Lava/Hyaloclastite Deltas: *Geology*, **2**, 381-384.
- FURNES, H., and STURT, B.A., 1976, Beach/shallow marine hyaloclastite deposits and their geological significance: an example from Gran Canaria: *The Journal of Geology*, 439-453.
- GABALDÓN, V., 1989, Formación detrítica de Las Palmas. Sus facies y evolución sedimentológica.
- GAILLOT, P., BREWER, T., PEZARD, P., and EN CHAO, Y., 2007, 'Borehole Imaging Tools– Principles and Applications': *Scientific Drilling*, 1-4.
- GERNON, T., UPTON, B., and HINCKS, T., 2013, Eruptive history of an alkali basaltic diatreme from Elie Ness, Fife, Scotland: *Bulletin of volcanology*, **75**, 1-20.
- GILBERT, J.S., and LANE, S., 1994, The origin of accretionary lapilli: *Bulletin of Volcanology*, **56**, 398-411.
- GODCHAUX, M.M., and BONNICHSEN, B., 2002, Syneruptive magma-water and posteruptive lava-water interactions in the Western Snake River Plain, Idaho, during the past 12 million years: *Tectonic and magmatic evolution of the Snake River Plain Volcanic Province. Idaho Geol Surv Bull*, **30**, 387-434.
- GODCHAUX, M.M., BONNICHSEN, B., and JENKS, M.D., 1992, Types of phreatomagmatic volcanoes in the western Snake River Plain, Idaho, USA: *Journal of Volcanology and Geothermal Research*, **52**, 1-25.
- GOTO, Y., and MCPHIE, J., 2004, Morphology and propagation styles of Miocene submarine basaltic lavas at Stanley, northwestern Tasmania, Australia: *Journal of Volcanology and Geothermal Research*, **130**, 307-328.
- GRABOWSKI, R.C., DROPPA, I.G., and WHARTON, G., 2011, Erodibility of cohesive sediment: The importance of sediment properties: *Earth-Science Reviews*, **105**, 101-120.
- GREGG, T.K.P., and FINK, J.H., 2000, A laboratory investigation into the effects of slope on lava flow morphology: *Journal of Volcanology and Geothermal Research*, **96**, 145-159.
- GREGG, T.K.P., and SMITH, D.K., 2003, Volcanic investigations of the Puna Ridge, Hawai'i: relations of lava flow morphologies and underlying slopes: *Journal of Volcanology and Geothermal Research*, **126**, 63-77.
- GRIFFITHS, R.W., and FINK, J.H., 1992, Solidification and morphology of submarine lavas: A dependence on extrusion rate: *Journal of Geophysical Research: Solid Earth*, **97**, 19729-19737.
- GROVE, C., 2013, Submarine hydrothermal vent complexes in the Paleocene of the Faroe-Shetland Basin: Insights from three-dimensional seismic and petrographical data: *Geology*, **41**, 71-74.
- GUILLOU, H., TORRADO, F.J.P., MACHIN, A.R.H., CARRACEDO, J.C., and GIMENO, D., 2004, The Plio-Quaternary volcanic evolution of Gran Canaria

- based on new K-Ar ages and magneto stratigraphy: *Journal of Volcanology and Geothermal Research*, **135**, 221-246.
- HALL, R.C.B., and ELS, B.G., 2002, The origin and significance of load-induced deformation structures in soft-sediment and lava at the base of the Archaean Ventersdorp Supergroup, South Africa: *Journal of African Earth Sciences*, **35**, 135-145.
- HANSON, R.E., HARGROVE, U.S., 1999, Processes of magma/wet sediment interaction in a large-scale Jurassic andesitic peperite complex, northern Sierra Nevada, California: *Bulletin of Volcanology*, **60**, 610-626.
- HANSON, R.E., and WILSON, T.J., 1993, Large-scale rhyolite peperites (Jurassic, southern Chile): *Journal of Volcanology and Geothermal Research*, **54**, 247-264.
- HAUGHTON, P., 1989, Structure of some Lower Old Red Sandstone conglomerates, Kincardineshire, Scotland: deposition from late-orogenic antecedent streams?: *Journal of the Geological Society*, **146**, 509-525.
- HAWLADER, H., 1990, Diagenesis and reservoir potential of volcanogenic sandstones—Cretaceous of the Surat Basin, Australia: *Sedimentary Geology*, **66**, 181-195.
- HELLAND-HANSEN, D., 2009, Rosebank-challenges to development from a subsurface perspective, Faroe Islands Exploration Conference: Proceedings of the 2nd Conference. *Annales Societatis Scientiarum, Færoensis, Supplementum*, Volume 50, p. 63-78.
- HELM-CLARK, C.M., RODGERS, D.W., and SMITH, R.P., 2004, Borehole geophysical techniques to define stratigraphy, alteration and aquifers in basalt: *Journal of applied geophysics*, **55**, 3-38.
- HOLE, M., JOLLEY, D., HARTLEY, A., LELEU, S., JOHN, N., and BALL, M., 2013, Lava-sediment interactions in an Old Red Sandstone basin, NE Scotland: *Journal of the Geological Society*, **170**, 641-655.
- HOLFORD, S., SCHOFIELD, N., MACDONALD, J., DUDDY, I., and GREEN, P., 2012, Seismic analysis of igneous systems in sedimentary basins and their impacts on hydrocarbon prospectivity: examples from the southern Australian margin.
- HON, K., KAUAHIKUAU, J., DENLINGER, R., and MACKAY, K., 1994, Emplacement and inflation of pahoehoe sheet flows - observations and measurements of active lava flows on Kilauea volcano, Hawaii: *Geological Society of America Bulletin*, **106**, 351-370.
- JEAN, M.M., HANAN, B.B., and SHERVAIS, J.W., 2014, Yellowstone hotspot-continental lithosphere interaction: *Earth and Planetary Science Letters*, **389**, 119-131.
- JENKS, M., BONNICHSEN, B., and GODCHAUX, M., 1998, Geologic map of the Grand View-Bruneau area, Owyhee County, Idaho. Technical Report 98-1. Idaho Geological Survey, University of Idaho, Moscow. 21 pp. plus map.
- JENKS, M.D., and BONNICHSEN, B., 1989, Subaqueous basalt eruptions into Pliocene Lake Idaho, Snake River Plain, Idaho: *Guidebook to the geology of northern and western Idaho and surrounding area: Idaho Geological Survey Bulletin*, **28**, 17-34.
- JERRAM, D.A., and STOLLHOFEN, H., 2002, Lava-sediment interaction in desert settings; are all peperite-like textures the result of magma-water interaction?: *Journal of Volcanology and Geothermal Research*, **114**, 231-249.
- JOLLEY, S.J., FISHER, Q.J., and AINSWORTH, R.B., 2010, Reservoir compartmentalization: an introduction: *Geological Society, London, Special Publications*, **347**, 1-8.

- JONES, J.G., and NELSON, P.H.H., 1970, The flow of basalt lava from air into water - its structural expression and stratigraphic significance: *Geological Magazine*, **107**, 13-19.
- KANO, K.-I., 1989, Interactions between andesitic magma and poorly consolidated sediments: Examples in the neogene shirahama group, South Izu, Japan: *Journal of Volcanology and Geothermal Research*, **37**, 59-75.
- KANO, K., 1991, Miocene pillowed sills in the Shimane Peninsula, SW Japan: *Journal of Volcanology and Geothermal Research*, **48**, 359-366.
- KATAOKA, K., 2005, Distal fluvio-lacustrine volcanoclastic resedimentation in response to an explosive silicic eruption: the Pliocene Mushono tephra bed, central Japan: *Geological Society of America Bulletin*, **117**, 3-17.
- KAUHIKAUA, J., CASHMAN, K.V., MATTOX, T.N., HELIKER, C.C., HON, K.A., MANGAN, M.T., and THORNER, C.R., 1998, Observations on basaltic lava streams in tubes from Kilauea Volcano, island of Hawai'i: *Journal of Geophysical Research: Solid Earth (1978-2012)*, **103**, 27303-27323.
- KNOTT, S., BURCHELL, M., JOLLEY, E., and FRASER, A., 1993, Mesozoic to Cenozoic plate reconstructions of the North Atlantic and hydrocarbon plays of the Atlantic margins, Geological Society, London, Petroleum Geology Conference series, Volume 4, Geological Society of London, p. 953-974.
- KOKELAAR, B.P., 1982, Fluidization of wet sediments during the emplacement and cooling of various igneous bodies: *Journal of the Geological Society*, **139**, 21-33.
- KOKELAAR, B.P., BEVINS, R.E., and ROACH, R.A., 1985, Submarine silicic volcanism and associated sedimentary and tectonic processes, Ramsey Island, SW Wales: *Journal of the Geological Society*, **142**, 591-613.
- KREISA, R.D., 1981, Storm-generated sedimentary structures in subtidal marine facies with examples from the Middle and Upper Ordovician of southwestern Virginia: *Journal of Sedimentary Research*, **51**.
- LAMERS, E., and CARMICHAEL, S., 1999, The Paleocene deepwater sandstone play West of Shetland, Geological Society, London, Petroleum Geology Conference series, Volume 5, Geological Society of London, p. 645-659.
- LARSEN, M., RASMUSSEN, T., and HJELM, L., 2010, Cretaceous revisited: exploring the syn-rift play of the Faroe-Shetland Basin, Geological Society, London, Petroleum Geology Conference series, Volume 7, Geological Society of London, p. 953-962.
- LEEDER, M.R., 2009, Sedimentology and sedimentary basins: from turbulence to tectonics, John Wiley & Sons.
- LEVIN, L., 1995, VOLCANOGENIC AND VOLCANICLASTIC RESERVOIR ROCKS IN MESOZOIC-CENOZOIC ISLAND ARCS: EXAMPLES FROM THE CAUCASUS AND THE NW PACIFIC: *Journal of Petroleum Geology*, **18**, 267-288.
- LIETZ, J., and SCHMINCKE, H.U., 1975, Miocene–pliocene sea-level changes and volcanic phases on gran Canaria (Canary islands) in the light of new K–Ar ages: *Palaeogeography, Palaeoclimatology, Palaeoecology*, **18**, 213-239.
- LONG, P.E., and WOOD, B.J., 1986, Structures, textures, and cooling histories of Columbia River basalt flows: *Geological Society of America Bulletin*, **97**, 1144-1155.
- LORENZ, B.E., 1984, Mud-magma interactions in the Dunnage Melange, Newfoundland. In: Kokelaar, B.P., Howells, M. (Eds.), Volcanic and Associated Sedimentary and Tectonic Processes in Modern and Ancient Marginal Basins: *Geol. Soc. London. Special Publication*, 271-277.

- LORENZ, V., ZIMANOWSKI, B., and BUETTNER, R., 2002, On the formation of deep-seated subterranean peperite-like magma-sediment mixtures: *Journal of Volcanology and Geothermal Research*, **114**, 107-118.
- LYLE, P., 2000, The eruption environment of multi-tiered columnar basalt lava flows: *Journal of the Geological Society*, **157**, 715-722.
- MACDONALD, G., 1953, Pahoehoe, 'a'a and block lava: *American Journal of Science*, **251**, 169-191.
- MACDONALD, R., and FETTES, D., 2007, The tectonomagmatic evolution of Scotland: *Transactions of the Royal Society of Edinburgh; Earth Sciences*, **97**, 213-295.
- MALDE, H.E., 1991, Quaternary geology and structural history of the Snake River Plain, Idaho and Oregon: *The Geology of North America*, **2**, 251-281.
- MALDE, H.E., and POWERS, H.A., 1962, Upper Cenozoic stratigraphy of western Snake River Plain, Idaho: *Geological Society of America Bulletin*, **73**, 1197-1220.
- MALDE, H.E., and POWERS, H.A., 1972, Geological map of the Glens Ferry-Hagerman area, west-central Snake River Plain, Idaho.
- MALTMAN, A.J., and BOLTON, A., 2003, How sediments become mobilized: *Geological Society, London, Special Publications*, **216**, 9-20.
- MANVILLE, V., NÉMETH, K., and KANO, K., 2009, Source to sink: A review of three decades of progress in the understanding of volcanoclastic processes, deposits, and hazards: *Sedimentary Geology*, **220**, 136-161.
- MARESH, J., WHITE, R.S., HOBBS, R.W., and SMALLWOOD, J.R., 2006, Seismic attenuation of Atlantic margin basalts: Observations and modeling: *Geophysics*, **71**, B211-B221.
- MATHISEN, M.E., and MCPHERSON, J.G., 1991, Volcanoclastic deposits: implications for hydrocarbon exploration: Tulsa, Ok, Society of Economic Paleontologists and Mineralogists Special Publication.
- MCLEAN, C.E., BROWN, D.J., and RAWCLIFFE, H.J., 2016, Extensive disruption at the base of the Jump Creek Rhyolite Lava, Owyhee Mountains, Idaho: *Bulletin of Volcanology*.
- MCPHIE, J., DOYLE, M.G., and ALLEN, R., 1993, Volcanic Textures: A guide to the interpretation of textures in volcanic rocks, CODES Key Centre, University of Tasmania, 196 p.
- MECO, J., KOPPERS, A.A.P., MIGGINS, D.P., LOMOSCHITZ, A., and BETANCORT, J.-F., 2015, The Canary record of the evolution of the North Atlantic Pliocene: New  $^{40}\text{Ar}/^{39}\text{Ar}$  ages and some notable palaeontological evidence: *Palaeogeography, Palaeoclimatology, Palaeoecology*, **435**, 53-69.
- MECO, J., SCAILLET, S., GUILLOU, H., LOMOSCHITZ, A., CARLOS CARRACEDO, J., BALLESTER, J., BETANCORT, J.-F., and CILLEROS, A., 2007, Evidence for long-term uplift on the Canary Islands from emergent Mio-Pliocene littoral deposits: *Global and Planetary Change*, **57**, 222-234.
- MIDDLETON, L.T., PORTER, M.L., and KIMMEL, P.G., 1985, Depositional settings of the Chalk Hills and Glens Ferry formations west of Bruneau, Idaho, Rocky Mountain Section (SEPM).
- MITSUHATA, Y., MATSUO, K., and MINEGISHI, M., 1999, Magnetotelluric survey for exploration of a volcanic-rock reservoir in the Yurihara oil and gas field, Japan\*: *Geophysical Prospecting*, **47**, 195-218.
- MOORE, J.G., 1975, Mechanism of formation of pillow lava *American Scientist*, 269-277.
- MOUNT, J.F., 1984, Mixing of siliciclastic and carbonate sediments in shallow shelf environments: *Geology*, **12**, 432-435.

- MOY, D., and IMBER, J., 2009, A critical analysis of the structure and tectonic significance of rift-oblique lineaments ('transfer zones') in the Mesozoic-Cenozoic succession of the Faroe-Shetland Basin, NE Atlantic margin: *Journal of the Geological Society*, **166**, 831-844.
- NELSON, C.E., JERRAM, D.A., and HOBBS, R.W., 2009, Flood basalt facies from borehole data: implications for prospectivity and volcanology in volcanic rifted margins: *Petroleum Geoscience*, **15**, 313-324.
- OWEN, G., 2003, Load structures: gravity-driven sediment mobilization in the shallow subsurface: *Geological Society, London, Special Publications*, **216**, 21-34.
- PALINKAŠ, L.A., BERMANEC, V., ŠOŠTARIĆ, S.B., KOLAR-JURKOVŠEK, T., PALINKAŠ, S.S., MOLNAR, F., and KNIEWALD, G., 2008, Volcanic facies analysis of a subaqueous basalt lava-flow complex at Hruškovec, NW Croatia—Evidence of advanced rifting in the Tethyan domain: *Journal of Volcanology and Geothermal Research*, **178**, 644-656.
- PAREDES, J.M., FOIX, N., PIÑOL, F.C., NILLNI, A., ALLARD, J.O., and MARQUILLAS, R.A., 2007, Volcanic and climatic controls on fluvial style in a high-energy system: The Lower Cretaceous Matasiete Formation, Golfo San Jorge basin, Argentina: *Sedimentary Geology*, **202**, 96-123.
- PEDERSEN, G.K., LARSEN, L.M., PEDERSEN, A.K., and HJORTKJÆR, B.F., 1998, The syn-volcanic Naajaat lake, Paleocene of West Greenland: *Palaeogeography, Palaeoclimatology, Palaeoecology*, **140**, 271-287.
- PÉREZ-TORRADO, F., CARRACEDO, J., and MANGAS, J., 1995, Geochronology and stratigraphy of the Roque Nublo Cycle, Gran Canaria, Canary Islands: *Journal of the Geological Society*, **152**, 807-818.
- PÉREZ-TORRADO, F., MARTI, J., MANGAS, J., and DAY, S., 1997, Ignimbrites of the Roque Nublo group, Gran Canaria, Canary Islands: *Bulletin of volcanology*, **58**, 647-654.
- PEREZ-TORRADO, F.J., GIMENO, D., AULINAS, M., CABRERA, M.C., GUILLOU, H., RODRIGUEZ-GONZALEZ, A., GISBERT, G., and FERNANDEZ-TURIEL, J.L., 2014, Polygonal feeder tubes filled with hydroclasts: a new volcanic lithofacies marking shoreline subaerial-submarine transition: *Journal of the Geological Society*.
- PÉREZ TORRADO, F.J., SANTANA, F., RODRÍGUEZ SANTANA, A., MELIÁN, A., LOMOSCHITZ MORA-FIGUEROA, A., GIMENO, D., CABRERA, M.C., and BAEZ, M., 2002, Reconstrucción paleogeográfica de depósitos volcanosedimentarios Pliocenos en el litoral NE de Gran Canaria (Islas Canarias) mediante métodos topográficos.
- PETRY, K., JERRAM, D.A., DE ALMEIDA, D.D.P.M., and ZERFASS, H., 2007, Volcanic-sedimentary features in the Serra Geral Fm., Paraná Basin, southern Brazil: Examples of dynamic lava-sediment interactions in an arid setting: *Journal of Volcanology and Geothermal Research*, **159**, 313-325.
- PLANKE, S., 1994, Geophysical response of flood basalts from analysis of wireline logs: Ocean Drilling Program Site 642, Voring volcanic margin: *J. geophys. Res.*, **99**, 9279-9296.
- PLANKE, S., RASMUSSEN, T., REY, S., and MYKLEBUST, R., 2005, Seismic characteristics and distribution of volcanic intrusions and hydrothermal vent complexes in the Vøring and Møre basins, Geological Society, London, Petroleum Geology Conference series, Volume 6, Geological Society of London, p. 833-844.

- PLANKE, S., SYMONDS, P.A., ALVESTAD, E., and SKOGSEID, J., 2000, Seismic volcanostratigraphy of large-volume basaltic extrusive complexes on rifted margins: *Journal of Geophysical Research*, **105**, 19335-19351.
- PORĘBSKI, S., and GRADZIŃSKI, R., 1990, Lava-Fed Gilbert-Type Delta in the Polonez Cove Formation (Lower Oligocene), King George Island, West Antarctica: *Coarse-grained deltas*, 333-351.
- PRENSKY, S.E., 1999, Advances in borehole imaging technology and applications: *Geological Society, London, Special Publications*, **159**, 1-43.
- RAMALHO, R.S., QUARTAU, R., TRENHAILE, A.S., MITCHELL, N.C., WOODROFFE, C.D., and ÁVILA, S.P., 2013, Coastal evolution on volcanic oceanic islands: A complex interplay between volcanism, erosion, sedimentation, sea-level change and biogenic production: *Earth-Science Reviews*, **127**, 140-170.
- REIDEL, S.P., 1998, Emplacement of Columbia River flood basalt: *Journal of Geophysical Research: Solid Earth (1978-2012)*, **103**, 27393-27410.
- REX, G.M., and SCOTT, A.C., 1987, The sedimentology, palaeoecology and preservation of the Lower Carboniferous plant deposits at Pettycur, Fife, Scotland: *Geological Magazine*, **124**, 43-66.
- RICHARDSON, J.F., and ZAKI, W.N., 1954, The sedimentation of a suspension of uniform spheres under conditions of viscous flow: *Chemical Engineering Science*, **3**, 65-73.
- RITCHIE, J., GATLIFF, R., and RICHARDS, P., 1999, Early Tertiary magmatism in the offshore NW UK margin and surrounds, Geological Society, London, Petroleum Geology Conference series, Volume 5, Geological Society of London, p. 573-584.
- RITCHIE, J., and HITCHEN, K., 1996, Early Paleogene offshore igneous activity to the northwest of the UK and its relationship to the North Atlantic Igneous Province: *Geological Society, London, Special Publications*, **101**, 63-78.
- RITCHIE, L., COLE, P., and SPARKS, R., 2002, Sedimentology of deposits from the pyroclastic density current of 26 December 1997 at Soufrière Hills Volcano, Montserrat: *Geological Society, London, Memoirs*, **21**, 435-456.
- ROHRMAN, M., 2007, Prospectivity of volcanic basins: Trap delineation and acreage de-risking: *AAPG bulletin*, **91**, 915-939.
- ROWLAND, S.K., and WALKER, G.P.L., 1990, Pahoehoe and aa in Hawaii: volumetric flow rate controls the lava structure: *Bulletin of Volcanology*, **52**, 615-628.
- SADLER, J., and LINK, P., 1996, The Tuana gravel: Early Pleistocene response to longitudinal drainage of a late-stage rift basin, western Snake River Plain: *Idaho: Northwest Geology*, **26**, 46-62.
- SAKATA, S., TAKAHASHI, M., IGARI, S.-I., and SUZUKI, N., 1989, Origin of light hydrocarbons from volcanic rocks in the "Green Tuff" region of northeast Japan: Biogenic versus magmatic: *Chemical geology*, **74**, 241-248.
- SCHIPPER, C.I., WHITE, J.D.L., ZIMANOWSKI, B., BÜTTNER, R., SONDER, I., and SCHMID, A., 2011, Experimental interaction of magma and "dirty" coolants: *Earth and Planetary Science Letters*, **303**, 323-336.
- SCHMID, R., 1981, Descriptive nomenclature and classification of pyroclastic deposits and fragments: Recommendations of the IUGS Subcommittee on the Systematics of Igneous Rocks: *Geology*, **9**, 41-43.
- SCHMINCKE, H., BEHNCKE, B., GRASSO, M., and RAFFI, S., 1997, Evolution of the northwestern Iblean Mountains, Sicily: Uplift, Pliocene/Pleistocene sea-level changes, paleoenvironment, and volcanism: *Geologische Rundschau*, **86**, 637-669.
- SCHNEIDER, J.L., TORRADO, F.J.P., TORRENTE, D.G., WASSMER, P., SANTANA, M.D.C., and CARRACEDO, J.C., 2004, Sedimentary signatures of the

- entrance of coarse-grained volcanoclastic flows into the sea: the example of the breccia units of the Las Palmas Detritic Formation (Mio-Pliocene, Gran Canaria, Eastern Atlantic, Spain): *Journal of Volcanology and Geothermal Research*, **138**, 295-323.
- SCHOFIELD, N., HEATON, L., HOLFORD, S.P., ARCHER, S.G., JACKSON, C.A.-L., and JOLLEY, D.W., 2012, Seismic imaging of 'broken bridges': linking seismic to outcrop-scale investigations of intrusive magma lobes: *Journal of the Geological Society*, **169**, 421-426.
- SCHOFIELD, N., and JOLLEY, D.W., 2013, Development of intra-basaltic lava-field drainage systems within the Faroe-Shetland Basin: *Petroleum Geoscience*, **19**, 273-288.
- SCHOFIELD, N., STEVENSON, C., and RESTON, T., 2010, Magma fingers and host rock fluidization in the emplacement of sills: *Geology*, **38**, 63-66.
- SCHUTTER, S.R., 2003, Hydrocarbon occurrence and exploration in and around igneous rocks: *Geological Society, London, Special Publications*, **214**, 7-33.
- SCOTT, A.C., 1990, Preservation, evolution, and extinction of plants in Lower Carboniferous volcanic sequences in Scotland: *Geological Society of America Special Papers*, **244**, 25-38.
- SELF, S., 1983, Large-scale phreatomagmatic silicic volcanism: a case study from New Zealand: *Journal of volcanology and geothermal research*, **17**, 433-469.
- SELF, S., KESZTHELYI, L., and THORDARSON, T., 1998, The importance of pahoehoe: *Annual Review of Earth and Planetary Sciences*, **26**, 81-110.
- SELF, S., SCHMIDT, A., and MATHER, T., 2014, Emplacement characteristics, time scales, and volcanic gas release rates of continental flood basalt eruptions on Earth: *Geological Society of America Special Papers*, **505**, SPE505-16.
- SERRA, O., WESTAWAY, P., and ABBOTT, H., 1984, Fundamentals of well-log interpretation, Elsevier Amsterdam.
- SHAHINPOUR, A., 2013, Borehole image log analysis for sedimentary environment and clay volume interpretation.
- SHERVAIS, J.W., KAUFFMAN, J.D., GILLERMAN, V.S., OTHBERG, K.L., VETTER, S.K., HOBSON, V.R., ZARNETSKE, M., COOKE, M.F., MATTHEWS, S.H., and HANAN, B.B., 2005, Basaltic volcanism of the central and western Snake River Plain: A guide to field relations between Twin Falls and Mountain Home, Idaho: *Interior Western United States*, **6**, 27.
- SHERVAIS, J.W., SHROFF, G., VETTER, S.K., MATTHEWS, S., HANAN, B.B., and MCGEE, J.J., 2002, Origin and evolution of the western Snake River Plain: Implications from stratigraphy, faulting, and the geochemistry of basalts near Mountain Home, Idaho: *Tectonic and Magmatic Evolution of the Snake River Plain Volcanic Province: Idaho Geological Survey Bulletin*, **30**, 343-361.
- SHIMAZU, M., 1985, Altered rhyolites as oil and gas reservoirs in the Minaminagaoka gas field (Niigata Prefecture, Japan): *Chemical geology*, **49**, 363-370.
- SILVESTRI, S., 1963, Proposal for a genetic classification of hyaloclastites: *Bulletin of Volcanology*, **25**, 315-321.
- SKILLING, I., 2002, Basaltic pahoehoe lava-fed deltas: large-scale characteristics, clast generation, emplacement processes and environmental discrimination: *Geological Society, London, Special Publications*, **202**, 91-113.

- SKILLING, I.P., WHITE, J.D.L., and MCPHIE, J., 2002, Peperite: a review of magma-sediment mingling: *Journal of Volcanology and Geothermal Research*, **114**, 1-17.
- SMALLWOOD, J.R., and MARESH, J., 2002, The properties, morphology and distribution of igneous sills: modelling, borehole data and 3D seismic from the Faroe-Shetland area: *Geological Society, London, Special Publications*, **197**, 271-306.
- SMEDLEY, P.L., 1986, The relationship between calc-alkaline volcanism and within-plate continental rift volcanism: evidence from Scottish Palaeozoic lavas: *Earth and Planetary Science Letters*, **77**, 113-128.
- SØRENSEN, A.B., 2003, Cenozoic basin development and stratigraphy of the Faroes area: *Petroleum Geoscience*, **9**, 189-207.
- SQUIRE, R.J., and MCPHIE, J., 2002, Characteristics and origin of peperite involving coarse-grained host sediment: *Journal of Volcanology and Geothermal Research*, **114**, 45-61.
- STEPHENSON, D., LOUGHLIN, S.C., MILLWARD, D., WATERS, C.N. & WILLIAMSON, I.T., 2003, Carboniferous and Permian Igneous Rocks of Great Britain North of the Variscan Front: Peterborough, Joint Nature Conservation Committee, 374 p.
- STEPHENSON, D., UPTON, B., WILLIAMSON, I., MILLWARD, D., WOODHALL, D., MACDONALD, J., and MONAGHAN, A., 2003, Dinantian volcanic rocks of the Midland Valley of Scotland and adjacent areas: *Carboniferous and Permian igneous rocks of Great Britain north of the Variscan Front*, 35-108.
- STEVENSON, J., MITCHELL, N., MOCHRIE, F., CASSIDY, M., and PINKERTON, H., 2012, Lava penetrating water: the different behaviours of pāhoehoe and 'a'ā at the Nesjahraun, Pingvellir, Iceland: *Bulletin of Volcanology*, **74**, 33-46.
- STOKER, M., HITCHEN, K., and GRAHAM, C., 1993, The geology of the Hebrides and West Shetland shelves, and adjacent deep-water areas, The Stationery Office/Tso.
- THIRLWALL, M., 1981, Implications for Caledonian plate tectonic models of chemical data from volcanic rocks of the British Old Red Sandstone: *Journal of the Geological Society*, **138**, 123-138.
- THIRLWALL, M., 1982, Systematic variation in chemistry and Nd-Sr isotopes across a Caledonian calc-alkaline volcanic arc: implications for source materials: *Earth and Planetary Science Letters*, **58**, 27-50.
- THORDARSON, T., and SELF, S., 1998, The Roza Member, Columbia River Basalt Group: A gigantic pahoehoe lava flow field formed by endogenous processes?: *Journal of Geophysical Research: Solid Earth (1978-2012)*, **103**, 27411-27445.
- TIERCELIN, J.J., and LEZZAR, K.E., 2002, A 300 Million Years History of Rift Lakes in Central and East Africa: An Updated Broad Review, in Odada, E., and Olago, D., eds., *The East African Great Lakes: Limnology, Palaeolimnology and Biodiversity*, Volume 12: Advances in Global Change Research, Springer Netherlands, p. 3-60.
- TORRADO, F.J.P., 1992, Volcanoestratigrafía del grupo Roque Nublo (Gran Canaria), Universidad de Las Palmas de Gran Canaria.
- TREWIN, and THIRLWALL, 2002, Old Red Sandstone, in Trewin, ed., *The Geology of Scotland*, The Geological Society.
- TUCKER, D.S., and SCOTT, K.M., 2009, Structures and facies associated with the flow of subaerial basaltic lava into a deep freshwater lake: The Sulphur

- Creek lava flow, North Cascades, Washington: *Journal of Volcanology and Geothermal Research*, **185**, 311-322.
- UMAZANO, A.M., BELLOSI, E.S., VISCONTI, G., and MELCHOR, R.N., 2008, Mechanisms of aggradation in fluvial systems influenced by explosive volcanism: an example from the Upper Cretaceous Bajo Barreal Formation, San Jorge Basin, Argentina: *Sedimentary Geology*, **203**, 213-228.
- UNDERHILL, J.R., MONAGHAN, A.A., and BROWNE, M.A., 2008, Controls on structural styles, basin development and petroleum prospectivity in the Midland Valley of Scotland: *Marine and Petroleum Geology*, **25**, 1000-1022.
- UPTON, B., STEPHENSON, D., SMEDLEY, P., WALLIS, S., and FITTON, J., 2004, Carboniferous and Permian magmatism in Scotland: *Geological Society, London, Special Publications*, **223**, 195-218.
- VAN EATON, A.R., MUIRHEAD, J.D., WILSON, C.J., and CIMARELLI, C., 2012, Growth of volcanic ash aggregates in the presence of liquid water and ice: an experimental approach: *Bulletin of volcanology*, **74**, 1963-1984.
- VISHER, G.S., and CUNNINGHAM, R.D., 1981, Convolute laminations – a theoretical analysis: example of a Pennsylvanian sandstone: *Sedimentary Geology*, **28**, 175-188.
- WAICHEL, B.L., DE LIMA, E.F., SOMMER, C.A., and LUBACHESKY, R., 2007, Peperite formed by lava flows over sediments: An example from the central Paraná Continental Flood Basalts, Brazil: *Journal of Volcanology and Geothermal Research*, **159**, 343-354.
- WALKER, G., 1971, Compound and simple lava flows and flood basalts: *Bulletin of Volcanology*, **35**, 579-590.
- WALKER, G.P., 1987, Pipe vesicles in Hawaiian basaltic lavas: their origin and potential as paleoslope indicators: *Geology*, **15**, 84-87.
- WATTON, T.J., CANNON, S., BROWN, R.J., JERRAM, D.A., and WAICHEL, B.L., 2014, Using formation micro-imaging, wireline logs and onshore analogues to distinguish volcanic lithofacies in boreholes: examples from Palaeogene successions in the Faroe-Shetland Basin, NE Atlantic: *Geological Society, London, Special Publications*, **397**, 173-192.
- WATTON, T.J., JERRAM, D.A., THORDARSON, T., and DAVIES, R.J., 2013, Three-dimensional lithofacies variations in hyaloclastite deposits: *Journal of Volcanology and Geothermal Research*, **250**, 19-33.
- WENTWORTH, C.K., 1922, A scale of grade and class terms for clastic sediments: *The Journal of Geology*, 377-392.
- WHITE, C.M., HART, W.K., BONNICHSEN, B., and MATTHEWS, D., 2002, Geochemical and Sr-isotopic variations in western Snake River Plain basalts, Idaho: *Tectonic and Magmatic Evolution of the Snake River Plain Volcanic Province. Idaho Geological Survey Bulletin*, **30**, 329-342.
- WHITE, J., and HOUGHTON, B., 2006, Primary volcaniclastic rocks: *Geology*, **34**, 677-680.
- WHITE, J.D.L., MCPHIE, J., and SKILLING, I., 2000, Peperite: a useful genetic term: *Bulletin of Volcanology*, **62**, 65-66.
- WILLIAMSON, I.T., and BELL, B.R., 1994, The Palaeocene lava field of west-central Skye, Scotland: Stratigraphy, palaeogeography and structure: *Earth and Environmental Science Transactions of the Royal Society of Edinburgh*, **85**, 39-75.
- WILLIAMSON, I.T., and BELL, B.R., 2012, The Staffa Lava Formation: graben-related volcanism, associated sedimentation and landscape character

- during the early development of the Palaeogene Mull Lava Field, NW Scotland: *Scottish Journal of Geology*, **48**, 1-46.
- WILLUMSEN, P., and SCHILLER, D.M., 1994, High quality volcanoclastic sandstone reservoirs in East Java, Indonesia.
- WILSON, M., NEUMANN, E.-R., DAVIES, G.R., TIMMERMAN, M., HEEREMANS, M., and LARSEN, B.T., 2004, Permo-Carboniferous magmatism and rifting in Europe: introduction: *Geological Society, London, Special Publications*, **223**, 1-10.
- WINTERWERP, J.C., and VAN KESTEREN, W.G.M., 2004, 3 - The Nature of Cohesive Sediment, in Johan, C.W., and Walther, G.M.v.K., eds., *Developments in Sedimentology*, Volume Volume 56, Elsevier, p. 29-85.
- WOHLETZ, K., 2002, Water/magma interaction: some theory and experiments on peperite formation: *Journal of Volcanology and Geothermal Research*, **114**, 19-35.
- WOOD, S.H., and CLEMENS, D.M., 2002, Geologic and tectonic history of the western Snake River Plain, Idaho and Oregon: *Tectonic and Magmatic Evolution of the Snake River Plain Volcanic Province: Idaho Geological Survey Bulletin*, **30**, 69-103.
- WOODCOCK, N., and STRACHAN, R., 2008, Geological history of Britain and Ireland, Wiley-Blackwell.
- WRIGHT, K., A., 2013, Seismic Stratigraphy and Geomorphology of Palaeocene Volcanic Rocks, Faroe-Shetland Basin.
- WRIGHT, K., DAVIES, R., JERRAM, D., MORRIS, J., and FLETCHER, R., 2012, Application of seismic and sequence stratigraphic concepts to a lava-fed delta system in the Faroe-Shetland Basin, UK and Faroes: *Basin Research*, **24**, 91-106.
- WU, C., GU, L., ZHANG, Z., REN, Z., CHEN, Z., and LI, W., 2006, Formation mechanisms of hydrocarbon reservoirs associated with volcanic and subvolcanic intrusive rocks: Examples in Mesozoic-Cenozoic basins of eastern China: *AAPG bulletin*, **90**, 137-147.
- ZIMANOWSKI, B., and BÜTTNER, R., 2002, Dynamic mingling of magma and liquefied sediments: *Journal of Volcanology and Geothermal Research*, **114**, 37-44.
- ZOU, C.-N., ZHAO, W.-Z., JIA, C.-Z., ZHU, R.-K., ZHANG, G.-Y., XIA, Z., and YUAN, X.-J., 2008, Formation and distribution of volcanic hydrocarbon reservoirs in sedimentary basins of China: *Petroleum Exploration and Development*, **35**, 257-271.
- ZOU, C., 2013, *Volcanic Reservoirs in Petroleum Exploration*, Newnes.

---

## Appendix 1

The following published manuscript is included as it provided a training exercise for field identification of some of the basic concepts covered within this thesis.

## Lithofacies architecture of basaltic andesite lavas and their interaction with wet-sediment: Port a' Chroinn, Kerrera, NW Scotland

HEATHER J. RAWCLIFFE\* & DAVID J. BROWN

*School of Geographical and Earth Sciences, Gregory Building, Lilybank Gardens, University of Glasgow, Glasgow G12 8QQ, Scotland, UK*

\*Corresponding author (e-mail: [H.Rawcliffe.1@research.gla.ac.uk](mailto:H.Rawcliffe.1@research.gla.ac.uk))

### Synopsis

Lavas of the Lorne Plateau Volcanic Succession (LPVS) crop out on the island of Kerrera, NW Scotland, and were emplaced during the Devonian Period, synchronous with Old Red Sandstone (ORS) terrestrial sedimentation. These flows are discontinuously exposed for c. 3 km at Port a' Chroinn, Kerrera, and typically comprise blocky, basal breccias, coherent, crystalline cores, and clinker flow tops, interpreted as basaltic andesite 'a'a lavas. Gradational zones are observed from coherent core, through highly vesicular core, to semi-coherent lava and normally graded clinker. Prismatic jointed, inflated pahoehoe lavas are also present, but have few characteristic morphological features. Localized domains of magma-sediment mingling occur at the bases of several lavas, with clasts of basaltic andesite within a sandstone matrix. These domains are interpreted as peperites, formed as lava flowed over and mingled with unconsolidated, wet sediment that had been deposited on the surfaces of underlying lavas during periods of volcanic quiescence.



### Introduction

In this study, we provide detailed descriptions of newly identified basaltic andesite 'a'a lavas and peperites on the island of Kerrera, western Scotland (Figs 1, 2). These lavas are interpreted as being of the 'a'a type and we describe their lithofacies architecture in detail. Peperite at the basal margins of pahoehoe lavas provides evidence for localized magma-sediment mingling. We discuss the morphological features of the 'a'a lavas, and the role of water during eruptions with respect to magma-sediment mingling.

During the Devonian Period Scotland was part of the continent of Laurussia, also known as the 'Old Red Sandstone Continent', which had formed through the amalgamation of Laurentia, Baltica and Avalonia (Woodcock & Strachan 2000). Old Red Sandstone sedimentation was widespread throughout the Devonian and related to Caledonian uplift, cooling and basin formation (Trewin & Thirlwall 2002). Associated volcanism, such as the Lorne Plateau Volcanic Succession (LPVS) (see below), was related to rapid post-orogenic uplift and extensional collapse (Macdonald & Fettes 2007).

The lavas of Kerrera form part of the LPVS, an extensive igneous episode, which occurred during the Early Devonian at c. 425–410 Ma. The succession covers more than 300 km<sup>2</sup> and is over 800 m thick (Groome & Hall 1974). The LPVS is dominated by basaltic andesite lavas with rarer interbedded volcanoclastic and sedimentary rocks (Lee *et al.* 1925; Trewin & Thirlwall 2002). On Kerrera the LPVS unconformably overlies Dalradian meta-sedimentary rocks and Lower Old Red Sandstone (ORS) sandstones and conglomerates.

<http://dx.doi.org/10.1144/sjg2013-018>

### Terminology

The majority of basaltic lavas can be classified as either 'a'a or pahoehoe, on the basis of their surface morphology (Macdonald 1953). 'A'a lava has a rough surface with characteristic 'clinker' or flow-top breccia, compared to the smooth or ropey surface of a pahoehoe lava (Macdonald 1953). Distinctive internal morphologies also aid classification: 'a'a have a massive central portion or core, and basal and flow-top breccias, whereas pahoehoe can be readily divided into flow units and individual lava tubes (Walker 1971; Rowland & Walker 1990). Morphological differences relate to the surface processes and flow dynamics that occur during lava emplacement.

Effusion rate of the lava determines whether the flow develops as an 'a'a or pahoehoe. A high effusion rate (volumetric flow rate) generally results in 'a'a development, whereas pahoehoe forms when flow rates are lower (below 5–10 m<sup>3</sup> s<sup>-1</sup>) and below a certain viscosity threshold which varies with flow velocity (Rowland & Walker 1990). Pahoehoe lavas advance slowly with small multiple flow lobes, typically <1 m<sup>2</sup>, active at any one time (Macdonald 1953; Self *et al.* 1998). The surface chills quickly, forming a crust that allows only the core of the lobe to continue to flow. This thermally efficient transport mechanism enables the lava to flow for significant lengths, potentially up to 1000 km (Hon *et al.* 1994; Self *et al.* 1998; Brown *et al.* 2011), and helps the lava to retain its heat from the vent to the flow margins.

'A'a lavas flow rapidly in narrow, open channels, typically 0.1–2.5 km wide. The margins of the flow stagnate and form levees through accretion, causing the central

Scottish Journal of Geology XX, (X), 1–7, 2014

2

H. J. RAWCLIFFE &amp; D. J. BROWN

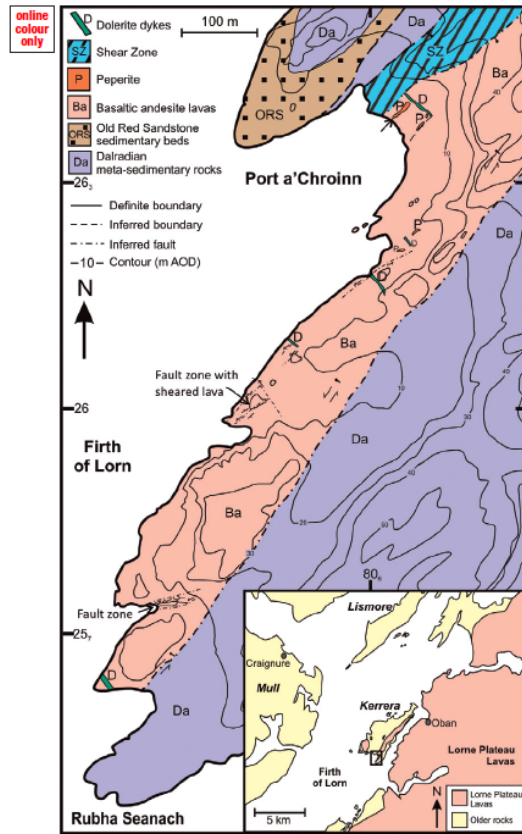


FIG. 1. Geological map of the area around Port a' Chroinn, south Kerrera. Inset shows the location of Kerrera, western Scotland, and the outcrop of the Lorne Plateau Lavas.

channelized portion to become more concentrated (Rowland & Walker 1990). The channelized part of the flow has a high flow velocity, up to  $60 \text{ km h}^{-1}$  (Macdonald 1953), but also a significant radiative heat loss, which leads to continual turnover of the flow and development of a rapidly cooling crust (Crisp & Baloga 1994). 'A'a clinker (spinose, ragged, slightly cooled clumps of lava) is produced when the cooler flow crust is continuously disrupted by the fast-moving flow, with shear stresses exceeding the tensile strength of the cooled crust (Brown *et al.* 2011). The clinker can be incorporated back into the flow as it is forced to the flow front and then falls to the base of the flow, resembling a caterpillar track motion (Macdonald 1953).

Magma-sediment interaction occurs as magma flows over, or is intruded into unconsolidated, typically wet sediment (White *et al.* 2000). The rock formed by this process of magma-sediment mingling is termed a peperite, and its formation is influenced by a number of factors, including the presence of water, grain size of the host sediment (coarse or fine), and magma-sediment density contrasts (White

*et al.* 2000). Peperites form at the margins of intrusions, where domains can be several cubic kilometres in thick volcano-sedimentary sequences, or in more minor occurrences at the base of lavas, typically  $<1 \text{ m}^3$  (Skilling *et al.* 2002). On contact with unconsolidated sediment, the magma disintegrates and fragments, forming juvenile clasts, which mix and mingle to varying degrees with the sediment. Juvenile clasts have a range of morphologies from blocky to globular/fluidal (Busby-Spera & White 1987), which reflect the brittle and ductile fragmentation processes, such as quenching and autobrecciation, that take place during peperite formation. Blocky clasts are sub-equant, polyhedral to tabular, with curvilinear to planar surfaces (Skilling *et al.* 2002). Groups of blocky clasts commonly display jigsaw-fit texture, which is characteristic of *in situ* fragmentation (Skilling *et al.* 2002). Fluidal clasts have globular morphologies, characterized by their intricate, irregular outlines, and range in shape from amoeboid to globules, to tendrils and wispy-like structures (Lorenz 1984; Busby-Spera & White 1987; Skilling *et al.* 2002). It is common for a mixture of juvenile clast morphologies to be present in the same peperite domain. The relative proportions of juvenile clasts and host sediment have been used to define dispersed and close-packed peperite (Hanson & Wilson 1993). Dispersed peperite has juvenile clasts well distributed throughout the host sediment; a close-packed peperite has a high concentration of juvenile clasts. Peperite is typically non-stratified, ungraded and highly discordant to bedding, and original stratification in the host sediment is commonly lost (Doyle 2000; White *et al.* 2000; Skilling *et al.* 2002).

#### Morphology and stratigraphic relationships of the lavas and peperites

The typical lithofacies architecture of the lavas and peperites described in this study is depicted in Figures 2 and 3. Below we discuss the field relationships and petrography of the lavas and peperite, and interpret their mode of formation.

#### 'A'a lavas

##### Field relationships

The lavas crop out discontinuously along the SW coast of Kerrera, between Port a' Chroinn and Rubha Seanach (Fig. 1) and are cross-cut by numerous Palaeogene dolerite dykes trending NW-SE. Multiple lavas are stacked on top of each other and the sequence has been heavily faulted (Figs 1, 2). The lavas are typically prismatically jointed, but have basal and flow-top breccias, comprising variably vesicular clinker that grades into coherent crystalline cores with abundant deformed, aligned vesicles (Figs 3, 4). The blocky, basal breccia is typically *c.* 50 cm thick, and sharply grades into a coherent, crystalline and poorly vesicular lava core, which is typically *c.* 1 m thick. Within this core, a central dense zone *c.* 60 cm thick, is present and vesicles are absent (Fig. 3a). Spherical and elongate vesicles *c.* 1–3 mm across are present and vesicularity increases towards the top of the lava core. A 'gradational zone', where spherical vesicles develop into abundant larger elongate vesicles, typically *c.* 3–5 cm across,

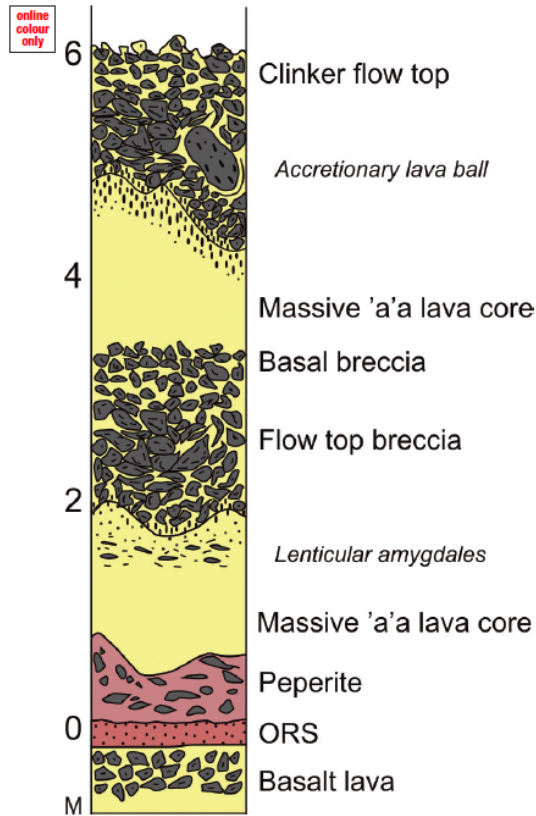


Fig. 2. Schematic summary log of characteristic lava and peperite morphology.

is present (Figs 3a, 4a). Above this gradational zone vesicular clasts, which have poorly defined shapes, grade into vesicular, subrounded to angular clinker *c.* 2.5 cm across, marking the top of the flow (Fig. 4b). In some lavas the clinker is normally graded and records a transition from coherent lava blebs *c.* 10–20 cm across, to rough, broken fragments *c.* 2 cm across (Figs 3b, 4b). The flow-top breccia is typically *c.* 90 cm thick and normally graded (Fig. 3b). Clasts fine upwards from 10–20 cm across at the base, to 2–3 cm across with a fine glassy 'matrix' at the top. The contact between the lava core and the flow-top breccia is irregular (Fig. 4c) and, locally, domains of coherent lava, up to 60 cm across, occur within the flow-top breccia (Fig. 4d). These irregular-shaped domains are interpreted as accretionary lava balls (see below).

#### Petrography

The lavas are of basaltic andesite composition with a fine-grained, intergranular microcrystalline groundmass of plagioclase, clinopyroxene and opaque minerals of <200  $\mu\text{m}$  in diameter (Fig. 5).

#### Interpretation

The lavas are interpreted as being of 'a' type, with clinkery flow tops and basal breccias surrounding a coherent core. The lavas display a transition from coherent to highly vesicular cores, through clumps of semi-coherent lava to normally graded clinker. The accretionary lava balls, found within the flow-top breccia, formed when fragments of coherent lava became detached from the main core.

#### Pahoehoe lavas and peperite

#### Field relationships

At Port a'Chroinn, isolated pale to dark grey, prismatic jointed lavas crop out. These lavas lack clinker flow-top breccias, but locally exhibit weathered brecciated flow tops. They lack basal breccias, but locally, at their bases, they show evidence of physical interaction with the sedimentary units.

At the base of some of these lavas a closely packed, blocky, peperite with clasts of basaltic andesite set in a sandstone matrix is observed. The peperite domains range in size, but are typically >2 m<sup>3</sup>. Clasts of basaltic andesite are angular to subrounded and range in size from 2–15 cm, with mixed morphologies of both blocky and fluidal clasts (Fig. 6). Groups of blocky clasts with characteristic jigsaw-fit texture are abundant (Fig. 6a, b); however, other clasts show irregular angular, fluidal (amoeboid), and globular morphologies (Fig. 6c, d). Larger pods of basaltic-andesite show fluidal margins. The host sedimentary matrix is red-brown, fine-grained sandstone (quartz arenite and arkosic arenite) (Fig. 6d). Locally, the sedimentary matrix fills 'developing' fractures in the igneous clasts. Stratification in the sedimentary matrix is typically absent; however, in places the host sediment displays thin laminae that are distorted and 'deformed' around the juvenile clasts (Fig. 6d).

#### Petrography

The fine-grained sandstone matrix is dominated by quartz, opaque minerals and feldspar and, locally, is altered to clay. Veins of quartz are abundant and typically present along clast-sediment boundaries (Fig. 7a). The juvenile clasts of basaltic andesite, which range in size from <0.5 mm to 2 cm are glassy to microcrystalline. Both blocky (Fig. 7b) and fluidal (amoeboid) (Fig. 7c, d) clasts are observed; however, some clasts are connected by thin necks to larger clasts. The majority of clasts at this scale have fluidal and crenulate margins. Cracks and vesicles in the lava are filled with sediment and quartz (Fig. 7).

#### Interpretation

The lavas are interpreted as inflated, basaltic pahoehoe; although typical ropey structures are lacking, some lavas have brecciated or rubbly tops, similar to those seen in the Columbia River Basalt Province and the Deccan Traps (Keszthelyi *et al.* 2006; Duraiswami *et al.* 2008). These are termed 'rubbly pahoehoe' (Keszthelyi *et al.* 2006), and are thought to form when the insulating, moving crust of the flow is disrupted by increases and fluctuations in effusion rate, away from the normal mode of emplacement. Rubbly pahoehoe flows generally have smooth basal crusts (Bondre *et al.* 2004; Duraiswami *et al.* 2008).

4

H. J. RAWCLIFFE &amp; D. J. BROWN

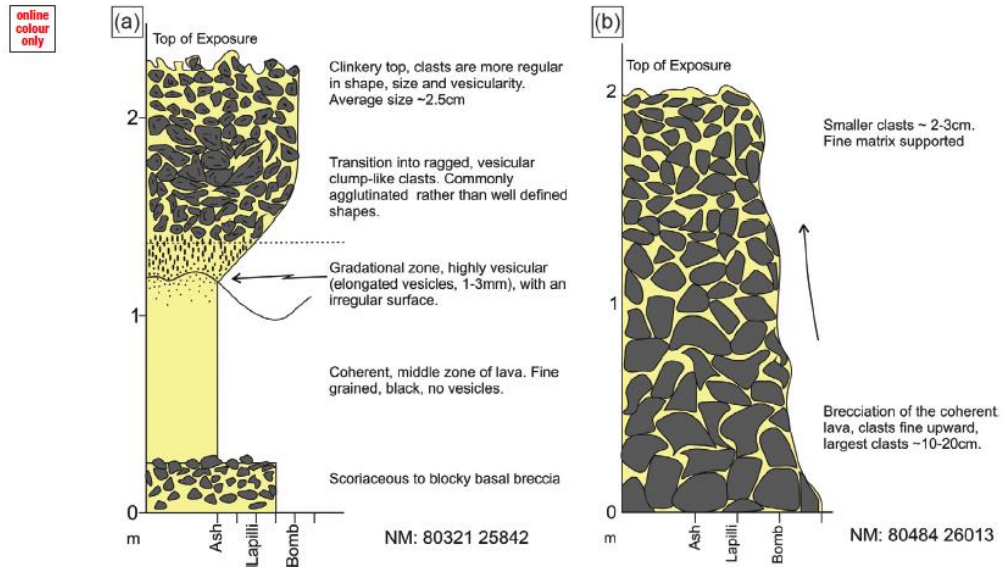


FIG. 3. (a) Schematic graphic log of a representative 'a' lava depicting the detail of the central, coherent zone of the lava, between the basal and flow-top breccias. (b) Schematic graphic log showing normal grading of flow-top breccia.

online colour only

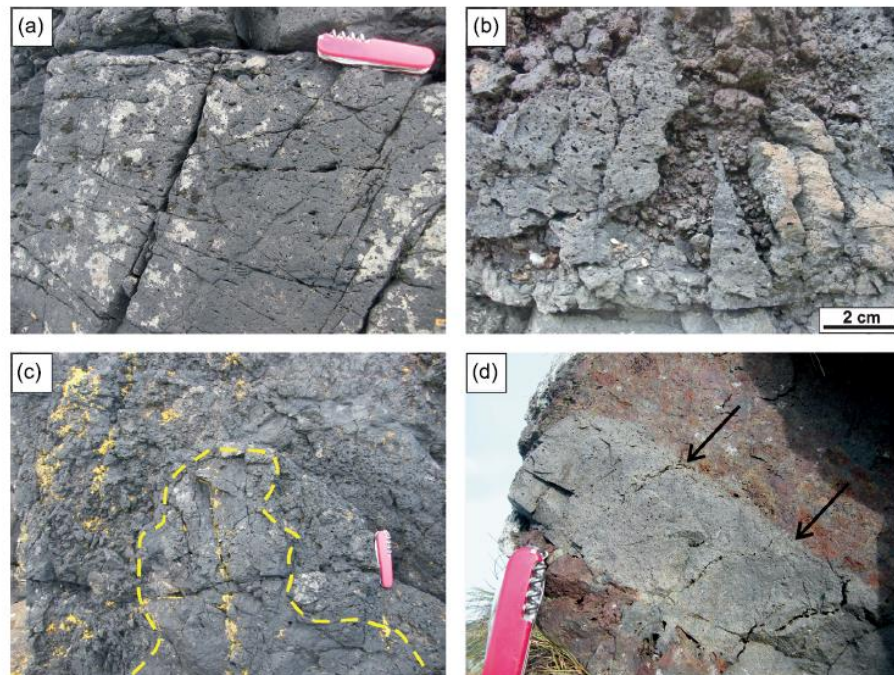


FIG. 4. Features of 'a' lavas. Size of pen knife is 8 cm. (a) Elongate vesicles within the 'gradational zone' of the core of the lava. (b) Transition zone from coherent lava with elongate vesicles to fragmented lava and clinker. (c) Irregular contact between the lava core and the flow-top breccia. Fragments of coherent lava become detached and form accretionary lava balls. (d) An accretionary lava ball within the flow-top breccia.

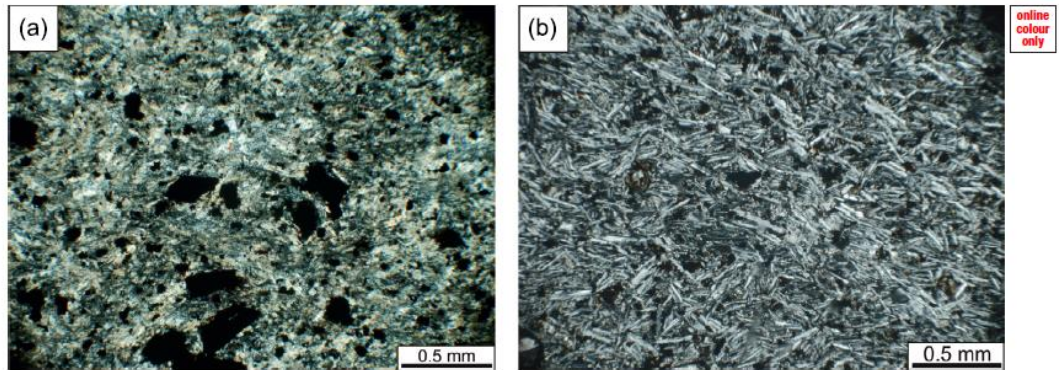


FIG. 5. Photomicrographs of 'a'a lavas in cross-polarized light. (a) Basaltic 'a'a lava with a fine-grained interstitial groundmass of plagioclase, clinopyroxene and microphenocrysts of Fe-Ti oxide. (b) Andesite from 'a'a lavas with a microcrystalline groundmass of pyroxene, plagioclase, amphibole and opaque minerals. Plagioclase crystals show preferential orientation in places.

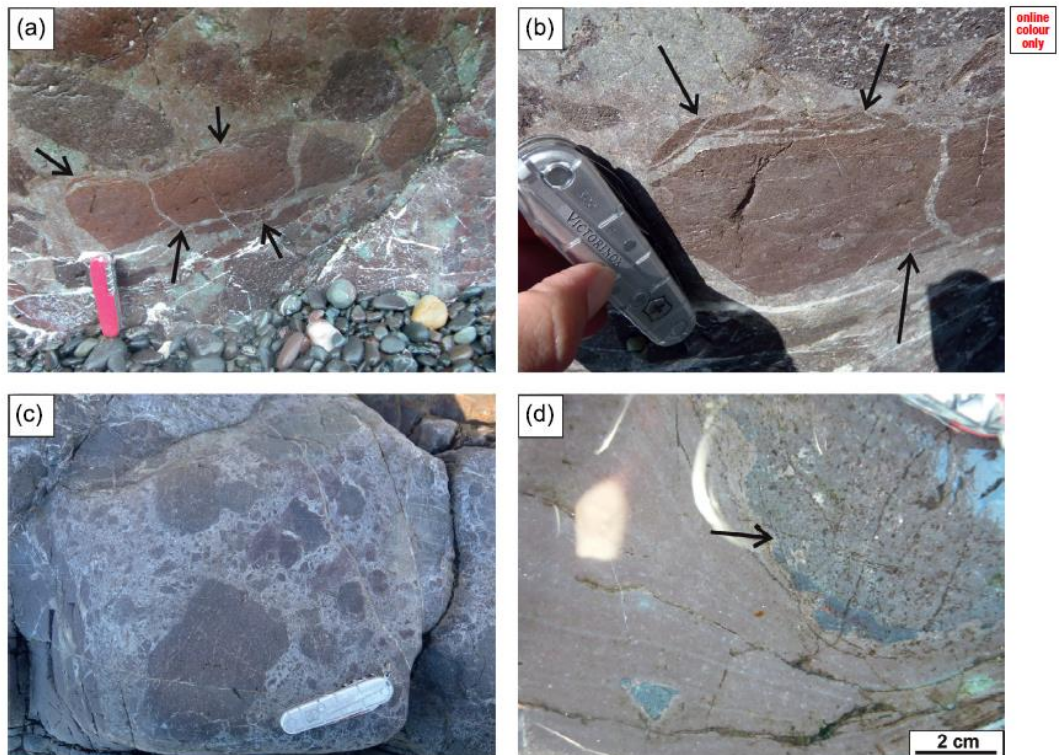


FIG. 6. Peperite with basaltic andesite clasts in a sandstone matrix. Size of pen knife is 8 cm. (a) and (b) show blocky peperite with sub-angular clasts displaying jig-saw fit texture. (c) Juvenile clasts range in size and from blocky to fluidal shapes within the peperite domain. (d) Fluidal juvenile clasts with crenulate margins (image taken through water). Note deformation of the laminae in the sedimentary matrix, indicating fluidization of these sediments during formation.

Where the lavas have interacted with unconsolidated sediment, peperite has formed. The presence of both blocky and fluidal juvenile clasts indicates that both brittle and ductile

processes occurred during formation of the peperite. Furthermore, the recognition of both fluidal and sub-planar margins on single juvenile clasts suggests multi-stage

6

H. J. RAWCLIFFE &amp; D. J. BROWN

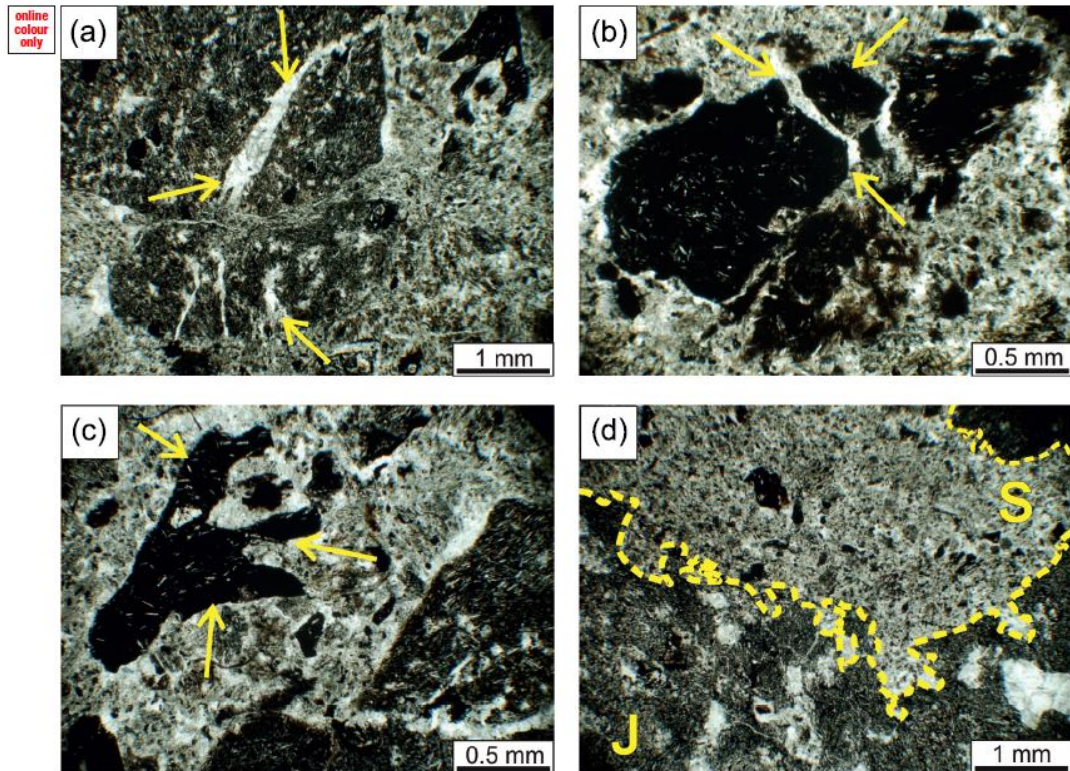


FIG. 7. Photomicrographs of the peperite. (a) Quartz veins filling the boundaries between lava clasts and sedimentary matrix. Vesicles of the juvenile clasts are also filled with the host sediment. (b) Blocky, angular juvenile clasts displaying a jigsaw-fit texture. (c) Fluidal/globular juvenile clast of basaltic andesite within fine-grained sediment host. (d) Irregular and globular margins of a large juvenile clast (J) within the host sediment (S).

fragmentation during this event (Skilling *et al.* 2002). Blocky clasts suggest a brittle regime, with fragmentation caused by quenching or mechanical stresses. The observed jigsaw-fit textures indicate that fragmentation occurred essentially *in situ* (Skilling *et al.* 2002). A ductile regime is implied for fluidal clasts, possibly caused by fluid instabilities within vapour films, magma–sediment density contrasts (Skilling *et al.* 2002) and hydromagmatic explosions (Busby-Spera & White 1987).

The disruption of laminae within the sedimentary matrix (Fig. 6d) indicates that fluidization of the host sediment occurred during emplacement and fragmentation of the lava. Fluidization of the host sediment within vapour films along magma–sediment contacts is thought to promote mingling of juvenile clasts within the host sediment and formation of fluidal clasts (Kokelaar 1982).

The presence of peperites implies that the host sediment was unconsolidated and, most likely, wet (peperite-like textures have been recognized in dry aeolian sands, for example, in Namibia; Jerram & Stollhofen 2002) when magma was emplaced into it and magma–sediment mingling took place. The observed textures suggest that, during periods of volcanic quiescence, sediment was deposited on the surface

of lavas, filling small depressions, which may also have held small, shallow bodies of water. These sediments were most likely of fluvial-lacustrine origin. Later lavas flowed over the sediment and locally bulldozed into it, resulting in magma–sediment interaction and the formation of peperite.

#### Discussion and conclusions

The dominant lavas of SW Kerrera are interpreted as being of 'a' lava type that display typical morphological features: basal and flow-top breccias comprising vesicular clinker, which surround a dense, coherent core. We have also identified a transition from coherent core through highly vesicular core to fragmented lava and flow-top clinker. Although flow-top breccias are, or have been, considered homogeneous (Brown *et al.* 2011), we provide evidence for normally graded clinker tops, whose formation we attribute to autobrecciation, thermal efficiency of the lava and sorting and erosion of the clinker.

As autobrecciation of the lava crust takes place some clinker is re-introduced to the main lava flow, although most clinker is carried along the top of the flow. As the lava continues to flow, the clinker abrades and mechanically

erodes. As more clinker is created the central fluidal part of the flow remains thermally efficient due to the thick crust and, therefore, continues to flow. Autobrecciation of the core region occurs, but the lava initially behaves in a more fluid fashion forming raggy, semi-coherent clumps, before progressively behaving in a more brittle fashion and generating more typical angular clinker. With continued flow the coarser clinker is continually abraded with lateral movement and, consequently, normal grading is developed in the flow-top breccias.

We have also identified localized peperites at the bases of pahoehoe lavas and discuss the role of water in their formation and the nature of the palaeo-land surface. The peperites provide evidence for lava flowing over and interacting with unconsolidated, most likely wet, sediment. We interpret the sediment to have accumulated on top of older lavas during periods of volcanic quiescence. Clast morphologies and evidence for fluidization suggest the sediment was water saturated; however, the amount of water remains uncertain. If the lavas had flowed over and into large bodies of water, we would expect to find a gradation from lava to hyaloclastite, and perhaps then peperite. However, at this location, only peperite is seen, and is confined to a relatively small area, suggesting only small ponds of water may have been present. We suggest it is relatively simple for sediment and small ponds of water to collect on the top of lavas, due to the typical undulating and hummocky nature of lava topography. The underlying lavas would have controlled the palaeo-drainage system, thus confining the sediment to localized 'channels', which were then exploited by later pahoehoe lavas. These geometries provide clear evidence of the partial 'drowning' of a syn-volcanic landscape, with the formation of isolated, topographically controlled occurrences of peperite, rather than the more typically observed peperite formed when lava covers large tabular bodies of sediment.

#### Acknowledgements

We would like to thank H. Emeleus and B. Upton for their positive, helpful reviews, and B. Bell for his comments on the manuscript and editorial support.

#### References

- BONDRE, N. R., DURAISWAMI, R. A. & DOLE, G. 2004. Morphology and emplacement of flows from the Deccan Volcanic Province, India. *Bulletin of Volcanology*, **66**, 29–45.
- BROWN, R., BLAKE, S., BONDRE, N., PHADNIS, V. & SELF, S. 2011. 'A'ā lava flows in the Deccan Volcanic Province, India, and their significance for the nature of continental flood basalt eruptions. *Bulletin of Volcanology*, **73**, 737–752.
- BUSBY-SPERA, C. & WHITE, J. 1987. Variation in peperite textures associated with differing host-sediment properties. *Bulletin of Volcanology*, **49**, 765–775.
- CRISP, J. & BALOGA, S. 1994. Influence of crystallization and entrainment of cooler material on the emplacement of basaltic aa lava flows. *Journal of Geophysical Research-Solid Earth*, **99**, 11819–11831.
- DOYLE, M. G. 2000. Clast shape and textural associations in peperite as a guide to hydromagmatic interactions: Upper Permian basaltic and basaltic andesite examples from Kiama, Australia. *Australian Journal of Earth Science*, **47**, 167–177.
- DURAISWAMI, R. A., BONDRE, N. R. & MANAGAVE, S. 2008. Morphology of rubbly pahoehoe (simple) flows from the Deccan Volcanic Province: Implications for style of emplacement. *Journal of Volcanology and Geothermal Research*, **177**, 822–836.
- GROOME, D. R. & HALL, A. 1974. Geochemistry of Devonian lavas of northern Lorne Plateau, Scotland. *Mineralogical Magazine*, **39**, 621–640.
- HANSON, R. E. & WILSON, T. J. 1993. Large-scale rhyolite peperites (Jurassic, southern Chile). *Journal of Volcanology and Geothermal Research*, **54**, 247–264.
- HON, K., KAUAHIKAUA, J., DENLINGER, R. & MACKAY, K. 1994. Emplacement and inflation of pahoehoe sheet flows – observations and measurements of active lava flows on Kilauea volcano, Hawaii. *Geological Society of America Bulletin*, **106**, 351–370.
- JERRAM, D. A. & STOLLHOFEN, H. 2002. Lava–sediment interaction in desert settings; are all peperite-like textures the result of magma–water interaction? *Journal of Volcanology and Geothermal Research*, **114**, 231–249.
- KESZTHELYI, L., SELF, S. & THORDARSON, T. 2006. Flood lavas on Earth, Io and Mars. *Journal of the Geological Society, London*, **163**, 253–264.
- KOKELAAR, B. P. 1982. Fluidization of wet sediments during the emplacement and cooling of various igneous bodies. *Journal of the Geological Society, London*, **139**, 21–33.
- LEE, G. W., BAILEY, E. B., BUCKMAN, S. S. & THOMAS, H. H. 1925. *The Pre-Tertiary Geology of Mull, Loch Aline, and Oban: (Being a Description of Parts of Sheets, 35, 43, 44, 45 and 52 of the One-inch Geological Map of Scotland)*. Printed under the authority of H.M. Stationery Office.
- LORENZ, B. E. 1984. Mud–magma interactions in the Dunnage Melange, Newfoundland. In Kokelaar, B. P. & Howells, M. (eds) *Marginal Basin Geology: Volcanic and Associated Sedimentary and Tectonic Processes in Modern and Ancient Marginal Basins*. Geological Society, London, Special Publications, **16**, 271–277.
- MACDONALD, G. 1953. Pahoehoe, 'a'ā and block lava. *American Journal of Science*, **251**, 169–191.
- MACDONALD, R. & FETTES, D. 2007. The tectonomagmatic evolution of Scotland. *Transactions of the Royal Society of Edinburgh; Earth Sciences*, **97**, 213–295.
- ROWLAND, S. K. & WALKER, G. P. L. 1990. Pahoehoe and aa in Hawaii: Volumetric flow rate controls the lava structure. *Bulletin of Volcanology*, **52**, 615–628.
- SELF, S., KESZTHELYI, L. & THORDARSON, T. 1998. The importance of pahoehoe. *Annual Review of Earth and Planetary Sciences*, **26**, 81–110.
- SKILLING, I. P., WHITE, J. D. L. & MCPHIE, J. 2002. Peperite: A review of magma–sediment mingling. *Journal of Volcanology and Geothermal Research*, **114**, 1–17.
- TREWIN, N. H. & THIRLWALL, M. F. 2002. Old Red Sandstone. In Trewin, N. H. (ed.) *The Geology of Scotland*. Geological Society, London.
- WALKER, G. 1971. Compound and simple lava flows and flood basalts. *Bulletin of Volcanology*, **35**, 579–590.
- WHITE, J. D. L., MCPHIE, J. & SKILLING, I. 2000. Peperite: A useful genetic term. *Bulletin of Volcanology*, **62**, 65–66.
- WOODCOCK, N. H. 2000. Devonian sedimentation and volcanism of the Old Red Sandstone Continent. In Woodcock, N. H. & Strachan, R. A. (eds) *Geological History of Britain and Ireland*. Wiley-Blackwell, Oxford.

MS. accepted for publication 22 January 2014